

A Crystallographic, Computational and Mechanistic Study of Rhodium Enaminoketonato Complexes

by

Gertruida Jacoba Susanna Venter

A thesis submitted in fulfillment of the requirements for the degree

Philosophiae Doctor

in

Chemistry

in the

Faculty of Agricultural and Natural Science

at the

University of the Free State

Supervisor: Professor Andreas Roodt

Co-supervisor: Professor Gideon Steyl

January 2013

Bedankings

Eerstens moet al die eer aan my Hemelse Vader gaan. Sonder die breinkrag wat ek van Hom gekry het, asook die seëninge wat Hy oor my pad bring, sou niks hiervan moontlik gewees het nie.

Ek kon nie vir `n beter promotor en mentor as Prof. André Roodt gevra het nie. Baie dankie vir al die geleenthede wat Prof. vir my gegee het – al die oorsese reise en konferensies die hele wêreld vol, die befondsingsgeleenthede sodat ek oor ander dinge as finansies kan stres, en `n kans om uit te vind dat ek daarvan hou om met studente te werk.

Prof. Gideon Steyl, dankie vir jou motivering en insette tydens hierdie projek.

My ouers, Henk en Fransina, dankie vir die opofferinge wat julle gemaak het om my te kry waar ek is. Ook die res van my gesin, Jaco, Hielien, Willem en Celia, baie dankie vir al julle liefde en ondersteuning. Ek is waarlik geseënd.

So baie vriende het my ondersteun wanneer ek wou mal word, maar ek wil `n paar uitsonder: Wilmari, Juan-Marie, Marianne en Alice. Sonder julle sou ek waarskynlik lankal my polse afgekou het.

Vir die anorganiese groep: dit was lekker om swaar en lekker tye met julle te deel. Dankie dat ek altyd op julle sin vir humor kon staatmaak. En koffie, moenie die koffie vergeet nie.

Finally, for financial assistance the University of the Free State Strategic Academic Cluster Initiative, SASOL, the South African National Research Foundation (SA-NRF/THRIP) and the Inkaba ye Afrika Research Initiative is gratefully acknowledged.

“Do not follow where the path may lead. Go, instead, where there is no path and leave a trail.” - Ralph Waldo Emerson

Table of contents

Abbreviations and symbols	...i
Abstract	...iii
Opsomming	...vii
Chapter 1 Introduction and Aim of Study	...1
1.1.Introduction	...1
1.2.Aim of this study	...3
Chapter 2 Literature Study	...5
2.1.Introduction	...5
2.2.Rhodium Chemistry	...6
2.1.2 Extraction of Platinum Group Metals	...6
2.2.2 Dicarbonyl Rhodium(I) Complexes with Bidentate Ligands	...7
2.3.2 Carbonyl Tertiary Phosphine Rhodium(I) Complexes	...11
2.3.Homogenously Catalysed Industrial Processes	...14
2.1.3 Introduction	...14
2.2.3 Rhodium in Homogeneous Catalysis	...15
2.3.3 The Monsanto Process	...17
2.4.3 The Cativa Process	...19
2.5.3 Oxidative Addition	...20
2.4.Nitrogen-Containing Complexes	...22
2.5.Halogens	...24
2.6.Conclusion	...25
Chapter 3 Experimental	...27
3.1.Introduction	...27
3.2.Apparatus detail	...28
3.2.1. Single-Crystal X-Ray Crystallography	...28

Table of contents

3.2.2.	Nuclear Magnetic Resonance Spectroscopy	...28
3.2.3.	Infrared Spectroscopy	...29
3.2.4.	Computational Data	...29
3.2.5.	Magnetic Spin Transfer Studies	...29
3.2.6.	UV/Vis Spectroscopy	...30
3.3.	Ligand Synthesis	...30
3.3.1.	Synthesis of 4-(2-Chlorophenylamino)pent-3-en-2-one (2-Cl-PhonyH)	...30
3.3.2.	Synthesis of 4-(4-Chlorophenylamino)pent-3-en-2-one (4-Cl-PhonyH)	...30
3.3.3.	Synthesis of 4-(2,4-Dichlorophenylamino)pent-3-en-2-one (2,4-Cl ₂ -PhonyH)	...31
3.3.4.	Synthesis of 4-(2,6-Dichlorophenylamino)pent-3-en-2-one (2,6-Cl ₂ -PhonyH)	...31
3.4.	Synthesis of [Rh(N,O-bid)(CO) ₂] Complexes	...31
3.4.1.	Synthesis of Dicarbonyl-[4-(Phenylamino)pent-3-en-2-onato]-Rhodium(I) [Rh(Phony)(CO) ₂]	...31
3.4.2.	Synthesis of Dicarbonyl-[4-(2-Chlorophenylamino)pent-3-en-2-onato]- Rhodium(I) [Rh(2-Cl-Phony)(CO) ₂]	...32
3.4.3.	Synthesis of Dicarbonyl-[4-(4-Chlorophenylamino)pent-3-en-2-onato]- Rhodium(I) [Rh(4-Cl-Phony)(CO) ₂]	...32
3.4.4.	Synthesis of Dicarbonyl-[4-(2,4-Dichlorophenylamino)pent-3-en-2-onato]- Rhodium(I) [Rh(2,4-Cl ₂ -Phony)(CO) ₂]	...33
3.4.5.	Synthesis of Carbonyl-[4-(2,6-Dichlorophenylamino)pent-3-en-2-onato]- Rhodium(I) [Rh(2,6-Cl ₂ -Phony)(CO) ₂]	...33
3.5.	Synthesis of [Rh(N,O-Bid)(CO)(PPh ₃)] Complexes	...34
3.5.1.	Synthesis of Carbonyl-[4-(4-Chlorophenylamino)pent-3-en-2-onato]- Triphenylphosphine-Rhodium(I) [Rh(4-Cl-Phony)(CO)(PPh ₃)]	...34
3.5.2.	Synthesis of Carbonyl-[4-(2,4-Dichlorophenylamino)pent-3-en-2-onato]- Triphenylphosphine-Rhodium(I) [Rh(2,4-Cl ₂ -Phony)(CO)(PPh ₃)]	...34
3.5.3.	Synthesis of Carbonyl-[4-(2,6-Dichlorophenylamino)pent-3-en-2-onato]- Triphenylphosphine-Rhodium(I) [Rh(2,6-Cl ₂ -Phony)(CO)(PPh ₃)]	...35

Table of contents

3.5.4.	Synthesis of Carbonyl-[4-(2,3-Dimethylphenylamino)pent-3-en-2-onato]-Triphenylphosphine-Rhodium(I) [Rh(2,3-Me ₂ -Phony)(CO)(PPh ₃)]	...35
3.5.5.	Synthesis of Carbonyl-[4-(2,6-Dimethylphenylamino)pent-3-en-2-onato]-Triphenylphosphine-Rhodium(I) [Rh(2,6-Me ₂ -Phony)(CO)(PPh ₃)]	...36
3.6.	Evaluation of Synthesis	...36
Chapter 4 X-Ray Crystallographic Study of 4-(Phenylamino)pent-3-en-2-one Functionalities		
		...39
4.1.	Introduction	...39
4.2.	Results	...41
4.2.1.	Crystal Structure of 4-(2-Chlorophenylamino)pent-3-en-2-one (2-Cl-PhonyH)	...43
4.2.2.	Crystal Structure of 4-(4-Chlorophenylamino)pent-3-en-2-one (4-Cl-PhonyH)	...46
4.2.3.	Crystal Structure of 4-(2,4-Dichlorophenylamino)pent-3-en-2-one (2,4-Cl ₂ -PhonyH)	...51
4.2.4.	Crystal Structure of 4-(2,6-Dichlorophenylamino)pent-3-en-2-one·0.5 [2,6-Dichlorophenylamine] Adduct [2,6-Cl ₂ -PhonyH·0.5(2,6-Cl ₂ -Phenylamine)]	...54
4.3.	Discussion	...57
4.4.	Conclusion	...61
Chapter 5 Theoretical Study of 4-(Phenylamino)pent-3-en-2-one Functionalities		
		...63
5.1.	Introduction	...63
5.2.	Results	...65
5.3.	Discussion	...69
5.4.	Conclusion	...72
Chapter 6 X-Ray Crystallographic Study of Functionalized Dicarboxyl-[4-(phenylamino)pent-3-en-2-onato]-rhodium(I) Complexes		
		...75
6.1.	Introduction	...75
6.2.	Results	...76

Table of contents

6.2.1. Crystal Structure of Dicarbonyl-[4-(phenylamino)pent-3-en-2-onato]-rhodium(I) [Rh(Phony)(CO) ₂]	...77
6.2.2. Crystal structure of Dicarbonyl-[4-(2-chlorophenylamino)pent-3-en-2-onato]- rhodium(I) [Rh(2-Cl-Phony)(CO) ₂]	...80
6.2.3. Crystal Structure of Dicarbonyl-[4-(4-chlorophenylamino)pent-3-en-2-onato]- rhodium(I) [Rh(4-Cl-Phony)(CO) ₂]	...83
6.2.4. Crystal Structure of Dicarbonyl-[4-(2,4-dichlorophenylamino)pent-3-en-2-onato]- rhodium(I) [Rh(2,4-Cl ₂ -Phony)(CO) ₂]	...86
6.2.5. Crystal Structure of Dicarbonyl-[4-(2,6-dichlorophenylamino)pent-3-en-2-onato]- rhodium(I) [Rh(2,6-Cl ₂ -Phony)(CO) ₂]	...89
6.3. Discussion	...93
6.4. Conclusion	...97
Chapter 7 Theoretical Study of Functionalized Dicarbonyl-[4-(phenylamino)pent-3-en-2-onato]- rhodium(I) Complexes	
7.1. Introduction	...99
7.2. Results	...99
7.3. Discussion	...104
7.4. Conclusion	...108
Chapter 8 X-Ray Crystallographic Study of Functionalized Carbonyl-[4-(phenylamino)pent-3-en-2-onato]-triphenylphosphine-rhodium(I) Complexes	
8.1. Introduction	...111
8.2. Results	...112
8.2.1. Crystal Structure of Carbonyl-[4-(4-chlorophenylamino)pent-3-en-2-onato]- triphenylphosphine-rhodium(I) [Rh(4-Cl-Phony)(CO)(PPh ₃)]	...113
8.2.2. Crystal Structure of Carbonyl-[4-(2,4-dichlorophenylamino)pent-3-en-2-onato]- triphenylphosphine-rhodium(I) [Rh(2,4-Cl ₂ -Phony)(CO)(PPh ₃)]	...116
8.2.3. Crystal Structure of Carbonyl-[4-(2,4-dichlorophenylamino)pent-3-en-2-onato]- triphenylphosphine-rhodium(I) 0.5 Acetone Solvate [Rh(2,6-Cl ₂ -Phony)(CO)(PPh ₃) ·0.5(CH ₃ COCH ₃)	...119

Table of contents

8.2.4. Crystal Structure of Carbonyl-[4-(2,3-dimethylphenylamino)pent-3-en-2-onato]-triphenylphosphine-rhodium(I) [Rh(2,3-Me ₂ -Phony)(CO)(PPh ₃)]	...122
8.2.5. Crystal Structure of Carbonyl-[4-(2,6-dimethylphenylamino)pent-3-en-2-onato]-triphenylphosphine-rhodium(I) 0.5 Acetone Solvate [Rh(2,6-Me ₂ -Phony)(CO)(PPh ₃)]·0.5(CH ₃ COCH ₃)	...125
8.3. Discussion	...128
8.4. Conclusion	...133
Chapter 9 Mechanistic Study of the Phosphine Exchange in Carbonyl-[4-(phenylamino)pent-3-en-2-onato]-triphenylphosphine-rhodium(I) Complexes	
9.1. Introduction	...135
9.2. Magnetization Transfer Study on the Exchange Reaction of [Rh(N,O-Bid)(CO)(PPh ₃)] Complexes with PPh ₃	...137
9.2.1. Theoretical Background	...137
9.2.2. Experimental Procedure	...140
9.2.3. Results	...142
9.3. Discussion and Conclusion	...147
Chapter 10 Evaluation of Study	
10.1. Evaluation of Study	...149
10.1.1. 4-(Phenylamino)pent-3-en-2-one Derivatives	...149
10.1.2. Dicarbonyl-[4-(phenylamino)pent-3-en-2-onato]-rhodium(I) Complexes	...150
10.1.3. Carbonyl-[4-(phenylamino)pent-3-en-2-onato]-triphenylphosphine-rhodium(I) Complexes	...150
10.1.4. Phosphine Exchange Reactions	...151
10.1.5. Oxidative Addition Reactions	...151
10.2. Future Research	...152
Appendix A Crystal Data of 4-(Phenylamino)pent-3-en-2-one Derivatives	...155
Appendix B DFT Calculated Data of 4-(Phenylamino)pent-3-en-2-one Derivatives	...187

Table of contents

Appendix C Crystal Data of Dicarboxyl-[4-(Phenylamino)pent-3-en-2-onato]-Rhodium(I) Derivatives	...193
Appendix D DFT Calculated Data of Dicarboxyl-[4-(Phenylamino)pent-3-en-2-onato]-Rhodium(I) Derivatives	...219
Appendix E Crystal Data of Carbonyl-[4-(Phenylamino)pent-3-en-2-onato]-Triphenylphosphine-Rhodium(I) Derivatives	...225

Abbreviations and Symbols

Å	Ångström
Arom	Aromatic
C ₆ D ₆	Deuterated benzene
CDCl ₃	Deuterated chloroform
CSD	Cambridge structural database
Cy	Cyclohexyl, -C ₆ H ₁₁
°	Degrees
°C	Degrees Celcius
d	Doublet in NMR spectra
d(...)	Distance
δ	Chemical shift
ΔE	Relative energy difference
ΔG [‡]	Gibbs free energy of activation
ΔH [‡]	Enthalpy of activation
ΔS [‡]	Entropy of activation
DFT	Density functional theory
DMF	Dimethylformamide
dm	Decimeter
Fc	Ferrocene
FID	Free induction decay
FT-NMR	Fourier transform nuclear magnetic resonance
g	Gram
HF	Hartree-Fock
Hz	Hertz
IR	Infrared
J	Coupling constant
K	Kelvin
L	Ligand

Abbreviations and Symbols

L,L'-Bid	Bidentate ligand
λ	Wavelength
M	Molar (Mol.dm ⁻³)
m	Multiplet in NMR spectra
Me	Methyl, -CH ₃
μ	Indicates bridging ligands in complexes
NHC	N-heterocyclic carbene
nm	Nanometer
NMR	Nuclear magnetic resonance
N,O-BidH	Derivatives of 4-(phenylamino)pent-3-en-2-one
PGM	Platinum group metal
Ph	Phenyl, -C ₆ H ₅
PhonyH	4-(Phenylamino)pent-3-en-2-one
ppm	Parts per million
PX ₃	Tertiary substituted phosphine
r _i	Interatomic distance for halide interactions
RMS	Quadratic mean (root-mean-square)
s	Singlet in NMR spectra
SS	Solid state
§	Section
t	Triplet in NMR spectra
τ	Molecular correlation time
<i>tert</i>	Tertiary
tBu	Tertiary Butyl, -C(CH ₃) ₃
θ	Angle
θ_E	Effective cone angle
UV/Vis	Ultraviolet/visible
Z	Number of molecules in unit cell

Abstract

This study includes the investigation of enamino-ketones as ligand systems in rhodium complexes with possible future application in catalysis. In order to evaluate the influence of substituents on the phenyl ring on activity of the complex, a range of 4-(phenylamino)pent-3-en-2-onate (PhonyH) derivatives with chloride substituents on different positions on the phenyl ring were synthesized and characterized through X-ray crystallography as well as infrared and NMR spectroscopy. The compounds crystallize in a range of space groups and varying crystal systems, are stable in air over a period of several years and soluble in most solvents. The optimized structures of these compounds were calculated using DFT methods. The relative energies of the optimized structures adopt a cumulative nature – the relative energy of 2,4-Cl₂-PhonyH with regard to unsubstituted PhonyH is roughly equal to the sum of the relative energies of 2-Cl-PhonyH and 4-Cl-PhonyH, while the relative energy of 2,6-Cl₂-PhonyH is twice the relative energy of 2-Cl-PhonyH. The distortion of the phenyl ring from the ideal planar position presented in the calculated structures corresponds to the distortion observed in the solid state.

The synthesis of the uncoordinated compounds was followed by the synthesis and characterization of a range of substituted dicarbonyl-[4-(phenylamino)pent-3-en-2-onato]-rhodium(I) complexes. The complexes crystallized in varying crystal systems and space groups. The *trans* influence of nitrogen was confirmed through the difference in the Rh-CO bonds: the Rh-C bond *trans* to the nitrogen atom is longer than the Rh-C bond *trans* to oxygen. The impact of the chloride substituents was observed from differences in geometrical parameters and is supported by information from the calculated structures and literature. The optimized structures of these complexes were calculated using DFT methods, and their optimized energies follow the same cumulative trend as observed in the uncoordinated compounds.

A range of carbonyl-[4-(phenylamino)pent-3-en-2-onato]-triphenylphosphine-rhodium(I) {[Rh(N,O-Bid)(CO)(PPh₃)]} complexes were synthesized and characterized, containing both electron-withdrawing chloride atoms and electron-donating methyl groups. These complexes displayed poor solubility, but once dissolved, were stable over a period of several months.

Isomorphism was observed between $[\text{Rh}(2,6\text{-Cl}_2\text{-Phony})(\text{CO})(\text{PPh}_3)]$ and $[\text{Rh}(2,6\text{-Me}_2\text{-Phony})(\text{CO})(\text{PPh}_3)]$.

$[\text{Rh}(2,6\text{-Cl}_2\text{-Phony})(\text{CO})(\text{PPh}_3)]$ and $[\text{Rh}(2,6\text{-Me}_2\text{-Phony})(\text{CO})(\text{PPh}_3)]$ were chosen to investigate the exchange of triphenylphosphine coordinated in $[\text{Rh}(\text{N,O-Bid})(\text{CO})(\text{PPh}_3)]$ complexes with the uncoordinated phosphine, allowing for the comparison of the electronic effect of the substituents on the phenyl rings. The method chosen for the investigation was magnetization spin transfer, an NMR technique which utilizes the magnetic properties of nuclei and determines the kinetic properties of the exchange reaction by following the rate at which magnetic equilibrium is restored.

The rate of the phosphine exchange reaction in $[\text{Rh}(2,6\text{-Cl}_2\text{-Phony})(\text{CO})(\text{PPh}_3)]$ was determined as approximately three times faster than the rate of reaction for phosphine exchange in $[\text{Rh}(2,6\text{-Me}_2\text{-Phony})(\text{CO})(\text{PPh}_3)]$. The decreased electron density surrounding the rhodium atom in $[\text{Rh}(2,6\text{-Cl}_2\text{-Phony})(\text{CO})(\text{PPh}_3)]$ allows for the reversal of the reaction as indicated by the k_{-1} values of approximately 11 s^{-1} calculated from the $[\text{Rh}(2,6\text{-Cl}_2\text{-Phony})(\text{CO})(\text{PPh}_3)]$ exchange reaction. This value is absent in the reaction of the $[\text{Rh}(2,6\text{-Me}_2\text{-Phony})(\text{CO})(\text{PPh}_3)]$ complex. The activation parameters of the exchange reaction in $[\text{Rh}(2,6\text{-Cl}_2\text{-Phony})(\text{CO})(\text{PPh}_3)]$ ($\Delta H^\ddagger = 25(3) \text{ kJ}\cdot\text{mol}^{-1}$ and $\Delta S^\ddagger = -117(9) \text{ J}\cdot\text{K}^{-1}\cdot\text{mol}^{-1}$) correlate well with the parameters of the exchange reaction in $[\text{Rh}(2,6\text{-Me}_2\text{-Phony})(\text{CO})(\text{PPh}_3)]$ ($\Delta H^\ddagger = 24(4) \text{ kJ}\cdot\text{mol}^{-1}$ and $\Delta S^\ddagger = -124(12) \text{ J}\cdot\text{K}^{-1}\cdot\text{mol}^{-1}$). In both cases the value for entropy, ΔS^\ddagger , is negative, indicating an associative mechanism. The relative contribution of $T\Delta S^\ddagger$ to ΔG^\ddagger is approximately 60% for both complexes, whereas the enthalpy (ΔH^\ddagger) terms are correspondingly small. This indicates that the activation process is primarily controlled by entropy and involves the formation of a stable, well-ordered transition state while bond weakening is less important. The relatively constant values for ΔG^\ddagger imply that the exchange reaction is not very sensitive to changes in temperature.

Keywords:

rhodium

enaminoketone

dicarbonyl

X-Ray crystallography

density functional theory

Abstract

phosphine exchange

NMR

magnetization spin transfer

activation parameters

Opsomming

Hierdie studie sluit die ondersoek van enaminketone as ligandstelsel in rodium komplekse in, met toepassingsmoontlikhede in katalise. Ten einde die invloed van substituentte op die fenielring op die aktiwiteit van die kompleks te evalueer is 'n reeks van 4-(fenielamino)pent-3-en-2-onaat (PhonyH) derivate met chloried substituentte op verskillende posisies op die feniel ring vervaardig en gekarakteriseer deur X-straal kristallografie sowel as KMR spektroskopie. Die verbindings kristalliseer in 'n reeks ruimtegroepe en verskeie kristalstelsels, is stabiel in lug oor 'n tydperk van 'n aantal jare en oplosbaar in die meeste oplosmiddels. Die geoptimeerde strukture van hierdie verbindings is bereken deur DFT metodes. Die relatiewe energieë van die geoptimeerde strukture neem 'n kumulatiewe natuur aan – die relatiewe energie van 2,4-Cl₂-PhonyH ten opsigte van ongewysigde PhonyH is ongeveer gelyk aan die som van die relatiewe energieë van 2-Cl-PhonyH en 4-Cl-PhonyH, terwyl die relatiewe energie van 2,6-Cl₂-PhonyH twee maal die energie van 2-Cl-PhonyH is. Die vervorming van die feniel ring uit die ideale planêre posisie soos voorgelê in die berekende strukture stem ooreen met die vervorming waargeneem in die vaste toestand.

Die sintese van die ongekoördineerde verbindings is opgevolg deur die sintese en karakterisering van 'n reeks gesubstitueerde dikarboniel-[4-(fenielamino)pent-3-en-2-onato]-rodium(I) komplekse. Die komplekse kristalliseer in verskillende kristalstelsels en ruimtegroepe. Die *trans* invloed van stikstof is bevestig deur die verskil in die Rh-CO bindings: die Rh-C binding *trans* ten opsigte van die stikstof atoom is langer as die Rh-C binding *trans* ten opsigte van die suurstof atoom. Die impak van die chloried substituent is waargeneem vanaf die verskille in geometriese parameters en word ondersteun deur inligting vanaf die berekende strukture en literatuur. Die geoptimeerde strukture van hierdie komplekse is bereken deur middel van DFT metodes en volg dieselfde kumulatiewe neiging as wat waargeneem is in die ongekoördineerde verbindings.

'n Reeks karboniel-[4-(fenielamino)pent-3-en-2-onato]-trifenilfosfen-rodium(I) {[Rh(N,O-Bid)(CO)(PPh₃)]} komplekse is vervaardig en gekarakteriseer, en bevat beide elektrononttrekkende chloried atome en elektronskenkende metiel groepe. Hierdie komplekse vertoon swak oplosbaarheid, maar is stabiel oor 'n tydperk van verskeie maande sodra dit

opgelos is. Isomorfisme is waargeneem tussen $[\text{Rh}(2,6\text{-Cl}_2\text{-Phony})(\text{CO})(\text{PPh}_3)]$ en $[\text{Rh}(2,6\text{-Me}_2\text{-Phony})(\text{CO})(\text{PPh}_3)]$.

$[\text{Rh}(2,6\text{-Cl}_2\text{-Phony})(\text{CO})(\text{PPh}_3)]$ en $[\text{Rh}(2,6\text{-Me}_2\text{-Phony})(\text{CO})(\text{PPh}_3)]$ is gekies om die uitruiling tussen trifenielfosfien gekoördineer in $[\text{Rh}(\text{N},\text{O}\text{-Bid})(\text{CO})(\text{PPh}_3)]$ komplekse met die ongekoördineerde fosfien te ondersoek, wat die vergelyking van die elektroniese effek van die substituentte op die feniel ringe toelaat. Die gekose metode vir die ondersoek is magnetisasie spin oordrag, 'n KMR tegniek wat die magnetiese eienskappe van nuklei benut en die kinetiese eienskappe van die uitruilingsreaksie bepaal deur die tempo van die herstel van die magnetiese ewewig te volg.

Die tempo van die fosfienuitruilingsreaksie in $[\text{Rh}(2,6\text{-Cl}_2\text{-Phony})(\text{CO})(\text{PPh}_3)]$ is vasgestel as ongeveer drie maal vinniger as die reaksietempo van fosfienuitruiling in $[\text{Rh}(2,6\text{-Me}_2\text{-Phony})(\text{CO})(\text{PPh}_3)]$. Die verminderde elektrondigtheid rondom die rodium atoom in $[\text{Rh}(2,6\text{-Cl}_2\text{-Phony})(\text{CO})(\text{PPh}_3)]$ laat die ommekeer van die reaksie toe, soos aangedui deur die k_{-1} waardes van ongeveer 11 s^{-1} , bereken vanaf die $[\text{Rh}(2,6\text{-Cl}_2\text{-Phony})(\text{CO})(\text{PPh}_3)]$ uitruilingsreaksie. Hierdie waarde is afwesig in die reaksie van die $[\text{Rh}(2,6\text{-Me}_2\text{-Phony})(\text{CO})(\text{PPh}_3)]$ kompleks. Die aktiveringsparameters van die uitruilingsreaksie in $[\text{Rh}(2,6\text{-Cl}_2\text{-Phony})(\text{CO})(\text{PPh}_3)]$ ($\Delta H^\ddagger = 25(3) \text{ kJ}\cdot\text{mol}^{-1}$ en $\Delta S^\ddagger = -117(9) \text{ J}\cdot\text{K}^{-1}\cdot\text{mol}^{-1}$) stem goed ooreen met die parameters van die uitruilingsreaksie in $[\text{Rh}(2,6\text{-Me}_2\text{-Phony})(\text{CO})(\text{PPh}_3)]$ ($\Delta H^\ddagger = 24(4) \text{ kJ}\cdot\text{mol}^{-1}$ en $\Delta S^\ddagger = -124(12) \text{ J}\cdot\text{K}^{-1}\cdot\text{mol}^{-1}$). In beide gevalle is die waarde vir entropie, ΔS^\ddagger , negatief, 'n aanduiding van 'n assosiatiewe meganisme. Die relatiewe bydraes van $T\Delta S^\ddagger$ tot ΔG^\ddagger is ongeveer 60% vir beide komplekse, terwyl die entalpie (ΔH^\ddagger) terme ooreenkomstig klein is. Dit dui aan dat die aktiveringsproses primêr deur entropie beheer word en behels die vorming van 'n stabiele, goed georganiseerde oorgangstoestand terwyl bindingsverswakking minder belangrik is. Die relatiewe konstante waardes vir ΔG^\ddagger impliseer dat die uitruilingsreaksie nie baie sensitief is ten opsigte van veranderinge in temperatuur nie.

1 Introduction and Aim of Study

1.1. Introduction

Rhodium is a rare, silvery-white, hard and chemically inert transition metal and a member of the platinum group. It is found in platinum- or nickel ores together with the other members of the platinum group metals and is predominantly implemented as an automotive catalyst where it is used together with platinum and palladium to control exhaust emissions¹. A comprehensive discussion of rhodium in oxidation states I to V can be found in *Advanced Inorganic Chemistry* by Cotton *et al.*² as well as the *Comprehensive Coordination Chemistry* series³.

Rhodium(I) dicarbonyl complexes of the formula $[\text{Rh}(\text{L},\text{L}'\text{-Bid})(\text{CO})_2]$ (where L,L'-Bid are chelating monoanionic ligands L,L'-coordinated to rhodium via O,O-, O,N- or O,S-donor atoms) have been studied extensively⁴ as catalyst precursors in hydroformylation, isomerization and hydrogenation of olefins as well as model compounds in studies of the key stages of catalytic cycles. Enaminoketones, also known as ketoamines, belong to this group of ligands and contain both a nitrogen and an oxygen atom as well as an unsaturated carbon-carbon bond. Due to their electron-rich quality these compounds are also of interest in various fields including liquid

¹ a) Amatayakul, W.; Ramnäs, O. *J. Clean. Prod.* **2001**, *9*, 345.

b) Heck, R.M.; Farrauto, R.J. *Appl. Catal. A-Gen.*, **2001**, *221*, 443.

² Cotton, F.A.; Wilkinson, G.; Murillo, C.A.; Bochmann, M. *Advanced Inorganic Chemistry*, 6th ed., John Wiley & Sons, Inc., New York, **1999**.

³ a) Wilkinson, G.; Gillard, R.D.; McCleverty, J.S. *Comprehensive Coordination Chemistry*, Volume I, Pergamon Press, Oxford, **1987**.

b) McCleverty, J.S.; Meyer, T.J. *Comprehensive Coordination Chemistry*, Volume II, Elsevier Pergamon Press, Oxford, **2004**.

⁴ a) Leipoldt, J.G.; Bok, L.D.C.; Van Vollenhoven, J.S.; Pieterse, A.I. *J. Inorg. Nucl. Chem.* **1978**, *40*, 61.

b) Heaton, B.T.; Jacob, C.; Markopoulos, J.; Markopoulou, O.; Nähring, J.; Skylaris, C.-K.; Smith, A.K. *J. Chem. Soc. Dalton Trans.* **1996**, 1701.

c) Cano, M.; Herras, J.V.; Lobo, M.A.; Pinilla, E.; Monge, M.A. *Polyhedron* **1994**, *13*, 1563.

d) Trzeciak, A.M.; Ziółkowski, J.J. *Coord. Chem. Rev.* **1999**, *190–192*, 883.

e) Pruchnik, F.P.; Smolenski, P.; Wajda-Hermanowicz, K. *J. Organomet. Chem.* **1998**, *570*, 63.

f) Van Rooy, A.; Orji, E.N.; Kramer, P.G.J.; Van Leeuwen, P.W.N.M. *Organometallics* **1995**, *14*, 34.

Chapter 1

crystals⁵, fluorescence studies⁶ as well as medical applications⁷ and catalysis⁸. In most CO-containing molecules, one or more CO groups can be substituted by a PX_3 or similar type of ligand. $[Rh(N,O-Bid)(CO)_2]$ complexes (where N,O-Bid = 4-(phenyl-amino)pent-3-en-2-one derivatives) react with PPh_3 to form $[Rh(N,O-Bid)(CO)(PPh_3)]$.

The electronic effect of tertiary aryl phosphines on a metal center can be described by the carbonyl stretching frequencies *trans* to the tertiary phosphine in square planar complexes⁹, known as the Tolman electronic parameter. Comparison of ν_{CO} gives an indication of the influence of PX_3 , since a decrease in electron-donating capability of the substituents on the tertiary phosphine leads to an increase in the CO stretching frequencies. This implies that an increase in ν_{CO} means less π -bond stabilization in the M-C moiety, caused by the decrease in metal-ligand $d \rightarrow \pi^*$ back donation due to the decrease in electron density on the metal center. X-ray structural studies¹⁰ have shown that for asymmetric bidentate ligands with different donor atoms, the *trans*-influence for oxygen, nitrogen and sulfur follows the reverse electronegativity range $S > N > O$.

Rhodium was first considered as catalyst following a report on the use of phosphines in a cobalt catalyzed process, in which preliminary data for the use of rhodium was included¹¹, which led to the application of phosphine ligands in rhodium catalyzed processes by many industries¹². A well-known catalyst in homogenous hydrogenation is Wilkinson's catalyst¹³, chloridetrakis(triphenylphosphine) rhodium(I) or $[RhCl(PPh_3)_3]$. Rhodium catalysts are generally faster and utilize milder reaction conditions than cobalt catalysts, and have better feedstock consumption. Since the mid-seventies cobalt catalysts were replaced by rhodium catalysts in

⁵ Pyżuk, W.; Krówczynsk, A.; Górecka, E. *Mol. Cryst. Liq. Cryst.* **1993**, 237, 75.

⁶ Xia, M.; Wu, B.; Xiang, G. *J. Flu. Chem.* **2008**, 129, 402.

⁷ a) Tan, H.Y.; Loke, W.K.; Tan, Y.T.; Nguyen, N.-T. *Lab Chip* **2008**, 8, 885.

b) Chen, H.; Rhodes, J. *J. Mol. Med.* **1996**, 74, 497.

⁸ Nair, V.A.; Suni, M.M.; Sreekumar, K. *Proc. Indian Acad. Sci. (Chem. Sci.)* **2002**, 114, 481.

⁹ Tolman, C.A. *J. Am. Chem. Soc.* **1970**, 92, 2953.

¹⁰ a) Graham, D.E.; Lamprecht, G.J.; Potgieter, I.M.; Roodt, A.; Leipoldt, J.G. *Transition Met. Chem.* **1991**, 16, 193.

b) Steyn, G.J.J.; Roodt, A.; Poetaeva, I.; Varshavsky, Y.S. *J. Organomet. Chem.* **1997**, 536/537, 197.

c) Botha, L.J.; Basson, S.S.; Leipoldt, J.G. *Inorg. Chim. Acta* **1987**, 126, 25.

d) Roodt, A.; Visser, H.G.; Brink, A. *Crystallogr. Rev.* **2011**, 17, 241.

¹¹ Slauch, L.H.; Mullineaux, R.D. US. Pat. 3,239,569 and 3,239,570 **1996** (to Shell); *J. Organomet. Chem.* **1968**, 13, 469.

¹² Onoda, T. *ChemTech.* **1993**, 34.

¹³ Osborn, J.A.; Jardine, F.H.; Young, J.A.; Wilkinson, G. *J. Chem. Soc. A* **1966**, 1711.

Chapter 1

propene and butene hydroformylation. A rhodium complex, $[\text{RhI}_2(\text{CO})_2]^+$, is also used in the carbonylation of alcohols which is known as the Monsanto process².

This study includes the investigation of enaminoketones as ligand systems in rhodium complexes with possible application in catalysis. A literature overview regarding ligand coordination, the carbonyl and phosphine groups, oxidative addition reactions, application of rhodium as an industrial catalyst and the extraction of rhodium are topics that will be discussed. For the purpose of this study phosphine exchange in $[\text{Rh}(\text{N},\text{O}\text{-Bid})(\text{CO})(\text{PPh}_3)]$ complexes is discussed, since exchange reactions play a major role in the activity of a complex. When varying the electronegativity of the ligand, the geometric parameters of the molecule are changed, which influences the reactivity of the molecule. For the purpose of this study, the position of the substituents on the phenyl moiety of the bidentate ligand was varied, and the substituents vary between electron-withdrawing chloride atoms and electron-donating methyl groups.

1.2. Aim of this study

A range of substituted enaminoketones were selected as ligand system in rhodium complexes of the type $[\text{Rh}(\text{N},\text{O}\text{-Bid})(\text{CO})(\text{PPh}_3)]$, where N,O-Bid is derivatives of 4-(phenyl-amino)pent-3-en-2-one. The use of a bulky phenyl moiety on the nitrogen atom of the enaminoketonato ligand prevents the formation of isomers, and all complexes crystallize with the triphenylphosphine ligand in the position *trans* to nitrogen. Electron-withdrawing chloride atoms as well as electron-donating methyl groups on different positions on the phenyl ring of the enaminoketonato ligand were chosen to evaluate the influence of electronic properties on the reaction of $[\text{Rh}(\text{N},\text{O}\text{-Bid})(\text{CO})(\text{PPh}_3)]$ complexes with methyl iodide.

With the above-mentioned in mind, the following specific aims were set for this study:

- The synthesis and characterization of a range of substituted 4-(phenylamino)pent-3-en-2-one (N,O-BidH) compounds, with electron-donating chloride atoms on different positions on the phenyl moiety. The X-Ray crystallographic data of these compounds will be compared with the theoretically optimized structures, with focus on differences between compounds with substitutions on different positions.

Chapter 1

- Synthesis and characterization of chloride-substituted dicarbonyl-[4-(phenylamino)pent-3-en-2-onato]-rhodium(I), or $[\text{Rh}(\text{N},\text{O}\text{-Bid})(\text{CO})_2]$ complexes, as well as the correlation between solid state X-Ray crystallographic data and the calculated structures with regard to geometric parameters.
- The optimized structures of the substituted PhonyH compounds and the $[\text{Rh}(\text{N},\text{O}\text{-Bid})(\text{CO})_2]$ complexes will be calculated using density functional theory, or DFT, calculations. The energies of these structures as well as the geometrical parameters will be compared between the optimized structures and their experimentally obtained counterparts.
- Synthesis and characterization of a range of substituted carbonyl-[4-(phenylamino)pent-3-en-2-onato]-triphenylphosphine-rhodium(I), or $[\text{Rh}(\text{N},\text{O}\text{-Bid})(\text{CO})(\text{PPh}_3)]$ complexes, and the influence of electron-donating and -withdrawing substituents on geometric parameters. These substituents include electron-withdrawing chloride atoms on different positions on the phenyl moiety of the bidentate ligand and electron-donating methyl groups.
- The evaluation of oxidative addition reactions of methyl iodide to $[\text{Rh}(\text{N},\text{O}\text{-Bid})(\text{CO})(\text{PPh}_3)]$ complexes using nuclear magnetic resonance, infrared and ultraviolet/visible spectroscopy.
- The evaluation of phosphine exchange reactions in $[\text{Rh}(\text{N},\text{O}\text{-Bid})(\text{CO})(\text{PPh}_3)]$ complexes using nuclear magnetic resonance spectroscopy, specifically the magnetization spin transfer technique.

2 Literature Overview

2.1 Introduction

This study includes the investigation of enaminoketones as ligand systems in rhodium complexes with possible application in catalysis, as noted in Chapter 1. A literature overview regarding ligand coordination, the carbonyl group, oxidative addition reactions, application of rhodium as an industrial catalyst and the extraction of rhodium are topics that will be discussed in this chapter. For the purpose of this study phosphine exchange in $[\text{Rh}(\text{N,O-Bid})(\text{CO})(\text{PPh}_3)]$ complexes is discussed, since exchange reactions play a major role in the activity of a complex.

Rhodium is a chemical element that is a rare, silvery-white, hard and chemically inert transition metal and a member of the platinum group with an atomic radius of $1.42(7) \text{ \AA}^1$. Naturally-occurring rhodium is composed of only one isotope, ^{103}Rh . First discovered in 1803 by William Hyde Wollaston², it is found in platinum- or nickel ores together with the other members of the platinum group metals. Rhodium usage is dominated by automotive catalyst applications where it is used together with platinum and palladium to control exhaust emissions³. Rhodium is inert against corrosion and most aggressive chemicals and is excessively rare. It is usually alloyed with platinum or palladium and applied in high-temperature and corrosion-resistive coatings⁴. White gold is often plated with a thin rhodium layer to improve its optical impression while sterling silver is rhodium plated for tarnish resistance. A comprehensive discussion of rhodium in oxidation states I to V can be found in Cotton *et al.*⁵

¹ Cordero B.; Gómez V.; Platero-Prats A.E.; Revés M.; Echeverría J.; Cremades E.; Barragán F.; Alvarez S. *Dalton Trans.* **2008**, 2832.

² Hinde, P.T. *J. Chem. Ed.* **1966**, *43*, 673.

³ a) Amatayakul, W.; Ramnäs, O. *J. Clean. Prod.* **2001**, *9*, 345.

b) Heck, R.M.; Farrauto, R.J. *Appl. Catal. A-Gen.*, **2001**, *221*, 443.

⁴ Ballinger, T.H.; Yates, J.T. *J. Phys. Chem.* **1991**, *95*, 1694.

⁵ Cotton, F.A.; Wilkinson, G.; Murillo, C.A.; Bochmann, M. *Advanced Inorganic Chemistry*, 6th ed., John Wiley & Sons, Inc., New York, **1999**.

2.2 Rhodium Chemistry

2.2.1 Extraction of Platinum Group Metals

Rhodium is part of the platinum group metals (PGM's), which also include ruthenium, osmium, iridium, palladium and platinum. The most significant source of PGM's is in South Africa⁶ followed by Russia and Northern America (mainly Canada). South Africa is the primary source of all the platinum group metals except for palladium, and is the nearly exclusive source for osmium, iridium, and ruthenium. These metals are found in two different forms: as ore found along the chromite vein in pyroxene deposits in South Africa's Bushveld complex or as a byproduct of nickel mining⁷. The first step in extracting PGM's from ore is the removal of the crude ore from the platinum-bearing iron-chromite reef layers along with small amounts of base metal sulfides, followed by crushing and gravity concentration on corduroy tables to separate the coarse particles of platinum-bearing minerals and the free metallic particles. The tailings from these tables are treated with thickeners before going to the flotation plant where most of the remaining PGM-bearing minerals are recovered. The flotation concentrates are sent to the smelter to be smelted into a copper-nickel-iron matte in a series of blast furnaces. The treatment of this material may be divided into two steps, first the removal of nickel and copper to produce a rich platinum group metal concentrate, followed by chemical treatment of this concentrate to separate and purify the individual metals. After removal of nickel and copper, gold, platinum and palladium is removed from the PGM concentrate, while the residue comprises iridium, rhodium, osmium and ruthenium.

After removing silver chloride, which is then further processed to produce silver metal, the filtrate is extracted with methyl isobutyl ketone to selectively extract gold along with other base metal impurities that are removed by washing the organic layer with dilute hydrochloric acid solution. Palladium is extracted from the platinum group metal concentrate with β -hydroxyoxime and the organic layer is washed with dilute hydrochloric acid solution to remove the base metals. Palladium is extracted from the organic layer and precipitates as ammonium hexachloropalladate salt with the use of ammonia. This salt is reduced with hydrogen to produce palladium metal. The PGM concentrate solution is neutralized with hydroxide solution, and ruthenium and

⁶ Kettler, P.B. *Org. Process Res. Dev.* **2003**, *7*, 342.

⁷ Hunt, L.B.; Lever, F.M. *Platinum Met. Rev.* **1969**, *13*, 126.

Chapter 2

osmium are distilled from the concentrate into a hydrochloric acid solution, followed by fractionally distillation to separate ruthenium from osmium. Concentrated hydrochloric acid solution is used to remove the platinum from the original concentrate and precipitated with ammonium chloride to produce ammonium hexachloroplatinate, which is burned to generate platinum metal. Iridium(III) is oxidized to iridium(IV) with hydrochloric acid and selectively extracted with trioctylamine, followed by re-extraction with dilute hydrochloric acid to bring the iridium back into the aqueous phase as a chloride-complex. Ammonium hexachloroiridate is precipitated upon addition of ammonium and then reduced under hydrogen to generate iridium metal. The extraction of rhodium is the final step in the refinement process. A mixture of sodium chloride and sodium sulfite solution is added to the concentrate to precipitate rhodium. The wet precipitate is dissolved in hydrochloric acid, and rhodium is precipitated by the addition of ammonium chloride to precipitate the ammonium hexachlororhodate salt. This salt is reduced under hydrogen to generate rhodium metal. The final purification steps for each of the metals will usually be repeated once or twice to attain the purity required for further value-added chemical products.

2.2.2 Dicarbonyl Rhodium(I) Complexes with Bidentate Ligands

Carbon monoxide is one of the most common ligands in organometallic chemistry and bonds to transition metals using synergistic π^* back-bonding⁸. The bond has three components, giving rise to a partial triple bond. Firstly, a σ bond is formed from overlap of a non-bonding electron pair on carbon with a blend of d , s , and p -orbitals on the metal centre. Secondly, a pair of π -bonds arise from overlap of filled d -orbitals on the metal centre with a pair of unoccupied π^* -orbitals projecting from the carbon of the CO. The π -bonding has the effect of weakening the carbon-oxygen bond compared with free carbon monoxide. Because of the multiple bond character of the M-CO linkage, the distance between the metal and carbon is relatively short, often $< 1.8 \text{ \AA}$. The interaction between a CO molecule and a metal atom is illustrated in Figure 2.1.

⁸ Miessler, G.L.; Tarr, D.A. *Inorganic Chemistry*, Prentice-Hall, Inc., Northfield, 1991.

Chapter 2

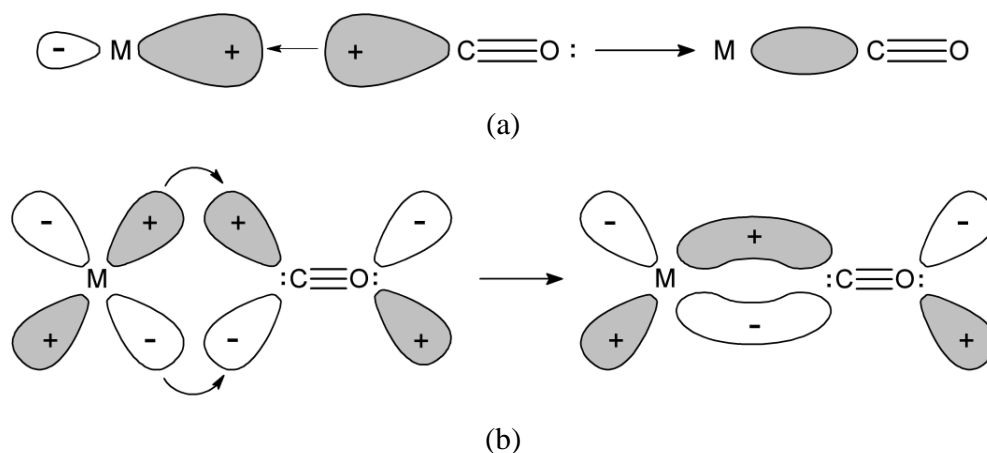


Figure 2.1. Illustration of a) σ -donation of a CO-molecule to a metal and b) π -backbonding of a metal to a CO-molecule⁵. The outer orbitals on the CO is omitted for clarity.

Metal carbonyl anions have a rich history in chemistry and are important precursors to a tremendous variety of organometallic, inorganic, and organic species⁸. They are also of considerable interest as the first compounds to contain transition metals in formally negative oxidation states⁹ and exhibit reactivity patterns that bear striking similarities to those of halides, chalcogenides, and pnictides¹⁰. Metal carbonyl mono-anions such as $[\text{Co}(\text{CO})_4]^-$, $[\text{Mn}(\text{CO})_5]^-$, $[\text{V}(\text{CO})_6]^-$, etc. are now often considered to be transition metal analogues of classic pseudohalides¹¹.

Infrared spectroscopy remains the single most powerful technique available for monitoring the reactions of metal carbonyls and for the provisional assignment of structures to new products, because the number, relative intensities, shapes, and energies of the IR-active carbonyl stretching modes, i.e., ν_{CO} absorptions, are extremely sensitive functions of the molecular structure and charge of a carbonyl complex. Carbonyl stretching frequencies for mononuclear metal carbonyls generally range from 2200 to 1500 cm^{-1} . Ion pairing between cations and metal carbonyl anions can cause dramatic changes in the ν_{CO} region, due to strong perturbation of the geometry of the anion. Classically the metal-carbonyl interaction involves synergistic bonding, with carbon monoxide acting as a σ -donor and a π -acceptor for *d*-block metals¹². This may however not be

⁹ Beck, W. *Angew. Chem., Int. Ed. Engl.* **1991**, 30, 168.

¹⁰ Ellis, J.E. *J. Organomet. Chem.* **1975**, 86, 1.

¹¹ a) Ellis, J.E. *J. Chem. Educ.* **1976**, 53, 2.

b) Golub, A.M.; Köhler, H.; Skopenko, V.V. *Chemistry of Pseudohalides*, Elsevier: Amsterdam, Chapter 1, **1986**.

¹² a) Yamamoto, S.; Kashiwagi, H. *Chem. Phys. Lett.* **1993**, 205, 306.

Chapter 2

accurate for all *d*-block metals. While there are many thousands of stable, isolable transition metal carbonyl complexes, there are few or none known for the metals at the extreme fringes of the *d*-block. For example, the group 3 ions Sc^{3+} , Y^{3+} , and La^{3+} have not yielded any isolable carbonyl complexes, presumably because their lack of *d* electrons precludes π -back-bonding and synergistic bonding. Additionally, no isolable carbonyls are known for the group 12 d^{10} ions Zn^{2+} and Cd^{2+} , possibly because their effective nuclear charges are too high to permit effective metal \rightarrow carbon $d\rightarrow\pi^*$ π -backbonding.

Rhodium(I) dicarbonyl complexes of the formula $\text{Rh}(\text{L},\text{L}'\text{-Bid})(\text{CO})_2$ with chelating monoanionic ligands L,L'-coordinated to rhodium via O,O-, O,N- or O,S-donor atoms represent a group of compounds that has recently been intensively studied^{13,14} as catalyst precursors in hydroformylation, isomerization and hydrogenation of olefins as well as model compounds in studies of the key stages of catalytic cycles. An important precursor in these complexes is tetracarbonyldichlororhodium, or $[\text{Rh}(\text{CO})_2(\mu\text{-Cl})_2]$, which is prepared by sublimation as red needles after CO saturated with ethanol is passed over powdered $\text{RhCl}_3\cdot 3\text{H}_2\text{O}$ at 100°C ¹⁵. It can also be prepared *in situ* by refluxing $\text{RhCl}_3\cdot 3\text{H}_2\text{O}$ in dimethylformamide at 180°C until the color changes to yellow. The halogen bridges are readily cleaved by a wide variety of donor ligands to give *cis*-dicarbonyl complexes such as in Scheme 2.1⁵:

b) Blomberg, M.R.A.; Siegbahn, P.E.M.; Lee, T.L.; Rendell, A.P.; Rice, J.E. *J. Chem. Phys.* **1991**, *95*, 5898.

c) Barnes, L.A.; Rosi, M.; Bauschlicher, C.W.J. *Chem. Phys.* **1991**, *94*, 2031.

d) Smith, S.; Hillier, I.H.; Von Niessen, W.; Guest, M.F. *Chem. Phys.* **1987**, *135*, 357.

e) Pierfoot, K.; Verhulst, J.; Verbeke, P.; Vanquickenborne, L.G. *Inorg. Chem.* **1989**, *28*, 3059.

f) Williamson, R.L.; Hall, M.B. *Int. J. Quantum Chem.* **1987**, *S21*, 503.

g) Shenvood, D.E.; Hall, M.B. *Inorg. Chem.* **1980**, *19*, 1805.

h) Hall, M.B.; Fenske, R.F. *Inorg. Chem.* **1972**, *11*, 1620.

¹³ Leipoldt, J.G.; Bok, L.D.C.; Van Vollenhoven, J.S.; Pieterse, A.I. *J. Inorg. Nucl. Chem.* **1978**, *40*, 61.

¹⁴ a) Heaton, B.T.; Jacob, C.; Markopoulos, J.; Markopoulou, O.; Nähring, J.; Skylaris, C.-K.; Smith, A.K. *J. Chem. Soc. Dalton Trans.* **1996**, 1701.

b) Cano, M.; Herras, J.V.; Lobo, M.A.; Pinilla, E.; Monge, M.A. *Polyhedron* **1994**, *13*, 1563.

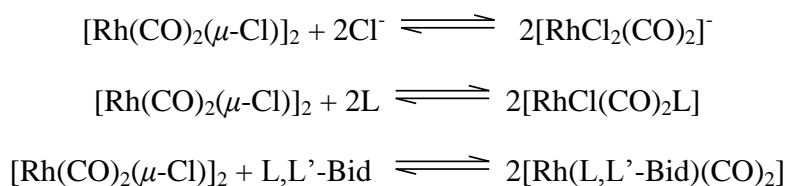
c) Trzeciak, A.M.; Ziółkowski, J.J. *Coord. Chem. Rev.* **1999**, *190–192*, 883.

d) Pruchnik, F.P.; Smolenski, P.; Wajda-Hermanowicz, K. *J. Organomet. Chem.* **1998**, *570*, 63.

e) Van Rooy, A.; Orji, E.N.; Kramer, P.G.J.; Van Leeuwen, P.W.N.M. *Organometallics* **1995**, *14*, 34.

¹⁵ McCleverty, J.A.; Wilkinson, G. *Inorg. Synth.* **1966**, *8*, 211.

Chapter 2



Scheme 2.1. Addition of ligands to tetracarbonyldichlororhodium.

In the crystalline state some of these compounds display dichroic properties¹⁶, suggesting the presence of a chain of weak metal-metal interactions such as have been reported previously in other d^8 systems¹⁷. The colors of these compounds in the solid state vary with the nature of the substituents on the coordinated β -diketone as well as with the transition metal, but are orange-red for rhodium. Acetylacetonatodicarbonylrhodium(I) crystallizes as elongated plates displaying an orange-green dichroism¹⁸. The geometry around the rhodium atom in dicarbonyl rhodium(I) complexes is square planar with possible slight displacement of the rhodium out of the plane, albeit with some exceptions¹⁹.

Dicarbonyl rhodium complexes have been studied extensively in the past and are a popular subject of investigation due to their vast application potential in, among others, catalysis²⁰, metal containing polymers²¹, C-H activation²² and bioinorganic support²³, with the donor atoms in the bidentate ligands comprising of a combination of carbon, oxygen, nitrogen, sulfur or phosphorus¹⁹. Crystal structures of complexes of the type $[\text{Rh}(\text{N,O-bid})(\text{CO})_2]$ are surprisingly limited though²⁴, while a few complexes employ diketonato ligands. $[\text{Rh}(\text{L,L}'\text{-bid})(\text{CO})_2]$ complexes adopt a square planar geometry, stabilized by a bite angle of $\sim 90^\circ$ with the chelating

¹⁶ Bailey, N.A.; Coates, E.; Robertson, G.B.; Bonati, F.; Ugo, R. *Chem. Commun.* **1967**, 1041.

¹⁷ a) Lewis, J.; Nyholm, R.S. *Sci. Progr.* **1964**, 52, 557.

b) Augoletta, M. *Gazzetta* **1959**, 89, 2359.

¹⁸ Huq, F.; Skapski, A.C. *J. Cryst. Mol. Struct.* **1974**, 4, 411.

¹⁹ Allen, F.H. The Cambridge Structural Database Version 1.9, *Acta Cryst.* **2002**, B58, 380.

²⁰ a) Rojas, S.; Garcia Fierro, J.L.; Fandos, R.; Rodriguez, A.; Terreros, P. *J. Chem. Soc., Dalton Trans.* **2001**, 2316.

b) Steyl, G.; Kruger, G.J.; Roodt, A. *Acta Cryst.* **2004**, C60, m473.

²¹ Hagadorn, J.R.; Arnold, J. *J. Organomet. Chem.* **2001**, 637, 521.

²² Gandelman, M.; Shimon, L.J.W.; Milstein, D. *Chem. Eur. J.* **2003**, 9, 4295.

²³ Green, K.N.; Jeffery, S.P.; Reibenspies, J.H.; Darensbourg, M.Y. *J. Am. Chem. Soc.* **2006**, 128, 6493.

²⁴ a) Gutierrez-Puebla, E.; Heras, J.V.; Monge, A.; Pinilla, E.; Rodrigues-Roldan, A.; Salvador, J.M. *Eur. Cryst. Meeting* **1985**, 9, 178.

b) Gopinathan, S.; Pardhy, S.A.; Gopinathan, C.; Puranik, V.G.; Tavale, S.S.; Row, T.N.G. *Inorg. Chim. Acta* **1986**, 111, 133.

c) Varshavsky, Y.S.; Galding, M.R.; Cherkasova, T.G.; Podkorytov, I.S.; Nikol'skii, A.B.; Trzeciak, A.M.; Olejnik, Z.; Lis, T.; Ziolkowski, J.J. *J. Organomet. Chem.* **2001**, 628, 195.

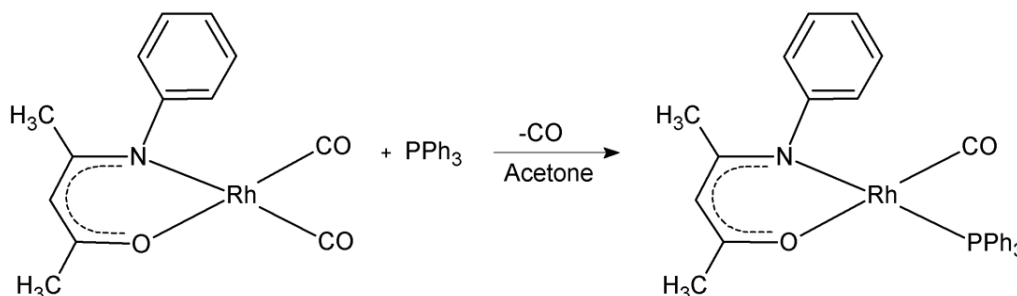
d) Doedens, R.J. *Inorg. Chem.* **1978**, 17, 1315.

Chapter 2

ligand²⁵. This is true even for very bulky ligands²⁶ as long as the criterion for the bite angle is met, with distortion of the ligand from its ideal geometry sometimes taking place to accommodate the geometry around the rhodium atom²⁷. The majority of dicarbonyl L,L'-bidentate rhodium complexes pack in a head-to-tail fashion, in other words the L,L'-bidentate ligand pack next to the carbonyl ligands of the adjacent molecules. While the bite angles appear to be larger when rhodium coordinates to more electron donating ligands, the steric properties of the ligands also play an important role in the geometric parameters of such complexes (see Chapter 6).

2.2.3 Carbonyl Tertiary Phosphine Rhodium(I) Complexes

In most CO-containing molecules, one or more CO groups can be substituted by a PX_3 or similar type of ligand. $[Rh^I(N,O-Bid)(CO)_2]$ complexes (where N,O-Bid = 4-(phenyl-amino)pent-3-en-2-one derivatives) react with PX_3 to form $[Rh(N,O-Bid)(CO)(PX_3)]$. The reaction between $[Rh(Phony)(CO)_2]$ and PPh_3 to form $[Rh(Phony)(CO)(PPh_3)]$ is shown in Scheme 2.2.



Scheme 2.2. Formation of $[Rh(Phony)(CO)(PPh_3)]$.

It has been shown²⁸ that in these substitution reactions only one carbonyl group is substituted by PX_3 , and in the case of asymmetric bidentate ligands (such as PhonyH), the product can be one of two possible isomers. However, it may be assumed that the final product will form with the PX_3 ligand situated *trans* to the donor atom with the largest *trans*-influence²⁹. In general, the most electronegative atom has the smallest *trans*-influence¹³ and in the case of β -diketones, this

²⁵ Van Leeuwen, P.W.N.M.; Kamer, P.C.J.; Reek, J.N.H. *Pure Appl. Chem.* **1999**, 71, 1443.

²⁶ Broussier, R.; Laly, M.; Perron, P.; Gautheron, B.; Nifant'ev, I.E.; Howard, J.A.K.; Kuz'mina, L.G.; Kalck, P. *J. Organomet. Chem.* **1999**, 587, 104.

²⁷ Mori, S.; Osuka, A. *Inorg. Chem.* **2008**, 47, 3937.

²⁸ Bonati, F.; Wilkinson, G. *J. Chem. Soc.* **1964**, 3156.

²⁹ Leipoldt, J.G.; Basson, S.S.; Grobler, E.C.; Roodt, A. *Inorg. Chim. Acta* **1985**, 99, 13.

Chapter 2

would be the oxygen atom nearest the strongest electron withdrawing substituent. This is in agreement with the polarization theory and the δ -*trans* effect, since the oxygen atom nearest to the more electron withdrawing group will be least polarizable and a weaker δ -donor. X-ray structural studies³⁰ have shown that for asymmetric bidentate ligands with different donor atoms, the *trans*-influence for oxygen, nitrogen and sulfur follows the reverse electronegativity range $S > N > O$.

The significant σ -donor ability and steric requirements of phosphine ligands is also important with regard to the structures of $[M(CO)_x(PX_3)_y]$ ($M = Rh, Ir, \text{etc.}$) type molecules. The electronic effect of tertiary aryl phosphines on a metal center can be described by the carbonyl stretching frequencies *trans* to the tertiary phosphine in square planar complexes³¹, known as the Tolman electronic parameter. Comparison of ν_{CO} gives an indication of the electronic influence of PX_3 , since a decrease in electron donating capability of the substituents on the tertiary phosphine leads to an increase in the CO stretching frequencies. This implies that an increase in ν_{CO} means less π -bond stabilization in the M-C moiety, caused by the decrease in metal-ligand $d \rightarrow \pi^*$ back donation due to the decrease in electron density on the metal center³².

The steric influence of tertiary phosphines can be expressed by the cone angle, θ_E , defined by Tolman³¹. For a symmetrical phosphine, this angle is defined as the tip of a cylindrical cone centered 2.28 Å from the center of the phosphorous atom, touching the Van der Waals radii of the outermost atoms in the phosphine model (Figure 2.2).

³⁰ a) Graham, D.E.; Lamprecht, G.J.; Potgieter, I.M.; Roodt, A.; Leipoldt, J.G. *Transition Met. Chem.* **1991**, *16*, 193.

b) Steyn, G.J.J.; Roodt, A.; Poetaeva, I.; Varshavsky, Y.S. *J. Organomet. Chem.* **1997**, *536/537*, 197.

c) Botha, L.J.; Basson, S.S.; Leipoldt, J.G. *Inorg. Chim. Acta* **1987**, *126*, 25.

³¹ Tolman, C.A. *J. Am. Chem. Soc.* **1970**, *92*, 2953.

³² a) Brink, A.; Roodt, A.; Steyl, G.; Visser, H.G. *Dalton Trans.* **2010**, *39*, 5572.

b) Muller, A.; Otto, S.; Roodt, A. *Dalton Trans.* **2008**, 650.

c) Roodt, A.; Otto, S.; Steyl, G. *Coord. Chem. Rev.* **2003**, *245*, 121.

Chapter 2

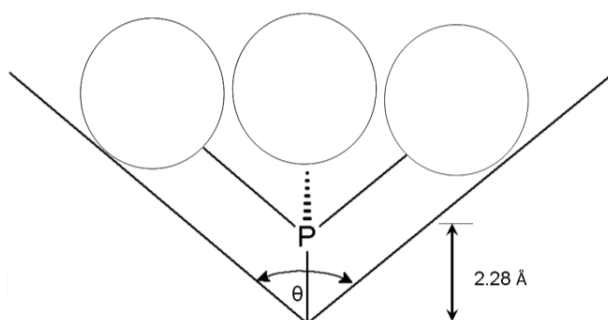


Figure 2.2. The cone angle (θ) for a symmetrical monodentate tertiary phosphine.

In the case of an asymmetrical phosphine ligand, $PX_1X_2X_3$ ($X_1 \neq X_2 \neq X_3$), the angle can be calculated by using a model which minimizes the sum of the cone half angles as seen in Figure 2.3, using Equation 2.1.

$$\theta = \frac{2}{3} \sum_{i=1}^3 \frac{\theta_i}{2}$$

Eq. 2.1

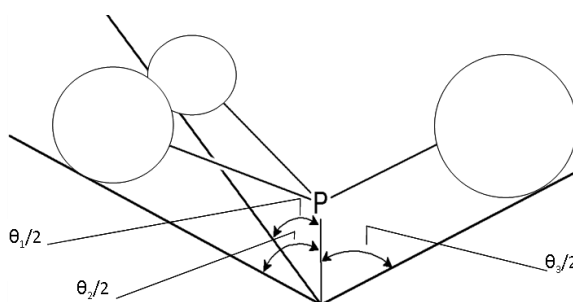


Figure 2.3. An illustration of the measurements needed for the calculation of the Tolman cone angle (θ) of an asymmetrical monodentate tertiary phosphine.

The calculation of the effective cone angle, θ_E , is based on the Tolman cone angle, with the specific metal-phosphorous distance being used as obtained from crystallographic data of the complex.

The application of carbonyl complexes of rhodium when combined with P-donor groups in basic catalytic reactions and related systems have been described previously³³. As with dicarbonyl

³³ a) Crous, R.; Datt, M.; Foster, D.; Bennie, L.; Steenkamp, C.; Huyser, J.; Kirsten, L.; Steyl, G.; Roodt, A. *Dalton Trans.* **2005**, 1108.

b) Purcell, W.; Basson, S.S.; Leipoldt, J.G.; Roodt, A.; Preston, H. *Inorg. Chim. Acta* **1995**, 234, 153.

c) Roodt, A.; Visser, H.G.; Brink, A. *Crystallogr. Rev.* **2011**, 17, 241.

d) Damoense, L.J.; Purcell, W.; Roodt, A. *Rhodium Express* **1995**, 4-14.

Chapter 2

rhodium complexes (§ 2.2.2.), carbonyl phosphine rhodium(I) complexes adopt a square planar geometry around the rhodium central atom. In $[\text{Rh}(\text{N},\text{O}\text{-Bid})(\text{CO})(\text{PPh}_3)]$ complexes an effective overlap between the π -orbital of the nitrogen atom and the d_π -orbital orbitals of the rhodium atom can be observed from the relatively longer Rh-P bond distance when compared to $[\text{Rh}(\text{O},\text{O}\text{-Bid})(\text{CO})(\text{PPh}_3)]$ complexes³⁴. The presence of free phosphine can cause labilization of the coordination sphere, followed by fast exchange between the coordinated and the free phosphine³⁵, possibly through a $\text{S}_{\text{N}}2$ mechanism which is possible with four-coordinate d^8 -metal complexes³⁶. Exchange reactions or substitution reactions play a fundamental role in many catalytic processes as well as synthetic routes.

2.3 Homogenously Catalysed Industrial Processes

2.3.1 Introduction

Catalysis plays an important role in producing liquid fuels and bulk chemicals. Heterogeneous catalysis is preferred for oil processes, with the exception of alkylation reaction for which liquid acids are used³⁷. For the production of fine chemicals a variety of sophisticated homogeneous catalysts are being employed, while both homogeneous and heterogeneous catalysts are used for the conversion of petrochemicals.

Homogeneous catalysis, by definition, implicates a catalytic system where the catalyst and reaction substrates are combined in one phase, most often as a liquid. Recently another definition has surfaced, where homogeneous catalysis involves metallic or organometallic complexes as catalysts. However, several reactions employing homogeneous catalysis do not necessarily involve organometallic complexes. Ligand effects are extremely important in homogeneous catalysis by metal complexes, since one metal can give a variety of products from one single substrate simply by changing the ligands around the metal centre. When allylnickel(II) complexes are used as catalysts, polymers are obtained while nickel(0) as the

e) Damoense, L.J.; Purcell, W.; Roodt, A.; Leipoldt, J.G. *Rhodium Express* **1994**, 10-4.

³⁴ a) Leipoldt, J.G.; Basson, S.S.; Bok, L.D.C.; Gerber, T.I.A. *Inorg. Chim. Acta* **1978**, 26, L35.

b) Lamprecht, D.; Lamprecht, G.J.; Botha, J.M.; Umakoshi, K.; Sasaki, Y. *Acta Cryst.* **1997**, C53, 1403.

³⁵ Trzeciak, A.M.; Ziółkowski, J.J. *Inorg. Chim. Acta* **1985**, 96, 15.

³⁶ Deeming, A.J.; Shaw, B.L. *J. Chem. Soc. A, Inorg. Phys. Theor.* **1969**, 597.

³⁷ Van Leeuwen, P.W.N.M. *Homogeneous Catalysis: Understanding the Art*, Kluwer Academic Publishers, Dordrecht, **2004**.

Chapter 2

catalyst precursor produces cyclic dimers and the all-*trans*-trimer. Linear dimerisation requires the presence of protic species.

2.3.2 Rhodium in Homogeneous Catalysis

The first interest in rhodium as catalyst was sparked by a report on the use of phosphines in a cobalt catalyzed process, in which preliminary data for the use of rhodium was included³⁸. This led to the application of phosphine ligands in rhodium catalyzed processes by many industries³⁹. The first ligand-modified process using rhodium catalysts came on line in 1974 (Celanese), followed by the Union Carbide Corporation in 1976⁴⁰ and the Mitsubishi Chemical Corporation in 1978, all using triphenylphosphine. A well-known catalyst in homogenous hydrogenation is Wilkinson's catalyst⁴¹, chlorotris(triphenylphosphine)rhodium(I). Rhodium catalysts are generally faster and therefore utilize milder reaction conditions than cobalt catalysts, and also have better feedstock utilization. Since the mid-seventies cobalt catalysts were replaced by rhodium catalysts in propene and butene hydroformylation. The production of detergent alcohol is an exception though, since no good alternative has yet been found to replace cobalt in the hydroformylation of internal higher alkenes to mainly linear products. The well-known mechanism of hydroformylation of ethene was first proposed by Heck⁴² and is depicted in Figure 2.4.

³⁸ Slauch, L.H.; Mullineaux, R.D. US. Pat. 3,239,569 and 3,239,570 **1996** (to Shell); *J. Organomet. Chem.*, **1968**, *13*, 469.

³⁹ Onoda, T. *ChemTech.* **1993**, 34.

⁴⁰ a) Parshall, G.W.; Ittel, S.D. *Homogeneous Catalysis*, 2nd Ed.; Wiley: New York, **1992**.

b) Cornils, B.; Herrmann, W.A. (Eds.), *Applied Homogeneous Catalysis with Organometallic Compounds. A Comprehensive Handbook*, VCH, Weinheim, **1996** (in two volumes).

⁴¹ Osborn, J. A.; Jardine, F. H.; Young, J. A.; Wilkinson, G. *J. Chem. Soc. A* **1966**, 1711.

⁴² Heck, R.F. *Acc. Chem. Res.* **1968**, *2*, 10.

Chapter 2

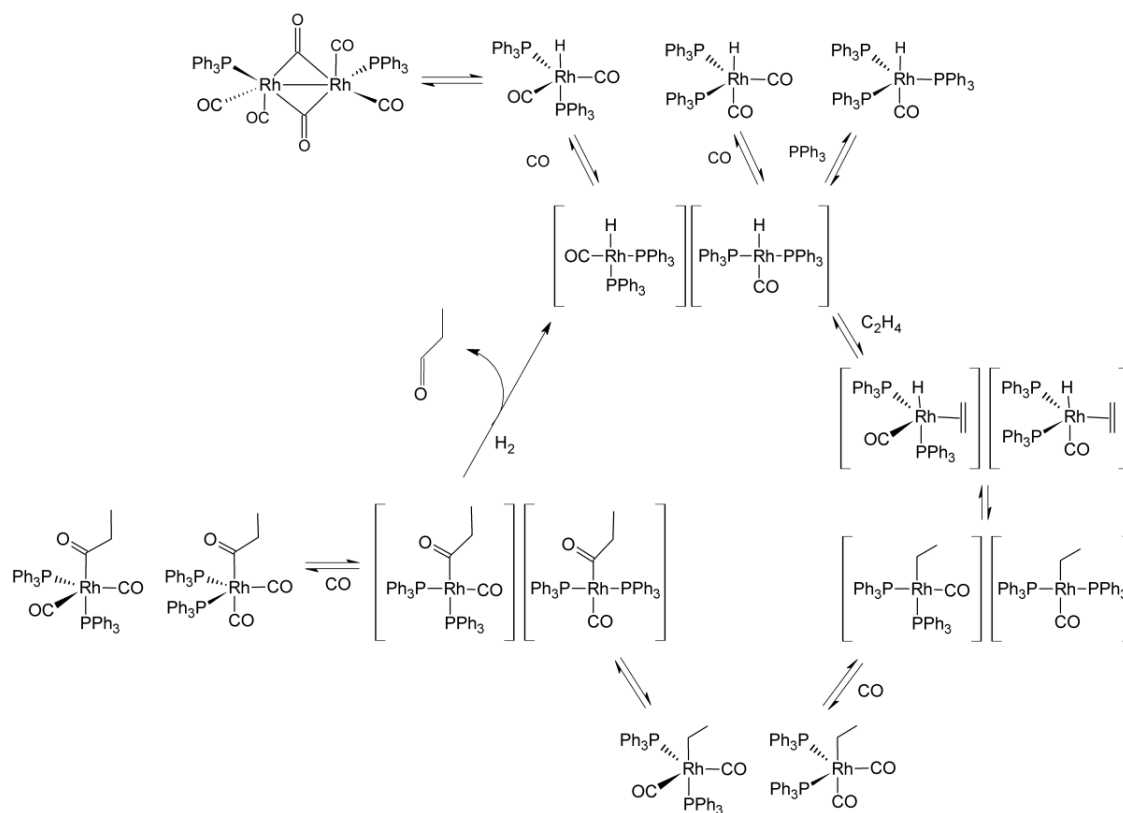


Figure 2.4. Simplified mechanism for hydroformylation of ethene as described by Heck⁴².

This corresponds to the dissociative mechanism described by Wilkinson⁴³. Although the complexes shown in Figure 2.4 include a minimum of two PPh_3 ligands, the equilibria of catalytically active species containing a single coordinated phosphine ligand play an active role in catalysis.

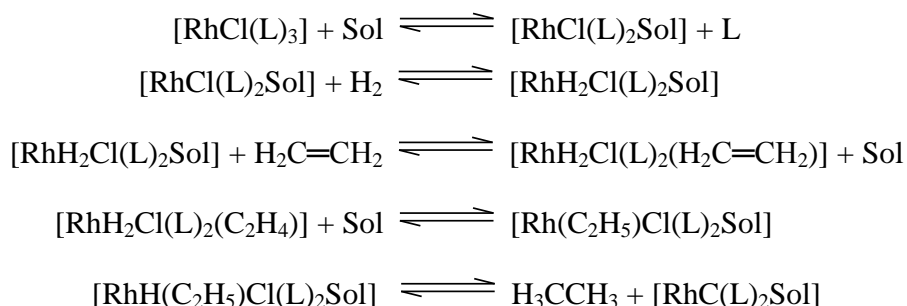
Wilkinson's catalyst, $[\text{RhCl}(\text{PPh}_3)_3]$, is well-known for its use in homogenous hydrogenation. Discovered in the sixties⁴¹, the reaction mechanism has been extensively studied. The commonly accepted reaction sequence is shown in Scheme 2.3:

⁴³ a) Young, J.F.; Osborn, J.A.; Jardine, F.A.; Wilkinson, G. *J. Chem. Soc. Chem. Commun.* **1965**, 131.

b) Evans, D.; Yagupsky, G.; Wilkinson, G. *J. Chem. Soc. A* **1968**, 2660.

c) Evans, D.; Osborn, J.A.; Wilkinson, G. *J. Chem. Soc. A* **1968**, 3133.

Chapter 2



Scheme 2.3. Reaction sequence for homogeneous hydrogenation of ethene.

In this scheme L symbolizes triarylphosphines and Sol represents the solvents ethanol and toluene. The first step involves the dissociation of one ligand L and the subsequent replacement thereof by a solvent molecule. Ligand dissociation is followed by oxidative addition of hydrogen, which occurs in *cis* fashion which can be promoted by the substitution of more electron rich phosphines on the rhodium complex. After substitution of the solvent with ethene, the hydride migrates to form the ethyl group. Reductive elimination of ethane completes the cycle, and the rate of this step can be improved by employing electron withdrawing ligands. Strong donor ligands, on the other hand, stabilizes the trivalent rhodium(III) chloride dihydride to such an extent that the complexes are no longer active. Some species have been observed in solution in addition to those shown in Scheme 2.3, for instance the dimers $[\text{RhCl}(\text{PPh}_3)]_2$, $[\text{RhCl}(\text{PPh}_3)_2(\text{olefin})]$ and dimers containing hydrides, to name a few. This indicates that the species actually observed may have little to do with the catalytic cycle. Conversely, few of the species mentioned in Scheme 2.3 can be observed and their existence is only known from the kinetic studies since the actual concentrations are below NMR detection level during the catalysis⁴⁴. Since knowledge of the effect of ligands on the reactivity of catalysts are limited⁴⁵, explaining the effect of electronic parameters of ligands require a careful study of all systems.

2.3.3 The Monsanto Process⁵

Carbonylation, the process of converting methanol to methyl acetate, was first performed in the 1940's. This method employed iodide-promoted cobalt salts as catalyst precursors and required

⁴⁴ a) Halpern, J.; Okamoto, T.; Zakhariiev, A. *J. Mol. Catal.* **1976**, *2*, 65.

b) Halpern, J.; Wong, C.S. *J. Chem. Soc. Chem. Commun.* **1973**, 629.

⁴⁵ O'Connor, C.; Wilkinson, G. *Tetrahedron Lett.* **1969**, *10*, 1375.

Chapter 2

very high pressures (600 bar) as well as high temperatures (230°C). In 1966 this method was improved by using rhodium, called the Monsanto process (Figure 2.5), which operates at 30-60 bar and 150-200°C.

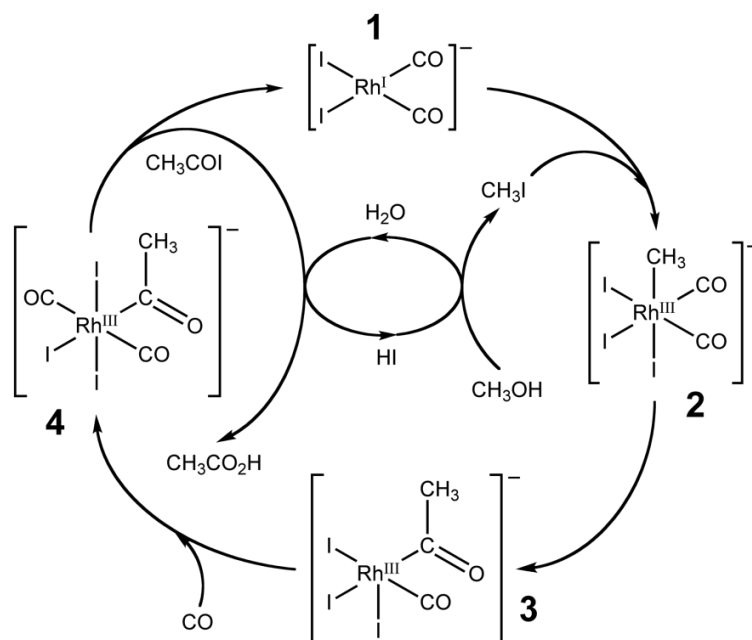


Figure 2.5. Simplified cycle for the rhodium catalyzed carbonylation of methanol; the Monsanto process⁵. The rate-limiting step is the addition of iodomethane to **1**⁴⁶.

In this process, two cycles are coupled with each other: (a) the iodide cycle, where iodide is converted to methanol and acetyl iodide to acetic acid; and (b) the main carbonylation cycle. The rate limiting step is the oxidative addition of MeI to $[\text{Rh}(\text{CO})_2\text{I}]^-$ (**1**), to give the aryl group (**2**). (**2**) is an unstable transition group that is usually observed in situ by infrared spectroscopy⁴⁶. Fast migration of the aryl group to the CO gives the acyl group (**3**). The monocarbonyl (**3**) decomposes by MeI elimination rather than MeCOI elimination, but the latter process is accelerated in the presence of excess CO to reform (**1**) with (**4**) as intermediate.

The key feature of this process is the presence of iodide in the cycle. Some water, present in the methanol feedstream, is also produced by the reaction in Equation 2.2:



⁴⁶ Maitlis, P.M.; Haynes, A.; Sunley, G.J.; Howard, M.J. *J. Chem. Soc., Dalton Trans.* **1996**, 2187.

Chapter 2

Water levels play a vital role as well; the use of very dry methanol leads to carbonylation of $\text{CH}_3\text{COOCH}_3$ to acetic anhydride.

2.3.4 The Cativa Process

Another well-known process in the carbonylation of methanol to acetic acid is the Cativa process, which differs from the Monsanto process in that iridium complexes are utilized instead of rhodium. Due to the limits on the water, methyl acetate, methyl iodide and rhodium concentrations and CO partial pressure imposed in the Monsanto process as well as the price difference between rhodium and iridium, research by British Petroleum (BP) on the Cativa process resumed in 1990⁴⁷. The anionic iridium cycle is similar to the rhodium cycle and is shown in Figure 2.6.

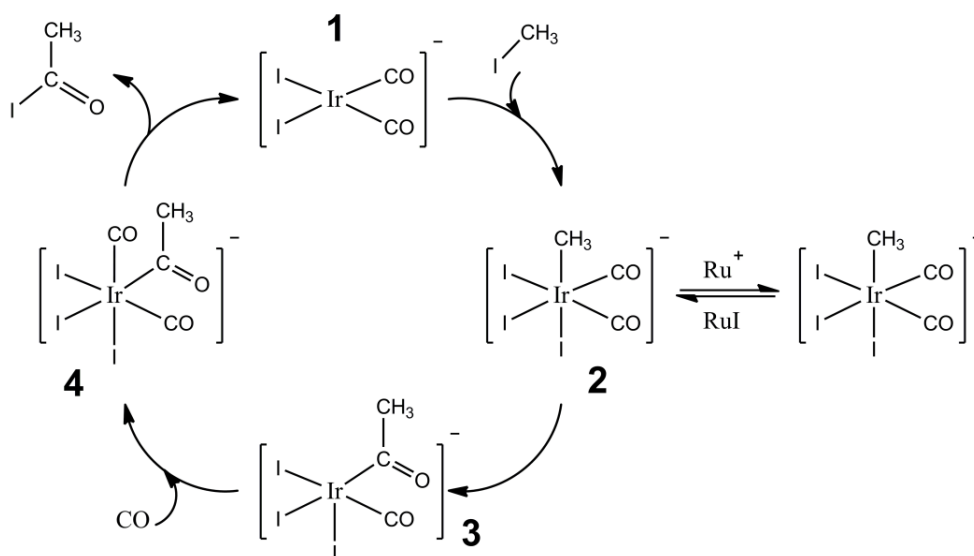


Figure 2.6. Simplified cycle for BP's Cativa process³⁷.

In the Cativa process the oxidative addition to iridium (step 1) is much faster than to the corresponding rhodium complex⁴⁸ and therefore not the limiting step. Instead, the subsequent migratory insertion of CO to form the iridium-acyl species (3) is the slowest step⁴⁹, making the

⁴⁷ Jones, J.H. *Platin. Met. Rev.* **2000**, *44*, 94.

⁴⁸ a) Ellis, P.R.; Pearson, J.M.; Haynes, A.; Adams, H.; Bailey, N.A.; Maitlis, P.M. *Organometallics* **1994**, *13*, 3215.

b) Griffin, T.R.; Cook, D.B.; Haynes, A.; Pearson, J.M.; Monti, D.; Morris, G.E. *J. Am. Chem. Soc.* **1996**, *118*, 3029.

⁴⁹ a) Sunley, G.J.; Watson, D.J. *Catal. Today* **2000**, *58*, 293.

Chapter 2

product of methyl iodide oxidative addition to the iridium(I) iodide complex (2) the most abundant iridium species. A full discussion of the Cativa process can be found in literature⁴⁷.

2.3.5 Oxidative Addition

Oxidative addition / reductive elimination processes are of great importance in a vast range of synthetically useful organometallic reactions and have been studied extensively^{32,50}. Oxidative addition can be generalized by Equation 2.3:



Oxidative addition requires the following conditions⁵:

- A non-bonding electron pair on the metal.
- Two vacant sites on the coordinatively unsaturated complex for accommodation of the incoming ligands.
- A M^{n+2} oxidation state which is energetically accessible and stable, since the process involves the oxidation of the metal by two units, from M^n to M^{n+2} .

Oxidative addition reactions can be generalized as the addition of molecules to coordinatively unsaturated d^8 or d^{10} transition metal complexes where the metal complex concurrently acts as Lewis acid and Lewis base. Square-planar 16-electron complexes of d^8 metals, containing two vacant sites, give octahedral 18-electron products after oxidative addition. Small covalent molecules H-X, C-X, H-H, C-H, C-C, etc. (X = halogen) can add to low oxidation state transition metal complexes, increasing both the coordination number and the oxidation number of the metal by two units⁵¹. These reactions can take two possible courses:

b) Ghaffar, T.; Charmant, J.P.H.; Sunley, G.J.; Morris, G.E.; Haynes, A.; Maitlis, P.M. *Inorg. Chem. Commun.* **2000**, 3, 11.

⁵⁰ a) Venter, J.A.; Leipoldt, J.G.; Van Eldik, R. *Inorg. Chem.* **1991**, 30, 2207.

b) Steyn, G.J.J.; Roodt, A.; Leipoldt, J.G. *Inorg. Chem.* **1992**, 31, 3477.

c) Parshall, G.W.; Mrowca, J.J. *Adv. Organomet. Chem.* **1968**, 7, 157.

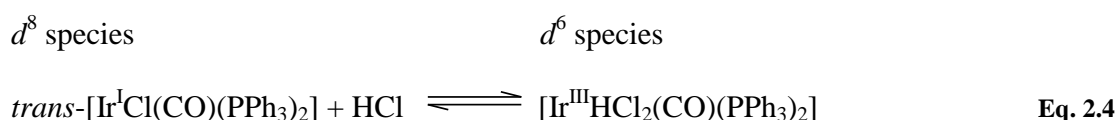
d) Van Koten, G.; Terheijden, J.; Van Beek, J.A.M.; Wehman-Ooyevaar, I.C.M.; Muller, F.; Stam, C.H. *Organometallics* **1990**, 9, 903.

e) Basson, S.S.; Leipoldt, J.G.; Roodt, A.; Venter, J.A. *Inorg. Chim. Acta* **1987**, 128, 31.

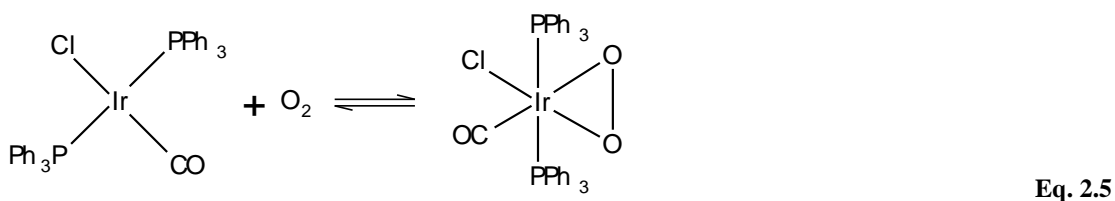
⁵¹ Koga, N.; Morokama, K. *Chem. Rev.* **1991**, 91, 823.

Chapter 2

1. Molecules that are added split into two η^1 -ligands; both are formally anionically bound to the metal center e.g. the central atom in the square-planar iridium complex gives up two electrons and is oxidized to Ir(III) (Equation 2.4).



2. Added molecules contain multiple bonds that are bound as η^2 -ligands without bond cleavage, resulting in a three-member ring system (Equation 2.5).



Oxidative addition is the initiating step for many catalytic carbonylation reactions, for example C-X (where X = halogen) addition to a rhodium(I) complex. The addition rate of these halogenated ligands to rhodium(I) complexes can be arranged in the order of C-I > C-Br >> C-Cl >>> C-F. Considering the bond energy of the halogenated ligands, they show a bond energy increase in the same order.

Coordinated ligands are of prime importance to oxidative addition reactions. An increase in σ -donor capability increases the electron density at the metal center and favors oxidative addition. Therefore electron donating (basic) ligands increase the metal ligand bonds strength while electron withdrawing (stronger π -acceptor) ligands weaken the metal ligand bonds.

The ligand steric effects should also be taken into consideration when a low reaction rate is observed, for example the strongly basic bulky ligand tris-*tert*-butylphosphine. Solvent effects cannot be ignored and it has been concluded⁵² that hydrogen bond formation may have an important role in the reaction rate of oxidative addition. Polar solvents like acetone are less capable of hydrogen bond formation and decrease the reaction rate. On the other hand ions in a reaction solution can coordinate to the metal center and enhance the reaction rate⁵³.

⁵² Parker, A.J. *Chem. Rev.* **1969**, 69, 1.

⁵³ a) Hichy, C.E.; Maitlis, P.M. *J. Chem. Soc. Chem. Comm.* **1984**, 1609.

b) Basson, S.S.; Leipold, J.G.; Roodt, A.; Venter, J.A. *Inorg Chim Acta.* **1987**, 128, 31.

2.4 Nitrogen-Containing Complexes

A well-known system in organometallic chemistry is the β -diketone compound AcacH (acetylacetonate). A multitude of derivatives have been synthesized to date, including nitrogen substituted versions known as enaminoketones, or α,β -unsaturated- β -ketoamines. Such nitrogen-containing compounds have enjoyed the interest of scientists over the span of many years with the earliest reports dating back as far as the 1880's⁵⁴, followed by renewed attention in the mid-20th century⁵⁵. Following the isolation of N-heterocyclic carbenes (NHC's) in 1991⁵⁶ and determination of their role in industrial processes⁵⁷, a focus was placed anew on nitrogen-containing compounds as ligand systems. One of the first examples of compounds containing electron donating nitrogen atoms used as a ligand is the complex tris(1,2-diaminocyclopentane)rhodium triperchlorate dodecahydrate, synthesized in 1928⁵⁸.

Reports of bidentate N,O-complexes cover a wide range of metals, including palladium⁵⁹, platinum⁶⁰, gold⁶¹, rhenium⁶², ruthenium⁶³ and rhodium⁶⁴, which constitute metals commonly used in catalysis. Compounds containing a nitrogen and an oxygen atom as well as an unsaturated carbon-carbon bond are known as enaminoketones (lesser name ketoamines). Since

⁵⁴ a) Combes, A.; Combes, C. *Compt. Rend.* **1889**, 108, 1252.

b) Combes, A.; Combes, C. *Bull. Soc. Chim. France* **1892**, 3, 778.

⁵⁵ a) McCarthy P.J.; Martell, A.E. *J. Am. Chem. Soc.* **1957**, 79, 264.

b) Holtzclaw, H.F.; Colmann, J.P.; Aire, R.M. *J. Am. Chem. Soc.* **1958**, 80, 1100.

⁵⁶ Arduengo, A.; Harlow, R.; Kline, M. *J. Am. Chem. Soc.* **1991**, 113, 361.

⁵⁷ a) Stetter, H. *Angew. Chem. Int. Ed.* **1976**, 15, 639.

b) Murry, J.; Frantz, D.; Soheili, A.; Tillyer, R.; Grabowski, E.; Reider, P. *J. Am. Chem. Soc.* **2001**, 123, 9696.

c) Frantz, D.; Morency, L.; Soheili, A.; Murry, J.; Grabowski, E.; Tillyer, R. *Org. Lett.* **2004**, 6, 843.

⁵⁸ Jaeger, F.M.; Blumendal, H.B. *Z. Anorg. Allg. Chem.* **1928**, 175, 161.

⁵⁹ a) Zharkova, G.I.; Baidina, I.A.; Igumenov, I.K. *Zh. Strukt. Khim. (Russ.) (J. Struct. Chem.)* **2008**, 49, 322.

b) Budzisz, E.; Malecka, M.; Lorenz, I.-P.; Mayer, P.; Kwiecien, R.A.; Paneth, P.; Krajewska, U.; Rozalski, M. *Inorg. Chem.* **2006**, 45, 9688.

c) Mikuriya, M.; Minowa, K.; Lim, J.-W. *Bull. Chem. Soc. Jpn.* **2001**, 74, 331.

⁶⁰ a) Crowley, J.D.; Goshe, A.J.; Steele, I.M.; Bosnich, B. *Chem. -Eur. J.* **2004**, 10, 1944.

b) Bermejo, E.; Castineiras, A.; Garcia-Santos, I.; Gomez-Rodriguez, L.; Sevillano, P. *Z. Anorg. Allg. Chem.* **2007**, 633, 2255.

⁶¹ Zharkova, G.I.; Baidina, I.A.; Igumenov, I.K. *Zh. Strukt. Khim. (Russ.) (J. Struct. Chem.)* **2007**, 48, 963.

⁶² Doney, J.J.; Bergman, R.G.; Heathcock, C.H. *J. Am. Chem. Soc.* **1985**, 107, 3724.

⁶³ a) Chou, T.-Y.; Lai, Y.-H.; Chen, Y.-L.; Chi, Y.; Prasad, K.R.; Carty, A.J.; Peng, S.-M.; Lee, G.-H. *Chem. Vap. Deposition* **2004**, 10, 149.

b) Hashimoto, T.; Hara, S.; Shiraishi, Y.; Natarajan, K.; Shimizu, K. *Chem. Lett.* **2003**, 32, 874.

c) Trivedi, M.; Chandra, M.; Pandey, D.S.; Puerta, M.C. Valerga, P. *J. Organomet. Chem.* **2004**, 689, 879.

d) Wilton-Ely, J.D.E.T.; Wang, M.; Honarkhah, S.J.; Tocher, D.A. *Inorg. Chim. Acta* **2005**, 358, 3218.

⁶⁴ a) Damoense, L.J.; Purcell, W.; Roodt, A. *Rhodium Express* **1994**, 10-5.

b) Damoense, L.J.; Purcell, W.; Roodt, A. *Rhodium Express* **1995**, 4-14.

Chapter 2

enaminoketones contain nitrogen and oxygen atoms as well as alkene functionality, these electron rich compounds are of interest in various fields including liquid crystals⁶⁵, fluorescence studies⁶⁶ as well as medical applications⁶⁷. It also has significant application possibilities in catalysis⁶⁸. An example of an enaminoketone is 4-(phenylamino)pent-3-en-2-one (PhonyH)⁶⁹, shown in Figure 2.7. Three tautomeric forms have been identified and are illustrated in Figure 2.8.

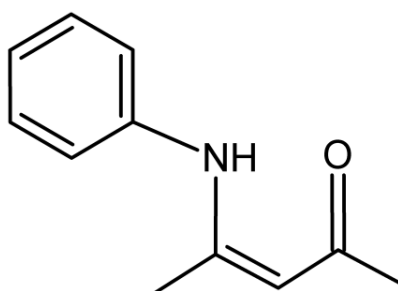


Figure 2.7. Unsubstituted 4-(phenylamino)pent-3-en-2-one (PhonyH).

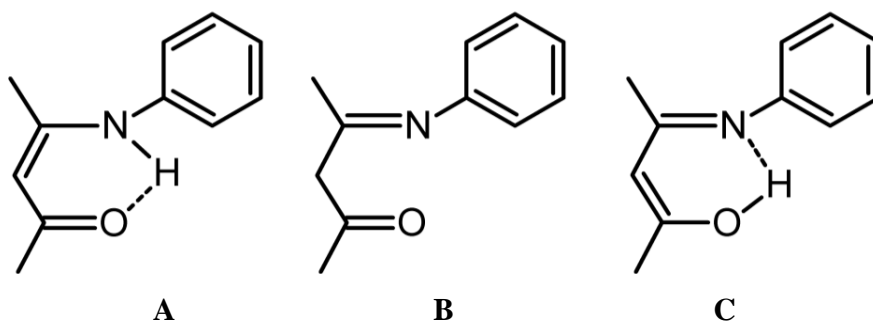


Figure 2.8. Tautomeric forms of enaminoketones.

The presence of form B has been ruled out by infrared spectroscopy due to the absence of a peak at 1700 cm^{-1} for a free carbonyl peak⁷⁰, while evidence has been found to validate the presence

⁶⁵ Pyżuk, W.; Krówczyński, A.; Górecka, E. *Mol. Cryst. Liq. Cryst.* **1993**, 237, 75.

⁶⁶ Xia, M.; Wu, B.; Xiang, G. *J. Flu. Chem.* **2008**, 129, 402.

⁶⁷ a) Tan, H.Y.; Loke, W.K.; Tan, Y.T.; Nguyen, N.-T. *Lab Chip* **2008**, 8, 885.

b) Chen, H.; Rhodes, J. *J. Mol. Med.* **1996**, 74, 497.

⁶⁸ Nair, V.A.; Suni, M.M.; Sreekumar, K. *Proc. Indian Acad. Sci. (Chem. Sci.)* **2002**, 114, 481.

⁶⁹ Shaheen, F.; Marchio, L.; Badshaha, A.; Khosac, M.K. *Acta Cryst.* **2006**, E62, o873.

⁷⁰ a) Ueno, K.; Martell, A.E. *J. Phys. Chem.*, **1955**, 59, 998.

b) Ueno, K.; Martell, A.E. *J. Phys. Chem.*, **1957**, 61, 257.

Chapter 2

of form A⁷¹. This has been confirmed by X-Ray crystallography, DFT calculations and nuclear magnetic resonance spectroscopy (see Chapters 3, 4 and 5).

Enaminoketones fall into the chelating bidentate monoanionic ligands category in which (O,O), (O,N), (O,S), (N,N) or (N,S) donor atoms represent a group of compounds that have been studied extensively^{14,40,72}. Complexes containing these compounds as ligands have been studied as catalyst precursors in hydroformylation, isomerization and hydrogenation of olefins as well as model compounds in studies of the key stages of catalytic cycles. The typical coordination number for these complexes is four, but some examples of pentacoordinate complexes, [Rh(LL)(CO)(PZ₃)₂], have also been reported^{14,a,73}. The study of these compounds as ligand systems and the accompanying effect of different substituents on subsequent reactions, for example the oxidative addition of methyl iodide, might provide an insight into how model catalysts could be designed in the future.

2.5 Halogens

Halogens are ever-present in both inorganic and organic chemistry, serving as monodentate, bridging ligands or substituents in organic compounds. In supramolecular chemistry and crystal engineering, wherein the halogen atoms are directly involved in forming intermolecular interactions, the steric impact of halogens has potential applications⁷⁴. The “chloride effect”, which was first described by Schmidt⁷⁵, is of interest in packing arrangements of halogenated compounds. This effect involves the presence of chloride substituents in aromatic compounds which frequently result in stacking arrangements with a resultant short (*ca.* 4 Å) crystallographic

⁷¹ Cromwell, N.H.; Miller, F.A.; Johnson, A.R.; Frank, R.L.; Wallace, D.J. *J. Am. Chem. Soc.*, **1949**, *71*, 3337.

⁷² a) Darenbourg, D.J.; Draper, J.D. *Inorg. Chem.* **1998**, *37*, 5383.

b) Hill, A.F.; White, A.J.P.; Williams, D.J. Wilton-Ely, J.D.E.T. *Organometallics* **1998**, *17*, 4249.

c) Romero, A.; Vegas, A.; Santos, A.; Martinez-Ripoll, M. *J. Organomet. Chem.* **1987**, *319*, 103.

d) López, J.; Santos, A.; Romero, A.; Echavarren, A.M. *J. Organomet. Chem.* **1993**, *443*, 221.

e) Brookhart, M.; Johnson, L.K.; Ittel, S.D. *Chem.Rev.* **2000**, *100*, 1169.

⁷³ a) Da Silva, M.F.C.G.; Trzeciak, A.M.; Ziolkowski, J.J.; Pombeiro, A.J.L. *J. Organomet. Chem.* **2001**, *620*, 174.

b) Herras, J.V.; Cano, M.; Lobo, M.A.; Pinilla, E. *Polyhedron* **1989**, *8*, 167.

⁷⁴ a) Fox, D.B.; Liantonio, R.; Metrangolo, P.; Pilati, T.; Resnati, G. *J. Fluorine Chem.*, **2004**, *125*, 271.

b) Csöregi, I.; Brehmer, T.; Bombicz, P.; Weber, E. *Cryst. Eng.* **2001**, *4*, 343.

⁷⁵ a) Green, B.S.; Schmidt, G. M. J. *Israel Chemical Society annual meeting abstracts*, **1971**, 197.

b) Cohen, M. D.; Schmidt G.M.J.; Sonntag, F.I. *J. Chem. Soc.* **1964**, 2000.

c) Schmidt, G. M. J. *J. Chem. Soc.* **1964**, 2014.

Chapter 2

axis⁷⁶. A chloride...chloride contact can be represented by the geometric parameters (θ_1 , θ_2 and r_i) of the C-Cl₁...Cl₂-C moieties (where $\theta_1 = \text{C}_1\text{-Cl}_1\text{...Cl}_2$, $\theta_2 = \text{Cl}_1\text{...Cl}_2\text{-C}_2$ and $r_i = \text{Cl}_1\text{...Cl}_2$ distance)⁷⁷. Cl...Cl close contacts are classified into two categories; for Type I $\theta_1 \sim \theta_2$ and for Type II $\theta_1 \sim 90^\circ$ and $\theta_2 \sim 180^\circ$ ^{77.b}. The distance r_i is classified as 'close' when it is shorter than the sum of the van der Waals radii of the two chloride atoms, 3.5 Å (using the CSD standard van der Waals radius for Cl as 1.75 Å¹⁹). The same principal applies for other halogens⁷⁸.

The electronic effect of a halogen substituent attached to a π -electron system is generally considered to be a combination of inductive and resonance effects. The inductive effect is one of electron withdrawal, presumably in the electronegativity order: F > Cl > Br > I⁷⁹. For most systems, the halogens have an apparent net electron withdrawing effect. The inductive properties of halogens have been employed to promote selectivity in catalytic processes⁸⁰, as well as change the properties in dyes⁸¹ and fluorescent probes⁸². It was also noted that regularity in changes in the characteristics of compounds is related to the halogen electron affinities⁸³. Based on these factors, the influence of halides on the mechanistic behavior of complexes was selected as contributing factor in this investigation topic.

2.6 Conclusion

With the above-mentioned in mind, the crystal structures of the ligands and the [Rh(N,O-Bid)(CO)₂] and [Rh(N,O-Bid)(CO)(PPh₃)] complexes will be discussed in Chapters 4, 6 and 8, with specific focus on the effect of chloride-substitution on the phenyl moiety of the enaminoketone ligand. Chloride was chosen as it occupies the same space as a methyl group, serving to compare the electron withdrawing group with an electron donating group while reducing influence of the steric factor between the two groups. The optimized structures of the

⁷⁶ Desiraju, G.R. *Crystal Engineering: The Design of Organic Solids*; Elsevier: Amsterdam, **1989**.

⁷⁷ a) Desiraju, G.R.; Parthasarathy, R. *J. Am. Chem. Soc.* **1989**, *111*, 8725.

b) Awwadi, F. F.; Willett, R. D.; Peterson, K.A.; Twamley, B. *Chem. Eur. J.* **2006**, *12*, 8952.

⁷⁸ Steyl, G.; Roodt, A. *Acta Cryst.* **2003**, *C59*, o525.

⁷⁹ Schubert, W.M.; Craven, J.M.; Steadly, H. *J. Am. Chem. Soc.*, **1959**, *81*, 2695.

⁸⁰ a) Lambert, R.M.; Cropley, R.L.; Husain, A.; Tikhov, M.S. *Chem. Commun.* **2003**, 1184.

b) Campbell, C.T.; Koel, B.E. *Journal of Catalysis* **1985**, *92*, 272.

⁸¹ Slyusarevaa, E.A., Tomilina, F.N., Sizykha, A.G., Tankevicha, E.Y., Kuzubova, A.A., Ovchinnikova, S.G. *Opt. Spectrosc.* **2012**, *112*, 671.

⁸² a) Kirillova, T.N., Gerasimova, M.A., Nemtseva, E.V., Kudryasheva, N.S. *Anal. Bioanal. Chem.* **2011**, *400*, 343.

⁸³ Kharchenko, V.I., Alexeikoa, L.N., Penkovskyb, V.V., Pavlenkoa, S.A., Kashim, A.V. *J. Mol. Struct. Theochem* **1991**, *233*, 35.

Chapter 2

enaminoketone compounds and the $[\text{Rh}(\text{N,O-Bid})(\text{CO})_2]$ complexes will be discussed in Chapters 5 and 7, respectively. The focus of Chapter 9 will be the mechanistic study of phosphine exchange in $[\text{Rh}(\text{N,O-Bid})(\text{CO})(\text{PPh}_3)]$ complexes, since ligand exchange plays a vital role in the activity of complexes.

3 Experimental

3.1. Introduction

A range of 4-(phenylamino)pent-3-en-2-one (PhonyH) ligands were synthesized where the substituent on the phenyl moiety is systematically changed from one compound to the next. As mentioned in Chapter 2, chloride was chosen as substituent as the atom occupies the same space as a methyl group, serving to compare the electron withdrawing group with an electron donating group while reducing influence of the steric factor between the two groups. These compounds were then coordinated to rhodium to form complexes of the type $[\text{Rh}(\text{N},\text{O}\text{-Bid})(\text{CO})_2]$ and $[\text{Rh}(\text{N},\text{O}\text{-Bid})(\text{CO})(\text{PPh}_3)]$, where N,O-Bid = derivatives of 4-(phenylamino)pent-3-en-2-one, to investigate the structural effects of changes in the number and position of the substituents on the various complexes. The ligands are illustrated in Figure 3.1.

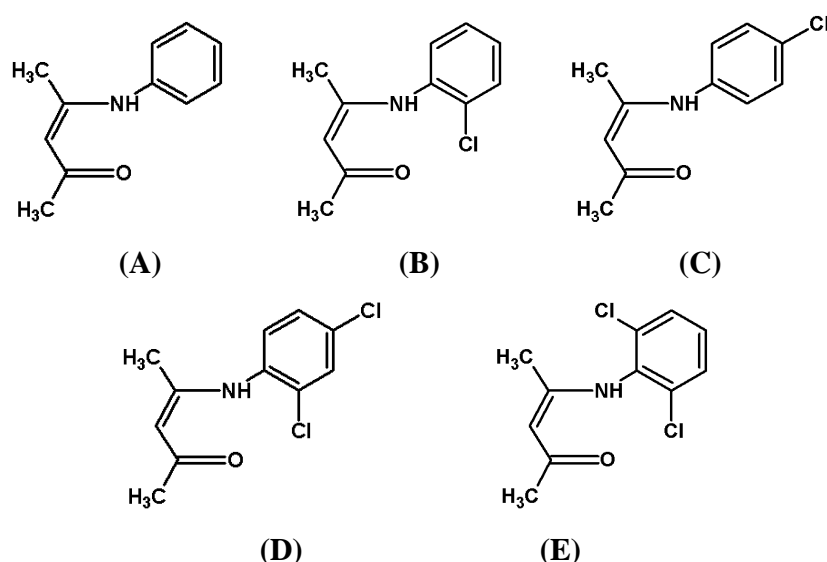


Figure 3.1. The 4-(phenylamino)pent-3-en-2-one (PhonyH) ligands synthesized, characterized and used in this study. (A) 4-(phenylamino)pent-3-en-2-one, PhonyH. (B) 4-(2-chlorophenylamino)pent-3-en-2-one, 2-Cl-PhonyH. (C) 4-(4-chlorophenylamino)pent-3-en-2-one, 4-Cl-PhonyH. (D) 4-(2,4-dichlorophenylamino)pent-3-en-2-one, 2,4-Cl₂-PhonyH. (E) 4-(phenylamino)pent-3-en-2-one, 2,6-Cl₂-PhonyH.

Chapter 3

The synthesis and characterization of the ligands will be discussed in this chapter, as well as synthesis and characterization for the [Rh(N,O-Bid)(CO)₂] and [Rh(N,O-Bid)(CO)(PPh₃)] complexes. Crystal data will be discussed in Chapters 4, 6 and 8.

3.2. Apparatus detail

3.2.1. Single-Crystal X-Ray Crystallography

The crystal data collection was done on a Bruker ApexII 4K CCD diffractometer using Mo $K\alpha$ (0.71073 Å) and ω -scans at 100(2) K. All reflections were merged and integrated with SAINT-PLUS¹ and were corrected for Lorentz, polarization and absorption effects using SADABS². The structures were solved by the heavy atom method and refined through full-matrix least-squares cycles using SHELX-97³ as part of the WinGX⁴ package with $\Sigma(|F_o| - |F_c|)^2$ being minimized. All non-H atoms were refined with anisotropic displacement parameters, while H atoms were constrained to parent atom sites using a riding model (aromatic C–H = 0.95 Å; aliphatic C–H = 0.98 Å). The graphics were done with the DIAMOND⁵ Visual Crystal Structure Information System software with 50% probability displacement ellipsoids for non-hydrogen atoms.

3.2.2. Nuclear Magnetic Resonance Spectroscopy

The ¹³C and ¹H FT-NMR solution-state spectra for the ligands were recorded at 75.48 and 300.13 MHz respectively on a Bruker AXS300 spectrometer at 25°C in C₆D₆, at 150.96 and 600.28 MHz respectively on a Bruker AXS600 spectrometer at 25°C in CDCl₃ for [Rh(N,O-bid)(CO)₂] complexes and at 150.96 and 600.28 MHz as well as at 242.99 MHz for ³¹P on a Bruker AXS600 spectrometer at 25°C in C₆D₆ for [Rh(N,O-bid)(CO)(PX₃)] complexes; chemical shifts are reported in ppm. The naming convention is defined in Chapters 4, 6 and 7: for the C atoms in the phenyl ring, the first digit indicates molecule number, the second digit indicates ring number and the third digit indicates the position of the atom in the ring. For

¹ Bruker SAINT-PLUS (including XPREP). Version 7.12, Bruker AXS Inc., Madison, WI, 2004.

² Bruker SADABS (Version 2004/1), Bruker AXS Inc., Madison, WI, 1998.

³ Sheldrick, G.M. *Acta Cryst.* **2008**, A64, 112.

⁴ Farrugia, L.J. *J. Appl. Cryst.* **1999**, 32, 837.

⁵ Brandenburg, K.; Putz, H. DIAMOND. Release 3.0e. Crystal Impact GbR, Bonn, Germany, 2004.

Chapter 3

substitutions on the phenyl ring, the first digit indicates molecule number while the second digit indicates position on the phenyl ring.

3.2.3. Infrared Spectroscopy

Solid state FT-IR spectra were recorded on a Bruker Tensor 27 spectrophotometer in the range of 4000-400 cm^{-1} with KBr pellets.

3.2.4. Computational Data

Calculation results were obtained using the GAUSSIAN-03W⁶ software package. DFT calculations were done at the B3LYP⁷ level of theory with the 6-31G++(d,p)⁸ basis set for the main group elements and LanL2DZ⁹ for rhodium atoms using the High Performance Computing Facility of the University of the Free State. Optimized structures were verified as a minimum through frequency analysis and from this data fingerprint stretching frequencies were identified. The energy values were corrected for differences in composition between the various compounds. The graphics were done with the DIAMOND⁵ Visual Crystal Structure Information System software and overlays with the Hyperchem¹⁰ software package.

3.2.5. Magnetic Spin Transfer Studies

³¹P magnetic spin transfer spectra were collected on a Bruker AXS600 spectrometer at 242.99 MHz in CD₂Cl₂ at 18°C, 25°C, 35°C and 45°C. Kinetic data was analyzed using the CIFIT2 software package¹¹.

⁶ Frisch, M.J.; Trucks, G.W.; Schlegel, H.B.; Scuseria, G.E.; Robb, M.A.; Cheeseman, J.R.; Montgomery Jr., J.A.; Vreven, T.; Kudin, K.N.; Burant, J.C.; Millam, J.M.; Iyengar, S.S.; Tomasi, J.; Barone, V.; Mennucci, B.; Cossi, M.; Scalmani, G.; Rega, N.; Petersson, G.A.; Nakatsuji, H.; Hada, M.; Ehara, M.; Toyota, K.; Fukuda, R.; Hasegawa, J.; Ishida, M.; Nakajima, T.; Honda, Y.; Kitao, O.; Nakai, H.; Klene, M.; Li, X.; Knox, J.E.; Hratchian, H.P.; Cross, J.B.; Bakken, V.; Adamo, C.; Jaramillo, J.; Gomperts, R.; Stratmann, R.E.; Yazyev, O.; Austin, A.J.; Cammi, R.; Pomelli, C.; Ochterski, J.W.; Ayala, P.Y.; Morokuma, K.; Voth, G.A.; Salvador, P.; Dannenberg, J.J.; Zakrzewski, V.G.; Dapprich, S.; Daniels, A.D.; Strain, M.C.; Farkas, O.; Malick, D.K.; Rabuck, A.D.; Raghavachari, K.; Foresman, J.B.; Ortiz, J.V.; Cui, Q.; Baboul, A.G.; Clifford, S.; Cioslowski, J.; Stefanov, B.B.; Liu, G.; Liashenko, A.; Piskorz, P.; Komaromi, I.; Martin, R.L.; Fox, D.J.; Keith, T.; Al-Laham, M.A.; Peng, C.Y.; Nanayakkara, A.; Challacombe, M.; Gill, P.M.W.; Johnson, B.; Chen, W.; Wong, M.W.; Gonzalez, C.; Pople, J.A. GAUSSIAN-03, Revision C.01, Gaussian, Inc., Wallingford, CT, **2004**.

⁷ Becke, A.D. *J. Chem. Phys.* **1993**, *98*, 5648.

⁸ a) Hariharan, P.C.; Pople, J.A. *Theoret. Chim. Acta* **1973**, *28*, 213.

b) Francl, M.M.; Petro, W.J.; Hehre, W.J.; Binkley, J.S.; Gordon, M.S.; DeFree, D.J.; Pople, J.A.; *J. Chem. Phys.* **1982**, *77*, 3654.

⁹ Hay, P.J.; Wadt, W.R. *J. Chem. Phys.* **1985**, *82*, 299.

¹⁰ HyperChem for Windows, Hypercube, Inc., Version 7.2, USA, **2002**.

¹¹ Bain, A. *Prog. Nucl. Mag. Res. Sp.* **2003**, *43*, 63.

3.2.6. UV/Vis Spectroscopy

UV/Vis absorbance spectra were collected on a Varian Cary 50 Conc. spectrophotometer in a 1.000(1) cm tandem quartz cuvette, which was equipped with a Julabo F12-mV temperature cell regulator accurate within 0.1°C. Spectra were collected at 25°C in dichloromethane.

3.3. Ligand Synthesis

3.3.1. Synthesis of 4-(2-Chlorophenylamino)pent-3-en-2-one (2-Cl-PhonyH)

A solution of acetylacetone (11.07 g, 0.1106 mol), 2-chloro-aniline (12.86 g, 0.1008 mol) and 2 drops of H₂SO₄(conc.) in 150 ml benzene was refluxed for 6 hours in a DeanStark trap, filtered and left to crystallize. Crystals suitable for X-Ray diffraction were obtained (19.94 g, 94.32 % yield).

IR (KBr): $\nu_{\text{NO(asy)}} 1357.4$ (s) cm^{-1} . ¹H NMR (300.13 MHz, C₆D₆, 25 °C): 1.46 (s, 5H), 2.00 (s, 1H), 5.01 (s, 3H), 6.63 (m, 114H; 116H), 6.69 (d, 113H), 7.06 (d, 115H). ¹³C NMR (75.48 MHz, C₆D₆, 25 °C): 19.30 (s, 1C), 29.24 (s, 5C), 98.85 (s, 3C), 126.36 (s, 112C), 126.75 (s, 114C), 127.06 (s, 115C), 129.82 (s, 116C), 130.13 (s, 113C), 136.97(s, 111C), 158.61 (s, 2C), 196.17 (s, 4C).

3.3.2. Synthesis of 4-(4-Chlorophenylamino)pent-3-en-2-one (4-Cl-PhonyH)

A solution of acetylacetone (11.07 g, 0.1106 mol), 4-chloro-aniline (12.77 g, 0.1001 mol) and 2 drops of H₂SO₄(conc.) in 150 ml benzene was refluxed for 6 hours in a DeanStark trap, filtered and left to crystallize. Crystals suitable for X-Ray diffraction were obtained (17.14 g, 81.67 % yield).

IR (KBr): $\nu_{\text{NO(asy)}} 1373.0$ (s) cm^{-1} . ¹H NMR (300.13 MHz, C₆D₆, 25 °C): 1.44 (s, 5H), 2.00 (s, 1H), 4.94 (s, 3H), 6.39 (m, 113H; 115H), 6.87 (d, 112H; 116H). ¹³C NMR (75.48 MHz, C₆D₆, 25 °C): 19.3 (s, 1C), 29.22 (s, 5C), 98.44 (s, 3C), 125.43 (s, 113C; 115C), 129.19 (s, 112C; 116C), 129.82 (s, 111C), 130.37 (s, 114C), 158.57 (s, 2C), 195.99 (s, 4C).

3.3.3. Synthesis of 4-(2,4-Dichlorophenylamino)pent-3-en-2-one (2,4-Cl₂-PhonyH)

A solution of acetylacetone (11.07 g, 0.1106 mol), 2,4-dichloro-aniline (16.36 g, 0.1010 mol) and 2 drops of H₂SO₄(conc.) in 150 ml benzene was refluxed for 6 hours in a DeanStark trap, filtered and left to crystallize. Crystals suitable for X-Ray diffraction were obtained (16.78 g, 68.07 % yield).

IR (KBr): $\nu_{\text{NO(asy)}} 1354.3$ (s) cm⁻¹. ¹H NMR (300.13 MHz, C₆D₆, 25 °C): 1.35 (s, 5H), 1.98 (s, 1H), 4.97 (s, 3H), 6.282 (d, 115H), 6.64 (d, 116H), 7.02 (s, 113H). ¹³C NMR (75.48 MHz, C₆D₆, 25 °C): 19.18 (s, 1C), 29.24 (s, 5C), 99.19 (s, 3C), 127.09 (s, 111C), 127.23 (s, 116C), 129.89 (s, 115C), 130.44 (s, 112C), 131.02 (s, 114C), 135.63(s, 113C), 158.12 (s, 2C), 196.45 (s, 4C).

3.3.4. Synthesis of 4-(2,6-Dichlorophenylamino)pent-3-en-2-one (2,6-Cl₂-PhonyH)

A solution of acetylacetone (11.07 g, 0.1106 mol), 2,6-dichloro-aniline (16.82 g, 0.1007 mol) and 2 drops of H₂SO₄(conc.) in 150 ml benzene was refluxed for 6 hours in a DeanStark trap, filtered and left to crystallize. Crystals suitable for X-Ray diffraction were obtained (19.55 g, 79.54 % yield).

IR (KBr): $\nu_{\text{NO(asy)}} 1357.4$ (s) cm⁻¹. ¹H NMR (300.13 MHz, C₆D₆, 25 °C): 1.41 (s, 5H), 1.99 (s, 1H), 5.09 (s, 3H), 6.80 (dd, 113H; 115H), 6.85 (d, 114H). ¹³C NMR (75.48 MHz, C₆D₆, 25 °C): 18.68 (s, 1C), 29.14 (s, 5C), 97.74 (s, 3C), 118.00 (s, 113C; 115C), 119.57 (s, 114C), 135.18 (s, 112C; 116C), 160.39 (s, 2C), 196.54 (s, 4C).

3.4. Synthesis of [Rh(N,O-bid)(CO)₂] Complexes

3.4.1. Synthesis of Dicarbonyl-[4-(Phenylamino)pent-3-en-2-onato]-Rhodium(I) [Rh(Phony)(CO)₂]

[RhCl(CO)₂]₂ was prepared *in situ* by heating RhCl₃·3H₂O (0.1046 g, 0.3973 mmol) in 2 ml DMF under reflux for 30 minutes. PhonyH (0.0786 g, 0.449 mmol, 1.14 eq) was added to the cooled DMF solution of [RhCl(CO)₂]₂. The product was precipitated by ice-water, followed by

Chapter 3

centrifuge. Crystals suitable for X-Ray diffraction were obtained from slow evaporation from a dichloromethane solution (0.0831 g, 65.84 % yield).

IR (KBr): $\nu_{\text{CO(asy)}} 1999.1$ (s) cm^{-1} ; $\nu_{\text{CO(sym)}} 2062.5$ (s) cm^{-1} . UV/Vis: $\lambda_{\text{max}(1)} = 329$ nm, $\epsilon_1 = 5102$ $\text{M}^{-1}\cdot\text{cm}^{-1}$; $\lambda_{\text{max}(2)} = 265$ nm, $\epsilon_2 = 6497$ $\text{M}^{-1}\cdot\text{cm}^{-1}$. ^1H NMR (600.28 MHz, CDCl_3 , 25 °C): 1.76 (s, 5H), 2.12 (s, 1H), 5.27 (s, 3H), 7.05 (d, 112; 116H), 7.17 (t, 114H), 7.34 (t, 113H; 115H). ^{13}C NMR (150.96 MHz, CDCl_3 , 25 °C): 23.31 (s, 1C), 25.95 (s, 5C), 99.05 (s, 3C), 123.97 (s, 112C; 116C), 125.52 (s, 114C), 128.82 (s, 113C; 115C), 157.25 (s, 111C), 165.53 (s, 2C), 178.31 (s, 4C), 183.70 (d, 14C), 184.58 (d, 13C).

3.4.2. Synthesis of Dicarbonyl-[4-(2-Chlorophenylamino)pent-3-en-2-onato]-Rhodium(I) [Rh(2-Cl-Phony)(CO)₂]

$[\text{RhCl}(\text{CO})_2]_2$ was prepared *in situ* by heating $\text{RhCl}_3\cdot 3\text{H}_2\text{O}$ (0.0522 g, 0.1982 mmol) in 2 ml DMF under reflux for 30 min. 2-Cl-PhonyH (0.0484 g, 0.2308 mmol) was added to the cooled DMF solution of $[\text{RhCl}(\text{CO})_2]_2$. The product was precipitated by ice-water, followed by centrifuge. Crystals suitable for X-Ray diffraction were obtained from slow evaporation from a dichloromethane solution (0.0527 g, 72.29% yield).

IR (KBr): $\nu_{\text{CO(asy)}} 2005.0$ (s) cm^{-1} ; $\nu_{\text{CO(sym)}} 2074.6$ (s) cm^{-1} . UV/Vis: $\lambda_{\text{max}(1)} = 329$ nm, $\epsilon_1 = 8469$ $\text{M}^{-1}\cdot\text{cm}^{-1}$; $\lambda_{\text{max}(2)} = 267$ nm, $\epsilon_2 = 8479$ $\text{M}^{-1}\cdot\text{cm}^{-1}$. ^1H NMR (600.28 MHz, CDCl_3 , 25 °C): 1.73 (s, 5H), 2.13 (s, 1H), 5.33 (s, 3H), 6.15 (m, 114H; 116H), 7.28 (d, 113H), 7.44 (d, 115H). ^{13}C NMR (150.96 MHz, CDCl_3 , 25 °C): 22.74 (s, 1C), 26.15 (s, 5C), 99.22 (s, 3C), 126.01 (s, 112C), 126.82 (s, 114C), 127.26 (s, 115C), 129.76 (s, 116C), 153.65 (s, 111C), 165.95 (s, 2C), 179.66 (s, 4C), 183.75 (d, 14C), 184.30 (d, 13C).

3.4.3. Synthesis of Dicarbonyl-[4-(4-Chlorophenylamino)pent-3-en-2-onato]-Rhodium(I) [Rh(4-Cl-Phony)(CO)₂]

$[\text{RhCl}(\text{CO})_2]_2$ was prepared *in situ* by heating $\text{RhCl}_3\cdot 3\text{H}_2\text{O}$ (0.1045 g, 0.3969 mmol) in 2 ml DMF under reflux for 30 minutes. 4-Cl-PhonyH (0.0944 g, 0.4502 mmol, 1.14 eq) was added to the cooled DMF solution of $[\text{RhCl}(\text{CO})_2]_2$. The product was precipitated by ice-water, followed

Chapter 3

by centrifuge. Crystals suitable for X-Ray diffraction were obtained from slow evaporation from a dichloromethane solution (0.1023 g, 70.12 % yield).

IR (KBr): $\nu_{\text{CO(asy)}} 1994.7 \text{ cm}^{-1}$; $\nu_{\text{CO(sym)}} 2064.8 \text{ (s) cm}^{-1}$. UV/Vis: $\lambda_{\text{max}} = 329 \text{ nm}$, $\epsilon = 6879 \text{ M}^{-1} \cdot \text{cm}^{-1}$. $^1\text{H NMR}$ (600.28 MHz, CDCl_3 , 25 °C): 1.75 (s, 5H), 2.12 (s, 1H), 5.28 (s, 3H), 7.00 (d, 113H; 115H), 7.31 (d, 112H; 116H). $^{13}\text{C NMR}$ (150.96 MHz, CDCl_3 , 25 °C): 23.40 (s, 1C), 26.01 (s, 5C), 99.22 (s, 3C), 125.44 (s, 113C; 115C), 128.94 (s, 112C; 116C), 131.04 (s, 111C), 155.66 (s, 114C), 165.62 (s, 2C), 179.03 (s, 4C), 183.80 (d, 14C), 184.33 (d, 13C).

3.4.4. Synthesis of Dicarbonyl-[4-(2,4-Dichlorophenylamino)pent-3-en-2-onato]-Rhodium(I) [Rh(2,4-Cl₂-Phony)(CO)₂]

[RhCl(CO)₂]₂ was prepared *in situ* by heating RhCl₃·3H₂O (0.0522 g, 0.1982 mmol) in 2 ml DMF under reflux for 30 min. 2,4-Cl₂-PhonyH (0.0558 g, 0.2286 mmol) was added to the cooled DMF solution of [RhCl(CO)₂]₂. The product was precipitated by ice-water, followed by centrifuge. Crystals suitable for X-Ray diffraction were obtained from slow evaporation from a dichloromethane solution (0.0903 g, 59.02 % yield).

IR (KBr): $\nu_{\text{CO(asy)}} 1990.1 \text{ (s) cm}^{-1}$; $\nu_{\text{CO(sym)}} 2068.8 \text{ (s) cm}^{-1}$. UV/Vis: $\lambda_{\text{max}} = 328 \text{ nm}$, $\epsilon = 12678 \text{ M}^{-1} \cdot \text{cm}^{-1}$. $^1\text{H NMR}$ (600.28 MHz, CDCl_3 , 25 °C): 1.73 (s, 5H), 2.13 (s, 1H), 5.38 (s, 3H), 7.09 (d, 116H), 7.27 (dd, 115H), 7.46 (d, 113H). $^{13}\text{C NMR}$ (150.96 MHz, CDCl_3 , 25 °C): 22.81 (s, 1C), 26.21 (s, 5C), 99.39 (s, 3C), 126.86 (s, 111C), 127.23 (s, 116C), 129.21 (s, 115C), 129.50 (s, 112C), 131.63 (s, 114C), 152.25 (s, 113C), 165.99 (s, 2C), 180.30 (s, 4C), 183.71 (d, 14C), 184.17 (d, 13C).

3.4.5. Synthesis of Carbonyl-[4-(2,6-Dichlorophenylamino)pent-3-en-2-onato]-Rhodium(I) [Rh(2,6-Cl₂-Phony)(CO)₂]

[RhCl(CO)₂]₂ was prepared *in situ* by heating RhCl₃·3H₂O (0.0997 g, 0.3789 mmol) in 2 ml DMF under reflux for 30 min. 2,6-Cl₂-PhonyH (0.1079 g, 0.4200 mmol) was added to the cooled DMF solution of [RhCl(CO)₂]₂. The product was precipitated by ice-water, followed by centrifuge. Crystals suitable for X-Ray diffraction were obtained from slow evaporation from a dichloromethane solution (0.1270 g, 83.44 % yield).

Chapter 3

IR (KBr): $\nu_{\text{CO(asy)}} 2000.8$ (s) cm^{-1} ; $\nu_{\text{CO(sym)}} 2072.3$ (s) cm^{-1} . UV/Vis: $\lambda_{\text{max}} = 327$ nm, $\epsilon_1 = 9279$ $\text{M}^{-1} \cdot \text{cm}^{-1}$; $\lambda_{\text{max(2)}} = 264$ nm, $\epsilon_2 = 7818$ $\text{M}^{-1} \cdot \text{cm}^{-1}$. ^1H NMR (600.28 MHz, CDCl_3 , 25 °C): 1.70 (s, 5H), 2.015 (s, 1H), 5.38 (s, 3H), 7.10 (t, 114H), 7.40 (d, 113H; 115H). ^{13}C NMR (150.96 MHz, CDCl_3 , 25 °C): 22.23 (s, 1C), 26.35 (s, 5C), 99.43 (s, 3C), 126.85 (s, 111H), 128.37 (s, 113C; 115C), 130.26 (s, 114C), 150.64 (s, 112C; 116C), 166.04 (s, 2C), 180.93 (s, 4C), 183.69 (d, 14C), 184.15 (d, 13C).

3.5. Synthesis of [Rh(N,O-Bid)(CO)(PPh₃)] Complexes

3.5.1. Synthesis of Carbonyl-[4-(4-Chlorophenylamino)pent-3-en-2-onato]-Triphenylphosphine-Rhodium(I) [Rh(4-Cl-Phony)(CO)(PPh₃)]

To a 5 ml acetone solution of [Rh(4-Cl-Phony)(CO)₂] (0.0200 g, 54.41 μmol) was added PPh₃ (0.0144 g, 54.90 μmol) resulting in the immediate evolution of gas. The solution was left to crystallize. Crystals suitable for X-Ray diffraction were obtained in quantitative yield (0.0327 g, 100%).

IR (KBr): $\nu_{\text{CO}} 1986.2$ (s) cm^{-1} . UV/Vis: $\lambda_{\text{max}} = 329$ nm, $\epsilon = 6880$ $\text{M}^{-1} \cdot \text{cm}^{-1}$. ^1H NMR (600.28 MHz, CD_2Cl_2 , 25 °C): 2.94 (s, 5H), 3.01 (s, 1H), 5.239 (s, 3H), 7.04 (d, 113H; 115H), 7.17 (d, 112H; 116H), 7.95 (m, Arom.). ^{13}C NMR (150.96 MHz, CD_2Cl_2 , 25 °C): 23.33 (s, 1C), 26.03 (s, 5C), 98.69 (s, 3C), 125.71 (s, 113C; 115C), 128.94 (s, 112C; 116C), 131.04 (s, 111C), 157.12 (s, 114C), 163.85 (s, 2C), 177.13 (s, 4C), 190.18 (d, 14C). ^{31}P NMR (242.99 MHz, CD_2Cl_2 , H_3PO_4 , 25 °C): 44.44 (d, $J_{\text{Rh-P}} 155.75$ Hz).

3.5.2. Synthesis of Carbonyl-[4-(2,4-Dichlorophenylamino)pent-3-en-2-onato]-Triphenylphosphine-Rhodium(I) [Rh(2,4-Cl₂-Phony)(CO)(PPh₃)]

To a 5 ml acetone solution of [Rh(2,4-Cl₂-Phony)(CO)₂] (0.0207 g, 51.49 μmol) was added PPh₃ (0.0137 g, 52.23 μmol) resulting in the immediate evolution of gas. The solution was left to crystallize. Crystals suitable for X-Ray diffraction were obtained in quantitative yield (0.0328 g, 100%).

Chapter 3

IR (KBr): ν_{CO} 1963.4 (s) cm^{-1} . UV/Vis: $\lambda_{\text{max}} = 328 \text{ nm}$, $\epsilon = 12678 \text{ M}^{-1} \cdot \text{cm}^{-1}$. ^1H NMR (600.28 MHz, CD_2Cl_2 , 25 °C): 1.34 (s, 5H), 1.98 (s, 1H), 4.98 (s, 3H), 6.26 (d, 116H), 6.62 (dd, 115H), 7.02 (m, Arom), 7.71 (d, 113H). ^{13}C NMR (150.96 MHz, CD_2Cl_2 , 25 °C): 19.15 (s, 1C), 29.22 (s, 5C), 99.17 (s, 3C), 127.18 (s, 111C), 127.21 (s, 116C), 128.07 (s, Arom), 128.31 (s, Arom), 128.44 (s, 115C), 129.91 (s, 112C), 130.59 (s, 114C), 152.25 (s, 113C), 165.99 (s, 2C), 180.30 (s, 4C), 188.20(d, 14C). ^{31}P NMR (242.99 MHz, CD_2Cl_2 , H_3PO_4 , 25 °C): 43.52 (d, $J_{\text{Rh-P}}$ 161.35Hz).

3.5.3. Synthesis of Carbonyl-[4-(2,6-Dichlorophenylamino)pent-3-en-2-onato]-Triphenylphosphine-Rhodium(I) [Rh(2,6-Cl₂-Phony)(CO)(PPh₃)]

To a 5 ml acetone solution of [Rh(2,6-Cl₂-Phony)(CO)₂] (0.0198 g, 49.25 μmol) was added PPh₃ (0.0132 g, 50.33 μmol) resulting in the immediate evolution of gas. The solution was left to crystallize. Crystals suitable for X-Ray diffraction were obtained in quantitative yield (0.0313 g, 100%).

IR (KBr): ν_{CO} 1969.2 (s) cm^{-1} . UV/Vis: $\lambda_{\text{max}} = 327 \text{ nm}$, $\epsilon = 9279 \text{ M}^{-1} \cdot \text{cm}^{-1}$. ^1H NMR (600.28 MHz, CD_2Cl_2 , 25 °C): 1.60 (s, 5H), 1.64 (s, 1H), 5.17 (s, 3H), 6.40 (t, 114H), 6.98 (m, Arom), 7.08 (d, 113H; 115H), 7.78 (m, Arom). ^{13}C NMR (150.96 MHz, CD_2Cl_2 , 25 °C): 22.28 (s, 1C), 26.30 (s, 5C), 98.91 (s, 3C), 125.68 (s, 111H), 128.08 (s, Arom), 128.31 (s, Arom), 128.38 (s, 113C; 115C), 130.42 (s, 114C), 135.07 (s, Arom), 135.15 (s, Arom), 152.33 (s, 112C; 116C), 164.51 (s, 2C), 179.24(s, 4C), 189.99 (d, 14C). ^{31}P NMR (242.99 MHz, CD_2Cl_2 , H_3PO_4 , 25 °C): 42.38 (d, $J_{\text{Rh-P}}$ 157.21 Hz).

3.5.4. Synthesis of Carbonyl-[4-(2,3-Dimethylphenylamino)pent-3-en-2-onato]-Triphenylphosphine-Rhodium(I) [Rh(2,3-Me₂-Phony)(CO)(PPh₃)]

To a 5 ml acetone solution of [Rh(2,3-Me₂-Phony)(CO)₂] (0.0204 g, 56.48 μmol) was added PPh₃ (0.0151 g, 57.57 μmol) resulting in the immediate evolution of gas. The solution was left to crystallize. Crystals suitable for X-Ray diffraction were obtained in quantitative yield (0.0336 g, 100%).

Chapter 3

IR (KBr): ν_{CO} 1966.9 (s) cm^{-1} . UV/Vis: $\lambda_{\text{max}} = 323 \text{ nm}$, $\epsilon = 7279 \text{ M}^{-1}.\text{cm}^{-1}$. ^1H NMR (600.28 MHz, CD_2Cl_2 , 25 °C): 1.77 (s, 5H), 1.88 (s, 18H), 2.25 (s, 1H), 2.60 (s, 17H), 5.32 (s, 3H), 7.01 (d, 116H), 7.18 (t, 115H), 7.30 (d, 114H), 7.97 (m, Arom). ^{13}C NMR (150.96 MHz, CD_2Cl_2 , 25 °C): 14.84 (s, 117C), 20.54 (s, 118C) 22.72 (s, 1C), 26.00 (s, 5C), 98.43 (s, 3C), 122.04 (s, 111H), 125.95 (s, 113C), 126.45 (s, 115C), 128.07 (s, Arom), 128.31 (s, Arom), 129.95 (s, 114C), 135.00 (s, Arom), 135.08 (s, Arom), 157.46 (s, 112C; 116C), 163.57(s, 2C), 176.32(s, 4C), 190.04 (d, 14C). ^{31}P NMR (242.99 MHz, CD_2Cl_2 , H_3PO_4 , 25 °C): 44.11 (d, $J_{\text{Rh-P}}$ 155.27 Hz).

3.5.5. Synthesis of Carbonyl-[4-(2,6-Dimethylphenylamino)pent-3-en-2-onato]-Triphenylphosphine-Rhodium(I) [Rh(2,6-Me₂-Phony)(CO)(PPh₃)]

To a 5 ml acetone solution of [Rh(2,6-Me₂-Phony)(CO)₂] (0.0302 g, 83.61 μmol) was added PPh₃ (0.0219 g, 83.50 μmol) resulting in the immediate evolution of gas. The solution was left to crystallize. Crystals suitable for X-Ray diffraction were obtained in quantitative yield (0.0498 g, 100%).

IR (KBr): ν_{CO} 1971.1 (s) cm^{-1} . UV/Vis: $\lambda_{\text{max}} = 330 \text{ nm}$, $\epsilon = 10279 \text{ M}^{-1}.\text{cm}^{-1}$. ^1H NMR (600.28 MHz, CD_2Cl_2 , 25 °C): 1.66 (s, 5H), 1.86 (s, 1H), 2.70 (s, 17H; 18H), 5.31 (s, 3H), 7.11 (t, 114H), 7.22 (d, 113H; 115H), 7.94 (m, Arom). ^{13}C NMR (150.96 MHz, CD_2Cl_2 , 25 °C): 19.51 (s, 117C; 118C), 21.75 (s, 1C), 26.01 (s, 5C), 98.44 (s, 3C), 124.94 (s, 111H), 128.08 (s, Arom), 128.31 (s, Arom), 129.97 (s, 113C), 131.52(s, 115C), 133.79 (s, 114C), 134.98 (s, Arom), 135.08 (s, Arom), 156.10 (s, 112C; 116C), 163.16 (s, 2C), 176.51 (s, 4C), 189.77 (d, 14C). ^{31}P NMR (242.99 MHz, CD_2Cl_2 , H_3PO_4 , 25 °C): 43.73 (d, $J_{\text{Rh-P}}$ 154.54 Hz).

3.6. Evaluation of Synthesis

A range of substituted 4-(phenylamino)pent-3-en-2-one (N,O-BidH) compounds, where the position of the chloride substituent on the phenyl moiety systematically changes in a combination of *ortho*- and *para*-positions, were synthesized in relatively high yields. These ligands are easily soluble in both polar and non-polar solvents and are stable in air over a period of several years. The dicarbonyl-[4-(phenylamino)pent-3-en-2-onato]-rhodium(I) [Rh(N,O-

Chapter 3

$\text{Bid}(\text{CO})_2$] complexes that were subsequently synthesized are insoluble in cold water but dissolves easily in polar solvents. The complexes decompose in solution but are stable in air over a period of several years. Carbonyl-[4-(phenylamino) pent-3-en-2-onato]-triphenylphosphine-rhodium(I) $[\text{Rh}(\text{N},\text{O}\text{-Bid})(\text{CO})(\text{PPh}_3)]$ complexes were synthesized in quantitative yields to form crystals of very high quality. These crystals are not very soluble but were found to dissolve in dichloromethane and benzene. The $[\text{Rh}(\text{N},\text{O}\text{-Bid})(\text{CO})(\text{PPh}_3)]$ complexes are stable in air and in solution over a period of several months.

Chapter 3

4 X-Ray Crystallographic Study of 4-(Phenylamino)pent-3-en-2-one Functionalities

4.1. Introduction

Compounds containing electron donating nitrogen atoms have elicited curiosity for many years, and one of the first examples of such a molecule used as a ligand is in the complex tris(1,2-diaminocyclopentane)rhodium triperchlorate dodecahydrate, synthesized in 1928¹. Such compounds containing a nitrogen and an oxygen atom as well as an unsaturated carbon-carbon bond are known as enaminoketones (lesser name ketoamines). These electron rich compounds are of interest in various fields including liquid crystals², fluorescence studies³ as well as medical applications⁴. It also has significant application possibilities in catalysis⁵. This study focuses on the modification of the electronic properties of these types of ligands for further application in mechanistic studies, or more specifically the effect of chloride substitution on the phenyl ring of the N,O-bidentate compound as ligand when applied in exchange reactions. The mechanistic study, however, will only be discussed later while the focus of this chapter will be on the properties of the uncoordinated N,O-bidentate compounds.

This chapter concentrates on 4-(phenylamino)pent-3-en-2-one (PhonyH⁶, Figure 4.1) derivatives with emphasis on electronic influence, which are determined by the effects of strong electron withdrawing groups, such as chloride moieties, on bond angles and distances. Differences in

¹ Jaeger, F.M.; Blumendal, H.B. *Z. Anorg. Allg. Chem.* **1928**, 175, 161.

² Pyżuk, W.; Krówczyński, A.; Górecka, E. *Mol. Cryst. Liq. Cryst.* **1993**, 237, 75.

³ Xia, M.; Wu, B.; Xiang, G. *J. Flu. Chem.* **2008**, 129, 402.

⁴ a) Tan, H.Y.; Loke, W.K.; Tan, Y.T.; Nguyen, N.-T. *Lab Chip* **2008**, 8, 885.

b) Chen, H.; Rhodes, J. *J. Mol. Med.* **1996**, 74, 497.

⁵ Nair, V.A.; Suni, M.M.; Sreekumar, K. *Proc. Indian Acad. Sci. (Chem. Sci.)* **2002**, 114, 481.

⁶ Shaheen, F.; Marchio, L.; Badshaha, A.; Khosac, M.K. *Acta Cryst.* **2006**, E62, o873.

Chapter 4

crystal packing styles between different derivatives are also addressed. The dihedral angle is defined as the angle between the planes through the phenyl ring and the N-C-C-C-O moieties and illustrated in Figure 4.2.

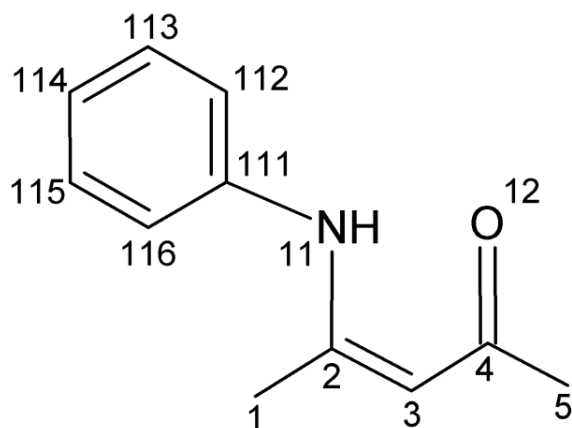


Figure 4.1. Representation of 4-(phenylamino)pent-3-en-2-one (PhonyH), illustrating the numbering scheme used throughout the thesis. For the C atoms in the phenyl ring, the first digit indicates molecule number, the second digit indicates ring number and the third digit indicates the position of the atom in the ring. For substitutions on the phenyl ring, the first digit indicates molecule number while the second digit indicates position on the phenyl ring.

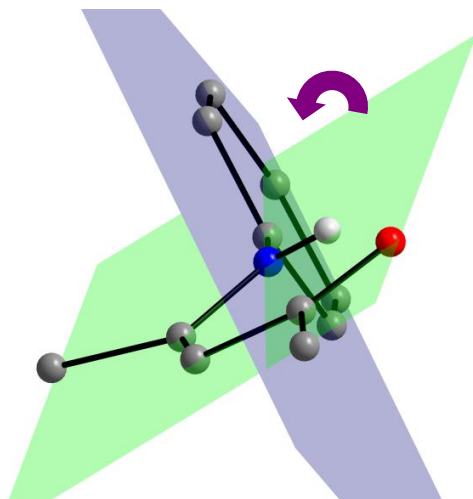


Figure 4.2. Illustration of the dihedral angle, calculated between the planes through the phenyl ring and H-N-C-C-O moieties.

Different interactions play a role in the crystal packing of a compound, the most common being intra- and intermolecular hydrogen bonds and π - π interactions. The term “halogen bonding” refers to the non-covalent interaction of a halogen atom in a molecule with a negative site, for

Chapter 4

example the lone pair electrons of a Lewis base, in an adjacent molecule. Halogen bonding has been observed for bromine and iodine, less frequently for chlorine and not yet for fluorine⁷. The strength of these halogen bonds increase in the order Cl<Br<I⁸. The “chloro effect” was first described by Schmidt⁹ in 1971 and is of interest in packing arrangements of halogenated compounds. This effect involves the presence of chloride substituents in aromatic compounds which frequently result in stacking arrangements with a resultant short (*ca.* 4 Å) crystallographic axis¹⁰. A chloride···chloride contact can be represented by the geometric parameters (θ_1 , θ_2 and r_i) of the C₁-Cl₁···Cl₂-C₂ moieties (where $\theta_1 = \text{C}_1\text{-Cl}_1\cdots\text{Cl}_2$, $\theta_2 = \text{Cl}_1\cdots\text{Cl}_2\text{-C}_2$ and $r_i = \text{Cl}_1\cdots\text{Cl}_2$ distance)¹¹. Cl···Cl close contacts are classified into two categories; for Type I $\theta_1 \sim \theta_2$ and for Type II $\theta_1 \sim 90^\circ$ and $\theta_2 \sim 180^\circ$ ^{11.b}. The distance r_i is classified as ‘close’ when it is shorter than the sum of the van der Waals radii of the two chloride atoms, 3.5 Å (using the CSD standard van der Waals radius for Cl as 1.75 Å¹²). The same principal applies to other halogens¹³. Since hydrogen bonds are long-range interactions, more than one acceptor A can bond to a group X-H. When there are two acceptors A₁ and A₂, the interaction is classified as a bifurcated hydrogen bond X-H···(A₁, A₂)¹⁴.

4.2. Results

Procedures for synthesis of the enaminoketones described here are discussed in Chapter 3. General crystal data and refinement parameters are presented in Table 4.1. A complete list of atomic coordinates, equivalent isotropic parameters, bond distances and angles, anisotropic displacement parameters and hydrogen coordinates for each individual dataset is given in Appendix A.

⁷ Clark, T.; Hennemann, M.; Murray, J.S.; Politzer, P. *J. Mol. Model.* **2007**, *13*, 291.

⁸ Politzer, P.; Lane, P.; Concha, M.C.; Ma, Y.; Murray, J.S. *J. Mol. Model.* **2007**, *13*, 305.

⁹ a) Green, B.S.; Schmidt, G.M. *J. Israel Chemical Society annual meeting abstracts*, **1971**, 197.

b) Cohen, M.D.; Schmidt G.M. J.; Sonntag, F. I. *J. Chem. Soc.* **1964**, 2000.

c) Schmidt, G.M.J. *J. Chem. Soc.* **1964**, 2014.

¹⁰ Desiraju, G.R. *Crystal Engineering: The Design of Organic Solids*; Elsevier: Amsterdam, **1989**.

¹¹ a) Desiraju, G.R.; Parthasarathy, R. *J. Am. Chem. Soc.* **1989**, *111*, 8725.

b) Awwadi, F.F.; Willett, R.D.; Peterson, K.A.; Twamley, B. *Chem. Eur. J.* **2006**, *12*, 8952.

¹² Allen, F.H. The Cambridge Structural Database Version 1.9, *Acta Cryst.* **2002**, *B58*, 380.

¹³ Steyl, G.; Roodt, A. *Acta Cryst.* **2003**, *C59*, o525.

¹⁴ Francl, M.M.; Petro, W.J.; Hehre, W.J.; Binkley, J.S.; Gordon, M.S.; DeFree, D.J.; Pople, J.A.; *J. Chem. Phys.* **1982**, *77*, 3654.

Chapter 4

Table 4.1. General crystal data for 2-Cl-PhonyH, 4-Cl-PhonyH, 2,4-Cl₂-PhonyH and 2,6-Cl₂-PhonyH. For label definition see Figure 4.1.

	2-Cl-PhonyH	4-Cl-PhonyH	2,4-Cl₂-PhonyH	2,6-Cl₂-PhonyH
Empirical formula	C11 H12 Cl N O	C11 H12 Cl N O	C11 H11 Cl2 N O	C11 H11 Cl2 N O, 0.5(C6 H5 Cl2 N)
Formula weight	209.67	209.67	244.11	325.12
Temperature (K)	100(2)	100(2)	100(2)	100(2)
Wavelength (Å)	0.71073	0.71069	0.71073	0.71073
Crystal system	Orthorhombic	Monoclinic	Triclinic	Monoclinic
Space group	<i>P</i> 2 ₁ 2 ₁ 2 ₁	<i>C</i> <i>c</i>	<i>P</i> $\bar{1}$	<i>C</i> 2/ <i>c</i>
<i>a</i> (Å)	7.3264(3)	14.137(5)	7.3893(8)	15.7140(1)
<i>b</i> (Å)	8.7103(4)	14.537(5)	10.933(1)	8.7210(2)
<i>c</i> (Å)	16.1960(7)	20.478(5)	13.764(2)	22.9950(4)
α (°)	90	90	90.040(5)	90
β (°)	90	100.516(5)	94.751(4)	104.794 (1)
γ (°)	90	90	99.251(5)	90
Volume (Å ³)	1033.55(8)	4138(2)	1093.6(2)	3046.81(9)
<i>Z</i>	4	16	4	8
Density _{cal} (Mg.m ⁻³)	1.347	1.346	1.483	1.418
μ (mm ⁻¹)	0.334	0.334	0.564	0.595
<i>F</i> (000)	440	1760	504	1336
Crystal size (mm ³)	0.60 x 0.42 x 0.21	0.18 x 0.13 x 0.10	0.33 x 0.21 x 0.08	0.31 x 0.25 x 0.19
$\theta_{\min} / \theta_{\max}$ (°)	2.52 / 26.99	2.14 / 27.00	1.48 / 28.30	1.83 / 28.36
Index ranges	-9 ≤ <i>h</i> ≤ 9 -11 ≤ <i>k</i> ≤ 11 -20 ≤ <i>l</i> ≤ 19	-18 ≤ <i>h</i> ≤ 17 -18 ≤ <i>k</i> ≤ 15 -26 ≤ <i>l</i> ≤ 26	-9 ≤ <i>h</i> ≤ 7 -14 ≤ <i>k</i> ≤ 14 -18 ≤ <i>l</i> ≤ 18	-20 ≤ <i>h</i> ≤ 20 -11 ≤ <i>k</i> ≤ 11 -30 ≤ <i>l</i> ≤ 30
Reflections collected	17399	21627	15163	34487
Independent reflections	2259	8986	5198	3791
<i>R</i> _{int}	0.0315	0.0303	0.0366	0.0343
Completeness to θ_{\max} (%)	99.6	100	96.6	99.7
Data / parameters	2259 / 130	8986 / 507	5198 / 283	3791 / 189
Goodness-of-fit on <i>F</i> ²	1.059	1.030	1.071	1.234
Final <i>R</i> indices, [<i>I</i> > 2σ(<i>I</i>)]	<i>R</i> ₁ = 0.0285 <i>wR</i> ₂ = 0.0809	<i>R</i> ₁ = 0.0378 <i>wR</i> ₂ = 0.0914	<i>R</i> ₁ = 0.0382 <i>wR</i> ₂ = 0.0937	<i>R</i> ₁ = 0.0312 <i>wR</i> ₂ = 0.0873
<i>R</i> indices (all data)	<i>R</i> ₁ = 0.0292 <i>wR</i> ₂ = 0.0819	<i>R</i> ₁ = 0.0447 <i>wR</i> ₂ = 0.0967	<i>R</i> ₁ = 0.0563 <i>wR</i> ₂ = 0.1033	<i>R</i> ₁ = 0.0400 <i>wR</i> ₂ = 0.1202
$\Delta\rho$ max / min (e.Å ⁻³)	0.333 / -0.255	0.361 / -0.250	0.396 / -0.377	0.545 / -0.535

4.2.1. Crystal Structure of 4-(2-Chlorophenylamino)pent-3-en-2-one (2-Cl-PhonyH)¹⁵

The compound 2-Cl-PhonyH, where PhonyH = 4-(phenylamino)pent-3-en-2-one, was prepared as discussed in § 3.3.1 and crystallizes in the orthorhombic space group $P2_12_12_1$ with $Z = 4$. The compound is shown in Figure 4.3, with important bond distances and angles reported in Table 4.2.

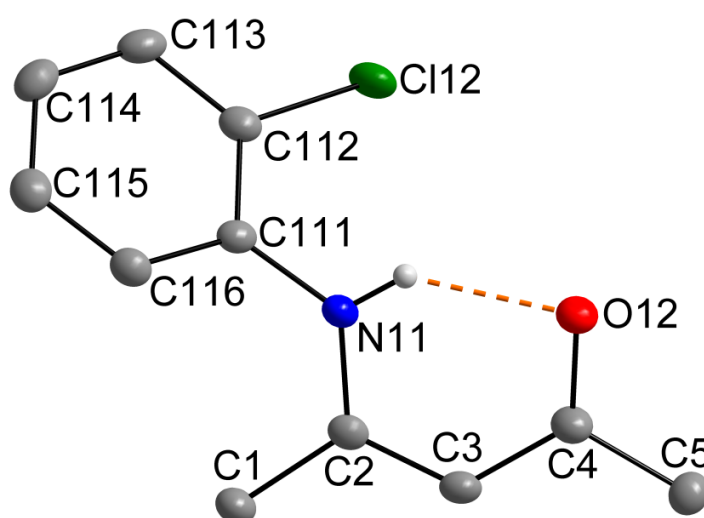


Figure 4.3. DIAMOND¹⁶ view of 2-Cl-PhonyH, where PhonyH = 4-(phenylamino)pent-3-en-2-one (50 % probability displacement ellipsoids). Selected hydrogen atoms and labels have been omitted for clarity. For the C atoms in the phenyl ring, the first digit indicates molecule number, the second digit indicates ring number and the third digit indicates the position of the atom in the ring. For the Cl atoms, the first digit indicates molecule number while the second digit indicates position on the phenyl ring.

Table 4.2. Selected bond distances (Å) and angles (°) for 2-Cl-PhonyH.

Atoms	Distances (Å)	Atoms	Angles (°)
N ₁₁ -C ₁₁₁	1.408(2)	N ₁₁ -H ₁₁ ⋯O ₁₂	138.9(2)
N ₁₁ -C ₂	1.347(2)	N ₁₁ -C ₂ ⋯C ₄ -O ₁₂	5.5(1)
O ₁₂ -C ₄	1.249(2)	Dihedral angle ^a	46.52(5)
C ₂ -C ₃	1.379(2)		
C ₃ -C ₄	1.428(2)		
N ₁₁ ⋯O ₁₂ (Bite distance)	2.633(2)		

^a Defined as the torsion angle between the N-C-C-C-O plane and the phenyl ring.

¹⁵ Venter, G.J.S., Steyl, G., Roodt, A. *Acta Cryst.* **2012**, E68, o3101.

¹⁶ Brandenburg, K.; Putz, H. DIAMOND. Release 3.0e. Crystal Impact GbR, Bonn, Germany, **2004**.

Chapter 4

The difference between $d(\text{C}_2\text{-C}_3)$ and $d(\text{C}_3\text{-C}_4)$ [1.379(2) Å and 1.428(2) Å, respectively] confirms the existence of an unsaturated carbon-carbon bond in the pentenone backbone between C_2 and C_3 . The pentenone backbone is slightly twisted as can be seen by the $\text{N}_{11}\text{-C}_2\cdots\text{C}_4\text{-O}_{12}$ torsion angle of $5.5(1)^\circ$. This could possibly be attributed to the orientation of the phenyl ring, where the less rigid pentenone moiety distorts to accommodate the bulky ring. Classical intra- and intermolecular hydrogen bonds exist between hydrogen atoms and oxygen and nitrogen atoms of adjacent molecules. Hydrogen interactions in the structure, illustrated in Figure 4.4, are shown in Table 4.3. The resulting packing style is shown in Figure 4.5 and Figure 4.6.

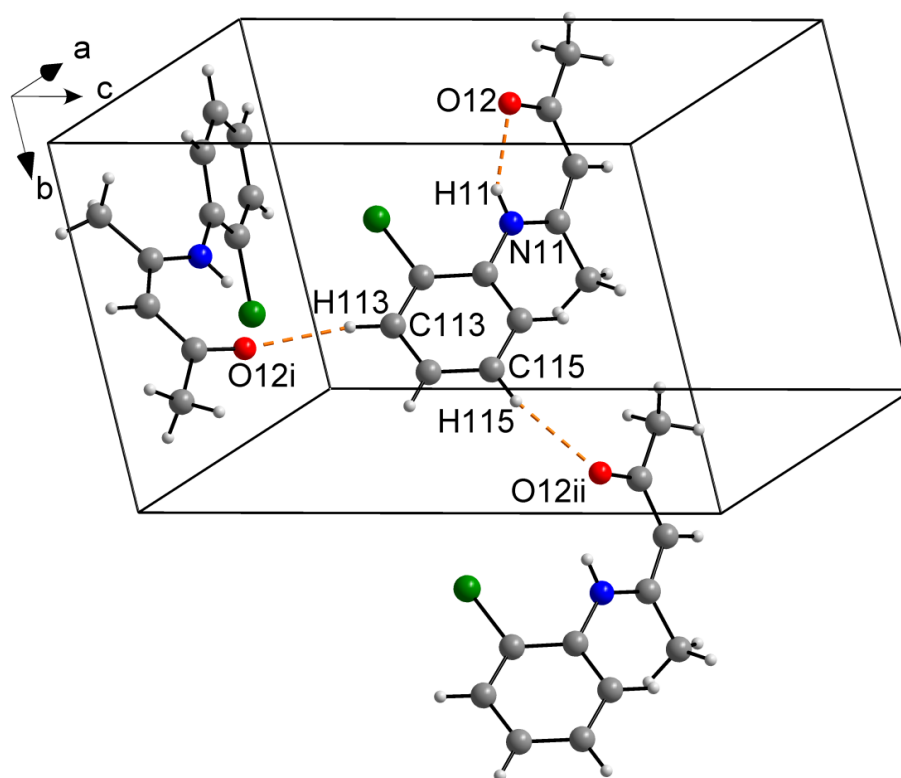


Figure 4.4. Partial unit cell for 2-Cl-PhonyH with important intra- and intermolecular hydrogen bonding interactions indicated with dashed lines. Symmetry operators are given in Table 4.3.

Table 4.3. Hydrogen bonds for 2-Cl-PhonyH (Å and $^\circ$).

D-H...A	$d_{\text{D-H}}$ (Å)	$d_{\text{H...A}}$ (Å)	$d_{\text{D...A}}$ (Å)	\angle_{DHA} ($^\circ$)
$\text{N}_{11}\text{-H}_{11}\cdots\text{O}_{12}$	0.84	1.94	2.633(2)	139.0
$\text{C}_{113}\text{-H}_{113}\cdots\text{O}_{12}^{\text{i}}$	0.95	2.43	3.356(2)	166.0
$\text{C}_{115}\text{-H}_{115}\cdots\text{O}_{12}^{\text{ii}}$	0.95	2.43	3.320(2)	157.0

Symmetry code: (i) $x - 1/2, -y + 1/2, -z + 1$ (ii) $x, y + 1, z$

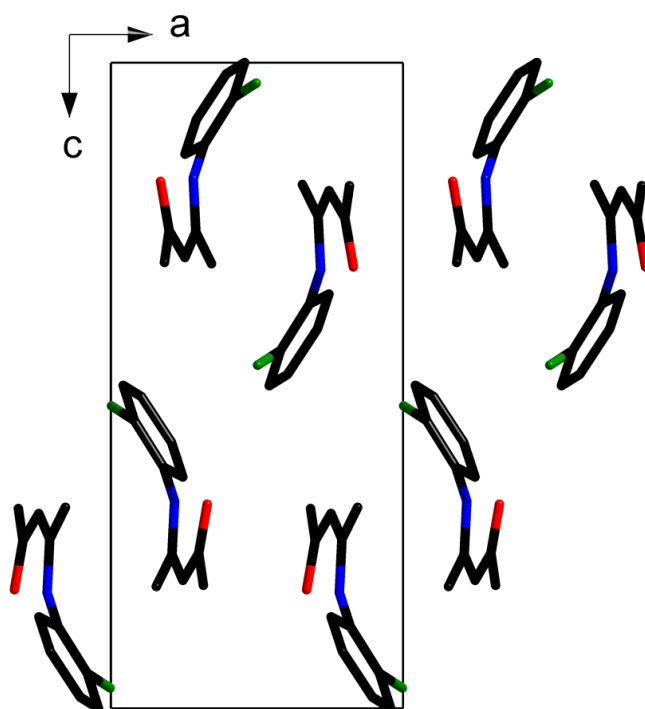


Figure 4.5. View of 2-Cl-PhonyH along the b-axis illustrating the packing style.

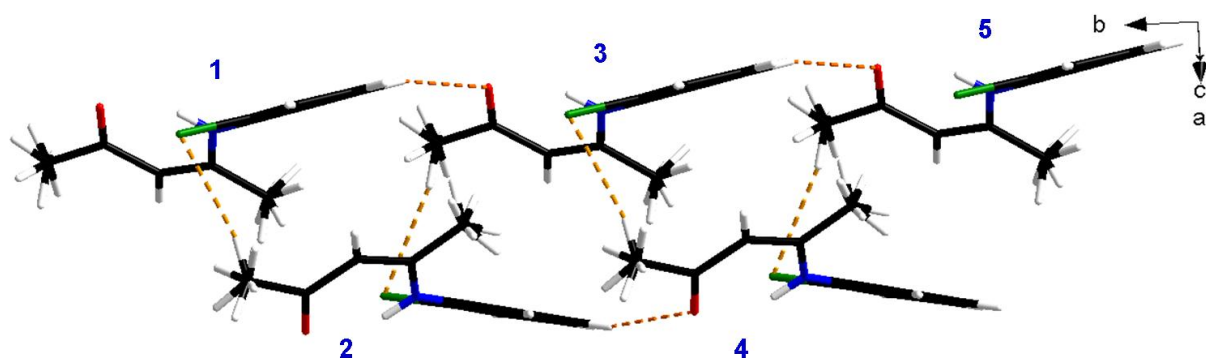


Figure 4.6. View of 2-Cl-PhonyH perpendicular to the b-axis illustrating the clockwise spiral packing style, influenced by the hydrogen-chloride and hydrogen-oxygen interactions.

2-Cl-PhonyH displays a linear stacking pattern, with C-H \cdots Cl interactions connecting the adjacent molecules in a right-handed (clockwise) screw along the b-axis (see Figure 4.6). This spiral stacking pattern is also supported by C-H \cdots O interactions in the direction of the b-axis. While the C-H \cdots Cl connects molecules in a +1 numerical order (refer to Figure 4.6), C-H \cdots O interactions are present in a +2 order, *i.e.* molecule 1 is connected to 3, which is connected to 5,

etc., while molecule 2 interacts with molecule 4, which in turn interacts with molecule 6. Each spiral column is connected to adjacent columns through C-H...N and C-H...O interactions.

4.2.2. Crystal Structure of 4-(4-Chlorophenylamino)pent-3-en-2-one (4-Cl-PhonyH)

The compound 4-Cl-PhonyH, where PhonyH = 4-(phenylamino)pent-3-en-2-one, was prepared as discussed in § 3.3.2 and crystallizes in the monoclinic space group Cc with $Z = 16$. The compound crystallizes with four independent molecules in the asymmetric unit and is shown in Figure 4.7, with important bond distances and angles reported in Table 4.4.

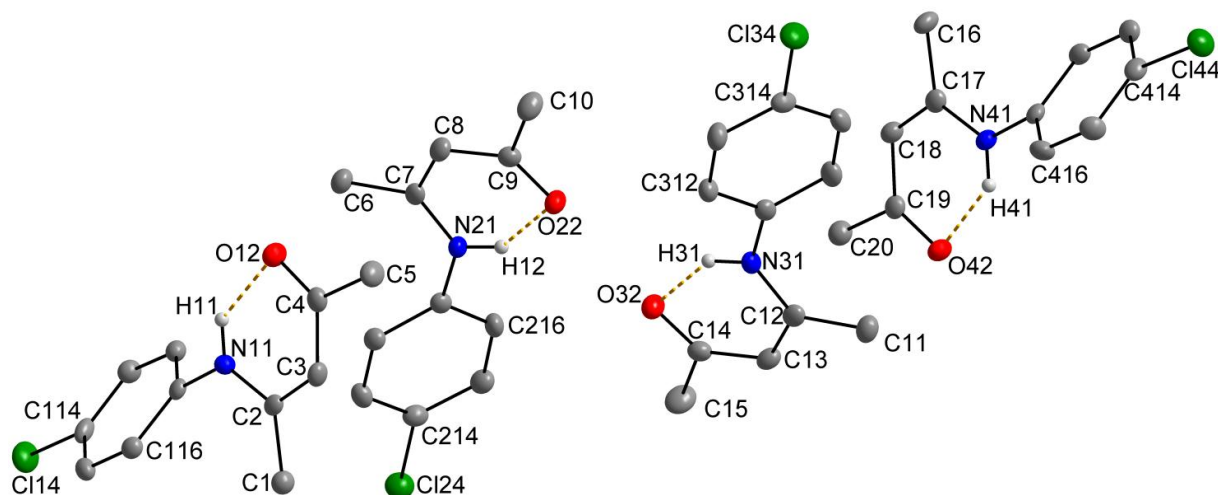


Figure 4.7. DIAMOND¹⁶ view of 4-Cl-PhonyH, where PhonyH = 4-(phenylamino)pent-3-en-2-one (50 % probability displacement ellipsoids). Selected hydrogen atoms and labels have been omitted for clarity. For the C atoms in the phenyl ring, the first digit indicates molecule number, the second digit indicates ring number and the third digit indicates the position of the atom in the ring. For the Cl atoms, the first digit indicates molecule number while the second digit indicates position on the phenyl ring.

Chapter 4

Table 4.4. Selected bond distances (Å) and angles (°) for 4-Cl-PhonyH.

	Molecule 1	Molecule 2	Molecule 3	Molecule 4
Atoms	Distances (Å)			
N ₁₁ -C ₁₁₁	1.423(3)	1.419(3)	1.406(3)	1.421(3)
N ₁₁ -C ₂	1.354(3)	1.347(3)	1.348(3)	1.353(3)
O ₁₂ -C ₄	1.248(3)	1.250(3)	1.252(3)	1.244(3)
C ₂ -C ₃	1.372(4)	1.376(4)	1.384(4)	1.373(4)
C ₃ -C ₄	1.424(4)	1.424(4)	1.418(4)	1.434(4)
N ₁₁ ⋯O ₁₂ (Bite distance)	2.676(3)	2.620(3)	2.634(3)	2.678(3)
Atoms	Angles (°)			
N ₁₁ -H ₁₁ ⋯O ₁₂	134.8(1)	137.5(2)	139.4(2)	134.7(2)
N ₁₁ -C ₂ ⋯C ₄ -O ₁₂	1.5(2)	1.7(2)	-3.0(2)	-1.7(2)
Dihedral angle ^a	51.71(8)	-41.30(8)	38.36(9)	-52.71(7)

^a Defined as the torsion angle between the N-C-C-C-O plane and the phenyl ring.

The packing modes of 4-Cl-PhonyH are mainly influenced by C-H⋯O and N-H⋯O interactions. Hydrogen interactions in the structure, illustrated in Figure 4.8, are shown in Table 4.5. The resulting packing style is shown in Figure 4.9.

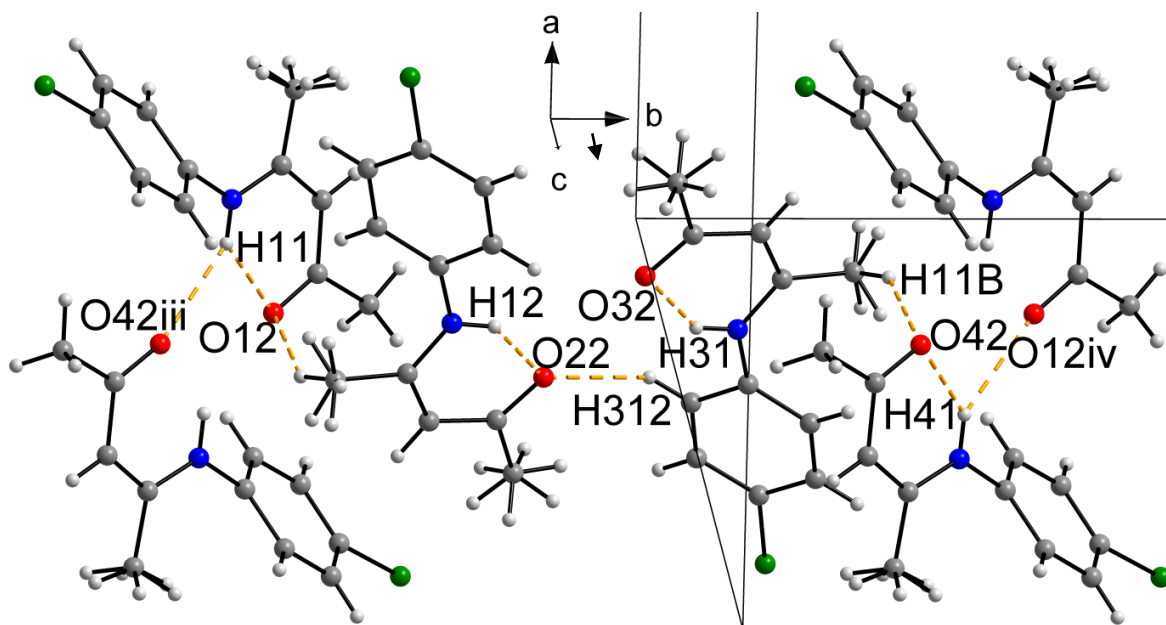


Figure 4.8. Partial unit cell for 4-Cl-PhonyH with important intra- and intermolecular hydrogen bonding interactions indicated with dashed lines. Symmetry operators are given in Table 4.5.

Chapter 4

Table 4.5. Hydrogen bonds for 4-Cl-PhonyH (Å and °).

D-H...A	d_{D-H} (Å)	$d_{H...A}$ (Å)	$d_{D...A}$ (Å)	\angle_{DHA} (°)
N ₁₁ -H ₁₁ ...O ₁₂	0.86	2.00	2.675(3)	134.9
N ₂₁ -H ₁₂ ...O ₂₂	0.86	1.92	2.620(3)	137.5
N ₃₁ -H ₃₁ ...O ₃₂	0.86	1.92	2.634(3)	139.4
N ₄₁ -H ₄₁ ...O ₄₂	0.86	2.00	2.678(3)	134.7
C ₆ -H _{6C} ...O ₁₂	0.96	2.53	3.341(3)	142.3
C ₁₁ -H _{11B} ...O ₄₂	0.96	2.44	3.266(3)	144.1
C ₃₁₂ -H ₃₁₂ ...O ₂₂	0.93	2.56	3.287(3)	135.5
N ₁₁ -H ₁₁ ...O ₄₂ ⁱⁱⁱ	0.86	2.43	3.137(3)	139.3
N ₄₁ -H ₄₁ ...O ₁₂ ^{iv}	0.86	2.45	3.164(3)	140.4

Symmetry code: (iii) x, y - 1, z (iv) x, y + 1, z

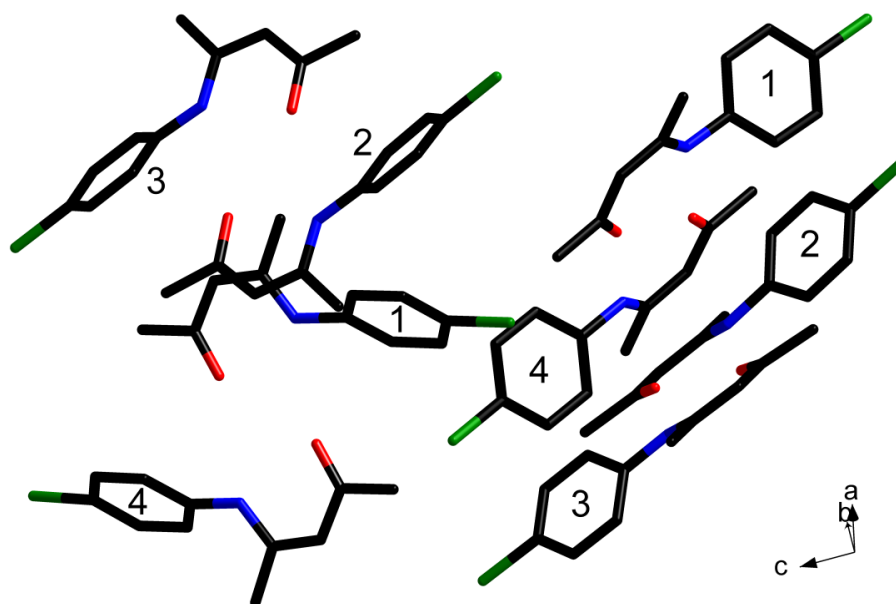


Figure 4.9. View of 4-Cl-PhonyH illustrating the packing style. The numbers '1', '2', '3' and '4' refer to the molecule number according to the previously defined numbering scheme (see Figure 4.1).

Crystallographic polymerism displayed by 4-Cl-PhonyH can clearly be seen from Figure 4.8, with bifurcated hydrogen bonds present for H₁₁ and H₄₁. This type of polymerism is made possible by the intermolecular N-H...O interactions between adjacent molecules. Since hydrogen bonds are long-range interactions, more than one acceptor A can bond to a group X-H. When there are two acceptors A₁ and A₂, the interaction is classified as a bifurcated hydrogen

Chapter 4

bond $X-H\cdots(A_1, A_2)$ ¹⁷, as was observed in this compound (see H_{11} and H_{41} in Figure 4.8). The packing modes of this compound are mainly influenced by $C-H\cdots O$ and $N-H\cdots O$ interactions. The compound crystallizes with four independent molecules in the asymmetric unit, which allows for an unusual opportunity to investigate the ranges of intramolecular bond parameters in the solid state (Table 4.4).

The majority of bond lengths and angles do not differ significantly between the different molecules with the exception of the dihedral angles, an indication that the orientation of the phenyl ring with respect to the $N_{11}-C_2-C_3-C_4-O_{12}$ structure plays a vital role in the single point energy of the molecules. The overlay of molecules one and three (a), two and four (b), one and four (c) and the mirror image of one with four (d) are shown in Figure 4.10.

¹⁷ Francl, M. M.; Petro, W. J.; Hehre, W. J.; Binkley, J. S.; Gordon, M. S.; DeFree, D. J.; Pople, J. A.; *J. Chem. Phys.* **1982**, *77*, 3654-3665.

Chapter 4

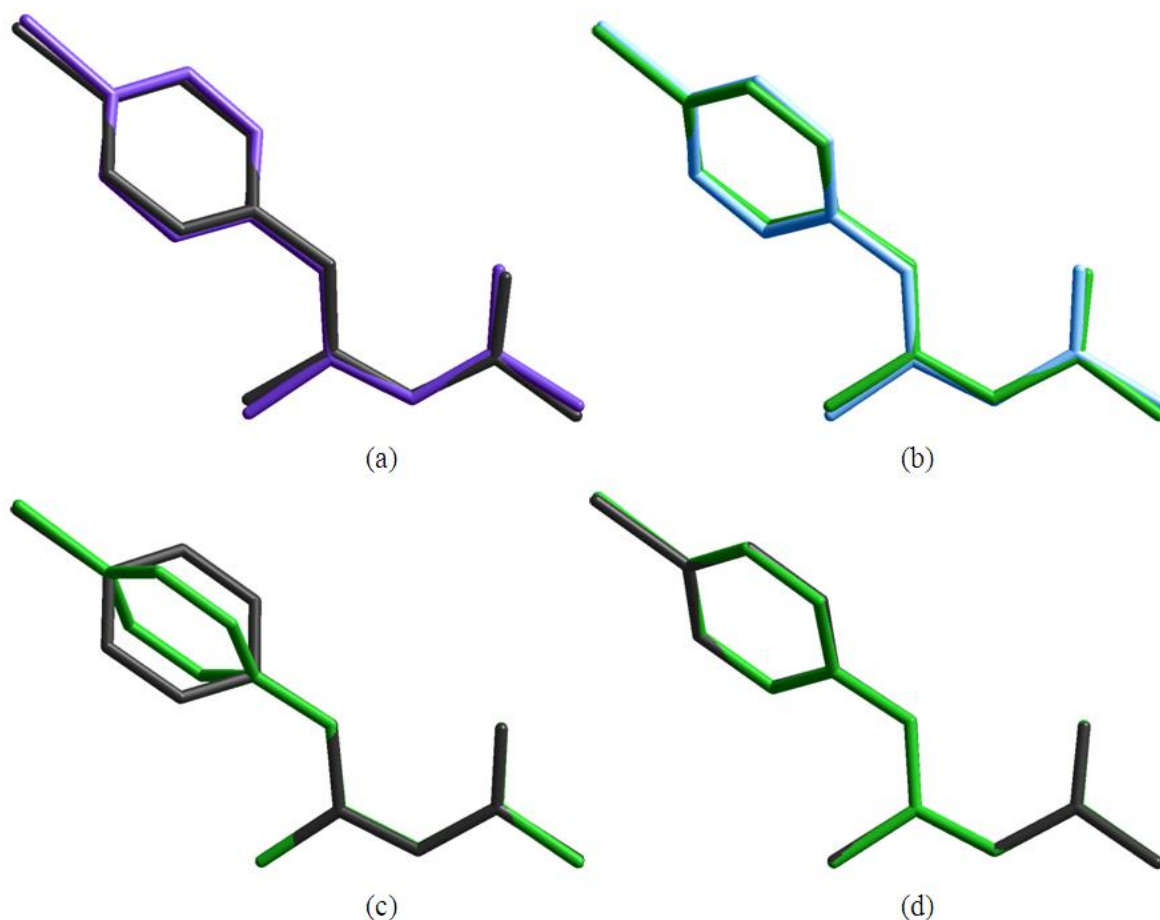


Figure 4.10. Overlay figures of the solid state structures of molecules (a) one (black) and three (violet), (b) two (light blue) and four (green), (c) one (black) and four (green) and (d) mirror image of one (black) and four (green) in 4-Cl-PhonyH. Overlay fit includes all non-hydrogen atoms. RMS value (a) = 0.169 Å; (b) = 0.136 Å; (c) = 0.895 Å; (d) = 0.055 Å.

Molecules one and three both display a positive dihedral angle, while molecules two and four are orientated towards a negative dihedral angle. Despite the resemblance in this regard, dihedral angles differ for molecules with similar orientations of the dihedral angles [$13.35(4)^\circ$ and $11.41(4)^\circ$ for one and three, and two and four, respectively]. The $N_{11}-C_2-C_3-C_4-O_{12}$ moieties of all molecules are only slightly distorted, as confirmed by the relatively small $N_{11}-C_2\cdots C_4-O_{12}$ torsion angles [smaller than $3.0(2)^\circ$].

4.2.3. Crystal Structure of 4-(2,4-Dichlorophenylamino)pent-3-en-2-one (2,4-Cl₂-PhonyH)

The compound 2,4-Cl₂-PhonyH, where PhonyH = 4-(phenylamino)pent-3-en-2-one, was prepared as discussed in § 3.3.3 and crystallizes in the triclinic space group $P\bar{1}$ with $Z = 4$. The compound crystallizes with two independent molecules in the asymmetric unit and is shown in Figure 4.11, with important bond distances and angles reported in Table 4.6.

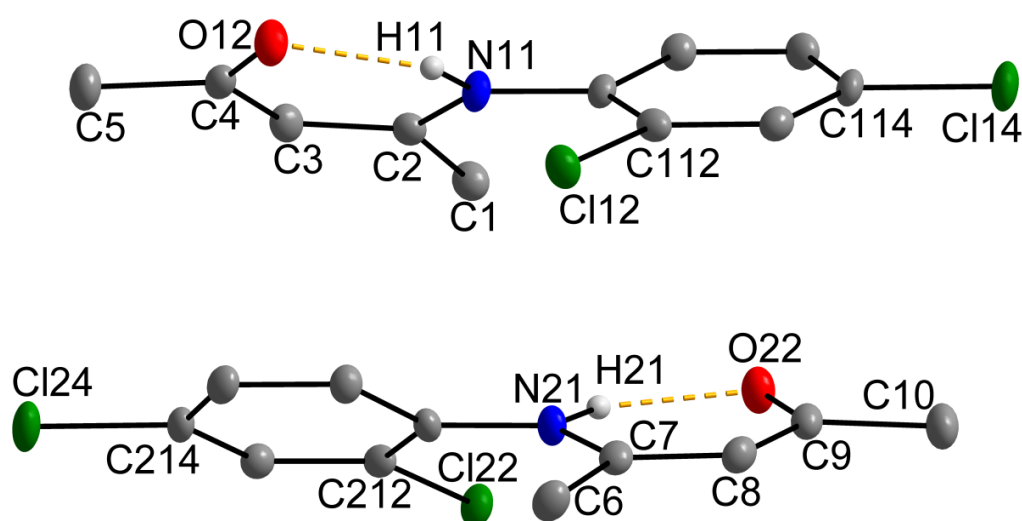


Figure 4.11. DIAMOND¹⁶ view of 2,4-Cl₂-PhonyH, where PhonyH = 4-(phenylamino)pent-3-en-2-one (50 % probability displacement ellipsoids). Selected hydrogen atoms and labels have been omitted for clarity. For the C atoms in the phenyl ring, the first digit indicates molecule number, the second digit indicates ring number and the third digit indicates the position of the atom in the ring. For the Cl atoms, the first digit indicates molecule number while the second digit indicates position on the phenyl ring.

Chapter 4

Table 4.6. Selected bond distances (Å) and angles (°) for 2,4-Cl₂-PhonyH.

	Molecule 1	Molecule 2
Atoms	Distances (Å)	
N ₁₁ -C ₁₁₁	1.403(3)	1.399(2)
N ₁₁ -C ₂	1.352(3)	1.353(2)
O ₁₂ -C ₄	1.254(3)	1.250(2)
C ₂ -C ₃	1.371(3)	1.372(3)
C ₃ -C ₄	1.428(3)	1.427(3)
N ₁₁ ⋯O ₁₂ (Bite distance)	2.628(2)	2.608(2)
Atoms	Angles (°)	
N ₁₁ -H ₁₁ ⋯O ₁₂	143(2)	141(2)
N ₁₁ -C ₂ ⋯C ₄ -O ₁₂	0.7(2)	0.1(2)
Dihedral angle ^a	42.00(6)	38.60(7)

^a Defined as the torsion angle between the N-C-C-C-O plane and the phenyl ring.

The packing modes of compound 2,4-Cl₂-PhonyH are influenced by intra- and intermolecular C-H⋯O and N-H⋯O interactions, as well as Type I Cl⋯Cl short contacts and π - π interactions {distances between centroids are 3.8125(4) Å and 3.6751(4) Å in either direction, with the phenyl ring and N₁₁-C₂-C₃-C₄-O₁₂ planes parallel to each other [interplanar angles of 3.19(7)° and 3.14(8)°]}. Hydrogen interactions in the structure, illustrated in Figure 4.12, are shown in Table 4.7. The resulting packing style is shown in Figure 4.13.

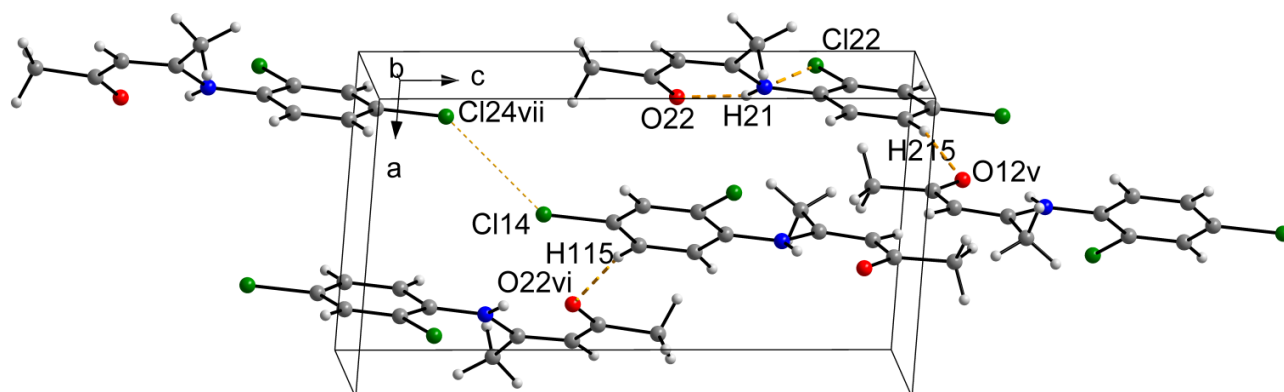


Figure 4.12. Partial unit cell for 2,4-Cl₂-PhonyH with important intra- and intermolecular hydrogen bonding interactions indicated with dashed lines. Symmetry operators are given in Table 4.7.

Chapter 4

Table 4.7. Hydrogen bonds for 2,4-Cl₂-PhonyH (Å and °).

D-H···A	d _{D-H} (Å)	d _{H···A} (Å)	d _{D···A} (Å)	< _{DHA} (°)
N ₂₁ -H ₂₁ ···Cl ₂₂	0.90(2)	2.64(2)	2.963(2)	102(2)
N ₂₁ -H ₂₁ ···O ₂₂	0.90(2)	1.85(2)	2.607(2)	141(2)
C ₁₁₅ -H ₁₁₅ ···O ₂₂ ^v	0.95	2.34	3.269(2)	167.0
C ₂₁₅ -H ₂₁₅ ···O ₁₂ ^{vi}	0.95	2.39	3.320(2)	167.1

Symmetry code: (v) -x + 1, -y + 2, -z + 1 (vi) -x + 1, -y + 1, -z + 2 (vii) x, y, z - 1

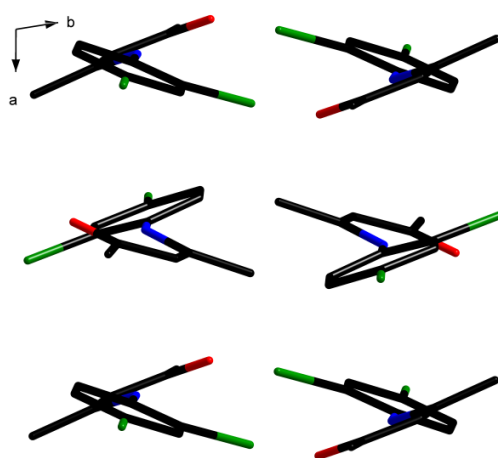


Figure 4.13. View of 2,4-Cl₂-PhonyH along the b-axis illustrating the packing style. π - π interactions between the phenyl ring and N-C-C-C-O moieties are clearly visible.

A short chloride-chloride contact was observed for Cl₁₄···Cl₂₄^{viii}, with a distance r_i of 3.4521(7) Å. θ_1 and θ_2 are 140.53(7)° and 141.05(6)° respectively, classifying the contact as Type I^{11.b}. The compound crystallizes with two independent molecules in the asymmetric unit with molecule two displaying the lowest single point energy (see Chapter 5). The overlay of molecules one and two are shown in Figure 4.14.

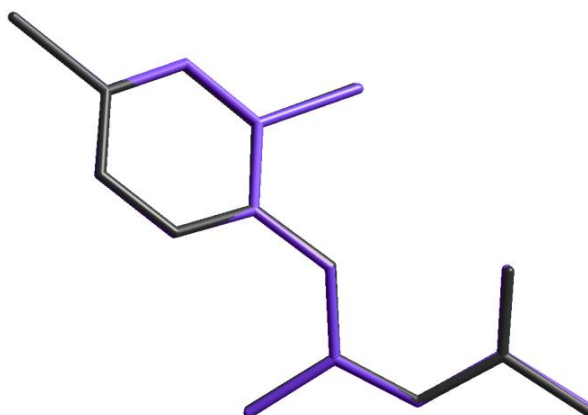


Figure 4.14. Overlay figures of the solid state structures of molecules one (black) and two (violet) in 2,4-Cl₂-PhonyH. Overlay fit includes all non-hydrogen atoms. RMS value = 0.049 Å.

Although the RMS value is very low, some subtle differences exist between the two molecules, resulting in an energy difference of 30.9 kJ.mol⁻¹. Both molecules display a positive dihedral angle; 42.00(6)° and 38.60(7)° for molecules one and two, respectively. While the N₁₁-C₁₁₁, N₁₁-C₂, O₁₂-C₄, C₂-C₃ and C₃-C₄ distances between the two molecules are similar, the N₁₁···O₁₂ distances differ significantly: 2.628(2) Å for molecule one *versus* 2.608(2) Å for molecule two.

4.2.4. Crystal Structure of 4-(2,6-Dichlorophenylamino)pent-3-en-2-one · 0.5 [2,6-Dichlorophenylamine] Adduct [2,6-Cl₂-PhonyH·0.5(2,6-Cl₂-Phenylamine)]¹⁸

The compound 2,6-Cl₂-PhonyH, where PhonyH = 4-(phenylamino)pent-3-en-2-one, was prepared as discussed in § 3.3.4 and crystallizes in the monoclinic space group *C2/c* with *Z* = 8. The compound, shown in Figure 4.15, crystallized with one amine adduct for every two compound molecules. Important bond distances and angles reported in Table 4.8.

¹⁸ Venter, G.J.S., Steyl, G., Roodt, A. *Acta Cryst.* **2013**, *E69*, o34.

Chapter 4

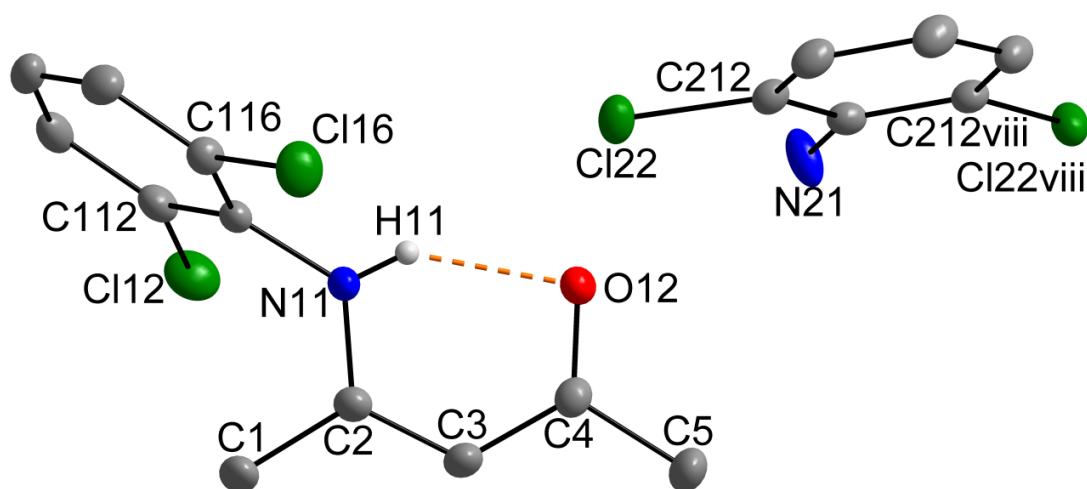


Figure 4.15. DIAMOND¹⁶ view of 2,6-Cl₂-PhonyH, where PhonyH = 4-(phenylamino)pent-3-en-2-one (50 % probability displacement ellipsoids). Selected hydrogen atoms and labels have been omitted for clarity. For the C atoms in the phenyl ring, the first digit indicates molecule number, the second digit indicates ring number and the third digit indicates the position of the atom in the ring. For the Cl atoms, the first digit indicates molecule number while the second digit indicates position on the phenyl ring. Atoms generated by symmetry are indicated by lower case roman numerical labels corresponding to the symmetry operator (viii) $-x, y, -z + \frac{1}{2}$.

Table 4.8. Selected bond distances (Å) and angles (°) for 2,6-Cl₂-PhonyH.

Atoms	Distances (Å)	Atoms	Angles (°)
N ₁₁ -C ₁₁₁	1.416(2)	N ₁₁ -H ₁₁ ⋯O ₁₂	143(2)
N ₁₁ -C ₂	1.346(2)	N ₁₁ -C ₂ ⋯C ₄ -O ₁₂	-0.9(1)
O ₁₂ -C ₄	1.251(2)	Dihedral angle ^a	81.79(6)
C ₂ -C ₃	1.376(2)		
C ₃ -C ₄	1.426(3)		
N ₁₁ ⋯O ₁₂ (Bite distance)	2.623(2)		

^a Defined as the torsion angle between the N-C-C-C-O plane and the phenyl ring.

Hydrogen interactions, both intra- and intermolecular, are present in 2,6-Cl₂-PhonyH (Figure 4.16, Table 4.9). Furthermore, π - π stacking occurs between phenyl rings in adjacent molecules, with a distance of 3.7247(1) Å between ring centroids and an angle of 0.00(8)° between parallel phenyl ring planes. The resulting packing style is shown in Figure 4.17.

Chapter 4

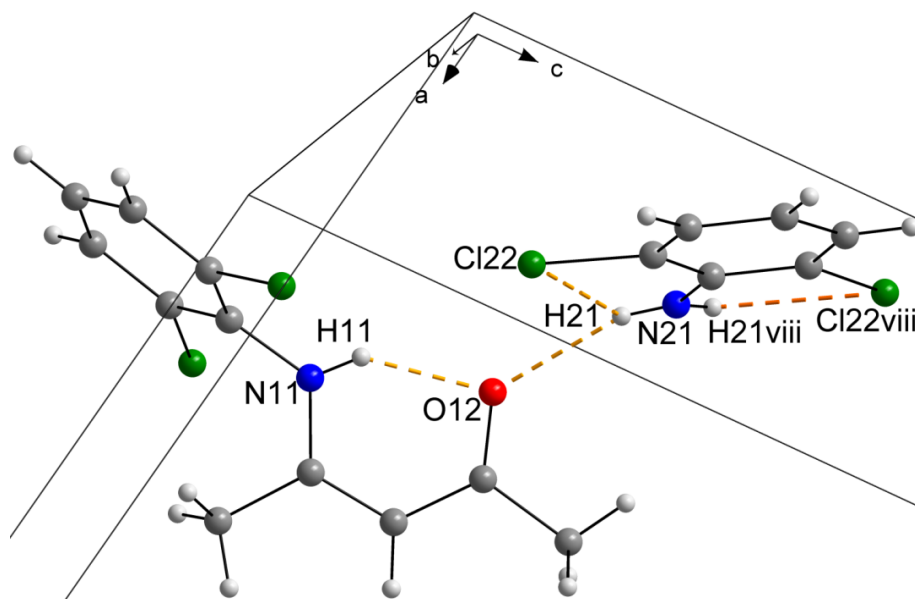


Figure 4.16. Partial unit cell for 2,6-Cl₂-PhonyH with important intra- and intermolecular hydrogen bonding interactions indicated with dashed lines. Symmetry operators are given in Table 4.9.

Table 4.9. Hydrogen bonds for 2,6-Cl₂-PhonyH (Å and °).

D-H...A	d_{D-H} (Å)	d_{H...A} (Å)	d_{D...A} (Å)	∠_{DHA} (°)
N ₁₁ -H ₁₁ ...O ₁₂	0.79(2)	1.94(2)	2.623(2)	143(2)
N ₂₁ -H ₂₁ ...Cl ₂₂	0.80(2)	2.56(2)	2.9694(9)	114(2)
N ₂₁ -H ₂₁ ...O ₁₂	0.80(2)	2.23(2)	2.975(2)	155(2)

Symmetry codes: (viii) -x, y, -z + ½

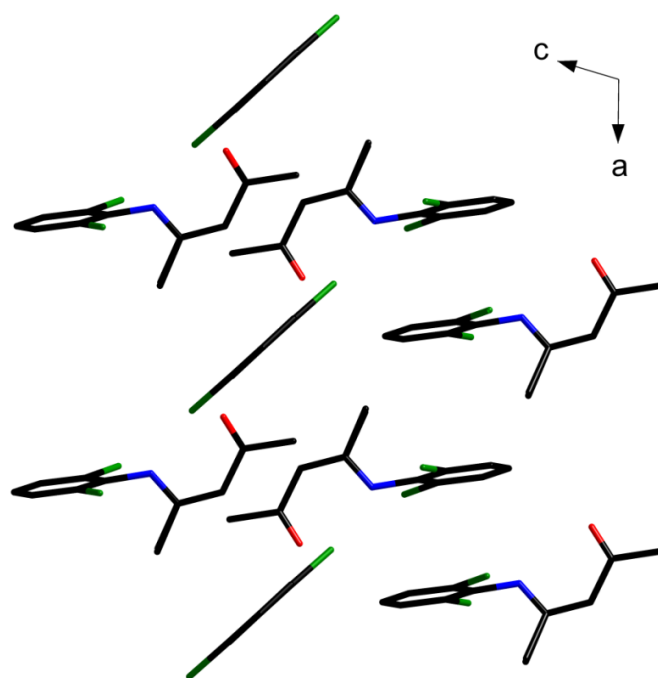


Figure 4.17. View of 2,6-Cl₂-PhonyH along the b-axis illustrating the packing style. π - π interactions between the phenyl ring moieties are clearly visible.

4.3. Discussion

All derivatives of PhonyH, as mentioned above, are isostructural and the structures have similar spatial arrangements; the enaminoketone fragment (N₁₁-C₂-C₃-C₄-O₁₂) is essentially planar due to the strong N₁₁-H₁₁···O₁₂ hydrogen bonds in the molecule, with the largest N₁₁-C₂···C₄-O₁₂ torsion angle being 5.5(1)° for 2-Cl-PhonyH (see Table 4.11). This angle varies for the range of compounds in the order of -3.0(2)° and 1.7(2)° for 4-Cl-PhonyH to 0.1(2)° and 0.7(2)° for 2,4-Cl₂-PhonyH, and is -1.2(2)° for 2,6-Cl₂-PhonyH. The dihedral angle between the enaminoketone fragment and the phenyl ring is 46.52(5)° for 2-Cl-PhonyH, varies between 51.71(8)° and -52.71(7)° for 4-Cl-PhonyH and between 38.60(7)° and 42.00(6)° for 2,4-Cl₂-PhonyH. The largest dihedral angle of 87.5(1)° is observed in compound 2,6-Cl₂-PhonyH, where the steric influence of the chloride atoms on the 2- and 6-positions have a significant influence on the geometry of the molecule. Disordered hydrogen atoms on the methyl moieties are observed for 2-Cl-PhonyH and 4-Cl-PhonyH, but are absent in 2,4-Cl₂-PhonyH and 2,6-Cl₂-PhonyH.

Chapter 4

The $N_{11}\cdots O_{12}$ distance in compound 2,6-Cl₂-PhonyH is 0.143(2) Å longer than the second longest distance, indicating a widening of the $N_{11}-C_2-C_3-C_4-O_{12}$ structure that is significantly larger than those of similar compounds (see Table 4.10). These compounds are illustrated in Figure 4.18 for comparison. In fact, 2,6-Cl₂-PhonyH differs from other compounds in several respects (see Table 4.11), which could possibly be attributed to the aniline adduct contained in the crystal.

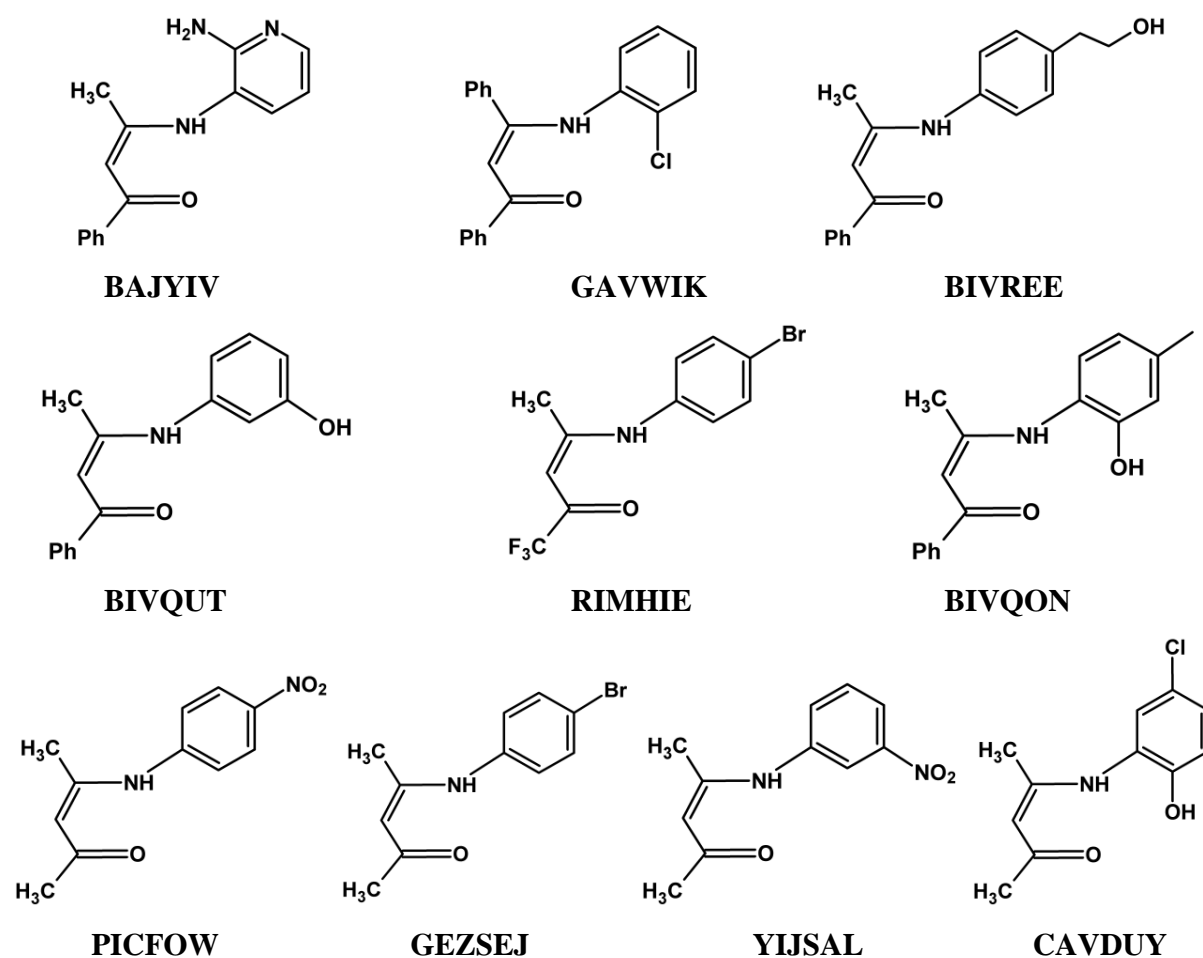


Figure 4.18. Illustrations of comparative enaminoketones found in literature, ordered according to ascending $N\cdots O$ distance. BAJYIV = 3-(2-aminopyridin-3-ylamino)-1-phenyl-2-buten-1-one; GAVWIK = 3-((2-chlorophenyl)amino)-1,3-diphenylprop-2-en-1-one; BIVREE = (Z)-3-(4-(2-hydroxyethyl)phenylamino)-1-phenylbut-2-en-1-one; BIVQUT = (Z)-3-(3-hydroxyphenylamino)-1-phenylbut-2-en-1-one; RIMHIE = *N*-(4-bromophenyl)-1,1,1-trifluoroacetylacetonimine; BIVQON = 3-(2-hydroxy-4-methylphenylamino)-1-phenylbut-2-en-1-one; PICFOW = 4-*p*-nitrophenylamino-pent-3-en-2-one; GEZSEJ = *N*-(4-bromophenyl)acetylacetonimine; YIJSAL = 2-(3-nitrophenylamino)-2-pent-3-en-4-one; CAVDUY = 4-chloro-2-(4-oxopent-2-en-2-ylamino)phenol. References are given in Table 4.10.

Chapter 4

Table 4.10. Comparison of selected geometrical parameters in reported compounds with similar enaminketones.

	CSD ¹² Reference code ^b	Displays dimerism	$d(\text{N}\cdots\text{O})$ (Å) ^c	$d(\text{N}_{11}\text{-C}_2)$ (Å) ^c	$d(\text{O}_{12}\text{-C}_4)$ (Å) ^c	$\text{N}_{11}\text{-C}_2\cdots\text{C}_4\text{-O}_{12}$ (°) ^c	Dihedral Angle ^a (°)
1	BAJYIV ¹⁹	No	2.563(2)	1.345(2)	1.257(2)	-0.8(1)	53.27(4)
2	GAVWIK ²⁰	No	2.670(3)	1.356(4)	1.250(3)	-5.7(2)	50.16(8)
3	BIVREE ²²	Yes	2.617(2)	1.338(2)	1.259(2)	-1.9(1)	39.26(5)
IV ^d		No	2.618(3)	1.353(5)	1.252(5)	0.4(3)	40.30(9)
V ^d		No	2.623(2)	1.346(2)	1.251(2)	-0.9(1)	81.79(6)
4	BIVQUT ²²	No	2.626(4)	1.326(5)	1.260(4)	0.5(3)	47.2(1)
5	RIMHIE ²¹	No	2.628(9)	1.363(9)	1.23(1)	0.0(7)	61.2(2)
II ^d		No	2.633(2)	1.347(2)	1.249(2)	5.5(1)	46.52(5)
6	BIVQON ²²	Yes	2.650(3)	1.341(3)	1.265(2)	8.1(2)	58.53(6)
III ^d		Yes	2.652(6)	1.351(6)	1.249(6)	2.0(4)	46.0(2)
I ^d	SEHGOC ⁶	No	2.658(3)	1.352(3)	1.244(3)	1.4(2)	32.03(9)
7	PICFOW ²³	No	2.660(3)	1.362(3)	1.245(4)	0.9(2)	14.6(1)
8	GEZSEJ ²⁴	Yes	2.70(1)	1.32(1)	1.25(1)	0.7(7)	47.9(2)
9	YIJSAL ²⁵	No	2.702(5)	1.352(5)	1.243(5)	-0.9(3)	38.3(1)
10	CAVDUY ²⁶	No	2.686(3)	1.339(3)	1.256(3)	-0.7(2)	44.64(7)
Average			2.6(1)	1.35(2)	1.25(2)	1(1)	46.8(4)

^a Defined as the torsion angle between the N-C-C-C-O plane and the phenyl ring.

^b BAJYIV = 3-(2-aminopyridin-3-ylamino)-1-phenyl-2-buten-1-one; GAVWIK = 3-((2-chlorophenyl) amino)-1,3-diphenylprop-2-en-1-one; BIVREE = (Z)-3-(4-(2-hydroxyethyl)phenylamino)-1-phenylbut-2-en-1-one; BIVQUT = (Z)-3-(3-hydroxyphenylamino)-1-phenylbut-2-en-1-one; RIMHIE = N-(4-bromophenyl)-1,1,1-trifluoroacetylacetoneimine; BIVQON = 3-(2-hydroxy-4-methylphenylamino)-1-phenylbut-2-en-1-one; PICFOW = 4-*p*-nitrophenylamino-pent-3-en-2-one; GEZSEJ = N-(4-bromophenyl)acetylacetoneimine; YIJSAL = 2-(3-nitrophenylamino)-2-pent-3-en-4-one; CAVDUY = 4-chloro-2-(4-oxopent-2-en-2-ylamino)phenol.

^c Average values are used for compounds with more than one independent molecule in the asymmetric unit.

^d I = PhonyH; II = 2-Cl-PhonyH; III = 4-Cl-PhonyH; IV = 2,4-Cl₂-PhonyH; V = 2,6-Cl₂-PhonyH.

¹⁹ Liszkiewicz, H.; Kowalska, M.W.; Glowiak, T.; Wietrzyk, J.; Opolski A. *Pol. J. Chem.* **2002**, 76, 1607.

²⁰ Shi, Y.-C.; Zhang, S.-H. *Acta Cryst.* **2005**, 61, o3748.

²¹ Sergienko, V.S.; Abramenko, V.L.; Ilyukhin, A.B. *Zh. Neorg. Khim. (Russ.)(Russ. J. Inorg. Chem.)* **1997**, 42, 945.

²² Rodriguez, M.; Santillan, R.; Lopez, Y.; Farfan, N.; Barba, V.; Nakatani, K.; Baez, E.V.G.; Padilla-Martinez, I.I. *Supramol. Chem.* **2007**, 19, 641.

²³ Da Silva, M.A.V.R.; Da Silva, M.D.M.C.R.; Paiva, J.P.A.; Nogueira, I.M.C.S.; Damas, A.M.; Barkley, J.V.; Harding, M.M.; Akello, M.J.; Pilcher, G. *J. Chem. Soc., Perkin Trans. 2* **1993**, 1765.

²⁴ Sergienko, V.S.; Garnovskii, A.D.; Abramenko, V.L.; Porai-Koshits, M.A. *Koord. Khim. (Russ.)(Coord. Chem.)* **1987**, 13, 1695.

²⁵ Olejnik, Z.; Lis, T.; Kowal, R.; Miniewicz, A. *Pol. J. Chem.* **1993**, 67, 347.

²⁶ Arici, C.; Tahir, M.N.; Ulku, D.; Atakol, O. *Acta Cryst.* **1999**, C55, 1691.

Chapter 4

Table 4.11. Selected bond lengths (Å) and angles (°) in PhonyH derivatives.

	II		III		IV		V	
	1	2	3	4	1	2		
N ₁₁ -C ₁₁₁	1.408(2)	1.423(3)	1.419(3)	1.406(3)	1.421(3)	1.403(3)	1.399(2)	1.416(2)
N ₁₁ -C ₂	1.347(2)	1.354(3)	1.347(3)	1.348(3)	1.353(3)	1.352(3)	1.353(2)	1.346(2)
O ₁₂ -C ₄	1.249(2)	1.248(3)	1.250(3)	1.252(3)	1.244(3)	1.254(3)	1.250(2)	1.251(2)
N ₁₁ ⋯O ₁₂	2.633(2)	2.676(3)	2.620(3)	2.634(3)	2.678(3)	2.628(2)	2.608(2)	2.623(2)
C ₂ -C ₃	1.379(2)	1.372(4)	1.376(4)	1.384(4)	1.373(4)	1.371(3)	1.372(3)	1.376(2)
C ₃ -C ₄	1.428(2)	1.424(4)	1.424(4)	1.418(4)	1.434(4)	1.428(3)	1.427(3)	1.426(3)
N ₁₁ -	138.9(2)	134.8(1)	137.5(2)	139.4(2)	134.7(2)	143(2)	141(2)	143(2)
H ₁₁ ⋯O ₁₂	5.5(1)	1.5(2)	1.7(2)	-3.0(2)	-1.7(2)	0.7(2)	0.1(2)	-0.9(1)
N ₁₁ -	46.52(5)	51.71(8)	-41.30(8)	38.36(9)	-52.71(7)	42.00(6)	38.60(7)	81.79(6)
C ₂ ⋯C ₄ -								
O ₁₂								
Dihedral								
angle ^a								

^a Defined as the torsion angle between the N-C-C-C-O plane and the phenyl ring as shown in Figure 4.2. A positive angle denotes a clockwise rotation.

In addition, the N₁₁-C₂ and O₁₂-C₄ distances are significantly shorter than other enaminoketone compounds. The dihedral angle of 2,6-Cl₂-PhonyH [87.5(1)°] is close to 90°, assumed due to the steric influence of the two chloride atoms on the 2- and 6-positions of the phenyl ring.

All compounds in Table 4.10 adhere to the criteria for enaminoketones, containing both oxygen and nitrogen atoms in positions enabling electron donation, as well as an unsaturated C-C bond in the backbone. Despite some significant differences between the compounds involved in this study and related structures found in literature, the compounds discussed in this chapter share characteristics with those complexes in Table 4.10. Generally speaking the compounds are nearly planar, with N₁₁-C₂⋯C₄-O₁₂ angles varying from 0.0(7)° for compound **5** to 8.1(2)° for compound **6**. The value for compound **6** is however of an outlying nature together with the value of 5.5(1)° for 2-Cl-PhonyH. Other compounds mostly display N₁₁-C₂⋯C₄-O₁₂ angles of less than 1° and only in rare cases between 1° and 3°. Dihedral angles greatly deviate from the ideal value of 0° for more effectively delocalized systems with values between 32.03(9)° for PhonyH and 81.79(6)° for 2,6-Cl₂-PhonyH. This can be contributed to the steric bulk of the phenyl

Chapter 4

moiety which takes precedence over the optimal position of π -orbitals for delocalization over the unsaturated C-C bond. The bite angles of the compounds can be described by the N \cdots O distances. These distances vary from 2.563(2) Å to 2.686(3) Å for compounds **1** and **10**, and are influenced by the electronic properties of the substituents on the phenyl moiety on the nitrogen atom. Compounds containing more electron withdrawing substituents tend to display smaller N \cdots O distances, which allows tailoring of a system to increase or decrease the bite angle of such a ligand as needed.

4.4. Conclusion

Large differences were observed regarding bond distances and angles between the separate compounds, confirmed through X-ray diffraction, infrared spectroscopy and NMR techniques. The compounds crystallize in a range of space groups and varying crystal systems. This emphasizes the influences of intra- and intermolecular hydrogen and π - π interactions as well as chloride-chloride short contacts on the packing modes of the solid state compounds, which is in turn influenced by the position of chloride atoms on the phenyl ring. The contribution of chloride on the geometrical parameters can clearly be seen in 4-Cl-PhonyH, where the dihedral angle is influenced by the position of the chloride moiety on the phenyl ring, as opposed to packing affects. This observation is supported by information from the calculated and literature structures, where the electronic properties of substituents on the phenyl ring impacts the geometrical parameters of the respective compounds. This property allows for the tailoring of enaminoketone compounds to suit different criteria for their utilization as ligand systems. The DFT calculated structures of these compounds will be discussed in Chapter 5.

Chapter 4

5 Theoretical Study of 4-Phenylamino pent-3-en-2-one Functionalities

5.1. Introduction

In the past decade the use of computational chemistry as aid to experimental data has greatly increased with the development of user-friendly software packages and affordable yet powerful computer systems. Various methods exist for investigating molecular geometry, energies of molecules, transition states and chemical reactivity and can be divided into five classes¹:

1. Molecular mechanics (MM)
2. *Ab initio* calculations
3. Semi-empirical (SE) calculations
4. Density functional theory (DFT) calculations
5. Molecular dynamics

Molecular mechanics is the simplest method and is based on calculating the total energy of a compound through simple algebraic expressions, without computing a wave function or total electron density. The energy expression consists of simple classical equations, such as the harmonic oscillator equation (Hooke's law) in order to describe the energy associated with bond stretching, bending, rotation and intermolecular forces, such as Van der Waals interactions and hydrogen bonding. All of the constants in these equations must be obtained from experimental data or an *ab initio* calculation².

¹ Lewars, E. *Computational Chemistry: Introduction to the theory and application of molecular and quantum mechanics*. Kluwer Academic Publishers, New York, **2004**.

² Cramer, C.J. *Essentials of Computational Chemistry: Theories and Models*. John Wiley & Sons Ltd., Chichester, **2004**.

Chapter 5

The term "*Ab Initio*" is latin for "from the beginning". For the purpose of these types of calculations mathematical and computational techniques were developed to describe computations directly from theoretical principles, with no inclusion of experimental data. This refers to an approximate quantum mechanical calculation. The most common type of *ab initio* calculation is called a Hartree Fock calculation (abbreviated HF), which is an approximate method for the determination of the ground-state wave function and ground-state energy of a quantum many-body system.

Semi-empirical calculations are set up with HF calculation as framework, but certain pieces of information, such as two electron integrals, are approximated or completely omitted. This is employed when treating large molecules where the full HF method without the approximations is too expensive. Semi-empirical calculations are much faster than their *ab initio* counterparts, but their results can be very wrong if the molecule being computed is not similar enough to the molecules in the database used to parameterize the method. In order to correct for the errors introduced by omitting part of the calculation, the method is parameterized by curve fitting in a few parameters or numbers, in order to give the best possible agreement with experimental data.

Molecular dynamics simulate physical, time-dependent movements of atoms and molecules. A series of time-correlated points are generated by propagating a starting set of coordinates and velocities according to Newton's equations of motion in a series of finite time steps³. The method was originally conceived within theoretical physics in the late 1950's and early 1960's, but is applied today mostly in materials science and the modeling of biomolecules.

DFT calculations, rather than being based on the wave function, express the total energy in terms of one-electron density. This originated with a theorem by Hohenburg and Kohn⁴. The electron density is calculated as a linear combination of basis functions similar to those employed to describe Hartree-Fock orbitals, but describes Kohn-Sham orbitals which are not mathematically equivalent to Hartree-Fock or natural orbitals³. Recently DFT calculations have become prominent with B3LYP⁵ being widely used. This functional, a hybrid between quicker methods

³ Jensen, F. *Introduction to Computational Chemistry*, 2nd Edition, John Wiley & Sons, Ltd. Chichester, **2007**.

⁴ Hohenburg, P.; Kohn, W. *Phys. Rev.* **1964**, *136*, B684.

⁵ Becke, A.D. *J. Chem. Phys.* **1993**, *98*, 5648-5652.

Chapter 5

with lower accuracy and more accurate, time-consuming methods, is known for its reasonable results and computational requirements while retaining fair accuracy.

In this study the focus will be on the DFT class of computational chemistry. In the following paragraphs a theoretical investigation is presented on the behavior of 4-phenylaminopent-3-en-2-one (PhonyH) type compounds in respect to functionalization and hydrogen bond formation. Electronic effects are included in the study to determine the effects of strong electron-withdrawing groups, such as chloride moieties.

5.2. Results

The calculated energies for the compounds as described in Chapter 4 are compared in Table 5.1. An overview of the cell dimensions in Chapter 4 are related in Table 5.2. The numbering scheme of the DFT optimized structures are the same as in Chapter 4, and are reported for convenience in Figure 5.2. Energy levels were adjusted such that the compound with the lowest energy for the optimized structures, PhonyH⁶, which is included for comparison, and single point structures obtained by using the solid state data given in Chapter 4 without any optimization, 2,4-Cl₂-PhonyH, are shown as the respective minima. The relative energies of the different compounds, as determined and optimized through DFT calculations using GAUSSIAN-03W⁷, are shown in Figure 5.1. Important bond distances and angles are reported in Table 5.3.

⁶ Shaheen, F.; Marchio, L.; Badshaha, A.; Khosac, M.K. *Acta Cryst.* **2006**, E62, o873.

⁷ Frisch, M.J.; Trucks, G.W.; Schlegel, H.B.; Scuseria, G.E.; Robb, M.A.; Cheeseman, J.R.; Montgomery Jr., J.A.; Vreven, T.; Kudin, K.N.; Burant, J.C.; Millam, J.M.; Iyengar, S.S.; Tomasi, J.; Barone, V.; Mennucci, B.; Cossi, M.; Scalmani, G.; Rega, N.; Petersson, G.A.; Nakatsuji, H.; Hada, M.; Ehara, M.; Toyota, K.; Fukuda, R.; Hasegawa, J.; Ishida, M.; Nakajima, T.; Honda, Y.; Kitao, O.; Nakai, H.; Klene, M.; Li, X.; Knox, J.E.; Hratchian, H.P.; Cross, J.B.; Bakken, V.; Adamo, C.; Jaramillo, J.; Gomperts, R.; Stratmann, R.E.; Yazyev, O.; Austin, A.J.; Cammi, R.; Pomelli, C.; Ochterski, J.W.; Ayala, P.Y.; Morokuma, K.; Voth, G.A.; Salvador, P.; Dannenberg, J.J.; Zakrzewski, V.G.; Dapprich, S.; Daniels, A.D.; Strain, M.C.; Farkas, O.; Malick, D.K.; Rabuck, A.D.; Raghavachari, K.; Foresman, J.B.; Ortiz, J.V.; Cui, Q.; Baboul, A.G.; Clifford, S.; Cioslowski, J.; Stefanov, B.B.; Liu, G.; Liashenko, A.; Piskorz, P.; Komaromi, I.; Martin, R.L.; Fox, D.J.; Keith, T.; Al-Laham, M.A.; Peng, C.Y.; Nanayakkara, A.; Challacombe, M.; Gill, P.M.W.; Johnson, B.; Chen, W.; Wong, M.W.; Gonzalez, C.; Pople, J.A. GAUSSIAN-03, Revision C.01, Gaussian, Inc., Wallingford, CT, **2004**.

Chapter 5

Table 5.1. Relative energy values for 4-(phenylamino)pent-3-en-2-one (PhonyH) and derivatives thereof, relative to the single point energy of the second molecule of 2,4-Cl₂-PhonyH and the optimized energy of PhonyH.

Compound	$\Delta E_{\text{Single point}}$ (kJ.mol ⁻¹)	$\Delta E_{\text{Optimized}}$ (kJ.mol ⁻¹)
PhonyH	183.0	0.00
2-Cl-PhonyH	112.4	9.56
4-Cl-PhonyH molecule 1	223.7	1.99
4-Cl-PhonyH molecule 2	226.2	1.99
4-Cl-PhonyH molecule 3	225.1	1.99
4-Cl-PhonyH molecule 4	221.0	1.99
2,4-Cl₂-PhonyH molecule 1	30.87	10.6
2,4-Cl₂-PhonyH molecule 2	0.000	10.6
2,6-Cl₂-PhonyH	158.1	18.0

Table 5.2. Cell dimension overview for 4-(phenylamino)pent-3-en-2-one (PhonyH) and the chloride derivatives thereof.

	PhonyH⁶	2-Cl-PhonyH	4-Cl-PhonyH	2,4-Cl₂-PhonyH	2,6-Cl₂-PhonyH
Crystal system	Monoclinic	Orthorhombic	Monoclinic	Triclinic	Monoclinic
Space group	<i>P2₁/c</i>	<i>P2₁2₁2₁</i>	<i>Cc</i>	<i>P$\bar{1}$</i>	<i>C2/c</i>
<i>a</i> (Å)	9.157(3)	7.3264(3)	14.137(5)	7.3893(8)	15.7140(1)
<i>b</i> (Å)	11.040(7)	8.7103(4)	14.537(5)	10.933(1)	8.7210(2)
<i>c</i> (Å)	10.130(5)	16.1960(7)	20.478(5)	13.764(2)	22.9950(4)
α (°)	90	90	90	90.040(5)	90
β (°)	106.10(3)	90	100.516(5)	94.751(4)	104.794 (1)
γ (°)	90	90	90	99.251(5)	90
<i>Z</i>	4	4	16	4	8

Chapter 5

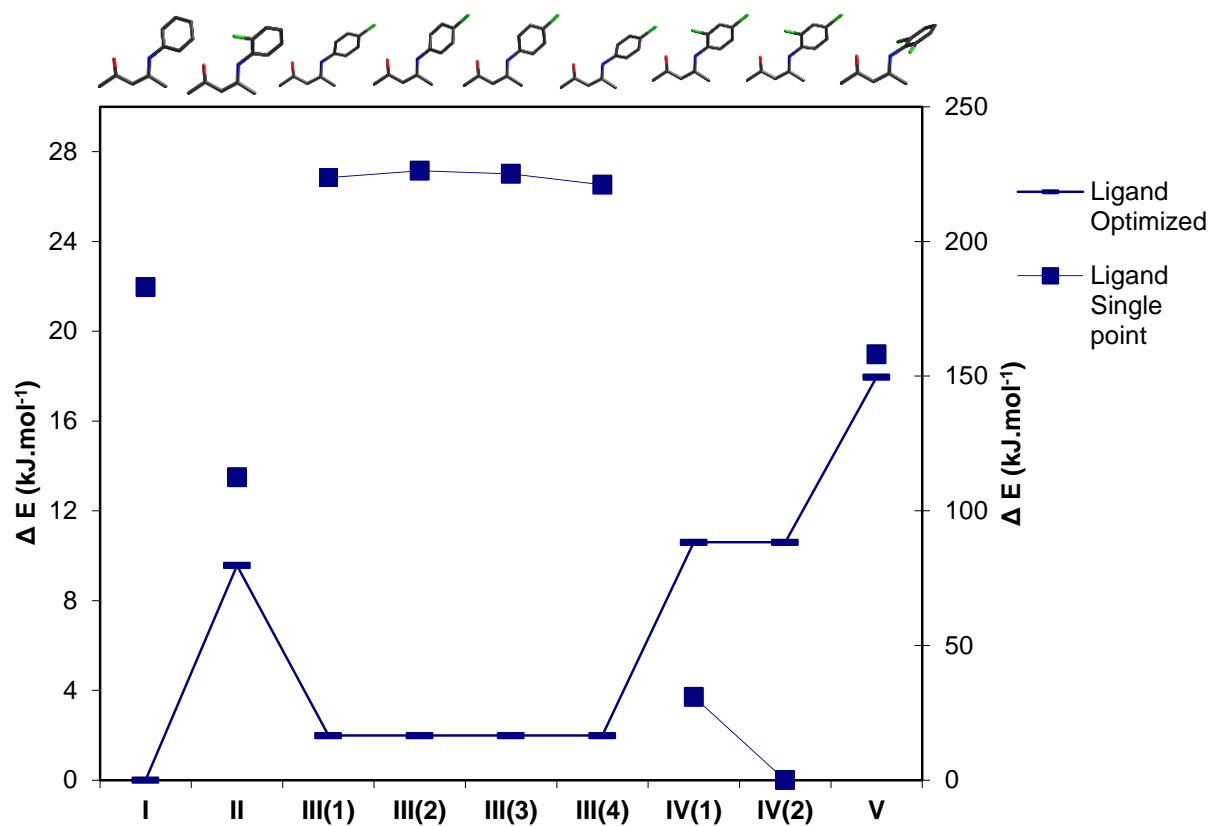


Figure 5.1. Calculated optimized and single point relative energies of compounds from GAUSSIAN-03W. The optimized energies are displayed on the primary axis and the single point energies on the secondary axis. Values in parentheses indicate the number of the independent molecule in the asymmetrical unit according to the numbering scheme defined in Chapter 4. **I** = PhonyH, **II** = 2-Cl-PhonyH, **III** = 4-Cl-PhonyH, **IV** = 2,4-Cl₂-PhonyH, **V** = 2,6-Cl₂-PhonyH.

Chapter 5

Table 5.3. Selected interatomic bond distances (Å) and angles (°) for solid state (Chapter 4; ss) and calculated (DFT) structures of PhonyH derivatives.

	PhonyH		2-Cl-PhonyH		4-Cl-PhonyH		2,4-Cl ₂ -PhonyH		2,6-Cl ₂ -PhonyH	
	SS ^a	DFT ^b	SS	DFT	SS ^c	DFT	SS ^d	DFT	SS	DFT
Atoms	Distances (Å)									
N ₁₁ -C ₁₁₁	1.412(3)	1.411	1.408(2)	1.4058	1.417(6)	1.408	1.401(3)	1.404	1.430(3)	1.412
N ₁₁ -C ₂	1.352(3)	1.357	1.347(2)	1.363	1.351(6)	1.357	1.353(5)	1.352	1.249(4)	1.356
O ₁₂ -C ₄	1.244(3)	1.254	1.249(2)	1.249	1.249(6)	1.246	1.252(5)	1.254	1.155(3)	1.245
N ₁₁ ⋯O ₁₂ ^e	2.658(3)	2.641	2.633(2)	2.657	2.652(6)	2.641	2.618(3)	2.638	2.821(2)	2.630
Atoms	Angles (°)									
N ₁₁ -H ₁₁ ⋯O ₁₂	140(2)	140.79	138.9(2)	138.22	136.6(4)	140.18	142(3)	143.04	145(2)	137.44
N ₁₁ -C ₂ ⋯C ₄ -O ₁₂	1.4(2)	0.816	5.5(1)	-0.43	2.0(4)	0.94	0.4(3)	0.73	-1.2(2)	-0.13
Dihedral angle ^f	32.03(9)	38.487	46.52(5)	48.370	46.5(2)	38.464	47.36(9)	41.912	87.5(1)	84.227

^a SS = solid state structure.

^b DFT = optimized calculated structure.

^c Average value of four independent molecules in asymmetrical unit.

^d Average value of two independent molecules in asymmetrical unit.

^e Bite distance.

^f The torsion angle between the N-C-C-C-O plane and the phenyl ring.

The overlay of the X-ray crystal structures with their theoretically optimized counterparts (Figure 5.2). is a graphical representation of the pair-wise differences of the related structures. This is represented mathematically by the root mean square (RMS) value, which is a measure of how far the average is from zero, providing information on the variations of bond lengths and angles and to a certain degree the orientation of the structures in relation to each other. The overlay figures of these structures in the solid state (red) and the calculated (DFT) structures (blue) are shown in Figure 5.2.

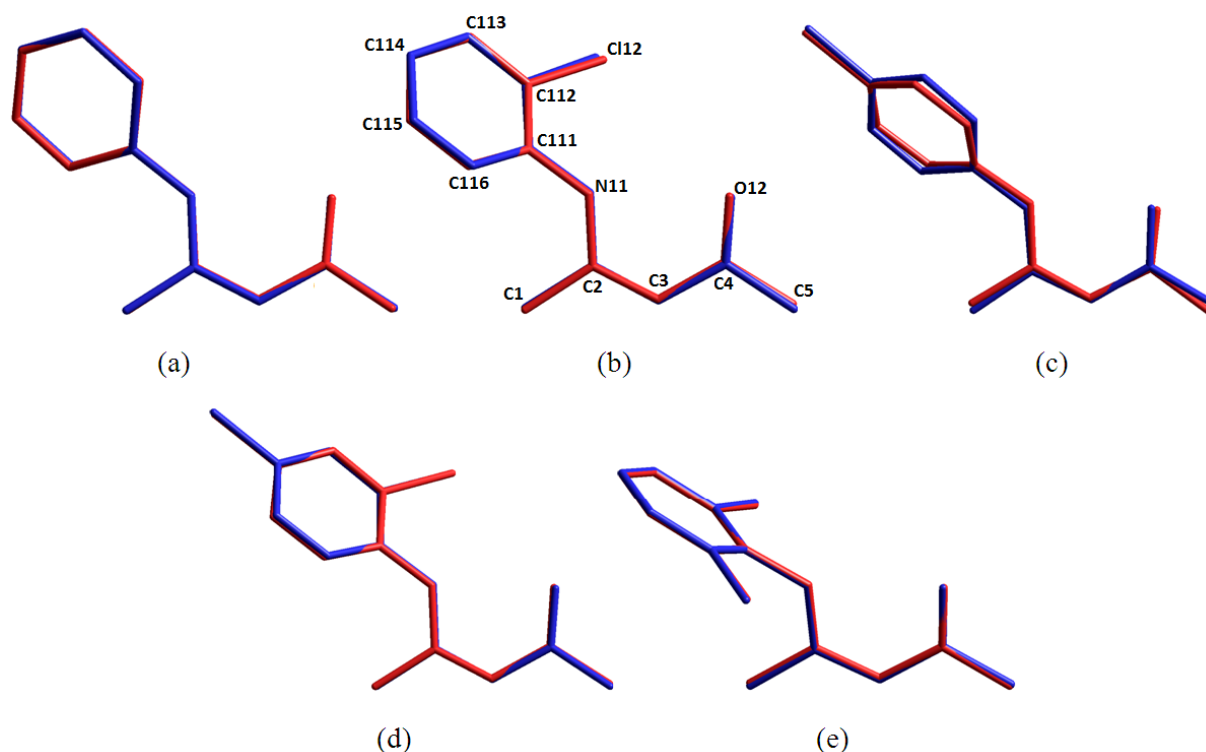


Figure 5.2. HyperChem⁸ overlay of the calculated (DFT) and solid state structures of a) PhonyH (RMS = 0.0728 Å); b) 2-Cl-PhonyH (RMS = 0.151 Å); c) 4-Cl-PhonyH (molecule 4; RMS = 0.183 Å); d) 2,4-Cl₂-PhonyH (molecule 2; RMS = 0.177 Å); e) 2,6-Cl₂-PhonyH (RMS = 0.0290 Å). Overlay fit includes all non-hydrogen atoms. The blue structure denotes the calculated (DFT) compound, while the red structure refers to the observed solid state compound. For the C atoms in the phenyl ring, the first digit indicates molecule number, the second digit indicates ring number and the third digit indicates the position of the atom in the ring. For substitutions on the phenyl ring, the first digit indicates molecule number while the second digit indicates position on the phenyl ring.

5.3. Discussion

Despite the low RMS values, angles and distances vary significantly between the solid state and calculated structures, demonstrating the impact of packing effects on the geometrical parameters of the solid state structures. The smallest difference in the dihedral angle (the angle between the planes through the phenyl ring and the N-C-C-C-O moieties) between solid state and calculated structure varies between 46.52(5)° and 48.4° for 2-Cl-PhonyH, a difference of 1.9°. The largest difference is for 4-Cl-PhonyH and varies between 46.5(2)° in the solid state and 38.5° for the calculated structure, a difference of 8.0°.

⁸ HyperChem 7.5.2 release for Windows; Hypercube, Inc., Gainesville, Florida, USA.

Chapter 5

In PhonyH, the optimized dihedral angle nears 90° , but this is not duplicated in the solid state, illustrating the influence of solid state packing effects on a system in contrast to the gaseous state implemented in the calculation. In 2,6-Cl₂-PhonyH, the optimized dihedral angle approaches 90° both in the optimized form and that observed in the solid state, indicating the pronounced steric effect due to the *ortho* substituents on the phenyl ring. Due to the symmetrical nature of compound 4-Cl-PhonyH, similar to that of PhonyH and 2,6-Cl₂-PhonyH, it could be expected that the dihedral angle of this compound might approach 90° . This is however not the case, and the structure adopts an average dihedral angle of 38.5° and $46.5(2)^\circ$ for the calculated and solid state, respectively. This might be explained by the electron-withdrawing nature of the chloride moiety, which on the 4-position of the phenyl ring disturbs the electron cloud of the ring in such a way as to lessen the interaction of this cloud with the filled *p*-orbitals of the N atom. This facilitates the rotation of the ring to a more favorable position, closer to a planar conformation regarding the N₁₁-C₂-C₃-C₄-O₁₂ plane. The large array of intermolecular interactions in the solid state 4-Cl-PhonyH (discussed in Chapter 4) also plays a part in stabilizing the molecules in a geometry vastly different from the optimized state with regard to angles.

The difference between the lowest and highest optimized energies, PhonyH and 2,6-Cl₂-PhonyH respectively, is $18 \text{ kJ}\cdot\text{mol}^{-1}$ (Figure 5.1.). The difference between the unsubstituted PhonyH and *ortho*-substituted 2-Cl-PhonyH is $9.6 \text{ kJ}\cdot\text{mol}^{-1}$, while the difference between PhonyH and *para*-substituted 4-Cl-PhonyH is $2.0 \text{ kJ}\cdot\text{mol}^{-1}$. The difference between PhonyH and 2,4-Cl₂-PhonyH, which is essentially a combination of *ortho*-substituted 2-Cl-PhonyH and *para*-substituted 4-Cl-PhonyH, is $11 \text{ kJ}\cdot\text{mol}^{-1}$, while PhonyH and 2,6-Cl₂-PhonyH, a combination of two *ortho*-substituted compounds, is $18 \text{ kJ}\cdot\text{mol}^{-1}$. The sum of the relative energies of 2-Cl-PhonyH and 4-Cl-PhonyH, *ortho*- and *para*-substituted compounds, is $12 \text{ kJ}\cdot\text{mol}^{-1}$ which is twice the energy of 2-Cl-PhonyH i.e. $19 \text{ kJ}\cdot\text{mol}^{-1}$. The calculated optimized energies of 2,4-Cl₂-PhonyH ($11 \text{ kJ}\cdot\text{mol}^{-1}$) and 2,6-Cl₂-PhonyH ($18 \text{ kJ}\cdot\text{mol}^{-1}$) roughly resembles the additive relative energies of 2-Cl-PhonyH and 4-Cl-PhonyH, therefore accentuating the cumulative nature of the energies with respect to the position of the chloride moieties on the phenyl ring.

The calculated optimized energies of PhonyH and 4-Cl-PhonyH are comparable, and their extremely close resemblance is confirmed by the similarities in bond distances and the small RMS (0.0144 \AA) value of their overlay, as demonstrated in Figure 5.3. Similarly, the optimized

Chapter 5

energy values of 2-Cl-PhonyH and 2,4-Cl₂-PhonyH are close in value, and the overlay of these two structures display a small RMS value of 0.0141 Å (Figure 5.4).

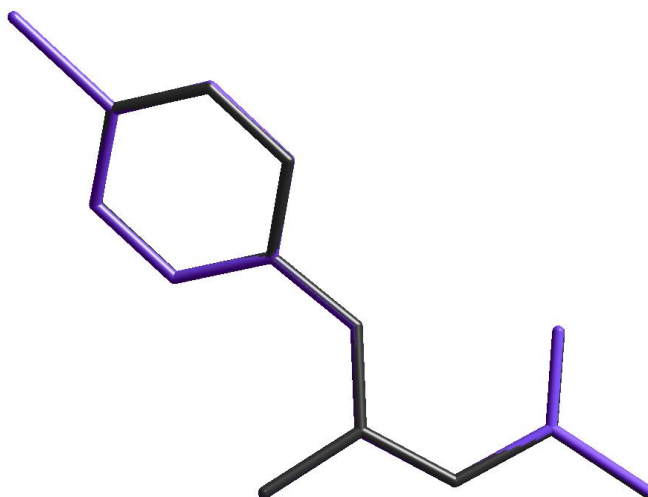


Figure 5.3. Overlay of the calculated (DFT) structures of PhonyH (black) with 4-Cl-PhonyH (Violet; RMS = 0.0144 Å).

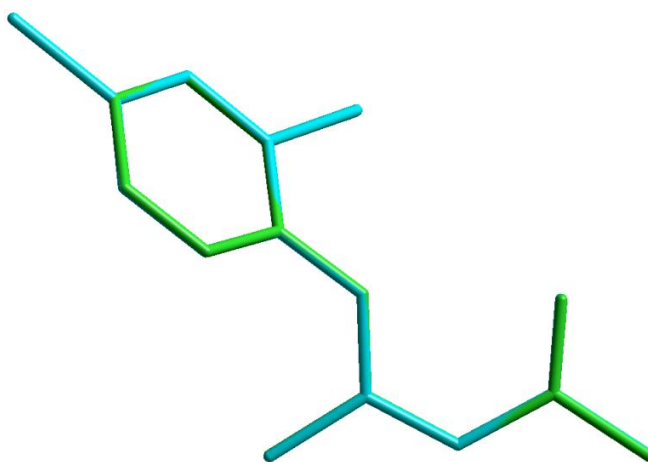


Figure 5.4. Overlay of the calculated (DFT) structures of 2-Cl-PhonyH (green) with 2,4-Cl₂-PhonyH (Cyan; RMS = 0.0141 Å).

The resemblance between the two pairs of structures is reflected in the bonding distances and angles, with angles comparing more closely for the first pair which is PhonyH and 4-Cl-PhonyH (Table 5.3). For these two compounds, the largest difference in distance is $d(\text{O}_{12}\text{-C}_4)$ and are 1.254 Å and 1.246 Å, respectively; a difference of 0.008 Å. Other distances, for instance $d(\text{N}_{11}\text{-C}_2)$ and $d(\text{N}_{11}\cdots\text{O}_{12})$, have the exact same values of 1.357 Å and 2.641 Å, respectively, for both

Chapter 5

compounds. Differences in angles are slightly more pronounced, with the $N_{11}-H_{11}\cdots O_{12}$ angle being 140.79° for PhonyH and 140.18° for 4-Cl-PhonyH, a difference of 0.61° , and the $N_{11}-C_2\cdots C_4-O_{12}$ angle 0.816° for PhonyH and 0.94° for 4-Cl-PhonyH, a difference of 0.12° . The dihedral angle for these two compounds correlates with a value of 38.5° .

For the 2-Cl-PhonyH/2,4-Cl₂-PhonyH pair the differences in bonding distances are more pronounced, with the largest differences being 0.011 \AA for $d(N_{11}-C_2)$ (1.363 \AA for 2-Cl-PhonyH and 1.352 \AA for 2,4-Cl₂-PhonyH) and 0.019 \AA for $d(N_{11}\cdots O_{12})$ (2.657 \AA for 2-Cl-PhonyH and 2.638 \AA for 2,4-Cl₂-PhonyH). The angles show differences as large as 6.46° for the dihedral angle (48.37° for 2-Cl-PhonyH and 41.91° for 2,4-Cl₂-PhonyH), with differences in the $N_{11}-H_{11}\cdots O_{12}$ and $N_{11}-C_2\cdots C_4-O_{12}$ angles of 4.8° and 1.16° , respectively (138.22° and -0.43° for 2-Cl-PhonyH and 143.04° and 0.73° for 2,4-Cl₂-PhonyH). Although these differences might seem large, it is an indication that the presence of a chloride on the *para*-position of the phenyl ring has an influence on the geometry of the compounds, albeit small. This influence is significantly more pronounced in the compounds containing an *ortho*-positioned chloride as well, as seen when comparing the second pair of compounds to the first set.

All distances and angles for 2,6-Cl₂-PhonyH closely correlate those for unsubstituted PhonyH. However, since the two chloride atoms contained in 2,6-Cl₂-PhonyH, both on *ortho*-positions, interferes sterically with the pentenone backbone, the compound distorts to allow for a considerably larger dihedral angle which results in the higher relative energy.

5.4. Conclusion

The calculated geometric parameters as seen in Table 5.3 differ significantly from the observed solid state parameters, supporting the postulated influence of different chloride substitutions on packing modes and bond lengths, where seemingly small differences in substitution causes large variations in packing modes. However, in spite of these differences, very good agreement exists between the DFT calculated and the solid state structures. This already suggests that in the free form, the geometries of these ligands are significantly dependent on the sterics introduced by the phenyl ring substituent on the N,O-backbone. The relative energies of the optimized structures adopt a cumulative nature – the relative energy of 2,4-Cl₂-PhonyH with regard to unsubstituted

Chapter 5

PhonyH is roughly equal to the sum of the relative energies of 2-Cl-PhonyH and 4-Cl-PhonyH, while the relative energy of 2,6-Cl₂-PhonyH equals twice the relative energy of 2-Cl-PhonyH. The distortion of the phenyl ring from the ideal planar position presented in the calculated structures corresponds to the distortion observed in the solid state. The behavior of these ligands when coordinated to Rh(I) is discussed in the following chapters.

Chapter 5

6 X-Ray Crystallographic Study of Functionalized Dicarbonyl-[4-(phenylamino)pent-3-en-2-onato]-rhodium(I) Complexes

6.1. Introduction

This chapter focuses on X-ray crystallographic studies on complexes of the type $[\text{Rh}(\text{N},\text{O-Bid})(\text{CO})_2]$ (where N,O-Bid is a derivative of 4-(phenylamino)pent-3-en-2-onate, Phony⁻), see Figure 6.1, and the effect of substitution of chloride on different positions on the phenyl ring.

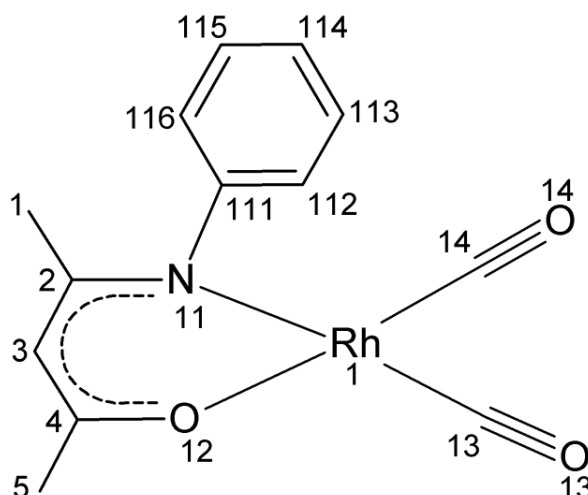


Figure 6.1. Schematic representation of $[\text{Rh}(\text{N},\text{O-Bid})(\text{CO})_2]$, illustrating the numbering scheme used throughout the chapter. For the C atoms in the phenyl ring, the first digit indicates complex number, the second digit indicates ring number and the third digit indicates the position of the atom in the ring. For substitutions on the phenyl ring, the first digit indicates complex number while the second digit indicates position on the phenyl ring.

Chapter 6

6.2. Results

Procedures for synthesis of the complexes are discussed in Chapter 3, while general crystal data and refinement parameters are presented in Table 6.1. A complete list of atomic coordinates, equivalent isotropic parameters, bond distances and angles, anisotropic displacement parameters and hydrogen coordinates for each individual dataset is given in Appendix B.

Table 6.1. General crystal data for [Rh(Phony)(CO)₂], [Rh(2-Cl-Phony)(CO)₂], [Rh(4-Cl-Phony)(CO)₂], [Rh(2,4-Cl₂-Phony)(CO)₂] and [Rh(2,6-Cl₂-Phony)(CO)₂]. For label definition see Figure 6.1.

	[Rh(Phony)(CO) ₂]	[Rh(2-Cl-Phony)(CO) ₂]	[Rh(4-Cl-Phony)(CO) ₂]	[Rh(2,4-Cl ₂ -Phony)(CO) ₂]	[Rh(2,6-Cl ₂ -Phony)(CO) ₂]
Empirical formula	C13 H12 N O3	C13 H11 Cl N	C13 H11 Cl N	C13 H10 Cl2 N	C13 H10 Cl2 N
	Rh	O3 Rh	O3 Rh	O3 Rh	O3 Rh
Formula weight	333.15	367.59	367.59	402.03	402.03
Temperature (K)	298(2)	100(2)	100(2)	100(2)	100(2)
Wavelength (Å)	0.71073	0.71073	0.71073	0.71069	0.71069
Crystal system	Monoclinic	Orthorhombic	Orthorhombic	Triclinic	Orthorhombic
Space group	<i>I</i> 2/ <i>a</i>	<i>Pbca</i>	<i>Pnma</i>	<i>P</i> $\bar{1}$	<i>P</i> 2 ₁ 2 ₁ 2 ₁
<i>a</i> (Å)	13.3756(2)	14.309(4)	13.163(2)	7.157(2)	7.8800(2)
<i>b</i> (Å)	96.193(1)	10.085(3)	6.8055(9)	9.983(2)	12.3010(3)
<i>c</i> (Å)	21.2210(3)	18.886(6)	14.962(2) Å	10.654(3)	15.0740(3)
α (°)	90	90	90	83.086(1)	90
β (°)	9.2915(1)	90	90	71.601(2)	90
γ (°)	90	90	90	82.059(1)	90
Volume (Å ³)	2621.94(6)	2725(1)	1340.2(3)	713.0(3)	1461.15(6)
<i>Z</i>	8	8	4	2	4
Density _{cal} (g.cm ⁻³)	1.688	1.792	1.822	1.873	1.828
μ (mm ⁻¹)	1.301	1.451	1.475	1.576	1.538
<i>F</i> (000)	1328	1456	728	396	792
Crystal size (mm ³)	0.23 x 0.10 x 0.08	0.37 x 0.28 x 0.13	0.30 x 0.06 x 0.04	0.26 x 0.22 x 0.16	0.41 x 0.33 x 0.12
$\theta_{\min}/\theta_{\max}$ (°)	2.40 / 27.00	2.16 / 28.32	2.06 / 26.98	2.02 / 27.00	2.14 / 28.27
Index ranges	-9 ≤ <i>h</i> ≤ 17 -11 ≤ <i>k</i> ≤ 11 -25 ≤ <i>l</i> ≤ 26	-13 ≤ <i>h</i> ≤ 19 -12 ≤ <i>k</i> ≤ 13 -25 ≤ <i>l</i> ≤ 23	-16 ≤ <i>h</i> ≤ 16 -8 ≤ <i>k</i> ≤ 5 -19 ≤ <i>l</i> ≤ 19	-9 ≤ <i>h</i> ≤ 9 -12 ≤ <i>k</i> ≤ 12 -13 ≤ <i>l</i> ≤ 13	-10 ≤ <i>h</i> ≤ 10 -16 ≤ <i>k</i> ≤ 16 -19 ≤ <i>l</i> ≤ 20
Reflections collected	9457	53966	12246	17679	37505

Chapter 6

Table 6.1. Continued.

	[Rh(Phony)(CO)₂]	[Rh(2-Cl-Phony)(CO)₂]	[Rh(4-Cl-Phony)(CO)₂]	[Rh(2,4-Cl₂-Phony)(CO)₂]	[Rh(2,6-Cl₂-Phony)(CO)₂]
Independent reflections	2854	3390	1579	3108	3632
R_{int}	0.0268	0.0577	0.0706	0.0298	0.0390
Completeness to θ_{max} (%)	99.5	99.7	99.6	99.7	100
Data / parameters	2854 / 165	3390 / 174	1579 / 105	3108 / 171	3632 / 183
Goodness-of-fit on F^2	1.010	1.081	1.293	1.076	0.963
Final R indices,	$R_1 = 0.0225$	$R_1 = 0.0296$	$R_1 = 0.0600$	$R_1 = 0.0211$	$R_1 = 0.0163$
$[I > 2\sigma(I)]$	$wR_2 = 0.0505$	$wR_2 = 0.0662$	$wR_2 = 0.1336$	$wR_2 = 0.0481$	$wR_2 = 0.0361$
R indices (all data)	$R_1 = 0.0295$	$R_1 = 0.0417$	$R_1 = 0.0735$	$R_1 = 0.0233$	$R_1 = 0.0172$
	$wR_2 = 0.0516$	$wR_2 = 0.0708$	$wR_2 = 0.1377$	$wR_2 = 0.0492$	$wR_2 = 0.0363$
$\Delta\rho$ max/ min (e.Å ⁻³)	0.800 / -0.498	1.294 / -0.539	1.746 / -2.905	0.872 / -0.951	0.276 / -0.328

6.2.1 Crystal Structure of Dicarboxyl-[4-(phenylamino)pent-3-en-2-onato]-rhodium(I) [Rh(Phony)(CO)₂]

The complex [Rh(Phony)(CO)₂], where Phony = 4-(phenylamino)pent-3-en-2-onate, was prepared as discussed in § 3.4.1 and crystallized in the monoclinic space group $I2/a$ with $Z = 8$. The complex is shown in Figure 6.2, with important bond distances and angles reported in Table 6.2.

Chapter 6

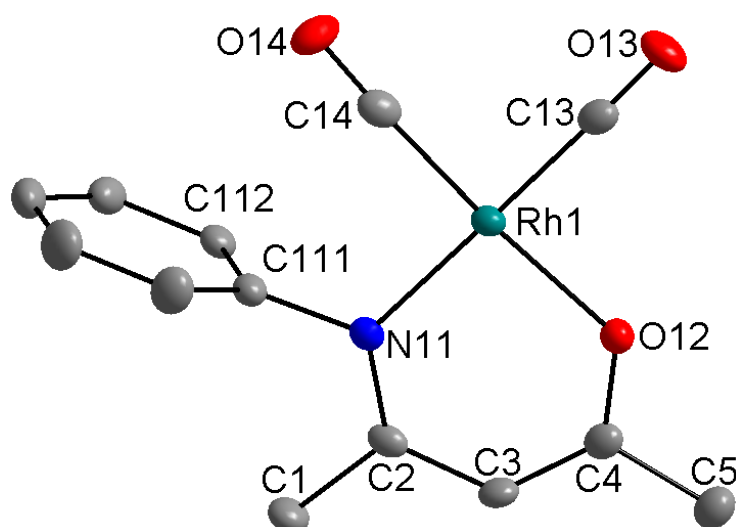


Figure 6.2. Ellipsoidal illustration of $[\text{Rh}(\text{Phony})(\text{CO})_2]$, where Phony = 4-(phenylamino)pent-3-en-2-onato (50 % probability displacement ellipsoids). Hydrogen atoms and selected labels have been omitted for clarity. For the C atoms in the phenyl ring, the first digit indicates molecule number, the second digit indicates ring number and the third digit indicates the position of the atom in the ring. For the C1 atoms, the first digit indicates molecule number while the second digit indicates position on the phenyl ring.

Table 6.2. Selected bond distances (\AA) and angles ($^\circ$) for $[\text{Rh}(\text{Phony})(\text{CO})_2]$.

Atoms	Distances (\AA)	Atoms	Angles ($^\circ$)
Rh ₁ -N ₁₁	2.058(2)	N ₁₁ -Rh ₁ -O ₁₂	90.55(6)
Rh ₁ -O ₁₂	2.032(2)	O ₁₂ -Rh ₁ -C ₁₃	89.75(8)
Rh ₁ -C ₁₃	1.866(2)	C ₁₃ -Rh ₁ -C ₁₄	86.5(1)
Rh ₁ -C ₁₄	1.841(3)	N ₁₁ -Rh ₁ -C ₁₄	93.13(9)
C ₁₃ -O ₁₃	1.142(3)	N ₁₁ -Rh ₁ -C ₁₃	178.94(8)
C ₁₄ -O ₁₄	1.143(3)	O ₁₂ -Rh ₁ -C ₁₄	175.99(9)
N ₁₁ -C ₁₁₁	1.448(3)	N ₁₁ -C ₂ ...C ₄ -O ₁₂	-0.4(2)
N ₁₁ -C ₂	1.139(3)	Dihedral angle ^a	87.88(8)
O ₁₂ -C ₄	1.294(2)		
N ₁₁ ...O ₁₂ (Bite distance)	2.906(2)		
Rh...Rh	3.4358(2)		

^a Defined as the torsion angle between the N-C-C-C-O plane and the phenyl ring.

The packing modes of $[\text{Rh}(\text{Phony})(\text{CO})_2]$ are influenced by classic intermolecular C-H...O as well as rhodium-rhodium interactions. Rh₁ is displaced from the plane formed by N₁₁, O₁₂, C₁₃ and C₁₄ by 0.0218(2) \AA . The distance between Rh₁ and Rh₁^{ix} is 3.4358(2) \AA , and the angle

Chapter 6

between the $N_{11}-O_{12}-C_{13}-C_{14}$ plane and the rhodium-rhodium interaction is $83.14(4)^\circ$. These interactions, illustrated in Figure 6.2, are shown in Table 6.3 and the resulting packing motif is shown in Figure 6.4.

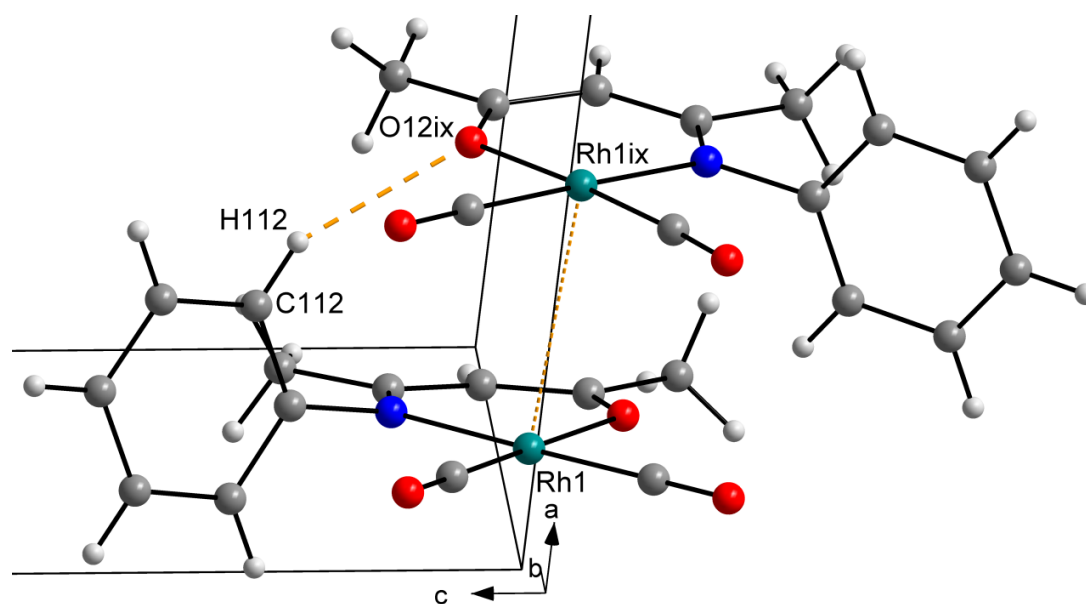


Figure 6.3. Partial unit cell for $[\text{Rh}(\text{Phony})(\text{CO})_2]$ with important intra- and intermolecular hydrogen bonding interactions indicated with dashed lines. The rhodium-rhodium interaction is indicated with a dotted line. Symmetry operator: (ix) $-x + \frac{1}{2}, y, -z$.

Table 6.3. Hydrogen bonds for $[\text{Rh}(\text{Phony})(\text{CO})_2]$ (\AA and $^\circ$).

$\text{D-H}\cdots\text{A}$	$d_{\text{D-H}}$ (\AA)	$d_{\text{H}\cdots\text{A}}$ (\AA)	$d_{\text{D}\cdots\text{A}}$ (\AA)	\angle_{DHA} ($^\circ$)
$\text{C}_{112}-\text{H}_{112}\cdots\text{O}_{12}^{\text{ix}}$	0.95	2.50	3.380(3)	153.6

Symmetry code: (ix) $-x + \frac{1}{2}, y, -z$

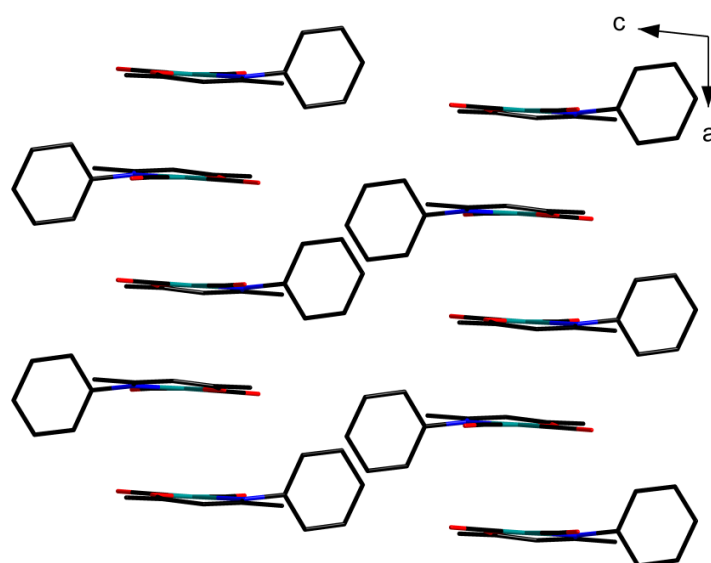


Figure 6.4. View of $[\text{Rh}(\text{Phony})(\text{CO})_2]$ along the b-axis illustrating the packing style. Linear stacking due to rhodium-rhodium interactions is clearly visible.

A linear packing arrangement between the rhodium atoms is clearly visible in Figure 6.4, resulting from the polymeric rhodium-rhodium interactions. This phenomenon can be perceived at a macroscopic level by the display of a yellow-green sheen on the solid state product in addition to an orange-red colour, illustrating the dichroic nature of the complex. A head-to-head packing arrangement is observed on one side of the molecule, where both carbonyl ligands are orientated in the same direction as the adjacent molecule, while the adjacent molecule on the other side of the molecule is rotated to conform to a head-to-tail packing arrangement.

6.2.2 Crystal structure of Dicarboxyl-[4-(2-chlorophenylamino)pent-3-en-2-onato]-rhodium(I) $[\text{Rh}(2\text{-Cl-Phony})(\text{CO})_2]$

The complex $[\text{Rh}(2\text{-Cl-Phony})(\text{CO})_2]$, where Phony = 4-(phenylamino)pent-3-en-2-onate, was prepared as discussed in § 3.4.2 and crystallized in the orthorhombic space group *Pbca* with $Z = 8$. The complex is shown in Figure 6.5, with important bond distances and angles reported in Table 6.4.

Chapter 6

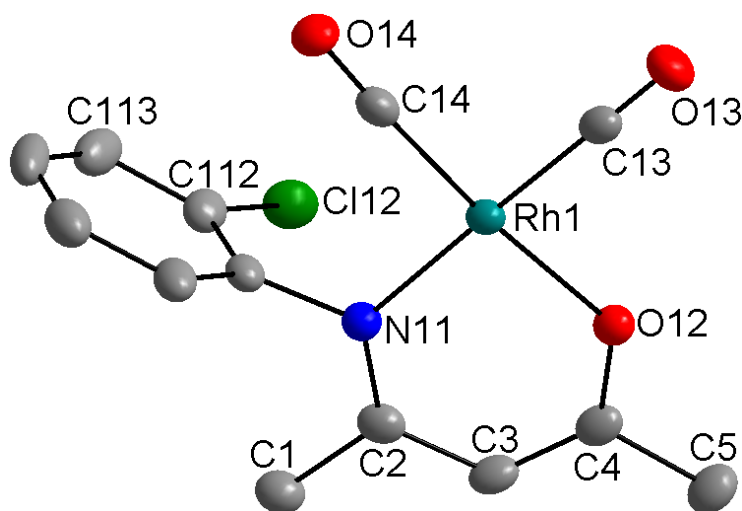


Figure 6.5. DIAMOND¹ view of [Rh(2-Cl-Phony)(CO)₂], where Phony = 4-(phenylamino)pent-3-en-2-onato (50% probability displacement ellipsoids). Hydrogen atoms and selected labels have been omitted for clarity. For the C atoms in the phenyl ring, the first digit indicates molecule number, the second digit indicates ring number and the third digit indicates the position of the atom in the ring. For the Cl atoms, the first digit indicates molecule number while the second digit indicates position on the phenyl ring.

Table 6.4. Selected bond distances (Å) and angles (°) for [Rh(2-Cl-Phony)(CO)₂].

Atoms	Distances (Å)	Atoms	Angles (°)
Rh ₁ -N ₁₁	2.054(2)	N ₁₁ -Rh ₁ -O ₁₂	90.08(8)
Rh ₁ -O ₁₂	2.019(2)	O ₁₂ -Rh ₁ -C ₁₃	88.5(1)
Rh ₁ -C ₁₃	1.858(3)	C ₁₃ -Rh ₁ -C ₁₄	87.2(1)
Rh ₁ -C ₁₄	1.849(3)	N ₁₁ -Rh ₁ -C ₁₄	94.2(1)
C ₁₃ -O ₁₃	1.135(4)	N ₁₁ -Rh ₁ -C ₁₃	178.6(1)
C ₁₄ -O ₁₄	1.143(3)	O ₁₂ -Rh ₁ -C ₁₄	174.7(1)
N ₁₁ -C ₁₁₁	1.436(4)	N ₁₁ -C ₂ ⋯C ₄ -O ₁₂	1.4(1)
N ₁₁ -C ₂	1.322(3)	Dihedral angle ^a	85.20(9)
O ₁₂ -C ₄	1.294(3)		
N ₁₁ ⋯O ₁₂ (Bite distance)	2.882(3)		
Rh⋯Rh	3.4151(7)		

^a Defined as the torsion angle between the N-C-C-C-O plane and the phenyl ring.

The introduction of a possible hydrogen-bonding atom in [Rh(2-Cl-Phony)(CO)₂] at the 2-position on the phenyl ring does not result in significant hydrogen interactions, instead the

¹ Brandenburg, K., Putz, H. DIAMOND. Release 3.0e. Crystal Impact GbR, Bonn, Germany.

Chapter 6

packing style is characterized by intermolecular rhodium-rhodium interactions, as illustrated in Figure 6.6. The complex exhibits crystallographic dimerism instead of polymerism, in contrast with $[\text{Rh}(2,4\text{-Cl}_2\text{-Phony})(\text{CO})_2]$ in which a chloride atom is located in the *ortho* position on the phenyl ring as well. Rh_1 is displaced from the plane formed by N_{11} , O_{12} , C_{13} and C_{14} by $0.0266(2)$ Å. The distance between Rh_1 and Rh_1^x in $[\text{Rh}(2\text{-Cl-Phony})(\text{CO})_2]$ is $3.4151(7)$ Å, and the angle between the $\text{N}_{11}\text{-O}_{12}\text{-C}_{13}\text{-C}_{14}$ plane and the direction of the rhodium-rhodium interaction is $78.44(4)^\circ$. The resulting packing style is shown in Figure 6.7.

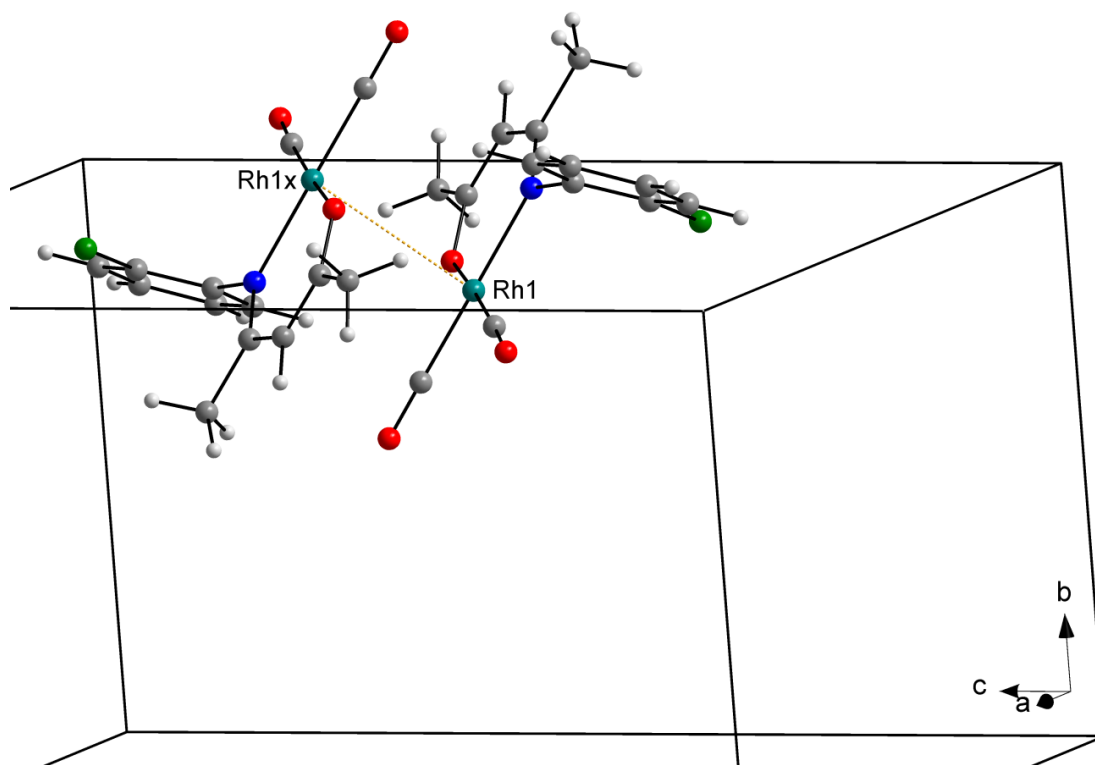


Figure 6.6. Partial unit cell for $[\text{Rh}(2\text{-Cl-Phony})(\text{CO})_2]$ with the rhodium-rhodium interaction is indicated with a dotted line. Symmetry code: $(x) -x + \frac{1}{2}, y, -z$.

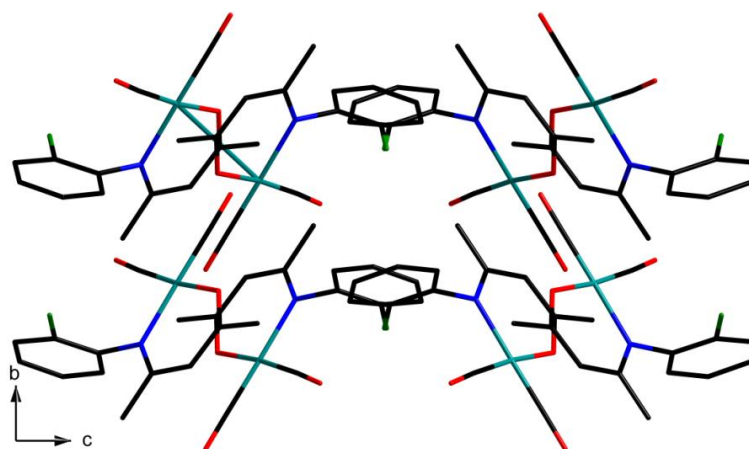


Figure 6.7. View of $[\text{Rh}(2\text{-Cl-Phony})(\text{CO})_2]$ along the a -axis illustrating the packing style.

Unlike the case with $[\text{Rh}(\text{Phony})(\text{CO})_2]$, intermolecular rhodium-rhodium interactions in $[\text{Rh}(2\text{-Cl-Phony})(\text{CO})_2]$ are of a dimeric nature, as shown in Figure 6.7. Although the chloride atoms appear to be very close to each other in the packing diagram, the shortest distance between two chloride atoms is $7.155(2) \text{ \AA}$.

6.2.3 Crystal Structure of Dicarboxyl-[4-(4-chlorophenylamino)pent-3-en-2-onato]-rhodium(I) $[\text{Rh}(4\text{-Cl-Phony})(\text{CO})_2]$

The complex $[\text{Rh}(4\text{-Cl-Phony})(\text{CO})_2]$, where Phony = 4-(phenylamino)pent-3-en-2-onate, was prepared as discussed in § 3.4.3 and crystallized in the orthorhombic space group $Pnma$ with $Z = 4$. The complex is shown in Figure 6.8, with important bond distances and angles reported in Table 6.5.

Chapter 6

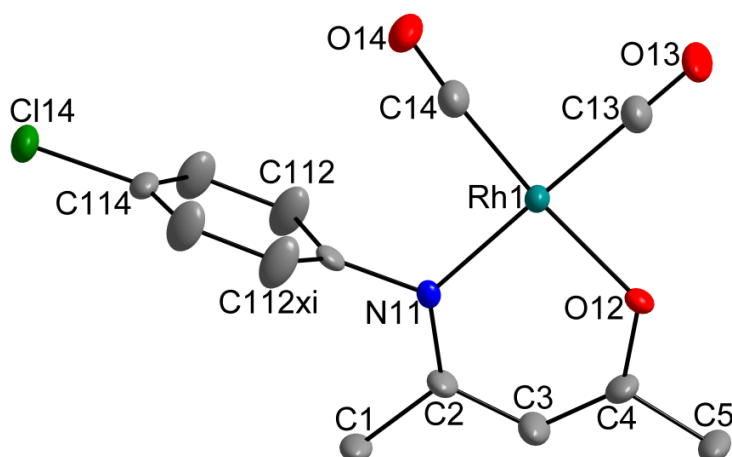


Figure 6.8. DIAMOND¹ view of [Rh(4-Cl-Phony)(CO)₂], where Phony = 4-(phenylamino)pent-3-en-2-onato (50% probability displacement ellipsoids). Hydrogen atoms and selected labels have been omitted for clarity. For the C atoms in the phenyl ring, the first digit indicates molecule number, the second digit indicates ring number and the third digit indicates the position of the atom in the ring. For the Cl atoms, the first digit indicates molecule number while the second digit indicates position on the phenyl ring. Atoms generated by symmetry are indicated by lower case roman numerical labels corresponding to the symmetry operator (xi) x, ½ - y, z.

Table 6.5. Selected bond distances (Å) and angles (°) for [Rh(4-Cl-Phony)(CO)₂].

Atoms	Distances (Å)	Atoms	Angles (°)
Rh ₁ -N ₁₁	2.065(8)	N ₁₁ -Rh ₁ -O ₁₂	91.2(3)
Rh ₁ -O ₁₂	2.033(6)	O ₁₂ -Rh ₁ -C ₁₃	87.9(4)
Rh ₁ -C ₁₃	1.86(1)	C ₁₃ -Rh ₁ -C ₁₄	87.0(5)
Rh ₁ -C ₁₄	1.84(1)	N ₁₁ -Rh ₁ -C ₁₄	94.0(4)
C ₁₃ -O ₁₃	1.14(1)	N ₁₁ -Rh ₁ -C ₁₃	179.1(4)
C ₁₄ -O ₁₄	1.15(1)	O ₁₂ -Rh ₁ -C ₁₄	174.8(4)
N ₁₁ -C ₁₁₁	1.45(1)	N ₁₁ -C ₂ ⋯C ₄ -O ₁₂	0.0(7)
N ₁₁ -C ₂	1.31(1)	Dihedral angle ^a	90.0(2)
O ₁₂ -C ₄	1.30(1)		
N ₁₁ ⋯O ₁₂ (Bite distance)	2.93(1)		
Rh⋯Rh	3.5477(5)		

^a Defined as the torsion angle between the N-C-C-C-O plane and the phenyl ring.

The packing modes of compound [Rh(4-Cl-Phony)(CO)₂] are influenced by classic intermolecular C-H⋯O and rhodium-rhodium interactions. The distance between Rh₁ and Rh₁^{xiv} is 3.5477(5) Å, and the angle between the N₁₁-O₁₂-C₁₃-C₁₄ plane and the rhodium-rhodium

Chapter 6

interaction is $73.56(2)^\circ$. These interactions are illustrated in Figure 6.9 and shown in Table 6.6. The resulting packing style is shown in Figure 6.10.

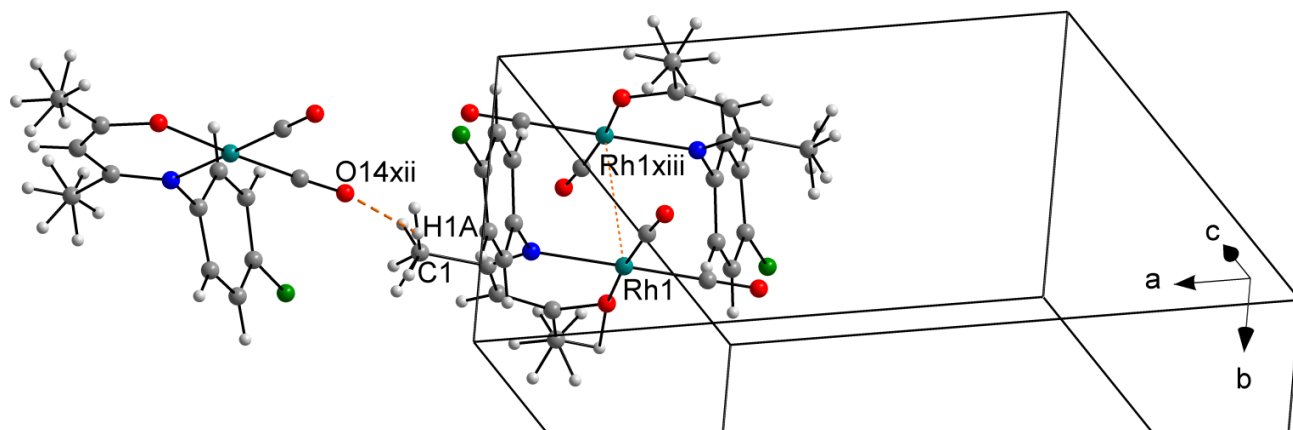


Figure 6.9. Partial unit cell for $[\text{Rh}(4\text{-Cl-Phony})(\text{CO})_2]$ with important intra- and intermolecular hydrogen bonding interactions indicated with dashed lines. The rhodium-rhodium interaction is indicated with a dotted line. Symmetry operators are given in Table 6.6.

Table 6.6. Hydrogen bonds for $[\text{Rh}(4\text{-Cl-Phony})(\text{CO})_2]$ (Å and $^\circ$).

D-H...A	$d_{\text{D-H}}$ (Å)	$d_{\text{H...A}}$ (Å)	$d_{\text{D...A}}$ (Å)	\angle_{DHA} ($^\circ$)
$\text{C}_1\text{-H}_{1\text{A}}\cdots\text{O}_{14}^{\text{xii}}$	0.98	2.41	3.23(1)	142.0

Symmetry codes: (xi) $x, \frac{1}{2} - y, z$ (xii) $x, -y + \frac{1}{2}, z$ (xiii) $2 - x, -\frac{1}{2} + y, 1 - y$

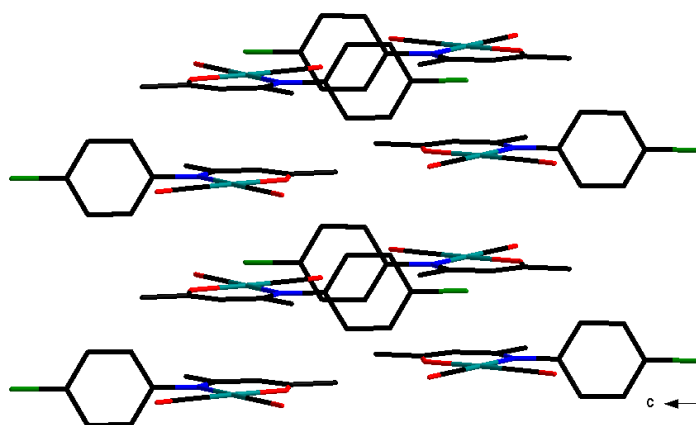


Figure 6.10. View of $[\text{Rh}(4\text{-Cl-Phony})(\text{CO})_2]$ along the a-axis illustrating the packing style. Linear stacking due to rhodium-rhodium interactions is clearly visible.

As is the case with $[\text{Rh}(\text{Phony})(\text{CO})_2]$, the linear packing arrangement is clearly visible in Figure 6.10, as a result of intermolecular rhodium-rhodium interactions. This phenomenon can be

observed by the yellow-green sheen on the solid state product in addition to an orange-red colour.

6.2.4 Crystal Structure of Dicarbonyl-[4-(2,4-dichlorophenylamino)pent-3-en-2-onato]-rhodium(I) [Rh(2,4-Cl₂-Phony)(CO)₂]

The complex [Rh(2,4-Cl₂-Phony)(CO)₂], where Phony = 4-(phenylamino)pent-3-en-2-onate, was prepared as discussed in § 3.4.4 and crystallized in the triclinic space group $P\bar{1}$ with $Z = 4$. The complex is shown in Figure 6.11, with important bond distances and angles reported in Table 6.7.

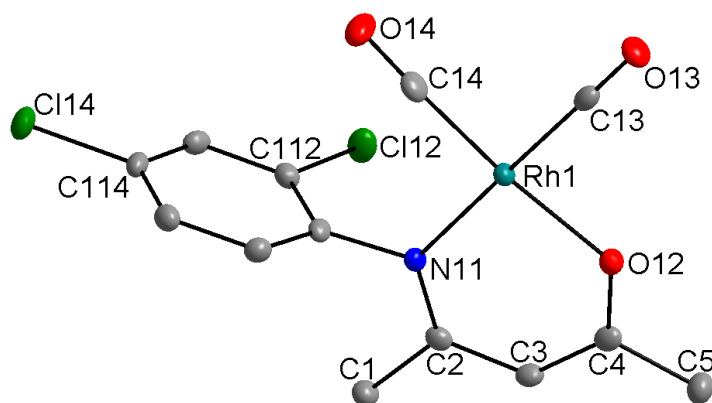


Figure 6.11. DIAMOND¹ view of [Rh(2,4-Cl₂-Phony)(CO)₂], where Phony = 4-(phenylamino)pent-3-en-2-onate (50% probability displacement ellipsoids). Hydrogen atoms and selected labels have been omitted for clarity. For the C atoms in the phenyl ring, the first digit indicates molecule number, the second digit indicates ring number and the third digit indicates the position of the atom in the ring. For the Cl atoms, the first digit indicates molecule number while the second digit indicates position on the phenyl ring.

Chapter 6

Table 6.7. Selected bond distances (Å) and angles (°) for [Rh(2,4-Cl₂-Phony)(CO)₂].

Atoms	Distances (Å)	Atoms	Angles (°)
Rh ₁ -N ₁₁	2.020(1)	N ₁₁ -Rh ₁ -O ₁₂	90.36(5)
Rh ₁ -O ₁₂	2.057(2)	O ₁₂ -Rh ₁ -C ₁₃	88.76(6)
Rh ₁ -C ₁₃	1.873(2)	C ₁₃ -Rh ₁ -C ₁₄	87.07(8)
Rh ₁ -C ₁₄	1.838(2)	N ₁₁ -Rh ₁ -C ₁₄	93.81(7)
C ₁₃ -O ₁₃	1.133(2)	N ₁₁ -Rh ₁ -C ₁₃	179.12(7)
C ₁₄ -O ₁₄	1.142(2)	O ₁₂ -Rh ₁ -C ₁₄	174.99(7)
N ₁₁ -C ₁₁₁	1.434(2)	N ₁₁ -C ₂ ...C ₄ -O ₁₂	-0.7(1)
N ₁₁ -C ₂	1.329(3)	Dihedral angle ^a	85.85(6)
O ₁₂ -C ₄	1.289(2)		
N ₁₁ ...O ₁₂ (Bite distance)	2.893(2)		
Rh...Rh	3.5836(9)		

^a Defined as the torsion angle between the N-C-C-C-O plane and the phenyl ring.

The packing modes of [Rh(2,4-Cl₂-Phony)(CO)₂] are influenced by classic intermolecular C-H...O and rhodium-rhodium interactions. Hydrogen and rhodium-rhodium interactions in the structure, illustrated in Figure 6.12, are shown in Table 6.8. Rh₁ is displaced from the plane formed by N₁₁, O₁₂, C₁₃ and C₁₄ by a distance of 0.0068(2) Å. The distance between Rh₁ and Rh₁^{xiv} is 3.5836(9) Å, and the angle between the N₁₁-O₁₂-C₁₃-C₁₄ plane and the rhodium-rhodium interaction is 72.46(3)°. Due to the short Cl₁₄-Cl₁₂ distance [3.963(1) Å] a chloride...chloride interaction can easily be assigned mistakenly, but the possibility is refuted by the C-Cl...Cl angles, which do not agree to one of the types assigned in literature². The packing style is shown in Figure 6.13.

² a) Desiraju, G.R.; Parthasarathy, R. *J. Am. Chem. Soc.* **1989**, *111*, 8725.

b) Awwadi, F.F.; Willett, R.D.; Peterson, K.A.; Twamley, B. *Chem. Eur. J.* **2006**, *12*, 8952.

Chapter 6

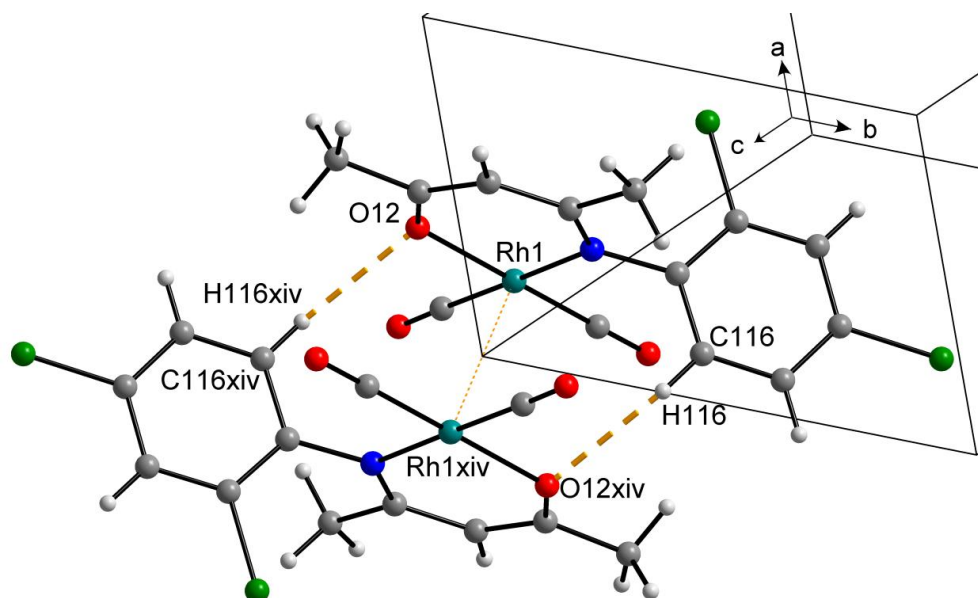


Figure 6.12. Partial unit cell for $[\text{Rh}(2,4\text{-Cl}_2\text{-Phony})(\text{CO})_2]$ with important intra- and intermolecular hydrogen bonding interactions indicated with dashed lines. The rhodium-rhodium interaction is indicated with a dotted line. Symmetry operators are given in Table 6.8.

Table 6.8. Hydrogen bonds for $[\text{Rh}(2,4\text{-Cl}_2\text{-Phony})(\text{CO})_2]$ (Å and °).

D-H...A	$d_{\text{D-H}}$ (Å)	$d_{\text{H...A}}$ (Å)	$d_{\text{D...A}}$ (Å)	\angle_{DHA} (°)
$\text{C}_{116}\text{-H}_{116}\cdots\text{O}_{12}^{\text{xiv}}$	0.95	2.50	3.289(3)	140.7

Symmetry code: (xiv) $-x, -y, -z + 2$

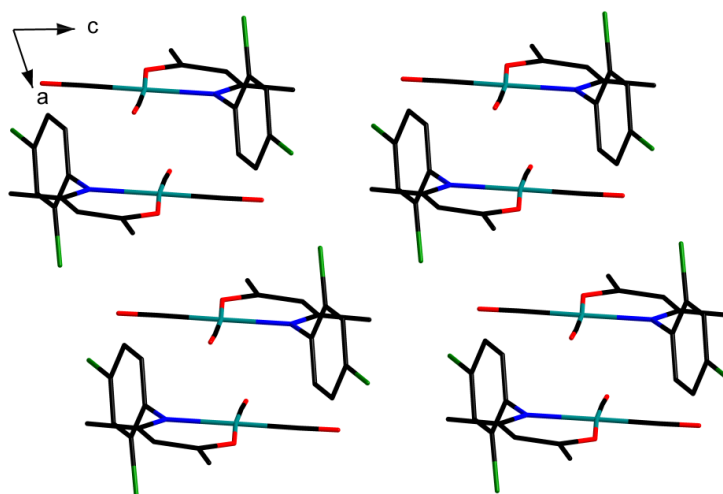


Figure 6.13. View of $[\text{Rh}(2,4\text{-Cl}_2\text{-Phony})(\text{CO})_2]$ along the b -axis illustrating the packing style. Linear stacking due to rhodium-rhodium interactions is clearly visible.

Chapter 6

As seen with previously discussed complexes, the linear packing arrangement in $[\text{Rh}(2,4\text{-Cl}_2\text{-Phony})(\text{CO})_2]$ is clearly visible in Figure 6.13, resulting from intermolecular rhodium-rhodium interactions. As with $[\text{Rh}(2\text{-Cl-Phony})(\text{CO})_2]$, the chloride atoms appear to be close to one another, but are separated by a minimum distance of 5.253(1) Å.

6.2.5 Crystal Structure of Dicarbonyl-[4-(2,6-dichlorophenylamino)pent-3-en-2-onato]-rhodium(I) $[\text{Rh}(2,6\text{-Cl}_2\text{-Phony})(\text{CO})_2]$

The complex $[\text{Rh}(2,6\text{-Cl}_2\text{-Phony})(\text{CO})_2]$, where Phony = 4-(phenylamino)pent-3-en-2-onate, was prepared as discussed in § 3.4.5 and crystallized in the orthorhombic space group $P2_12_12_1$ with $Z = 4$. The complex is shown in Figure 6.14, with important bond distances and angles reported in Table 6.9.

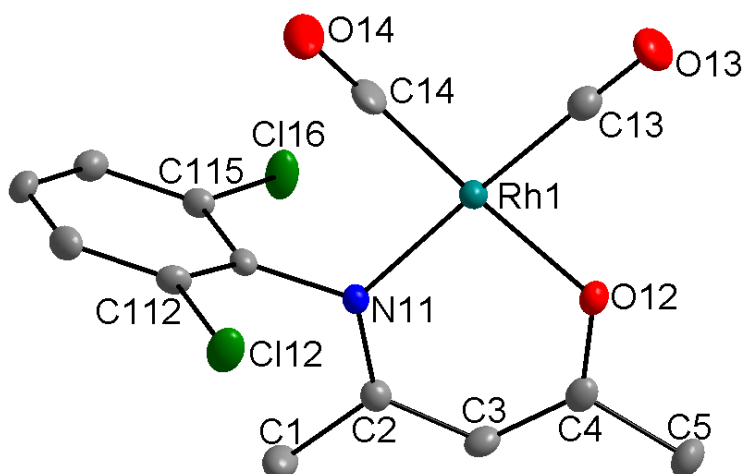


Figure 6.14. DIAMOND¹ view of $[\text{Rh}(2,6\text{-Cl}_2\text{-Phony})(\text{CO})_2]$, where Phony = 4-(phenylamino)pent-3-en-2-onato (50% probability displacement ellipsoids). Hydrogen atoms and selected labels have been omitted for clarity. For the C atoms in the phenyl ring, the first digit indicates molecule number, the second digit indicates ring number and the third digit indicates the position of the atom in the ring. For the Cl atoms, the first digit indicates molecule number while the second digit indicates position on the phenyl ring.

Chapter 6

Table 6.9. Selected bond distances (Å) and angles (°) for [Rh(2,6-Cl₂-Phony)(CO)₂].

Atoms	Distances (Å)	Atoms	Angles (°)
Rh ₁ -N ₁₁	2.051(1)	N ₁₁ -Rh ₁ -O ₁₂	90.15(6)
Rh ₁ -O ₁₂	2.017(1)	O ₁₂ -Rh ₁ -C ₁₃	87.63(7)
Rh ₁ -C ₁₃	1.872(2)	C ₁₃ -Rh ₁ -C ₁₄	89.45(9)
Rh ₁ -C ₁₄	1.834(2)	N ₁₁ -Rh ₁ -C ₁₄	92.77(8)
C ₁₃ -O ₁₃	1.134(2)	N ₁₁ -Rh ₁ -C ₁₃	177.76(8)
C ₁₄ -O ₁₄	1.140(3)	O ₁₂ -Rh ₁ -C ₁₄	176.98(8)
N ₁₁ -C ₁₁₁	1.429(2)	N ₁₁ -C ₂ ...C ₄ -O ₁₂	3.7(2)
N ₁₁ -C ₂	1.324(2)	Dihedral angle ^a	89.35(7)
O ₁₂ -C ₄	1.287(3)		
N ₁₁ ...O ₁₂ (Bite distance)	2.880(2)		

^a Defined as the torsion angle between the N-C-C-C-O plane and the phenyl ring.

No dz^2 rhodium-rhodium interactions were observed in [Rh(2,6-Cl₂-Phony)(CO)₂] due to the steric bulk of the chloride atoms, although intermolecular hydrogen interactions are present. The packing modes are influenced by classic intermolecular C-H...O interactions, as well as C-H...Cl interactions. Hydrogen interactions in the structure are illustrated in Figure 6.15, and shown in Table 6.10. Rh₁ is displaced from the plane formed by N₁₁, O₁₂, C₁₃ and C₁₄ by a distance of 0.0987(1) Å. The absence of rhodium-rhodium interactions in this complex can be explained by the steric influence of the phenyl ring of the 2,6-Cl₂-Phony moiety, since the dihedral angle of the phenyl ring with regard to Rh₁-N₁₁-C₂-C₃-C₄-O₁₂ is 87.20(5)°. The packing style is shown in Figure 6.16.

Chapter 6

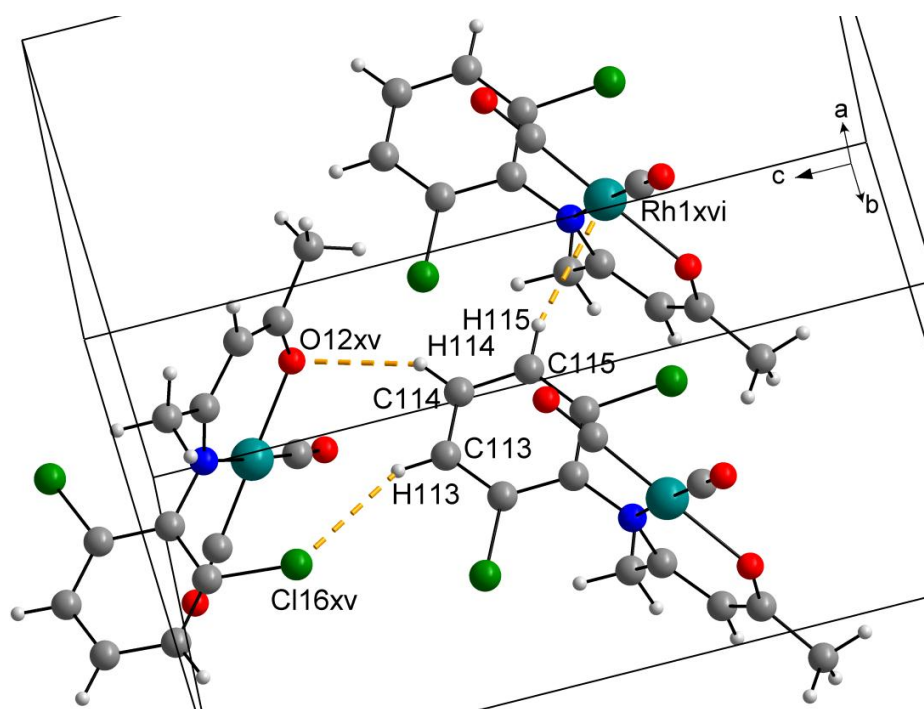


Figure 6.15. Partial unit cell for [Rh(2,6-Cl₂-Phony)(CO)₂] with important intra- and intermolecular hydrogen bonding interactions indicated with dashed lines. The symmetry operator is given in Table 6.10.

Table 6.10. Hydrogen bonds for [Rh(2,6-Cl₂-Phony)(CO)₂] (Å and °).

D-H...A	d_{D-H} (Å)	d_{H...A} (Å)	d_{D...A} (Å)	<DHA (°)
C ₁₁₃ -H ₁₁₃ ...Cl ₁₆ ^{xv}	0.95	2.79	3.663(2)	152.6
C ₁₁₄ -H ₁₁₄ ...O ₁₂ ^{xv}	0.95	2.50	3.342(2)	147.4
C ₁₁₅ -H ₁₁₅ ...Rh ₁ ^{xvi}	0.95	3.04	3.972(2)	166.1

Symmetry code: (xv) $-x + 1/2, -y + 2, z + 1/2$ (xvi) $1 + x, y, z$

Chapter 6

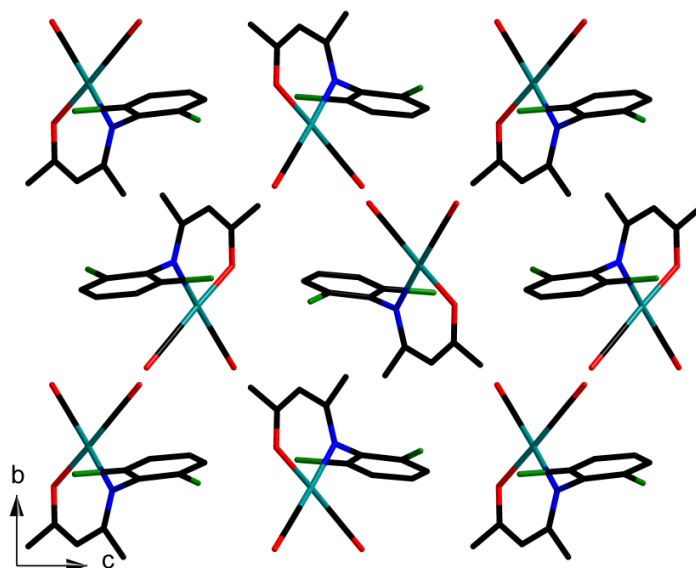


Figure 6.16. View of $[\text{Rh}(2,6\text{-Cl}_2\text{-Phony})(\text{CO})_2]$ along the a -axis illustrating the packing style.

$[\text{Rh}(2,6\text{-Cl}_2\text{-Phony})(\text{CO})_2]$ differs from the other complexes discussed in this chapter in a few respects, of which the lack of rhodium-rhodium interactions is one. A chloride-chloride interaction of distance $3.6279(6) \text{ \AA}$ is mimicked, but is disregarded due to the $\text{C-Cl}\cdots\text{Cl}$ angles of $162.73(6)^\circ$ and $97.17(6)^\circ$ (see discussion on halide interactions in § 4.1). While these types of interactions are absent in this complex, a $\text{C-H}\cdots\text{Rh}$ interaction is present, another anomaly in this range of complexes since no similar interactions could be observed in the other complexes discussed in this chapter. The $\text{H}_{115}\cdots\text{Rh}_1$ distance is 3.04 \AA , with a $\text{C}_{115}\text{-H}_{115}\cdots\text{Rh}_1$ angle of 116.1° . According to Desiraju and Steiner³ metals that act as hydrogen bond acceptors are generally late transition metals in low oxidation states, and contains a filled orbital that is sterically accessible. Metals typically associated with these types of interactions include Fe, Co, Ir, Pd and Pt. The intermolecular interaction of hydrogen atoms with electron-rich metals is a common phenomenon⁴ and has been observed for all types of non-traditional hydrogen bonding donor groups. As per definition of weak hydrogen interactions, the intermolecular hydrogen interaction with Rh in this case fills the criteria³ that the interatomic distance should be smaller than the sum of their Van der Waals radii, which is 3.35 \AA .

³ Desiraju, R.D.; Steiner, T. *The Weak Hydrogen Bond In Structural Chemistry and Biology*, Oxford University Press, New York, **1999**.

⁴ Braga, D.; Grepioni, F.; Desiraju, R.D. *Chem. Rev.* **1998**, *98*, 1375.

6.3. Discussion

Hydrogen interactions are present in all complexes except $[\text{Rh}(2\text{-Cl-Phony})(\text{CO})_2]$ and play a vital role in the packing of these complexes, along with intermolecular rhodium-rhodium interactions, which are present in all complexes except $[\text{Rh}(2,6\text{-Cl}_2\text{-Phony})(\text{CO})_2]$. Yellow-green dichroism was frequently observed in all the complexes and was most prominent in $[\text{Rh}(\text{Phony})(\text{CO})_2]$. Disorders of the hydrogen atoms on the methyl groups in these complexes are absent, with the exception of $[\text{Rh}(4\text{-Cl-Phony})(\text{CO})_2]$. Although the complexes are chemically similar, packing styles are influenced by different contributing factors such as $\text{Rh}\cdots\text{Rh}$ interactions as well as intermolecular $\text{C-H}\cdots\text{O}$, $\text{C-H}\cdots\text{Cl}$ and $\text{C-H}\cdots\text{Rh}$ interactions. The crystal-packing diagrams of complexes $[\text{Rh}(\text{Phony})(\text{CO})_2]$, $[\text{Rh}(4\text{-Cl-Phony})(\text{CO})_2]$ and $[\text{Rh}(2,4\text{-Cl}_2\text{-Phony})(\text{CO})_2]$ reveal one-dimensional coordination polymers, while complex $[\text{Rh}(2\text{-Cl-Phony})(\text{CO})_2]$ displays dimeric coordination packing. Packing occurs in a head-to-tail fashion with regard to the carbonyl groups for the above complexes, with $[\text{Rh}(2,6\text{-Cl}_2\text{-Phony})(\text{CO})_2]$ being the exception to this rule. This is consistent with literature, where the majority of rhodium L,L'-bidentate dicarbonyl complexes pack in a head-to-tail fashion due to steric constraints (Table 6.11). For comparative purposes the complexes in Table 6.11 are visually illustrated in Figure 6.17. The complexes are ordered according to increasing $\text{N}\cdots\text{O}$ distances, which is a manifestation of the bite angle.

Chapter 6

Table 6.11. Comparison of [Rh(N,O-Bid)(CO)₂] complexes with [Rh(L,L'-bid)(CO)₂] complexes. The complexes are ordered according to increasing N...O distances.

	CSD ⁵ Reference code ^b	L,L' Type	d(Rh...Rh) (Å)	Packing style ^c	d(N...O) ^d (Å)	d(R ₁ -N ₁₁) ^d (Å)	d(R ₁ -O ₁₂) ^d (Å)	N ₁₁ -Rh- O ₁₂ ^d (°)	N ₁₁ -C ₂ ... C ₄ -O ₁₂ ^d (°)
1	DEXHJ ⁶	O,O	6.668(3)	HT	2.771(5)	2.016(3)	2.015(3)	86.8(1)	1.4(4)
2	KEFJUB ⁷	O,O	4.587(1)	O	2.809(6)	2.008(5)	2.007(4)	88.8(2)	-1.0(5)
3	KEFJOV ⁷	O,O	3.2337(4)	HT	2.831(2)	2.021(2)	2.018(2)	89.00(7)	0.7(2)
4	BTFARH ⁸	O,O	3.5368(0)	D	2.8583(0)	2.0264(0)	2.0346(0)	89.751(0)	1.692(0)
5	QUNBAC ⁹	N,O	3.399(3)	HT	2.869(4)	2.034(4)	2.040(4)	89.5(1)	1.2(4)
V ^e		N,O	N/A	O	2.880(2)	2.051(1)	2.017(1)	90.15(6)	3.7(2)
II ^e		N,O	3.4151(7)	HT	2.882(3)	2.054(2)	2.019(2)	90.08(8)	1.4(1)
6	KAKYUR ¹⁰	O,O	3.346(1)	D	2.887(8)	2.016(6)	2.049(6)	90.1(3)	1.0(8)
7	VAVJUX ¹¹	O,O	3.4187(9)	D	2.89(7)	2.04(1)	2.03(1)	90.6(4)	2(1)
IV ^e		N,O	3.5477(5)	HT	2.893(2)	2.020(1)	2.057(2)	90.36(5)	-0.7(1)
I ^e		N,O	3.4358(2)	O	2.906(2)	2.058(2)	2.032(2)	90.55(6)	-0.4(2)
8	ACABRH02 ¹²	O,O	3.2711(3)	HT	2.9089(4)	2.0443(3)	2.0401(2)	90.827(6)	0.12(1)
III ^e		N,O	3.5836(9)	HT	2.93(1)	2.065(8)	2.033(6)	91.2(3)	0.0(7)
9	BUPCUK ¹³	O,O	N/A	HT	2.9960(8)	2.1339(6)	2.0089(6)	92.58(1)	26.48(3) ^f
Average					2.88(7)	2.03(2)	2.03(2)	90.0(6)	1(2) ^g

^b ACABRH02 = acetylacetonato-dicarbonyl-rhodium(I); BTFARH = benzoyl-1,1,1-trifluoroacetato-dicarbonyl-rhodium(I); BUPCUK = dicarbonyl-(1*S*)-3-trifluoroacetylcamphorate-rhodium(I) dicarbonyl-(1*R*)-3-trifluoroacetylcamphorate-iridium(I); DEXHJ = (1*RS*,4*SR*)-(trifluoroacetyl-menthonato-O,O')-dicarbonyl-rhodium(I); KAKYUR = dicarbonyl-(1-ferrocenyl-4,4,4-trifluoro-1,3-butanedionato)-rhodium(I); KEFJOV = dicarbonyl-(5-methyl-9-oxophenalen-1-one-O,O')-rhodium(I); KEFJUB = dicarbonyl-(9-oxophenalen-1-one-O,O')-rhodium(I); VAVJUX = tetracarbonyl-(μ2-3,3'-hexafluoro-glutaryl-bis-(1*R*)-camphorato-O,O',O",O"-dirhodium(I); QUNBAC = dicarbonyl-(4-amino-1,1,1-trifluoro-3-penten-2-onato-N,O)-rhodium(I).

^c HT: head-to-tail; HH: head-to-head; D: Diagonal; O: Other.

^d Average values are used for complexes with more than one independent molecule in the asymmetric unit.

^e **I** = [Rh(Phony)(CO)₂]; **II** = [Rh(2-Cl-Phony)(CO)₂]; **III** = [Rh(4-Cl-Phony)(CO)₂]; **IV** = [Rh(2,4-Cl₂-Phony)(CO)₂]; **V** = [Rh(2,6-Cl₂-Phony)(CO)₂].

^f Torsion angle excluded in the calculation of the average value due to outlier nature.

^g Average calculated for absolute values of angles.

⁵ Allen, F.H. The Cambridge Structural Database Version 1.9, *Acta Cryst.* **2002**, B58, 380.

⁶ Schurig, V.; Pille, W.; Peters, K.; Von Schnering, H.G. *Mol. Cryst. Liq. Cryst.* **1985**, 120, 385.

⁷ Mochida, T.; Torigoe, R.; Koinuma, T.; Asano, C.; Satou, T.; Koike, K.; Nikaido, T. *Eur. J. Inorg. Chem.* **2006**, 558.

⁸ Leipoldt, J.G.; Bok, L.D.C.; Basson, S.S.; Van Vollenhoven, J.S.; Gerber, T.I.A. *Inorg. Chim. Acta* **1977**, 25, L63.

⁹ Varshavsky, Y.S.; Galding, M.R.; Cherkasova, T.G.; Podkorytov, I.S.; Nikol'skii, A.B.; Trzeciak, A.M.; Olejnik, Z.; Lis, T.; Ziolkowski, J.J. *J. Organomet. Chem.* **2001**, 628, 195.

¹⁰ Conradie, J.; Cameron, T.S.; Aquino, M.A.S.; Lamprecht, G.J.; Swarts, J.C. *Inorg. Chim. Acta* **2005**, 358, 2530.

¹¹ Schurig, V.; Gaus, H.; Scheer, P.; Walz, L.; Von Schnering, H.G. *Angew. Chem., Int. Ed.* **1989**, 28, 1019.

¹² Huq, F.; Skapski, A.C. *J. Cryst. Mol. Struct.* **1974**, 4, 411.

¹³ Schurig, V.; Pille, W.; Winter, W. *Angew. Chem., Int. Ed.* **1983**, 22, 327.

Chapter 6

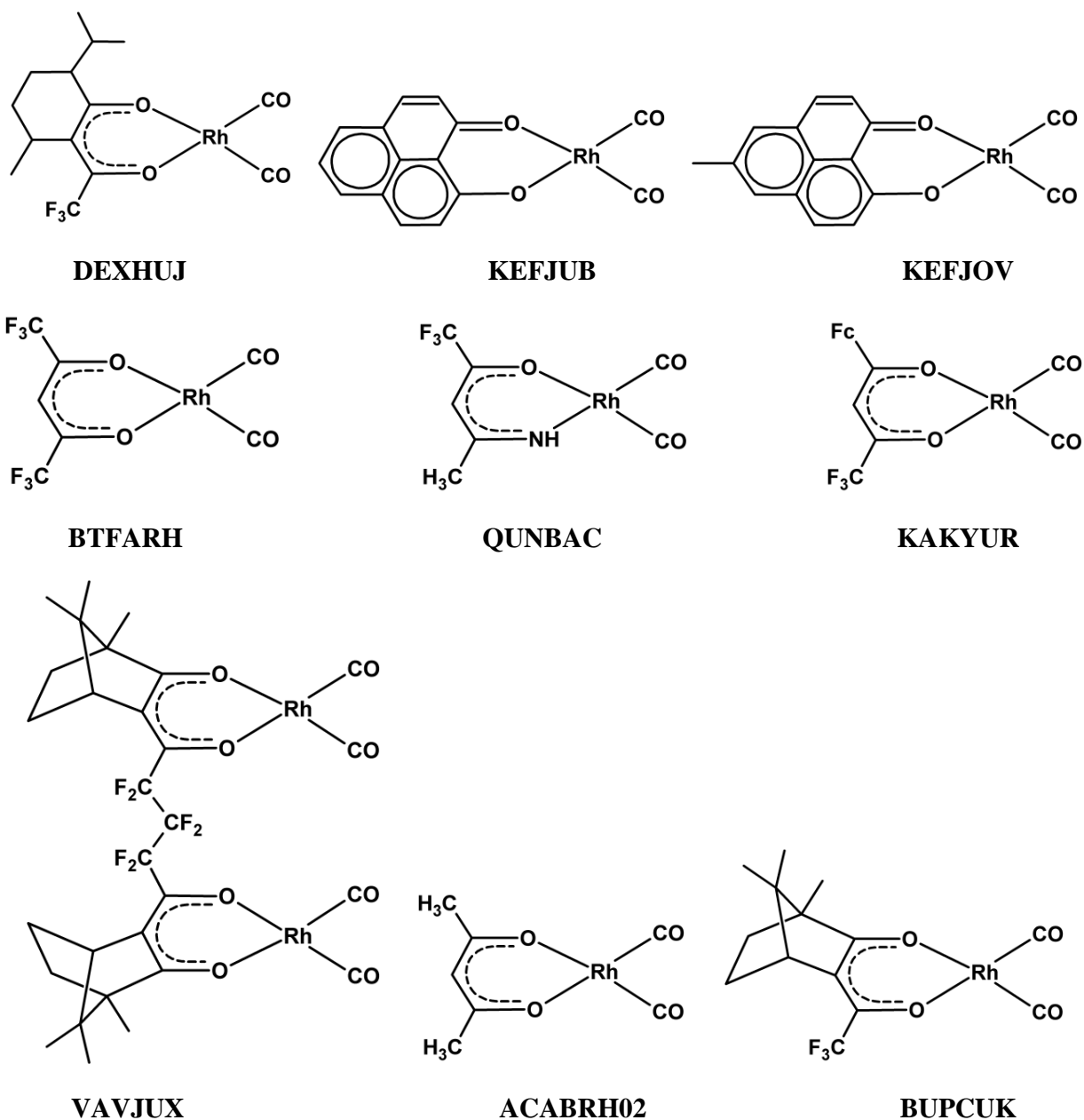


Figure 6.17. Illustrations of comparative $[\text{Rh}(\text{L},\text{L}'\text{-bid})(\text{CO})_2]$ complexes found in literature, ordered according to ascending $\text{N}\cdots\text{O}$ distance. ACABRH02 = acetylacetonato-dicarbonyl-rhodium(I); BTFARH = benzoyl-1,1,1-trifluoroacetato-dicarbonyl-rhodium(I); BUPCUK = dicarbonyl-(1*S*)-3-trifluoroacetylcamphorate-rhodium(I) dicarbonyl-(1*R*)-3-trifluoroacetyl-camphorate-iridium(I); DEXHUJ = (1*RS*,4*SR*)-(trifluoroacetyl-menthonato-*O,O'*)-dicarbonyl-rhodium(I); KAKYUR = dicarbonyl-(1-ferrocenyl-4,4,4-trifluoro-1,3-butanedionato)-rhodium(I); KEFJOV = dicarbonyl-(5-methyl-9-oxophenalen-1-one-*O,O'*)-rhodium(I); KEFJUB = dicarbonyl-(9-oxophenalen-1-one-*O,O'*)-rhodium(I); VAVJUX = tetracobonyl-(μ 2-3,3'-hexafluoro-glutarylbis-(1*R*)-camphorate-*O,O',O'',O'''*)-di-rhodium(I); QUNBAC = dicarbonyl-(4-amino-1,1,1-trifluoro-3-penten-2-onato-*N,O*)-rhodium(I).

Chapter 6

The absence of rhodium-rhodium interactions in $[\text{Rh}(2,6\text{-Cl}_2\text{-Phony})(\text{CO})_2]$ and the accompanying lack of linear $\text{Rh}\cdots\text{Rh}$ packing can be attributed to the steric intervention of the Cl-atoms on the phenyl ring. The packing of the complex is instead influenced by both $\text{C-H}\cdots\text{O}$ and $\text{C-H}\cdots\text{Cl}$ interactions, as well as a $\text{C-H}\cdots\text{Rh}$ interaction which compensates for the lack of $\text{Rh}\cdots\text{Rh}$ interaction.

Crystal structures of complexes of the type $[\text{Rh}(\text{N,O-bid})(\text{CO})_2]$ are surprisingly limited⁵, while more complexes employ diketonato type ligands. Upon coordination of the bidentate ligand, the unsaturated carbon-carbon bond of the pentenone backbone becomes delocalized and $\text{C}_2\text{-C}_3$ and $\text{C}_3\text{-C}_4$ distances no longer vary significantly. The $\text{N}_{11}\text{-C}_2\cdots\text{C}_4\text{-O}_{12}$ torsion angles seem to be independent of the electronic properties of substituents on the ligand and do not follow a clear trend when compared with the $\text{N}_{11}\text{-Rh-O}_{12}$ bite angles, displaying angles of less than 2° with the exception of $[\text{Rh}(2,6\text{-Cl}_2\text{-Phony})(\text{CO})_2]$ and complex **9**. In both these cases the steric bulk of the ligand has a significant influence on the distortion of the $\text{N}_{11}\text{-C}_2\text{-C}_3\text{-C}_4\text{-O}_{12}$ backbone of the ligand. The complexes adopt a square planar geometry, with the most significant distortion of the rhodium atom from the $\text{N}_{11}\text{-O}_{12}\text{-C}_{13}\text{-C}_{14}$ plane being $0.0987(1)$ Å for $[\text{Rh}(2,6\text{-Cl}_2\text{-Phony})(\text{CO})_2]$, with the second largest being $0.0298(8)$ Å for complex **6**. While the $\text{N}_{11}\text{-Rh-O}_{12}$ bite angles appear to be larger when rhodium is coordinated to more electron-donating ligands, the steric properties of the ligands also play an important role in the geometric parameters of such complexes. The $\text{Rh}_1\text{-C}_{13}$ and $\text{Rh}_1\text{-C}_{14}$ distances do not disagree significantly in complexes with O,O-bidentate ligands, however, in complexes containing N,O-bidentate ligands an elongation of the $\text{Rh}_1\text{-C}_{13}$ distances is presented due to the higher *trans* influence of the nitrogen atom. While no significant trend could be observed with regard to ‘head-to-tail’ orientation in complexes containing O,O-bidentate ligands, complexes containing N,O-bidentate ligands investigated in this chapter were orientated in a head-to-tail fashion, in other words in each case the N,O-bidentate ligand was packed next to the carbonyl ligands of the adjacent molecules. Once again $[\text{Rh}(2,6\text{-Cl}_2\text{-Phony})(\text{CO})_2]$ was the exception, although this does not appear to be related to rhodium-rhodium interactions, packing style, $\text{N}\cdots\text{O}$ distance or even steric bulk of the bidentate ligand. $[\text{Rh}(2,6\text{-Cl}_2\text{-Phony})(\text{CO})_2]$ does however exhibit a $\text{C-H}\cdots\text{Rh}$ interaction which is not present in any of the other complexes.

6.4. Conclusion

Slight differences were observed regarding bond distances and angles between the separate complexes, confirmed through both X-ray diffraction and NMR techniques. The *trans* influence of nitrogen was confirmed through the elongation of the Rh₁-C₁₃ bond with respect to the Rh₁-C₁₄ bond. The contribution of the chloride substituents on the geometrical parameters can clearly be seen in the differences in Rh₁-C₁₃ and Rh₁-C₁₄ distances. This is supported by information from the calculated structures (see Chapter 7) and literature, where the electronic properties of substituents on the phenyl ring impacts the geometrical parameters of the respective complexes. This property allows for the tailoring of [Rh(N,O-bid)(CO)₂] complexes to suit different criteria for their utilization as possible catalysts. Large differences between stretching frequencies of the solid state complexes can be explained by the influences of intra- and intermolecular hydrogen, rhodium-rhodium and π - π interactions on the packing modes. The position of the chloride atoms on the ring, and the subsequent influence on the packing modes, is also clearly signified in the variation in crystal systems and space groups as the position and number of the chloride atoms on the phenyl ring changes.

Chapter 6

7 Theoretical Study of Functionalized Dicarbonyl-[4-(phenyl- amino)pent-3-en-2-onato]-rhodium(I) Complexes

7.1. Introduction

In the following chapter a theoretical investigation is presented on the behavior of dicarbonyl-[4-(phenylamino)pent-3-en-2-onato]-rhodium(I), or $[\text{Rh}(\text{N},\text{O}\text{-Bid})(\text{CO})_2]$ type compounds (where N,O-Bid is a derivative of 4-(phenylamino)pent-3-en-2-onate, Phony⁻) in respect to functionalization and hydrogen bond formation. Electronic effects are included in the study by incorporating substituents on the phenyl ring of the N,O-Bid ligand to determine the effects of strong electron withdrawing groups, such as chloride moieties. General aspects of computational chemistry have been included in Chapter 5 and the reader is referred to § 5.1 for more information if required.

7.2. Results

The calculated energies for the compounds described in Chapter 6, optimized through DFT calculations using GAUSSIAN-03W¹, are compared in Table 7.1. Energy levels were adjusted

¹ Frisch, M.J.; Trucks, G.W.; Schlegel, H.B.; Scuseria, G.E.; Robb, M.A.; Cheeseman, J.R.; Montgomery Jr., J.A.; Vreven, T.; Kudin, K.N.; Burant, J.C.; Millam, J.M.; Iyengar, S.S.; Tomasi, J.; Barone, V.; Mennucci, B.; Cossi, M.; Scalmani, G.; Rega, N.; Petersson, G.A.; Nakatsuji, H.; Hada, M.; Ehara, M.; Toyota, K.; Fukuda, R.; Hasegawa, J.; Ishida, M.; Nakajima, T.; Honda, Y.; Kitao, O.; Nakai, H.; Klene, M.; Li, X.; Knox, J.E.; Hratchian, H.P.; Cross, J.B.; Bakken, V.; Adamo, C.; Jaramillo, J.; Gomperts, R.; Stratmann, R.E.; Yazyev, O.; Austin, A.J.; Cammi, R.; Pomelli, C.; Ochterski, J.W.; Ayala, P.Y.; Morokuma, K.; Voth, G.A.; Salvador, P.; Dannenberg, J.J.;

Chapter 7

such that the compound with the lowest energy for the optimized (DFT) structures, [Rh(Phony)(CO)₂], and single point structures obtained by using the solid state data given in Chapter 6 without any optimization, [Rh(2,4-Cl₂-Phony)CO)₂], are shown as the respective minima. The relative energies of the different compounds are shown in red in Figure 7.1 and compared with the energies from the free ligands described earlier (blue, see Chapter 5). An overview of the cell dimensions in Chapter 6 is related in Table 7.3 while important bond distances and angles are reported in Table 7.2. The overlay figures of these structures in the solid state (red) and the calculated optimized (DFT) structures (blue) are shown in Figure 7.2. Observed solid state (KBr) and calculated carbonyl stretching frequencies (ν_{CO}) for the complexes are shown in Table 7.4.

Table 7.1. Calculated optimized and single point energies of complexes relative to energy of [Rh(Phony)(CO)₂] for optimized complexes and [Rh(2-Cl-Phony)(CO)₂] for single point calculations.

N,O-Bid ligands	$\Delta E_{\text{Single point}} \text{ (kJ.mol}^{-1}\text{)}$	$\Delta E_{\text{Optimized}} \text{ (kJ.mol}^{-1}\text{)}$
Phony	76.06	0.00
2-Cl-Phony	49.56	7.30
4-Cl-Phony	49.96	2.48
2,4-Cl ₂ -Phony	0.00	8.40
2,6-Cl ₂ -Phony	8.77	13.14

Zakrzewski, V.G.; Dapprich, S.; Daniels, A.D.; Strain, M.C.; Farkas, O.; Malick, D.K.; Rabuck, A.D.; Raghavachari, K.; Foresman, J.B.; Ortiz, J.V.; Cui, Q.; Baboul, A.G.; Clifford, S.; Cioslowski, J.; Stefanov, B.B.; Liu, G.; Liashenko, A.; Piskorz, P.; Komaromi, I.; Martin, R.L.; Fox, D.J.; Keith, T.; Al-Laham, M.A.; Peng, C.Y.; Nanayakkara, A.; Challacombe, M.; Gill, P.M.W.; Johnson, B.; Chen, W.; Wong, M.W.; Gonzalez, C.; Pople, J.A. GAUSSIAN-03, Revision C.01, Gaussian, Inc., Wallingford, CT, **2004**.

Chapter 7

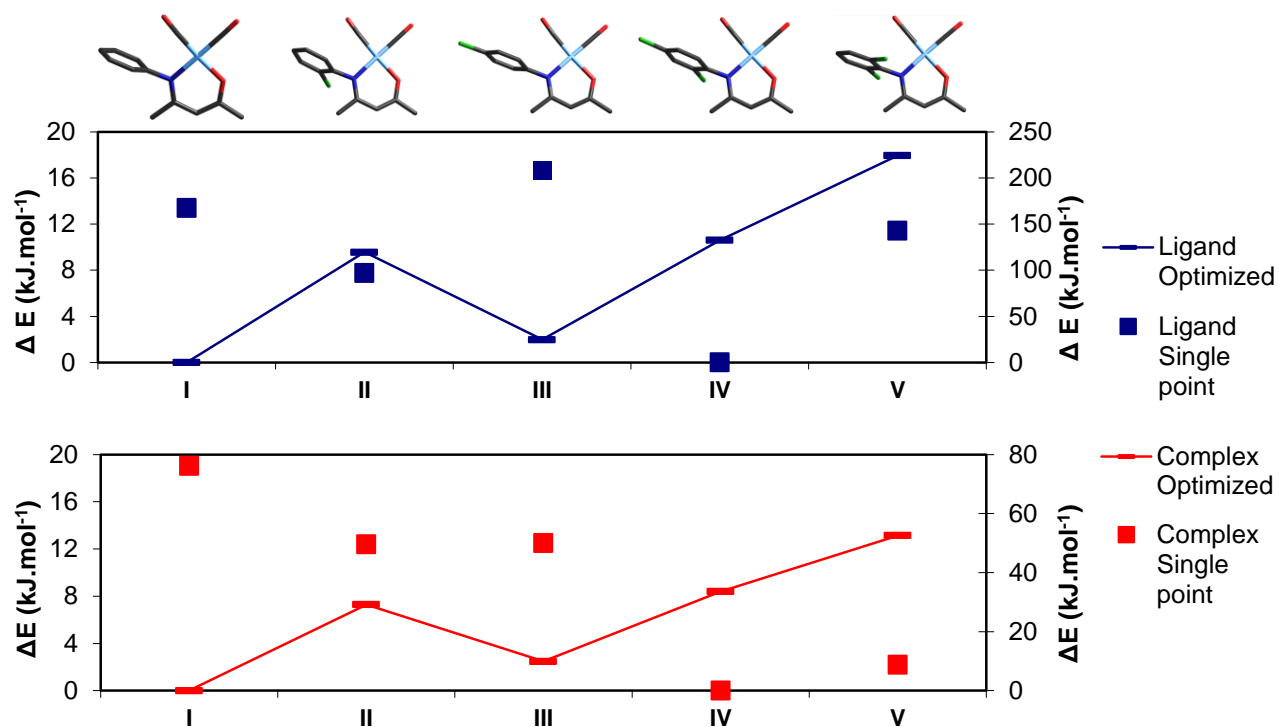


Figure 7.1. Diagram of solid state single point and DFT calculated optimized relative energies of free N,O-BidH (blue) and $[\text{Rh}(\text{N,O-Bid})(\text{CO})_2]$ complexes (red) from GAUSSIAN-03W. DFT calculated energies for the compounds are reported relative to PhonyH at 0.00 kJ.mol^{-1} and relative to $[\text{Rh}(\text{Phony})(\text{CO})_2]$ at 0.00 kJ.mol^{-1} for the complexes.

Table 7.2. Comparison of selected geometrical parameters of solid state structures of [Rh(N,O-Bid)(CO)₂] complexes with their DFT optimized counterparts (Å, °).

	[Rh(Phony)(CO) ₂]		[Rh(2-Cl-Phony)(CO) ₂]		[Rh(2,4-Cl ₂ -Phony)(CO) ₂]		[Rh(2,6-Cl ₂ -Phony)(CO) ₂]			
	SS ^a	DFT ^b	SS	DFT	SS	DFT	SS	DFT		
Interatomic distance										
Rh ₁ -N ₁₁	2.058(2)	2.105	2.054(2)	2.107	2.065(8)	2.104	2.057(2)	2.064	2.051(1)	2.112
Rh ₁ -O ₁₂	2.032(2)	2.064	2.019(2)	2.064	2.033(6)	2.064	2.020(1)	2.107	2.017(1)	2.065
Rh ₁ -C ₁₃	1.866(2)	1.900	1.858(3)	1.899	1.86(1)	1.900	1.873(2)	1.900	1.872(2)	1.898
Rh ₁ -C ₁₄	1.841(3)	1.874	1.849(3)	1.873	1.84(1)	1.874	1.838(2)	1.872	1.834(2)	1.871
C ₁₃ -O ₁₃	1.142(3)	1.140	1.135(4)	1.140	1.14(1)	1.140	1.133(2)	1.139	1.134(2)	1.140
C ₁₄ -O ₁₄	1.143(3)	1.144	1.143(3)	1.143	1.15(1)	1.143	1.142(2)	1.143	1.140(3)	1.143
N ₁₁ ...O ₁₂	2.906(2)	2.940	2.882(3)	2.940	2.93(1)	2.939	2.893(2)	2.939	2.880(2)	2.940
Rh displacement ^c	0.0218(2)	0.0000	0.0266(2)	0.0039	0.0000(0)	0.0002	0.0206(2)	0.0026	0.0089(1)	0.0002
Interatomic angle										
Angles (°)										
N ₁₁ -Rh ₁ -O ₁₂	90.55(6)	89.75	90.08(8)	89.63	91.2(3)	89.70	90.36(5)	89.56	90.15(6)	89.48
O ₁₂ -Rh ₁ -C ₁₃	89.75(8)	86.58	88.5(1)	86.59	87.9(4)	86.56	88.76(6)	86.63	87.63(7)	86.65
C ₁₃ -Rh ₁ -C ₁₄	86.5(1)	89.39	87.2(1)	89.41	87.0(5)	89.41	87.07(8)	89.38	89.45(9)	89.37
N ₁₁ -Rh ₁ -C ₁₄	93.13(9)	94.28	94.2(1)	94.38	94.0(4)	94.33	93.81(7)	94.43	92.77(8)	94.50
N ₁₁ -C ₂ ...C ₄ -O ₁₂	-0.4(2)	0.30	1.4(1)	0.17	0.0(7)	0.02	-0.7(1)	0.11	3.7(2)	-0.01
Dihedral angle ^d	87.88(8)	89.99	85.20(9)	86.74	90.0(2)	89.95	85.85(6)	87.06	89.35(7)	89.99

^a SS = solid state structure.

^b DFT = optimized calculated structure.

^c Displacement of the Rh atom from the N₁₁-O₁₂-C₁₃-C₁₄ plane – see Figure 6.1.

^d The torsion angle between the N₁₁-C₂-C₃-C₄-O₁₂ plane and the N-substituted phenyl ring – see Figure 6.1.

Chapter 7

Table 7.3. Cell dimension overview for dicarbonyl-[4-(phenylamino)pent-3-en-2-onato]-rhodium(I) [Rh(Phony)(CO)₂] and the chloride derivatives thereof.

	[Rh(Phony)(CO) ₂]	[Rh(2-Cl-Phony)(CO) ₂]	[Rh(4-Cl-Phony)(CO) ₂]	[Rh(2,4-Cl ₂ -Phony)(CO) ₂]	[Rh(2,6-Cl ₂ -Phony)(CO) ₂]
Crystal system	Monoclinic	Orthorhombic	Orthorhombic	Triclinic	Orthorhombic
Space group	<i>I2/a</i>	<i>Pbca</i>	<i>Pnma</i>	<i>P</i> $\bar{1}$	<i>P2₁2₁2₁</i>
<i>a</i> (Å)	13.3756(2)	14.309(4)	13.163(2)	7.157(2) 9.983(2)	7.8800(2)
<i>b</i> (Å)	96.193(1)	10.085(3)	6.8055(9)	10.654(3)	12.3010(3)
<i>c</i> (Å)	21.2210(3)	18.886(6)	14.962(2) Å	83.086(1)	15.0740(3)
α (°)	90	90	90	71.601(2)	90
β (°)	9.2915(1)	90	90	82.059(1)	90
γ (°)	90	90	90	2	90
<i>Z</i>	8	8	4		4

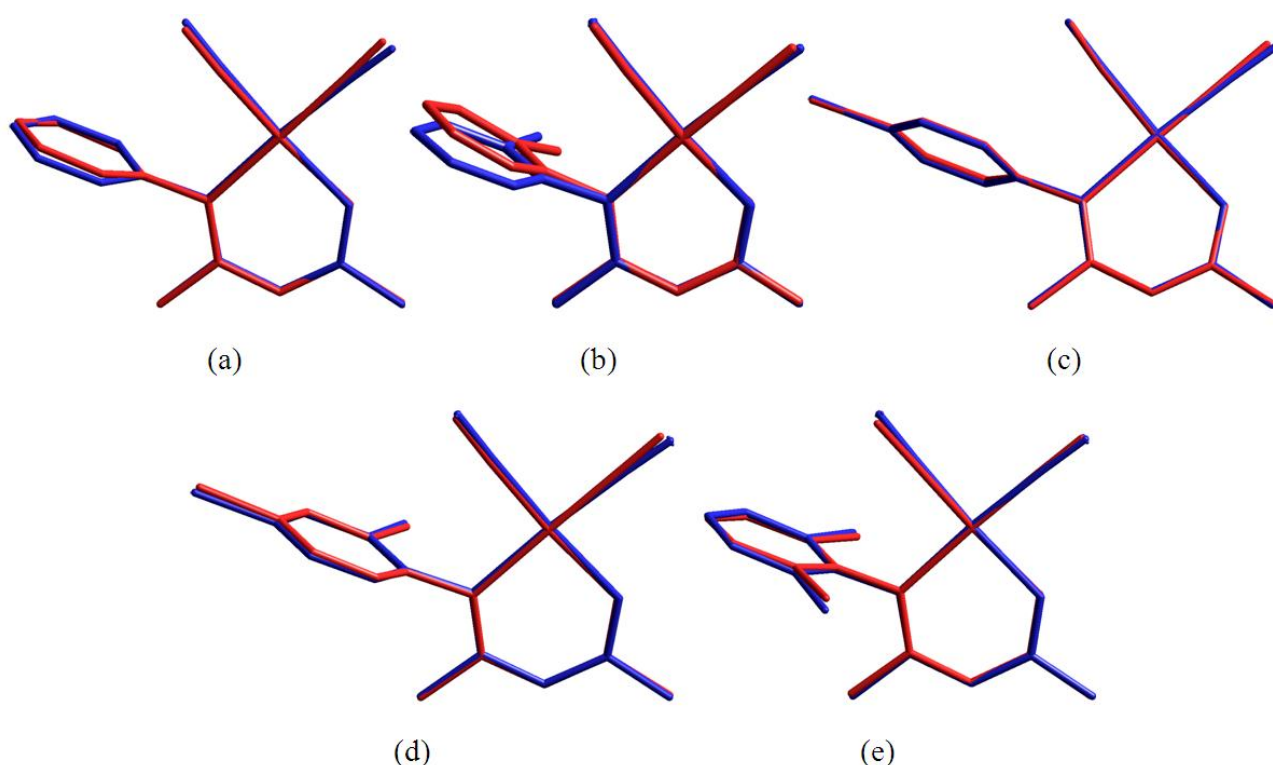


Figure 7.2. Overlay figures of the calculated (DFT) and solid state structures of a) [Rh(Phony)(CO)₂], RMS value = 0.163 Å; b) [Rh(2-Cl-Phony)(CO)₂], RMS value = 0.233 Å; c) [Rh(4-Cl-Phony)(CO)₂], RMS value = 0.062 Å; d) [Rh(2,4-Cl₂-Phony)(CO)₂], RMS value = 0.088 Å; e) [Rh(2,6-Cl₂-Phony)(CO)₂], RMS value = 0.126 Å. Overlay fit includes all non-hydrogen atoms. The blue structures denote the calculated complexes, while the red structures refer to the single point observed solid state complexes.

Chapter 7

Table 7.4. Observed solid state and calculated ν_{CO} for [Rh(N,O-Bid)(CO)₂] complexes.

Compound	$\nu_{\text{CO(asy)}} (\text{cm}^{-1})$		$\nu_{\text{CO(sym)}} (\text{cm}^{-1})$	
	Observed	Calculated	Observed	Calculated
	(Solid state)		(Solid state)	
[Rh(Phony)(CO) ₂]	1999	2001	2062	2056
[Rh(2-Cl-Phony)(CO) ₂]	2005	2001	2075	2057
[Rh(4-Cl-Phony)(CO) ₂]	1995	2001	2065	2057
[Rh(2,4-Cl ₂ -Phony)(CO) ₂]	1990	2002	2069	2058
[Rh(2,6-Cl ₂ -Phony)(CO) ₂]	2001	2001	2072	2058

7.3. Discussion

The solid state structures of the above-mentioned complexes show good correlation with the calculated (DFT) structures, with RMS overlay values ranging from 0.664 Å to 0.713 Å (Figure 7.2). Angles and distances are compared in Table 7.2. The calculated energy (Figure 7.1) of [Rh(2,6-Cl₂-Phony)(CO)₂] is significantly larger than the first four complexes, with [Rh(Phony)(CO)₂] having the lowest energy.

Despite the large differences in energy, the geometric parameters of the optimized complexes are surprisingly similar. The Rh₁-N₁₁ distances, for example, are 2.105 Å, 2.107 Å, 2.104 Å, 2.107 Å and 2.112 Å for the respective complexes and represent a difference of only 0.007 Å between the highest and lowest values. Other parameters display even smaller differences and generally differ by only 0.001 or 0.002 Å.

Differences in bond angles are more pronounced than the bond distances, albeit still small. The N₁₁-Rh₁-O₁₂ angle varies between 89.75° for [Rh(Phony)(CO)₂] and 89.48° for [Rh(2,6-Cl₂-Phony)(CO)₂], a difference of 0.27°. It is unexpected that these values should differ at all, since $d(\text{N}_{11}\cdots\text{O}_{12})$ was calculated as 2.940 Å for both complexes, and varied with 0.001 Å for [Rh(4-Cl-Phony)(CO)₂] and [Rh(2,4-Cl₂-Phony)(CO)₂]. The range for O₁₂-Rh₁-C₁₃ is from 86.56° for [Rh(4-Cl-Phony)(CO)₂] to 86.65° for [Rh(2,6-Cl₂-Phony)(CO)₂], a difference of 0.09°. The C₁₃-Rh₁-C₁₄ range is even smaller; from 89.37° for [Rh(2,6-Cl₂-Phony)(CO)₂] to 89.41° for [Rh(2-Cl-Phony)(CO)₂] and [Rh(4-Cl-Phony)(CO)₂], a difference of 0.04°. The N₁₁-Rh₁-C₁₄ angle has

Chapter 7

a slightly larger range; 94.28° for $[\text{Rh}(\text{Phony})(\text{CO})_2]$ to 94.50° for $[\text{Rh}(2,6\text{-Cl}_2\text{-Phony})(\text{CO})_2]$, a difference of 0.22° , however, the most significant differences in parameters is displayed in the dihedral angle (the angle between the $\text{N}_{11}\text{-C}_2\text{-C}_3\text{-C}_4\text{-O}_{12}$ plane and the phenyl ring). Complexes with symmetrical substitutions of chlorides – either no substitution like $[\text{Rh}(\text{Phony})(\text{CO})_2]$, *para*-substitution like $[\text{Rh}(4\text{-Cl-Phony})(\text{CO})_2]$ or substitution on both *ortho* positions like $[\text{Rh}(2,6\text{-Cl}_2\text{-Phony})(\text{CO})_2]$ - share a value for the dihedral angle of 89.99° while the dihedral angles for $[\text{Rh}(2\text{-Cl-Phony})(\text{CO})_2]$ and $[\text{Rh}(2,4\text{-Cl}_2\text{-Phony})(\text{CO})_2]$ are 86.74° and 87.06° , respectively; amounting to differences of 3.25° and 2.93° .

Considering the above-mentioned information it is to be expected that the complexes would exhibit energies closer to each other. It would seem, however, that the presence and position of the chloride atoms plays a significant role in the total energy of the complex. Although $[\text{Rh}(2\text{-Cl-Phony})(\text{CO})_2]$ and $[\text{Rh}(4\text{-Cl-Phony})(\text{CO})_2]$, and $[\text{Rh}(2,4\text{-Cl}_2\text{-Phony})(\text{CO})_2]$ and $[\text{Rh}(2,6\text{-Cl}_2\text{-Phony})(\text{CO})_2]$ have the same chemical formulae, large differences in energy indicate the influence of electronic factors on the energy of the complexes. Despite the low RMS values, angles and distances vary significantly between the solid state and calculated structures. The $\text{Rh}_1\text{-N}_{11}$ distances for complex $[\text{Rh}(4\text{-Cl-Phony})(\text{CO})_2]$ differ by 0.036 \AA between the solid state and calculated structures, while the corresponding distances differ by as much as 0.087 \AA for $[\text{Rh}(2,4\text{-Cl}_2\text{-Phony})(\text{CO})_2]$. The differences in $\text{Rh}_1\text{-O}_{12}$ distances provide a contrast with the $\text{Rh}_1\text{-N}_{11}$ distances since the complex with the largest discrepancy between the $\text{Rh}_1\text{-N}_{11}$ distances, $[\text{Rh}(2,4\text{-Cl}_2\text{-Phony})(\text{CO})_2]$, only differs with 0.007 \AA for $\text{Rh}_1\text{-O}_{12}$. The largest difference in $\text{Rh}_1\text{-O}_{12}$ distances is manifested in $[\text{Rh}(2,6\text{-Cl}_2\text{-Phony})(\text{CO})_2]$, with a difference of 0.048 \AA . While both the $\text{Rh}_1\text{-C}_{13}$ and the $\text{Rh}_1\text{-C}_{14}$ bonds show differences between the solid state and calculated structures of 0.041 \AA for $[\text{Rh}(2\text{-Cl-Phony})(\text{CO})_2]$ and 0.037 \AA for $[\text{Rh}(2,6\text{-Cl}_2\text{-Phony})(\text{CO})_2]$ for the respective distances, the $\text{C}_{13}\text{-O}_{13}$ and $\text{C}_{14}\text{-O}_{14}$ distances show no significant difference. The differences in the $\text{Rh}_1\text{-C}_{13}$ and $\text{Rh}_1\text{-C}_{14}$ distances are reflected in the CO stretching frequencies (ν_{CO} , see Table 7.4), where the complex with the smallest difference between $\text{Rh}_1\text{-C}_{13}$ and $\text{Rh}_1\text{-C}_{14}$ $\{[\text{Rh}(2\text{-Cl-Phony})(\text{CO})_2]$, with $d(\text{Rh}_1\text{-C}_{13})$ and $d(\text{Rh}_1\text{-C}_{14})$ values of $1.858(3) \text{ \AA}$ and $1.849(3) \text{ \AA}$, respectively} displays the highest CO stretching frequencies while the complex with the greatest differences $\{[\text{Rh}(2,4\text{-Cl}_2\text{-Phony})(\text{CO})_2]$, with $d(\text{Rh}_1\text{-C}_{13})$ and $d(\text{Rh}_1\text{-C}_{14})$ values of $1.873(2) \text{ \AA}$ and $1.838(2) \text{ \AA}$, respectively} exhibit the lowest.

Chapter 7

The discrepancies between solid state and calculated structures continue in the angles around the Rh atom, with the differences being consistently the largest for $[\text{Rh}(\text{Phony})(\text{CO})_2]$: 0.80° for $\text{N}_{11}\text{-Rh}_1\text{-O}_{12}$, 3.17° for $\text{O}_{12}\text{-Rh}_1\text{-C}_{13}$ and 2.9° for $\text{C}_{13}\text{-Rh}_1\text{-C}_{14}$. An exception is the angle $\text{N}_{11}\text{-Rh}_1\text{-C}_{14}$ where the largest difference of 1.73° is observed in $[\text{Rh}(2,6\text{-Cl}_2\text{-Phony})(\text{CO})_2]$. The impact of packing effects and intermolecular bonds on the geometrical parameters of the solid state structure as previously discussed is also reflected in the calculated energies for the optimized and solid state structures. The dihedral angles for all the complexes, both solid state and calculated, generally near 90° as a result of steric interference from the metal atom and carbonyl groups. This is in contrast with the free ligands discussed in Chapter 5 regarding PhonyH and the derivatives thereof, where dihedral angles of the free ligands can be as small as $38.36(9)^\circ$. The difference between the lowest and highest optimized energies, $[\text{Rh}(\text{Phony})(\text{CO})_2]$ and $[\text{Rh}(2,6\text{-Cl}_2\text{-Phony})(\text{CO})_2]$ respectively, is 13.1 kJ.mol^{-1} (Figure 7.1). The calculated energies of *ortho*-substituted $[\text{Rh}(2\text{-Cl-Phony})(\text{CO})_2]$ and *para*-substituted $[\text{Rh}(4\text{-Cl-Phony})(\text{CO})_2]$ differ from the energy of $[\text{Rh}(\text{Phony})(\text{CO})_2]$ by 7.3 kJ.mol^{-1} and 2.5 kJ.mol^{-1} , respectively, while the difference between $[\text{Rh}(\text{Phony})(\text{CO})_2]$ and $[\text{Rh}(2,4\text{-Cl}_2\text{-Phony})(\text{CO})_2]$ and $[\text{Rh}(2,6\text{-Cl}_2\text{-Phony})(\text{CO})_2]$ are respectively 8.4 kJ.mol^{-1} and 13.1 kJ.mol^{-1} . $[\text{Rh}(2,4\text{-Cl}_2\text{-Phony})(\text{CO})_2]$ can be described as a combination of *ortho*- and *para*-substituted $[\text{Rh}(2\text{-Cl-Phony})(\text{CO})_2]$ and $[\text{Rh}(4\text{-Cl-Phony})(\text{CO})_2]$ while $[\text{Rh}(2,6\text{-Cl}_2\text{-Phony})(\text{CO})_2]$ is similar to two *ortho*-substituted complexes. The calculated optimized energies of $[\text{Rh}(2,4\text{-Cl}_2\text{-Phony})(\text{CO})_2]$ and $[\text{Rh}(2,6\text{-Cl}_2\text{-Phony})(\text{CO})_2]$ of 8.4 kJ.mol^{-1} and 13.1 kJ.mol^{-1} roughly resemble the relative energies of $[\text{Rh}(2\text{-Cl-Phony})(\text{CO})_2]$ and $[\text{Rh}(4\text{-Cl-Phony})(\text{CO})_2]$ when added in this fashion: the energy of *ortho*-substituted $[\text{Rh}(2\text{-Cl-Phony})(\text{CO})_2]$ added to *para*-substituted $[\text{Rh}(4\text{-Cl-Phony})(\text{CO})_2]$ is 9.8 kJ.mol^{-1} , simulating $[\text{Rh}(2,4\text{-Cl}_2\text{-Phony})(\text{CO})_2]$, while twice the energy of *ortho*-substituted $[\text{Rh}(2\text{-Cl-Phony})(\text{CO})_2]$ is 14.6 kJ.mol^{-1} and simulates $[\text{Rh}(2,6\text{-Cl}_2\text{-Phony})(\text{CO})_2]$. The similarities between the energies accentuate the cumulative nature of the energies with respect to the position of the chloride atoms on the phenyl moiety. The relative energy differences between $[\text{Rh}(\text{Phony})(\text{CO})_2]$ to $[\text{Rh}(2,6\text{-Cl}_2\text{-Phony})(\text{CO})_2]$ follow the same trend as the relative energy differences for the uncoordinated ligands (see Chapter 5) which also display a cumulative nature. This was illustrated in Figure 7.1.

Another aspect in which the $[\text{Rh}(\text{N,O-Bid})(\text{CO})_2]$ complexes follow the trend set in the N,O-BidH compounds, is that complexes with optimized energies close in value display similarities in

Chapter 7

geometric parameters. The optimized energy of $[\text{Rh}(4\text{-Cl-Phony})(\text{CO})_2]$ is $2.5 \text{ kJ}\cdot\text{mol}^{-1}$ with respect to the minimum energy of $[\text{Rh}(\text{Phony})(\text{CO})_2]$ (see Table 7.1), and their small overlay RMS overlay value of 0.005 \AA confirms these similarities (see Figure 7.3). Similarly, the optimized energy values for $[\text{Rh}(2\text{-Cl-Phony})(\text{CO})_2]$ and $[\text{Rh}(2,4\text{-Cl}_2\text{-Phony})(\text{CO})_2]$ are $7.3 \text{ kJ}\cdot\text{mol}^{-1}$ and $8.4 \text{ kJ}\cdot\text{mol}^{-1}$, respectively, a difference of $1.1 \text{ kJ}\cdot\text{mol}^{-1}$. The overlay of these two complexes with a RMS value of 0.015 \AA is displayed in Figure 7.4 and shows the remarkable agreement between these two sets of complexes.

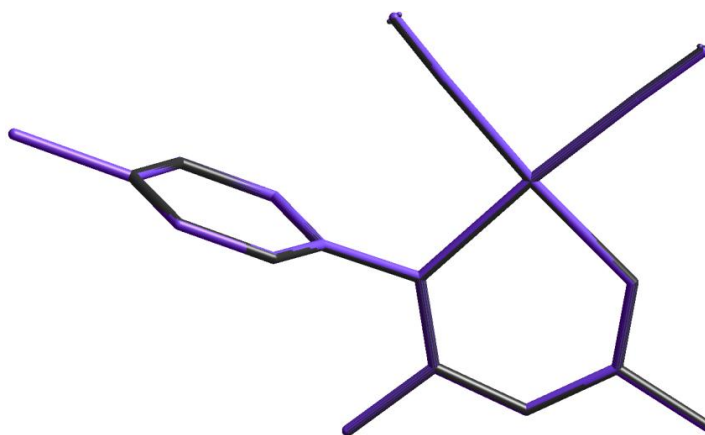


Figure 7.3. Overlay of the calculated (DFT) structures of $[\text{Rh}(\text{Phony})(\text{CO})_2]$ (black) with $[\text{Rh}(4\text{-Cl-Phony})(\text{CO})_2]$ (violet; RMS = 0.005 \AA).

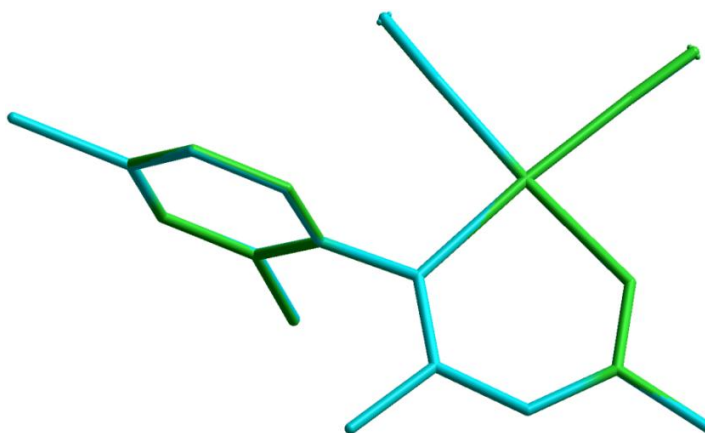


Figure 7.4. Overlay of the calculated (DFT) structures of $[\text{Rh}(2\text{-Cl-Phony})(\text{CO})_2]$ (green) with $[\text{Rh}(2,4\text{-Cl}_2\text{-Phony})(\text{CO})_2]$ (cyan; RMS = 0.015 \AA).

The agreement between the sets of structures as demonstrated in the overlays can be more closely investigated in the bonding distances and angles, reported in Table 7.2. In the first pair

Chapter 7

of complexes, $[\text{Rh}(\text{Phony})(\text{CO})_2]$ and $[\text{Rh}(4\text{-Cl-Phony})(\text{CO})_2]$, the largest difference in distance is for $d(\text{N}_{11}\cdots\text{O}_{12})$, with values of $2.906(2)$ Å and $2.93(1)$ Å, respectively, a difference of $0.02(1)$ Å. This is followed by the distance $d(\text{Rh}_1\text{-N}_{11})$, where the values are $2.058(2)$ Å and $2.065(8)$ Å, respectively, a difference of $0.007(8)$ Å. The displacement of Rh_1 from the $\text{N}_{11}\text{-O}_{12}\text{-C}_{13}\text{-C}_{14}$ plane is more prominent in $[\text{Rh}(\text{Phony})(\text{CO})_2]$ with a value of $0.0218(2)$ Å, versus no displacement in $[\text{Rh}(4\text{-Cl-Phony})(\text{CO})_2]$. No other noteworthy distances show significant differences. Differences in angles are more pronounced than in distances, and the largest difference, when disregarding the dihedral angle, is for $\text{O}_{12}\text{-Rh}_1\text{-C}_{13}$, a difference of $1.85(4)^\circ$ between the respective values of $89.75(8)^\circ$ and $87.9(4)^\circ$. The respective dihedral angles for $[\text{Rh}(\text{Phony})(\text{CO})_2]$ and $[\text{Rh}(4\text{-Cl-Phony})(\text{CO})_2]$ are $87.88(8)^\circ$ and $90.0(2)^\circ$, a difference of $2.12(2)^\circ$.

For the second pair of complexes, $[\text{Rh}(2\text{-Cl-Phony})(\text{CO})_2]$ and $[\text{Rh}(2,4\text{-Cl}_2\text{-Phony})(\text{CO})_2]$, differences in geometric parameters are less pronounced than for the first pair, but occur more frequently. The largest difference is for the distance $d(\text{Rh}_1\text{-C}_{13})$, a difference of $0.015(4)$ Å between $1.858(3)$ Å and $1.873(2)$ Å. The displacement of Rh_1 from the $\text{N}_{11}\text{-O}_{12}\text{-C}_{13}\text{-C}_{14}$ plane is $0.0266(2)$ Å and $0.0206(2)$ Å, respectively, a difference of $0.0060(3)$ Å. The largest variation in angles is $2.1(1)^\circ$ for the $\text{N}_{11}\text{-C}_2\cdots\text{C}_4\text{-O}_{12}$ torsion angle, calculated between $1.4(1)^\circ$ and $-0.7(1)^\circ$. The difference is $0.4(1)^\circ$ for the $\text{N}_{11}\text{-Rh}_1\text{-C}_{14}$ angle with respective values of $94.2(1)^\circ$ and $93.81(7)^\circ$.

Unlike the case with the free ligands, the geometric parameters for $[\text{Rh}(2,6\text{-Cl}_2\text{-Phony})(\text{CO})_2]$ do not correlate to the parameters for $[\text{Rh}(\text{Phony})(\text{CO})_2]$, although the dihedral angle more closely correspond than is the case in the ligands, which should be taken in consideration when comparing the trend in optimized energies of the complexes with the ligand compounds (Figure 7.1).

7.4. Conclusion

The calculated IR stretching frequencies, as seen in Table 7.4, differ significantly from the observed solid state stretching frequencies, supporting the postulated influence of different chloride substitutions on packing modes and bond lengths, where seemingly small differences in

Chapter 7

substitution causes large variations in packing modes. No significant difference between stretching frequencies for the calculated complexes were observed, but large differences between stretching frequencies of the solid state complexes can be explained by the influences of intra- and intermolecular hydrogen, rhodium-rhodium and π - π interactions on the packing modes. The cumulative nature of the energies as displayed in the free ligands as discussed in Chapter 5 is repeated in the $[\text{Rh}(\text{N},\text{O}\text{-Bid})(\text{CO})_2]$ complexes: the relative energy of $[\text{Rh}(2,4\text{-Cl}_2\text{-Phony})(\text{CO})_2]$ with regard to unsubstituted $[\text{Rh}(\text{Phony})(\text{CO})_2]$ is roughly equal to the sum of the relative energies of $[\text{Rh}(2\text{-Cl-Phony})(\text{CO})_2]$ and $[\text{Rh}(4\text{-Cl-Phony})(\text{CO})_2]$, while the relative energy of $[\text{Rh}(2,6\text{-Cl}_2\text{-Phony})(\text{CO})_2]$ approaches twice the relative energy of $[\text{Rh}(2\text{-Cl-Phony})(\text{CO})_2]$. The solid state behavior of the $[\text{Rh}(\text{Phony})(\text{CO})(\text{PPh}_3)]$ type complexes following monodentate substitution by P-donor ligands is described in the next chapter.

Chapter 7

8 X-Ray Crystallographic Study of Functionalized Carbonyl-[4-(phenylamino)pent-3-en-2-onato]-triphenylphosphine-rhodium(I) Complexes

8.1. Introduction

This chapter focuses on complexes of the type $[\text{Rh}(\text{N},\text{O-Bid})(\text{CO})(\text{PPh}_3)]$ (where N,O-Bid is a derivative of 4-(phenylamino)pent-3-en-2-onate, Phony⁻) as seen in Figure 8.1, and the effect of substitution of methyl groups and chloride on different positions on the N-functionalized phenyl ring as observed from solid state X-ray crystallographic studies.

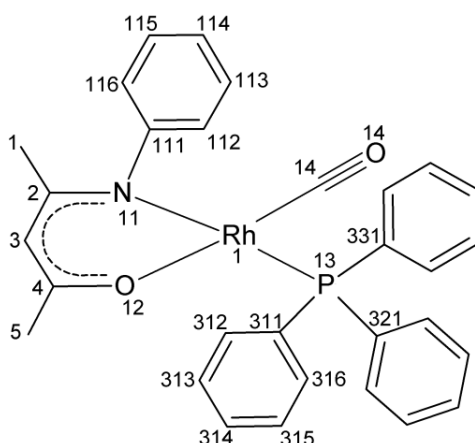


Figure 8.1. Schematic representation of $[\text{Rh}(\text{N},\text{O-Bid})(\text{CO})(\text{PPh}_3)]$, illustrating the naming method used throughout the chapter. For the C atoms in the phenyl ring, the first digit indicates molecule number, the second digit indicates ring number and the third digit indicates the position of the atom in the ring. For substitutes on the phenyl ring, the first digit indicates the molecule number while the second digit indicates position on the phenyl ring.

Chapter 8

8.2. Results

General crystal data and refinement parameters are presented in Table 8.1 for [Rh(4-Cl-Phony)(CO)(PPh₃)], [Rh(2,4-Cl₂-Phony)(CO)(PPh₃)] and [Rh(2,6-Cl₂-Phony)(CO)(PPh₃)], [Rh(2,3-Me₂-Phony)(CO)(PPh₃)] and [Rh(2,6-Me₂-Phony)(CO)(PPh₃)]. A complete list of atomic coordinates, equivalent isotropic parameters, bond distances and angles, anisotropic displacement parameters and hydrogen coordinates for each individual dataset is given in Appendix C.

Table 8.1. General crystal data for [Rh(4-Cl-Phony)(CO)(PPh₃)], [Rh(2,4-Cl₂-Phony)(CO)(PPh₃)], [Rh(2,6-Cl₂-Phony)(CO)(PPh₃)], [Rh(2,3-Me₂-Phony)(CO)(PPh₃)] and [Rh(2,6-Me₂-Phony)(CO)(PPh₃)].

	[Rh(4-Cl-Phony)(CO)(PPh ₃)]	[Rh(2,4-Cl ₂ -Phony)(CO)(PPh ₃)]	[Rh(2,6-Cl ₂ -Phony)(CO)(PPh ₃)]·0.5(C ₆ H ₅ COCH ₃)	[Rh(2,3-Me ₂ -Phony)(CO)(PPh ₃)]	[Rh(2,6-Me ₂ -Phony)(CO)(PPh ₃)]·0.5(C ₆ H ₅ COCH ₃)
Empirical formula	C ₃₀ H ₂₆ ClN O ₂ P Rh	C ₃₀ H ₂₅ Cl ₂ N O ₂ P Rh	C _{31.75} H ₂₅ Cl ₂ N O ₃ P Rh	C ₃₂ H ₃₁ N O ₂ P Rh	C _{33.50} H ₃₄ N O _{2.50} P Rh
Formula weight	601.85	636.29	673.31	595.46	624.50
Temperature (K)	100(2)	100(2)	100(2)	100(2)	100(2)
Wavelength (Å)	0.71073	0.71073	0.71073	0.71073	0.71073
Crystal system	Triclinic	Orthorhombic	Monoclinic	Monoclinic	Monoclinic
Space group	<i>P</i> $\bar{1}$	<i>P</i> 2 ₁ 2 ₁	<i>P</i> 2 ₁ / <i>c</i>	<i>P</i> 2 ₁ / <i>c</i>	<i>P</i> 2 ₁ / <i>c</i>
<i>a</i> (Å)	7.4570(7)	7.6656(5)	17.3242(5)	14.9077(3)	16.8558(8)
<i>b</i> (Å)	9.3350(9)	16.610(1)	11.3170(3)	11.6202(3)	11.4028(5)
<i>c</i> (Å)	20.502(2)	20.942(1)	15.4753(4)	16.0256(4)	16.4059(8)
α (°)	101.202(5)	90	90	90	90
β (°)	91.635(5)	90	108.197(1)	93.521(1)	108.733(1)
γ (°)	112.403(4)	90	90	90	90
Volume (Å ³)	1286.0(2)	2666.4(3)	2882.3(1)	2770.9(1)	2986.2(2)
<i>Z</i>	2	4	4	4	4
Density _{cal} (g·cm ⁻³)	1.554	1.585	1.552	1.427	1.389
μ (mm ⁻¹)	0.859	0.930	0.868	0.703	0.657
<i>F</i> (000)	612	1288	1362	1224	1288
Crystal size (mm ³)	0.30 x 0.18 x 0.16	0.22 x 0.15 x 0.08	0.41 x 0.36 x 0.17	0.25 x 0.15 x 0.13	0.31 x 0.15 x 0.11
$\theta_{\min} / \theta_{\max}$ (°)	1.02 / 25.00	1.56 / 28.29	1.24 / 28.30	1.37 / 28.51	1.28 / 28.33

Chapter 8

Table 8.1. Continued.

	[Rh(4-Cl-Phony)(CO)(PPh ₃)]	[Rh(2,4-Cl ₂ -Phony)(CO)(PPh ₃)]	[Rh(2,6-Cl ₂ -Phony)(CO)(PPh ₃)]·0.5(CH ₃ COCH ₃)	[Rh(2,3-Me ₂ -Phony)(CO)(PPh ₃)]	[Rh(2,6-Me ₂ -Phony)(CO)(PPh ₃)]·0.5(CH ₃ COCH ₃)
Index ranges	-8 ≤ h ≤ 8 -11 ≤ k ≤ 11 -24 ≤ l ≤ 24	-6 ≤ h ≤ 10 -22 ≤ k ≤ 14 -27 ≤ l ≤ 22	-23 ≤ h ≤ 23 -13 ≤ k ≤ 15 -14 ≤ l ≤ 20	-19 ≤ h ≤ 19 -15 ≤ k ≤ 14 -21 ≤ l ≤ 18	-21 ≤ h ≤ 22 -15 ≤ k ≤ 11 -21 ≤ l ≤ 21
Reflections collected	16712	9908	21503	30367	2315
Independent reflections	4383	6128	7162	6985	7425
R_{int}	0.0463	0.0515	0.0350	0.0398	0.0415
Completeness to θ_{max} (%)	96.8	98.9	99.8	99.4	99.8
Data / parameters	4383 / 327	6128 / 330	7162 / 364	6985 / 0 / 305	7425 / 354
Goodness-of-fit on F^2	1.064	1.071	1.046	1.043	1.085
Final R indices, [$I > 2\sigma(I)$]	$R_1 = 0.0308$ $wR_2 = 0.0732$	$R_1 = 0.0649$ $wR_2 = 0.1422$	$R_1 = 0.0331$ $wR_2 = 0.0776$	$R_1 = 0.0330$ $wR_2 = 0.0691$	$R_1 = 0.0384$ $wR_2 = 0.1007$
R indices (all data)	$R_1 = 0.0372$ $wR_2 = 0.0808$	$R_1 = 0.0830$ $wR_2 = 0.1681$	$R_1 = 0.0426$ $wR_2 = 0.0869$	$R_1 = 0.0437$ $wR_2 = 0.0756$	$R_1 = 0.0495$ $wR_2 = 0.1121$
$\Delta\rho$ max / min (e.Å ⁻³)	1.006 / -0.636	2.938 / -1.158	1.391 / -0.815	0.603 / -0.694	1.539 / -1.319

8.2.1. Crystal Structure of Carbonyl-[4-(4-chlorophenylamino)pent-3-en-2-onato]-triphenylphosphine-rhodium(I) [Rh(4-Cl-Phony)(CO)(PPh₃)]

The compound [Rh(4-Cl-Phony)(CO)(PPh₃)], where Phony⁻ = 4-(phenylamino)pent-3-en-2-onate, crystallized in the triclinic space group $P\bar{1}$ with $Z = 2$. The discrete [Rh(4-Cl-Phony)(CO)(PPh₃)] molecule is shown in Figure 8.2, with important bond distances and angles reported in Table 8.2.

Chapter 8

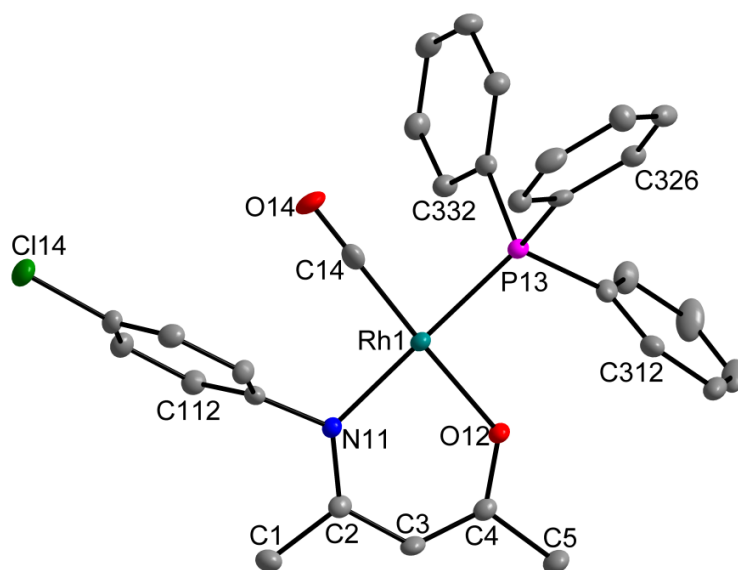


Figure 8.2. DIAMOND¹ view of [Rh(4-Cl-Phony)(CO)(PPh₃)], where Phony⁻ = 4-(phenylamino)pent-3-en-2-onate (50% probability displacement ellipsoids). Selected hydrogen atoms and labels have been omitted for clarity. For the C atoms in the phenyl ring, the first digit indicates molecule number, the second digit indicates ring number and the third digit indicates the position of the atom in the ring. For the Cl atoms, the first digit indicates molecule number while the second digit indicates position on the phenyl ring.

Table 8.2. Selected bond distances (Å) and angles (°) for [Rh(4-Cl-Phony)(CO)(PPh₃)].

Atoms	Distances (Å)	Atoms	Angles (°)
Rh ₁ -N ₁₁	2.080(2)	N ₁₁ -Rh ₁ -O ₁₂	89.04(9)
Rh ₁ -O ₁₂	2.034(2)	O ₁₂ -Rh ₁ -P ₁₃	90.75(6)
Rh ₁ -P ₁₃	2.2627(8)	P ₁₃ -Rh ₁ -C ₁₄	86.56(9)
Rh ₁ -C ₁₄	1.814(3)	N ₁₁ -Rh ₁ -C ₁₄	93.7(1)
C ₁₃ -O ₁₄	1.146(4)	N ₁₁ -Rh ₁ -C ₁₃	178.39(7)
N ₁₁ -C ₁₁₁	1.443(5)	O ₁₂ -Rh ₁ -P ₁₄	176.6(1)
N ₁₁ -C ₂	1.315(4)	N ₁₁ -C ₂ ⋯C ₄ -O ₁₂	0.4(3)
O ₁₂ -C ₄	1.284(3)	Dihedral angle ^a	83.76(9)
N ₁₁ ⋯O ₁₂ (Bite distance)	2.885(4)	θ_E^b	154.89(3)

^a Defined as the torsion angle between the N-C-C-C-O plane and the phenyl ring.

^b The Tolman cone angle, as defined in § 2.2.3.

No classic hydrogen interactions were observed for compound [Rh(4-Cl-Phony)(CO)(PPh₃)], with the shortest intermolecular C-H⋯O distance being 2.713(2) Å for H₃₂₄ and O₁₂. Rh₁ is

¹ Brandenburg, K., Putz, H. DIAMOND. Release 3.0e. Crystal Impact GbR, Bonn, Germany.

Chapter 8

displaced from the plane formed by N₁₁, O₁₂, P₁₃ and C₁₄ by 0.0077(2) Å. An anagostic C-H···Rh interaction of distance 2.90 Å with C-H···Rh angle of 155.5° is present in this complex between H₁₁₃ and Rh_{1^{xviii}} which compensates for the lack of other types of interactions. The packing diagram is shown in Figure 8.4. Hydrogen interactions in the structure are illustrated in Figure 8.9, and shown in Table 8.3.

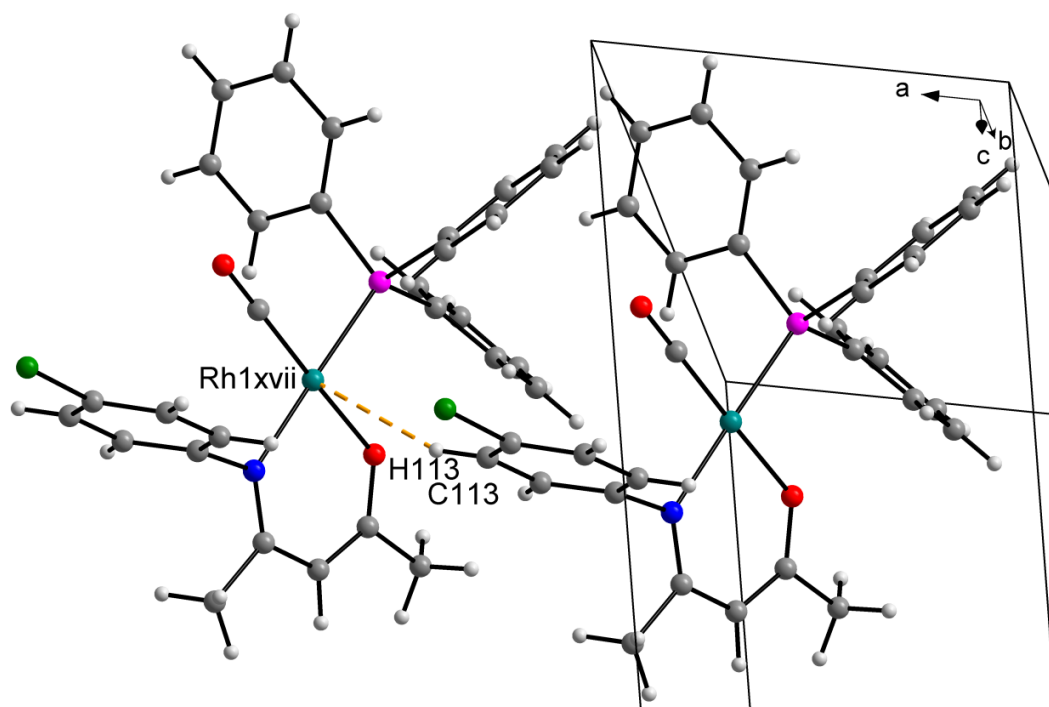


Figure 8.3. Partial unit cell for [Rh(4-Cl-Phony)(CO)(PPh₃)] demonstrating the anagostic hydrogen-rhodium interaction indicated with dashed lines. The symmetry operator is given in Table 8.3.

Table 8.3. Hydrogen bond for [Rh(4-Cl-Phony)(CO)(PPh₃)] (Å and °).

D-H···A	d _{D-H} (Å)	d _{H···A} (Å)	d _{D···A} (Å)	<DHA (°)
C ₁₁₅ -H ₁₁₅ ···Rh _{1^{xvii}}	0.95	2.90	3.782(3)	155.5

Symmetry code: (xvii) 1 + x, y, z

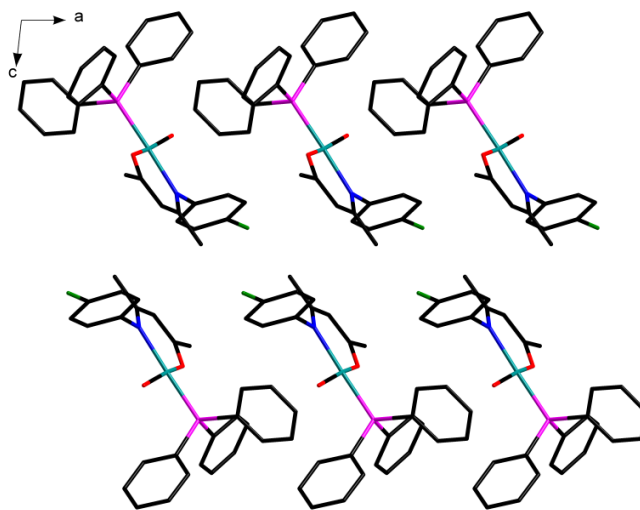


Figure 8.4. View of $[\text{Rh}(4\text{-Cl-Phony})(\text{CO})(\text{PPh}_3)]$ along the b -axis illustrating the packing style.

From the packing the chloride atoms appear to be close enough to one another to justify a chloride \cdots chloride interaction, but the shortest chloride \cdots chloride distance of 4.462(2) Å, which far exceeds the sum of the Van der Waals radii (see Chapter 4), as well as the C-Cl \cdots Cl angles of 52.1(1)° in either direction refutes this possibility. The rhodium-rhodium interactions which were observed in the dicarbonyl complexes are absent in the triphenylphosphine-containing complexes due to the steric bulk of said ligand, and no π -interactions were observed despite the abundance of delocalized electrons in the system.

8.2.2. Crystal Structure of Carbonyl-[4-(2,4-dichlorophenylamino)pent-3-en-2-onato]-triphenylphosphine-rhodium(I) $[\text{Rh}(2,4\text{-Cl}_2\text{-Phony})(\text{CO})(\text{PPh}_3)]$

The compound $[\text{Rh}(2,4\text{-Cl}_2\text{-Phony})(\text{CO})(\text{PPh}_3)]$, where Phony $^-$ = 4-(phenylamino)pent-3-en-2-onate, crystallized in the triclinic space group $P\bar{1}$ with $Z = 4$. The complex is shown in Figure 8.5, with important bond distances and angles reported in Table 8.4.

Chapter 8

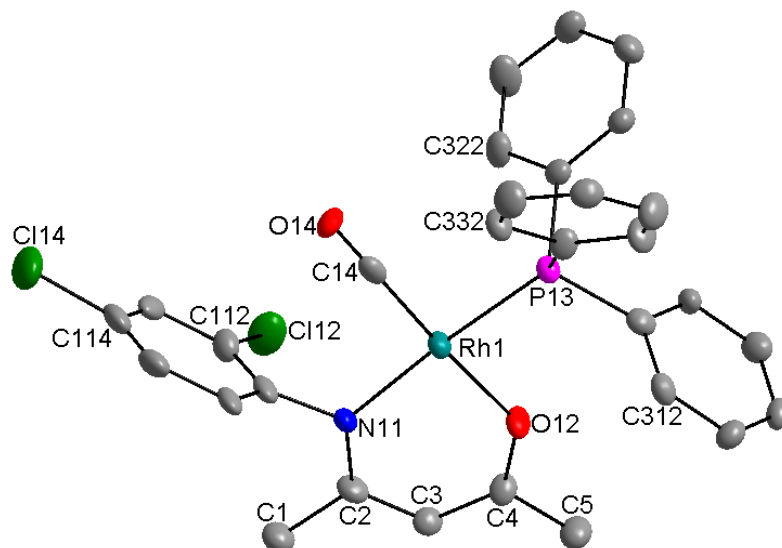


Figure 8.5. DIAMOND¹ view of [Rh(2,4-Cl₂-Phony)(CO)(PPh₃)], where Phony⁻ = 4-(phenylamino)pent-3-en-2-onate (50% probability displacement ellipsoids). Selected hydrogen atoms and labels have been omitted for clarity. For the C atoms in the phenyl ring, the first digit indicates molecule number, the second digit indicates ring number and the third digit indicates the position of the atom in the ring. For the Cl atoms, the first digit indicates molecule number while the second digit indicates position on the phenyl ring.

Table 8.4. Selected bond distances (Å) and angles (°) for [Rh(2,4-Cl₂-Phony)(CO)(PPh₃)].

Atoms	Distances (Å)	Atoms	Angles (°)
Rh ₁ -N ₁₁	2.076(6)	N ₁₁ -Rh ₁ -O ₁₂	88.7(2)
Rh ₁ -O ₁₂	2.033(6)	O ₁₂ -Rh ₁ -P ₁₃	87.3(1)
Rh ₁ -P ₁₃	2.268(2)	P ₁₃ -Rh ₁ -C ₁₄	90.1(2)
Rh ₁ -C ₁₄	1.825(8)	N ₁₁ -Rh ₁ -C ₁₄	93.9(3)
C ₁₄ -O ₁₄	1.13(1)	N ₁₁ -Rh ₁ -C ₁₃	175.9(2)
N ₁₁ -C ₁₁₁	1.44(1)	O ₁₂ -Rh ₁ -P ₁₄	176.1(3)
N ₁₁ -C ₂	1.33(3)	N ₁₁ -C ₂ ⋯C ₄ -O ₁₂	-1.0(7)
O ₁₂ -C ₄	1.286(9)	Dihedral angle ^a	85.3(2)
N ₁₁ ⋯O ₁₂ (Bite distance)	2.871(8)	θ _E ^b	155.80(9)

^a Defined as the torsion angle between the N-C-C-C-O plane and the phenyl ring.

^b The Tolman cone angle, as defined in § 2.2.3.

Only intramolecular C-H⋯O interactions were observed in the compound [Rh(2,4-Cl₂-Phony)(CO)(PPh₃)]. Rh₁ is displaced from the plane formed by N₁₁, O₁₂, P₁₃ and C₁₄ by

Chapter 8

0.0102(5) Å. The hydrogen interaction in the structure, illustrated in Figure 8.6, is shown in Table 8.5, with the resultant packing diagram shown in Figure 8.7.

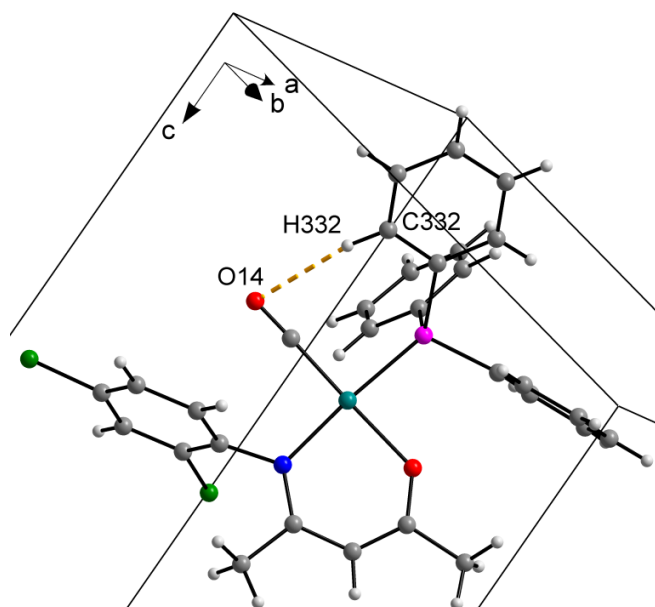


Figure 8.6. Partial unit cell for [Rh(2,4-Cl₂-Phony)(CO)(PPh₃)] with the intramolecular hydrogen bonding interaction indicated with dashed lines.

Table 8.5. Hydrogen bonds for [Rh(2,4-Cl₂-Phony)(CO)(PPh₃)] (Å and °).

D-H...A	d_{D-H} (Å)	d_{H...A} (Å)	d_{D...A} (Å)	<DHA (°)
C ₃₃₂ -H ₃₃₂ ...O ₁₄	0.95	2.54	3.45(1)	159.3

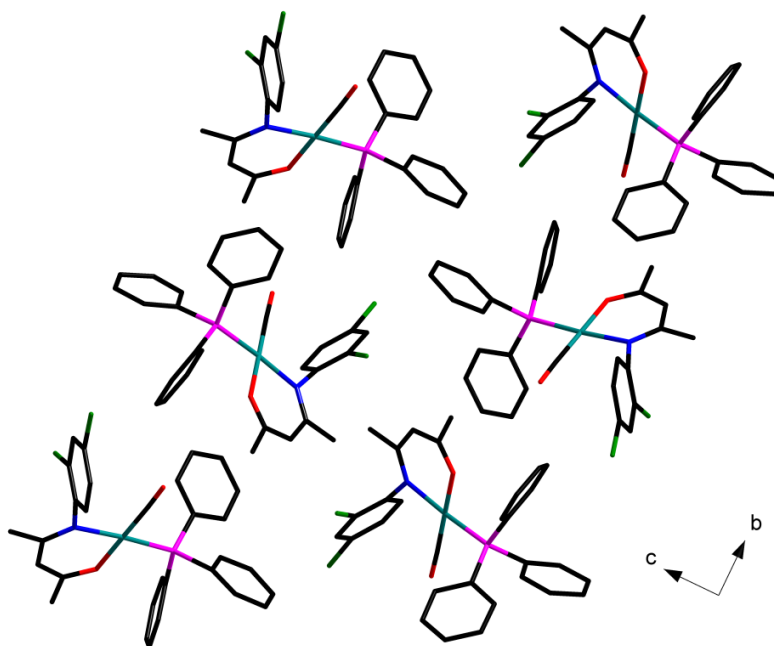


Figure 8.7. View of $[\text{Rh}(2,4\text{-Cl}_2\text{-Phony})(\text{CO})(\text{PPh}_3)]$ along the a-axis illustrating the packing style.

A $\text{C-O}\cdots\pi$ interaction might be possible between the carbonyl oxygen, O_{14} , and the delocalized electrons of the phenyl ring of the bidentate ligand, with the distance from O_{14} to the centroid of the phenyl moiety of the bidentate N,O-ligand being $3.393(5)$ Å. However, the angle between a line between the O_{14} atom to the centroid and a plane through the phenyl ring is 75.0° , and this angle, in conjunction with the $\text{C}_{14}\text{-O}_{14}\cdots\text{centroid}$ angle of 81.2° refutes this possibility.

8.2.3. Crystal Structure of Carbonyl-[4-(2,4-dichlorophenylamino)pent-3-en-2-onato]-triphenylphosphine-rhodium(I) 0.5 Acetone Solvate $[\text{Rh}(2,6\text{-Cl}_2\text{-Phony})(\text{CO})(\text{PPh}_3)]\cdot 0.5(\text{CH}_3\text{COCH}_3)$

The compound $[\text{Rh}(2,6\text{-Cl}_2\text{-Phony})(\text{CO})(\text{PPh}_3)]\cdot 0.5(\text{CH}_3\text{COCH}_3)$, where Phony = 4-(phenylamino) pent-3-en-2-onate, crystallized in the orthorhombic space group $P2_12_12_1$ with four discrete $[\text{Rh}(2,6\text{-Cl}_2\text{-Phony})(\text{CO})(\text{PPh}_3)]$ molecules and two disordered acetone molecules in the unit cell. The complex is shown in Figure 8.8, with important bond distances and angles reported in Table 8.6.

Chapter 8

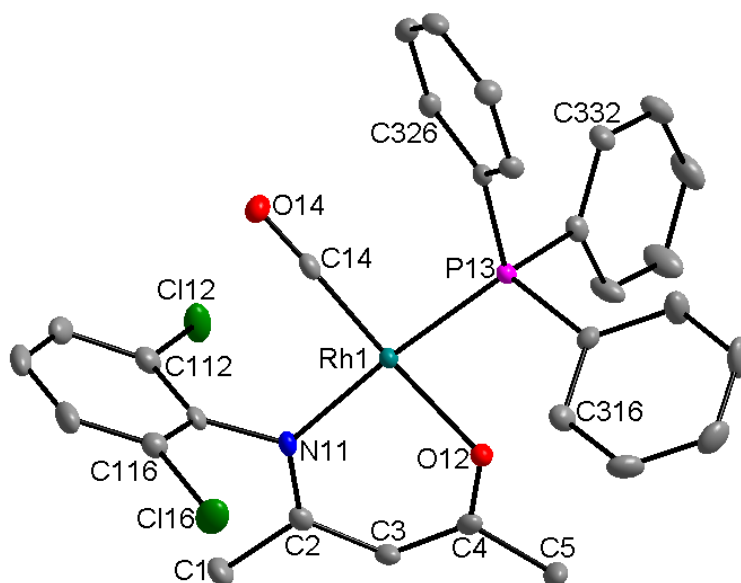


Figure 8.8 DIAMOND¹ view of [Rh(2,6-Cl₂-Phony)(CO)(PPh₃)], where Phony⁻ = 4-(phenylamino)pent-3-en-2-onate (50% probability displacement ellipsoids). Selected hydrogen atoms and labels as well as the acetone solvate molecule have been omitted for clarity. For the C atoms in the phenyl ring, the first digit indicates molecule number, the second digit indicates ring number and the third digit indicates the position of the atom in the ring. For the Cl atoms, the first digit indicates molecule number while the second digit indicates position on the phenyl ring.

Table 8.6. Selected bond distances (Å) and angles (°) for [Rh(2,6-Cl₂-Phony)(CO)(PPh₃)].

Atoms	Distances (Å)	Atoms	Angles (°)
Rh ₁ -N ₁₁	2.085(2)	N ₁₁ -Rh ₁ -O ₁₂	88.61(9)
Rh ₁ -O ₁₂	2.035(2)	O ₁₂ -Rh ₁ -P ₁₃	86.80(6)
Rh ₁ -P ₁₃	2.2688(7)	P ₁₃ -Rh ₁ -C ₁₄	91.60(8)
Rh ₁ -C ₁₄	1.808(3)	N ₁₁ -Rh ₁ -C ₁₄	93.0(1)
C ₁₄ -O ₁₄	1.150(4)	N ₁₁ -Rh ₁ -C ₁₃	175.41(6)
N ₁₁ -C ₁₁₁	1.426(4)	O ₁₂ -Rh ₁ -P ₁₄	175.4(1)
N ₁₁ -C ₂	1.322(4)	N ₁₁ -C ₂ ⋯C ₄ -O ₁₂	3.4(2)
O ₁₂ -C ₄	1.286(4)	Dihedral angle ^a	84.06(8)
N ₁₁ ⋯O ₁₂ (Bite distance)	2.879(3)	θ _E ^b	155.29(3)

^a Defined as the torsion angle between the N-C-C-C-O plane and the phenyl ring.

^b The Tolman cone angle, as defined in § 2.2.3.

The packing modes of compound [Rh(2,6-Cl₂-Phony)(CO)(PPh₃)] are influenced by classic intra- and intermolecular C-H⋯O interactions. Hydrogen interactions in the structure are

Chapter 8

illustrated in Figure 8.9, and shown in Table 8.7. Rh₁ is displaced from the plane formed by N₁₁, O₁₂, P₁₃ and C₁₄ by 0.0286(2) Å. The resultant packing is given in Figure 8.10.

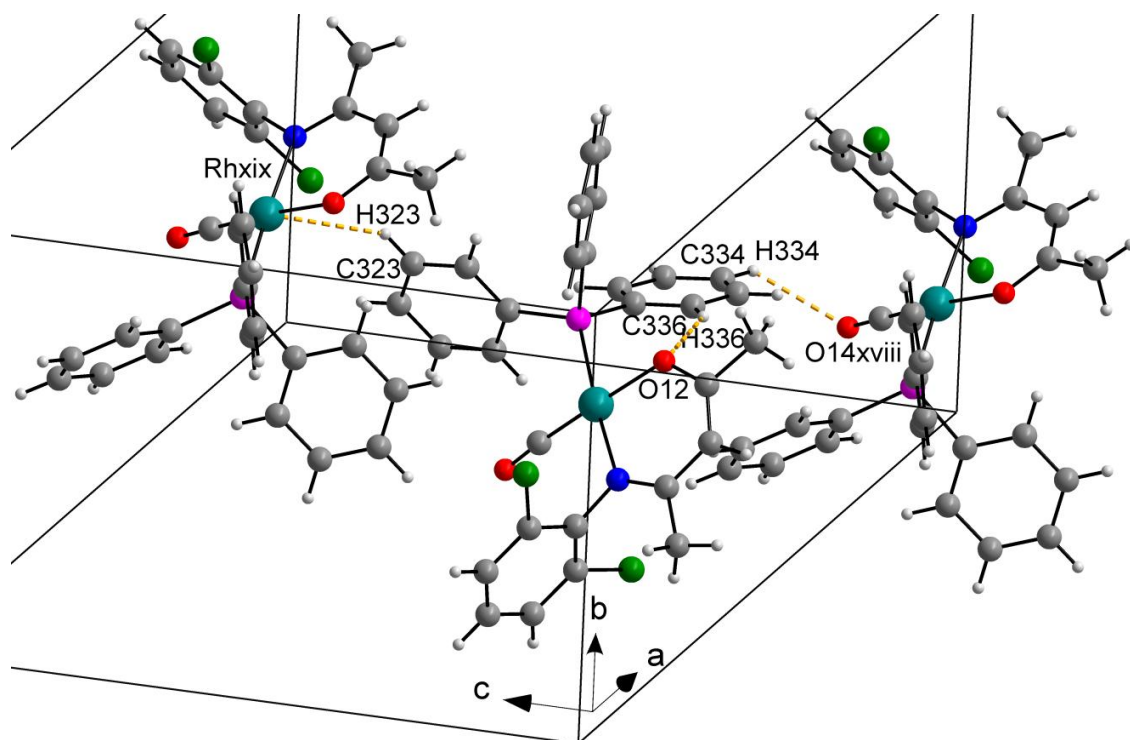


Figure 8.9. Partial unit cell for [Rh(2,6-Cl₂-Phony)(CO)(PPh₃)] with important intra- and intermolecular hydrogen bonding interactions indicated with dashed lines. The symmetry operators are given in Table 8.7.

Table 8.7. Hydrogen bonds for [Rh(2,6-Cl₂-Phony)(CO)(PPh₃)] (Å and °).

D-H...A	d _{D-H} (Å)	d _{H...A} (Å)	d _{D...A} (Å)	<DHA (°)
C ₃₃₆ -H ₃₃₆ ...O ₁₂	0.95	2.46	3.266(3)	143.0
C ₃₃₄ -H ₃₃₄ ...O ₁₄ ^{xviii}	0.95	2.52	3.185(4)	127.2

Symmetry code: (xviii) x, -y + 1½, z - ½ (xix) x, -y + 1½, x + ½

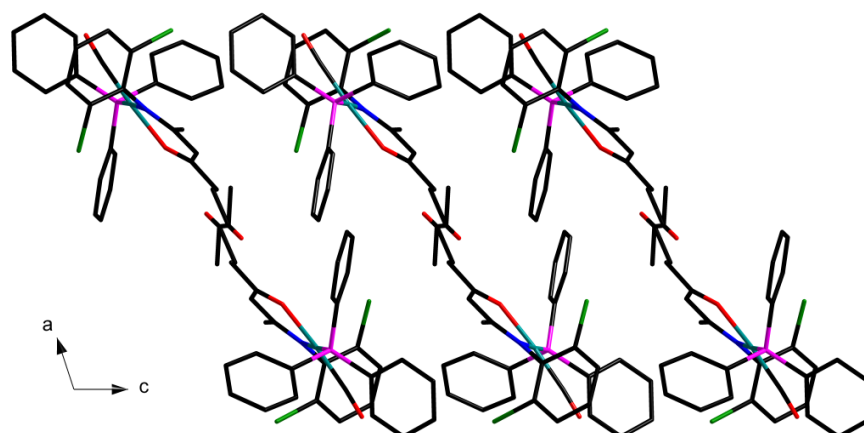


Figure 8.10. View of $[\text{Rh}(2,6\text{-Cl}_2\text{-Phony})(\text{CO})(\text{PPh}_3)] \cdot 0.5(\text{CH}_3\text{COCH}_3)$ along the b-axis illustrating the packing style.

In this complex, as with $[\text{Rh}(4\text{-Cl-Phony})(\text{CO})_2]$, a $\text{C-H}\cdots\text{Rh}$ interaction is present. The $\text{H}_{323}\cdots\text{Rh}_1^{\text{xx}}$ distance is $2.9936(2)$ Å, with a $\text{C}_{323}\text{-H}_{323}\cdots\text{Rh}_1^{\text{xx}}$ angle of $143.6(2)^\circ$. However, in addition to the $\text{C-H}\cdots\text{Rh}$ interaction, intra- and intermolecular interaction influence the packing of this complex which were absent in $[\text{Rh}(4\text{-Cl-Phony})(\text{CO})_2]$.

8.2.4. Crystal Structure of Carbonyl-[4-(2,3-dimethylphenylamino)pent-3-en-2-onato]-triphenylphosphine-rhodium(I) $[\text{Rh}(2,3\text{-Me}_2\text{-Phony})(\text{CO})(\text{PPh}_3)]^2$

The compound $[\text{Rh}(2,3\text{-Me}_2\text{-Phony})(\text{CO})(\text{PPh}_3)]$, where $\text{Phony}^- = 4\text{-(phenylamino)pent-3-en-2-onate}$, crystallized in the monoclinic space group $P2_1/c$ with $Z = 4$. The compound is shown in Figure 8.11, with important bond distances and angles reported in Table 8.8.

² Venter, G.J.S.; Steyl, G.; Roodt, A. *Acta Cryst.* **2009**, *E65*, m1321.

Chapter 8

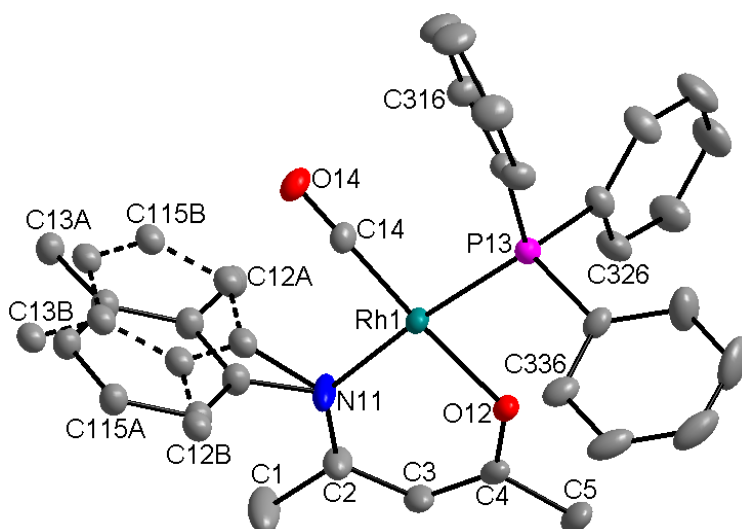


Figure 8.11. DIAMOND view of $[\text{Rh}(2,3\text{-Me}_2\text{-Phony})(\text{CO})(\text{PPh}_3)]$, where $\text{Phony}^- = 4\text{-}(\text{phenylamino})\text{pent-3-en-2-onate}$ (50% probability displacement ellipsoids). Selected hydrogen atoms and labels have been omitted for clarity. For the C atoms in the phenyl ring, the first digit indicates molecule number, the second digit indicates ring number and the third digit indicates the position of the atom in the ring. The dashed lines indicate the 41% disorder on the phenyl ring of the Phony moiety.

Table 8.8. Selected bond distances (Å) and angles (°) for $[\text{Rh}(2,3\text{-Me}_2\text{-Phony})(\text{CO})(\text{PPh}_3)]$.

Atoms	Distances (Å)	Atoms	Angles (°)
Rh ₁ -N ₁₁	2.069(2)	N ₁₁ -Rh ₁ -O ₁₂	88.61(8)
Rh ₁ -O ₁₂	2.028(2)	O ₁₂ -Rh ₁ -P ₁₃	84.97(5)
Rh ₁ -P ₁₃	2.2634(6)	P ₁₃ -Rh ₁ -C ₁₄	91.87(7)
Rh ₁ -C ₁₄	1.807(2)	N ₁₁ -Rh ₁ -C ₁₄	93.6(1)
C ₁₄ -O ₁₄	1.152(3)	N ₁₁ -Rh ₁ -C ₁₃	174.49(6)
N ₁₁ -C ₁₁₁	1.492(5) ^c	O ₁₂ -Rh ₁ -P ₁₄	176.48(8)
N ₁₁ -C ₂	1.320(4)	N ₁₁ -C ₂ ⋯C ₄ -O ₁₂	4.1(2)
O ₁₂ -C ₄	1.290(3)	Dihedral angle ^a	88.4(1) ^d
N ₁₁ ⋯O ₁₂ (Bite distance)	2.885(3)	θ _E ^b	156.39(3)

^a Defined as the torsion angle between the N-C-C-C-O plane and the phenyl ring.

^b The Tolman cone angle, as defined in § 2.2.3.

^c Average value for two disordered rings. Individual values: 1.521(4) for ring A and 1.463(3) for ring B.

^d Average value for two disordered rings. Individual values: 87.47(7) for ring A and 89.36(8) for ring B.

The packing modes of compound $[\text{Rh}(2,3\text{-Me}_2\text{-Phony})(\text{CO})(\text{PPh}_3)]$ are influenced by classic intramolecular C-H⋯O interactions. Hydrogen interactions in the structure are illustrated in

Chapter 8

Figure 8.12, and shown in Table 8.9. Rh₁ is displaced from the plane formed by N₁₁, O₁₂, P₁₃ and C₁₄ by 0.0168(2) Å. The phenyl ring of the ligand moiety is disordered in a 59:41% ratio as calculated from the Fourier map. The packing diagram is given in Figure 8.13.

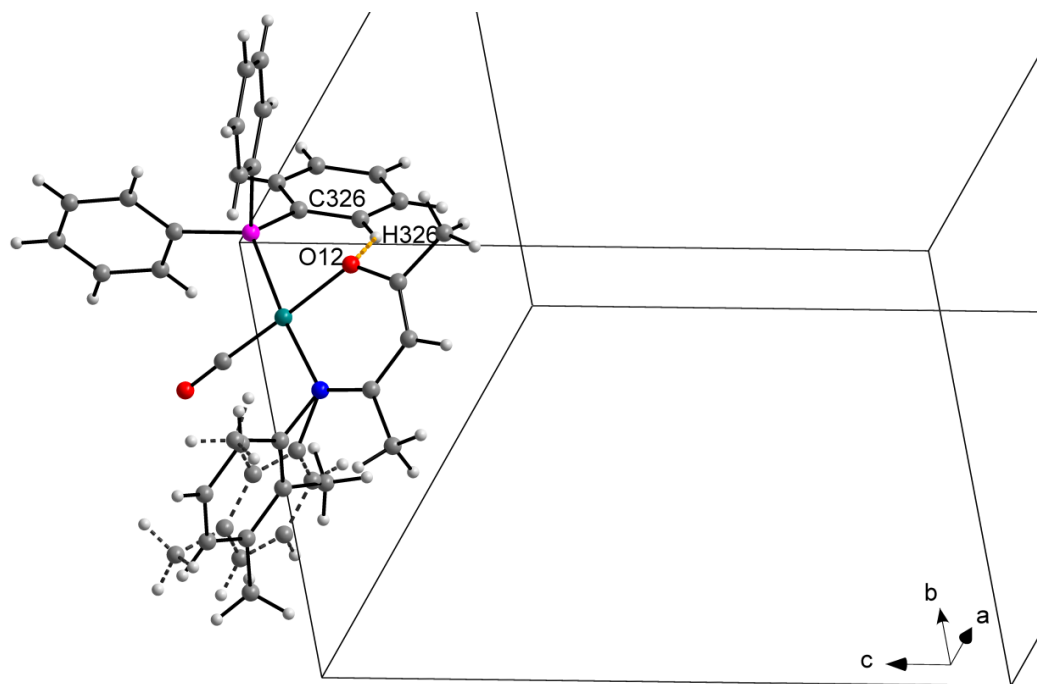


Figure 8.12. Partial unit cell for [Rh(2,3-Me₂-Phony)(CO)(PPh₃)] with the intramolecular hydrogen interaction indicated with a dashed orange line.

Table 8.9. Hydrogen bonds for [Rh(2,3-Me₂-Phony)(CO)(PPh₃)] (Å and °).

D-H···A	d _{D-H} (Å)	d _{H···A} (Å)	d _{D···A} (Å)	<DHA (°)
C ₃₂₆ -H ₃₂₆ ···O ₁₂	0.95	2.36	3.177(3)	143.2

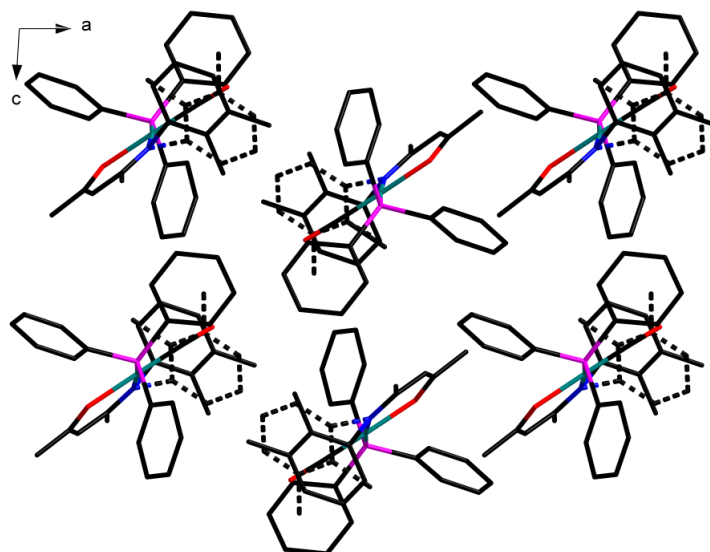


Figure 8.13. View of $[\text{Rh}(2,3\text{-Me}_2\text{-Phony})(\text{CO})(\text{PPh}_3)]$ along the *b*-axis illustrating the packing style.

8.2.5. Crystal Structure of Carbonyl-[4-(2,6-dimethylphenylamino)pent-3-en-2-onato]-triphenylphosphine-rhodium(I) 0.5 Acetone Solvate $[\text{Rh}(2,6\text{-Me}_2\text{-Phony})(\text{CO})(\text{PPh}_3)] \cdot 0.5(\text{CH}_3\text{COCH}_3)^3$

The compound $[\text{Rh}(2,6\text{-Me}_2\text{-Phony})(\text{CO})(\text{PPh}_3)] \cdot 0.5(\text{CH}_3\text{COCH}_3)$, where $\text{Phony}^- = 4\text{-(phenylamino)pent-3-en-2-onate}$, crystallized in the monoclinic space group $P2_1/c$ with four discrete $[\text{Rh}(2,6\text{-Me}_2\text{-Phony})(\text{CO})(\text{PPh}_3)]$ molecules and two disordered acetone molecules per unit cell. The compound is shown in Figure 8.14, with important bond distances and angles reported in Table 8.10.

³ Venter, G.J.S.; Steyl, G.; Roodt, A. *Acta Cryst.* **2009**, *E65*, m1606.

Chapter 8

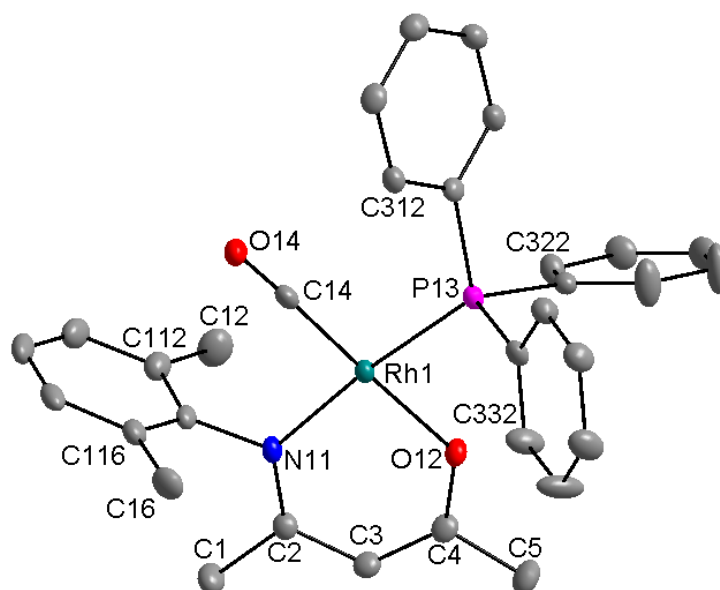


Figure 8.14. DIAMOND view of $[\text{Rh}(2,6\text{-Me}_2\text{-Phony})(\text{CO})(\text{PPh}_3)] \cdot 0.5(\text{CH}_3\text{COCH}_3)$, where Phony = 4-(phenylamino)pent-3-en-2-onate (50% probability displacement ellipsoids). Selected hydrogen atoms and labels as well as the acetone solvate molecule have been omitted for clarity. For the C atoms in the phenyl ring, the first digit indicates molecule number, the second digit indicates ring number and the third digit indicates the position of the atom in the ring.

Table 8.10. Selected bond distances (Å) and angles (°) for $[\text{Rh}(2,6\text{-Me}_2\text{-Phony})(\text{CO})(\text{PPh}_3)] \cdot 0.5(\text{CH}_3\text{COCH}_3)$.

Atoms	Distances (Å)	Atoms	Angles (°)
Rh ₁ -N ₁₁	2.076(2)	N ₁₁ -Rh ₁ -O ₁₂	89.43(8)
Rh ₁ -O ₁₂	2.028(2)	O ₁₂ -Rh ₁ -P ₁₃	85.94(5)
Rh ₁ -P ₁₃	2.2701(6)	P ₁₃ -Rh ₁ -C ₁₄	91.60(8)
Rh ₁ -C ₁₄	1.808(3)	N ₁₁ -Rh ₁ -C ₁₄	93.0(1)
C ₁₄ -O ₁₄	1.151(4)	N ₁₁ -Rh ₁ -C ₁₃	174.35(6)
N ₁₁ -C ₁₁₁	1.441(4)	O ₁₂ -Rh ₁ -P ₁₄	177.4(1)
N ₁₁ -C ₂	1.321(4)	N ₁₁ -C ₂ ···C ₄ -O ₁₂	-2.6(2)
O ₁₂ -C ₄	1.290(4)	Dihedral angle ^a	85.58(8)
N ₁₁ ···O ₁₂ (Bite distance)	2.886(3)	θ _E ^b	155.77(3)

^a Defined as the torsion angle between the N-C-C-C-O plane and the phenyl ring.

^b The Tolman cone angle, as defined in § 2.2.3.

The packing modes of compound $[\text{Rh}(2,6\text{-Me}_2\text{-Phony})(\text{CO})(\text{PPh}_3)] \cdot 0.5(\text{CH}_3\text{COCH}_3)$ are influenced by classic intra- and intermolecular C-H···O interactions. Hydrogen interactions in the structure are illustrated in Figure 8.15, and shown in Table 8.11. Rh₁ is displaced from the

Chapter 8

plane formed by N₁₁, O₁₂, P₁₃ and C₁₄ by 0.0456(2) Å. The packing diagram is given in Figure 8.16.

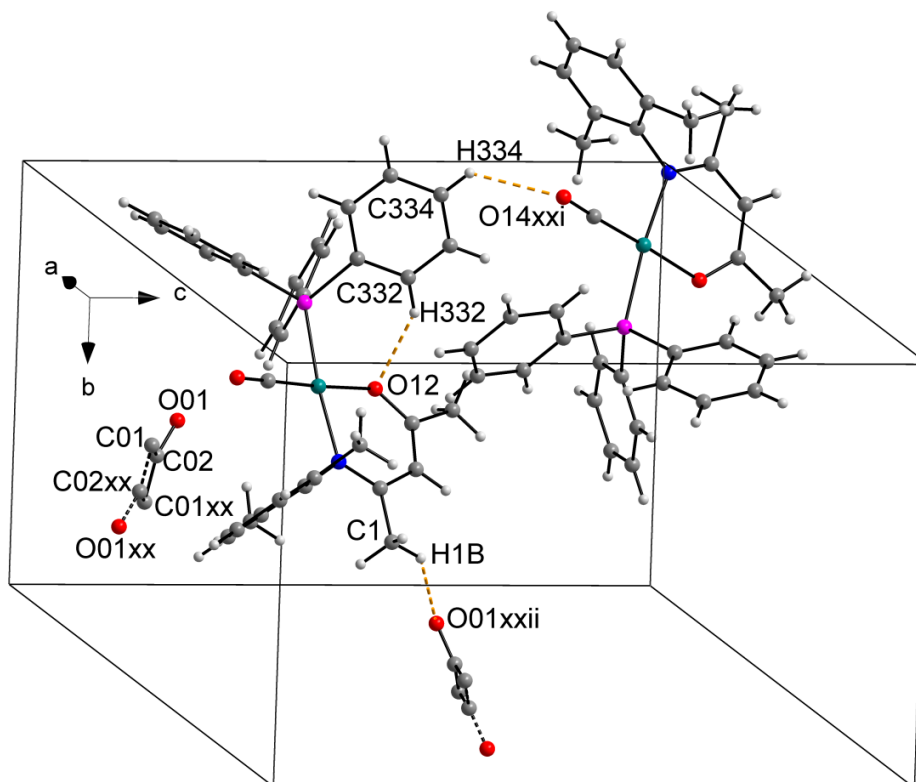


Figure 8.15. Partial unit cell for [Rh(2,6-Me₂-Phony)(CO)(PPh₃)]·0.5(CH₃COCH₃) with important intra- and intermolecular hydrogen bonding interactions indicated with dashed lines. The symmetry operators are given in Table 8.11.

Table 8.11. Hydrogen bonds for [Rh(2,6-Me₂-Phony)(CO)(PPh₃)]·0.5(CH₃COCH₃) (Å and °).

D-H...A	d _{D-H} (Å)	d _{H...A} (Å)	d _{D...A} (Å)	<DHA (°)
C ₃₃₂ -H ₃₃₂ ...O ₁₂	0.95	2.38	3.201(3)	144.1
C ₃₃₄ -H ₃₃₄ ...O ₁₄ ^{xxi}	0.95	2.51	3.201(4)	129.7
C ₁ -H _{1B} ...O ₀₁ ^{xxii}	0.98	2.54	3.372(9)	142.4

Symmetry code: (xx) -x + 1, -y + 1, -z (xxi) x, -y + ½, z + ½ (xxii) -x + 1, y + ½, -z + ½

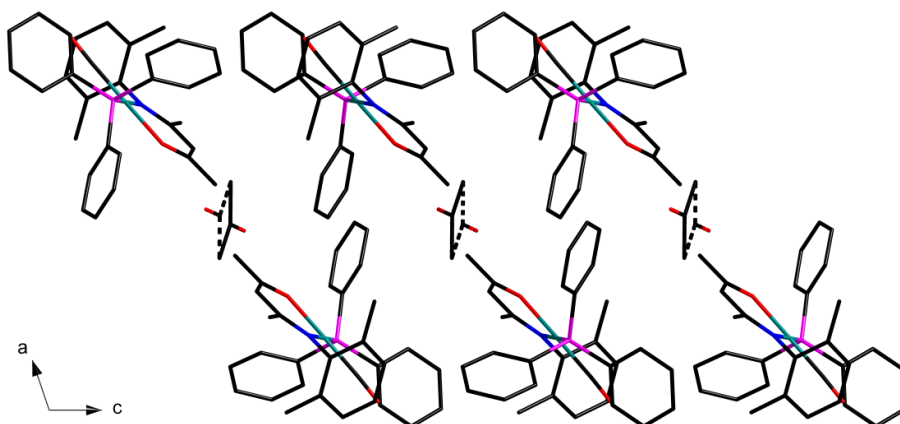


Figure 8.16. View of $[\text{Rh}(2,6\text{-Me}_2\text{-Phony})(\text{CO})(\text{PPh}_3)] \cdot 0.5(\text{CH}_3\text{COCH}_3)$ along the b-axis illustrating the packing style.

8.3. Discussion

Isomorphism was observed between the complexes $[\text{Rh}(2,6\text{-Cl}_2\text{-Phony})(\text{CO})(\text{PPh}_3)]$ and $[\text{Rh}(2,6\text{-Me}_2\text{-Phony})(\text{CO})(\text{PPh}_3)]$, with similar unit cell parameters (Table 8.1) and an RMS overlay value of 0.196 \AA (Figure 8.17).

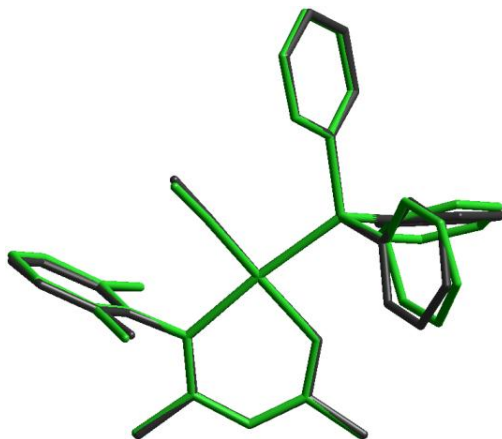


Figure 8.17. Overlay figures of $[\text{Rh}(2,6\text{-Cl}_2\text{-Phony})(\text{CO})(\text{PPh}_3)]$ (green) and $[\text{Rh}(2,6\text{-Me}_2\text{-Phony})(\text{CO})(\text{PPh}_3)]$ (black). Overlay fit includes all non-hydrogen atoms. RMS value = 0.195 \AA .

The cell volume of $[\text{Rh}(2,6\text{-Me}_2\text{-Phony})(\text{CO})(\text{PPh}_3)]$ [$2986.2(2) \text{ \AA}^3$] is slightly larger than the cell volume of $[\text{Rh}(2,6\text{-Cl}_2\text{-Phony})(\text{CO})(\text{PPh}_3)]$ [$2882.3(1) \text{ \AA}^3$]; although the a-axis of $[\text{Rh}(2,6\text{-Me}_2\text{-Phony})(\text{CO})(\text{PPh}_3)]$ is shorter than the a-axis for $[\text{Rh}(2,6\text{-Cl}_2\text{-Phony})(\text{CO})(\text{PPh}_3)]$ [$16.8558(8) \text{ \AA}$ versus $17.3242(5) \text{ \AA}$], the b- and c-axes are slightly longer for $[\text{Rh}(2,6\text{-Me}_2\text{-$

Chapter 8

Phony)(CO)(PPh₃)] than for [Rh(2,6-Cl₂-Phony)(CO)(PPh₃)] [11.4028(5) Å and 16.4059(8) Å *versus* 11.3170(3) Å and 15.4753(4) Å, respectively]. The C-H...Rh interaction present in [Rh(2,6-Cl₂-Phony)(CO)(PPh₃)] is absent in [Rh(2,6-Me₂-Phony)(CO)(PPh₃)], and the disorder of the acetone solvate differs slightly. Bonding distances and angles in these two complexes do not differ significantly (Table 8.12), as reflected in the low RMS overlay value.

Table 8.12. Summary of important distances (Å) and angles (°) in [Rh(N,O-Bid)(CO)(PPh₃)] complexes.

	[Rh(4-Cl-Phony) (CO)(PPh ₃)]	[Rh(2,4-Cl ₂ - Phony)(CO) (PPh ₃)]	[Rh(2,6-Cl ₂ - Phony)(CO) (PPh ₃)]	[Rh(2,3-Me ₂ - Phony)(CO) (PPh ₃)]	[Rh(2,6-Me ₂ - Phony)(CO) (PPh ₃)]
Rh ₁ -N ₁₁	2.080(2)	2.076(6)	2.085(2)	2.069(2)	2.076(2)
Rh ₁ -O ₁₂	2.034(2)	2.033(6)	2.035(2)	2.028(2)	2.028(2)
Rh ₁ -P ₁₃	2.2627(8)	2.268(2)	2.2688(7)	2.2634(6)	2.2701(6)
Rh ₁ -C ₁₄	1.814(3)	1.825(8)	1.808(3)	1.807(2)	1.808(3)
N ₁₁ -Rh ₁ -O ₁₂	89.04(9)	88.7(2)	88.61(9)	88.61(8)	89.43(8)
O ₁₂ -Rh ₁ -P ₁₃	90.75(6)	87.3(1)	86.80(6)	84.97(5)	85.94(5)
P ₁₃ -Rh ₁ -C ₁₄	86.56(9)	90.1(2)	91.60(8)	91.87(7)	91.60(8)
N ₁₁ -Rh ₁ -C ₁₄	93.7(1)	93.9(3)	93.0(1)	93.6(1)	93.0(1)
N ₁₁ -C ₂ -C ₄ -O ₁₂	0.4(3)	-1.0(7)	3.4(2)	4.1(2)	-2.6(2)
Dihedral angle ^a	83.76(9)	85.3(2)	84.06(8)	88.4(1)	85.58(8)
θ _E ^b	154.89(3)	155.80(9)	155.29(3)	156.39(3)	155.77(3)

^a Defined as the torsion angle between the N-C-C-C-O plane and the phenyl ring.

^b The Tolman cone angle, as defined in § 2.2.3.

The [Rh(N,O-Bid)(CO)(PPh₃)] complexes are chemically similar, and display a surprising lack of intermolecular hydrogen interactions, and very few intramolecular hydrogen interactions. Unlike the N,O-BidH compounds and [Rh(N,O-Bid)(CO)₂] complexes discussed in Chapters 4 and 6, no disordered methyl hydrogen atoms were observed, although the phenyl ring of the 2,3-Me₂-Phony⁻ ligand in [Rh(2,3-Me₂-Phony)(CO)(PPh₃)] displays a 59:41 disorder. The complexes adopt a square planar coordination geometry of the rhodium(I) atom, with the largest displacement of the rhodium atom from the N₁₁-O₁₂-P₁₃-C₁₄ plane being 0.0456(2) Å for [Rh(2,6-Me₂-Phony)(CO)(PPh₃)]. The presence of an electron donating methyl group instead of an electron withdrawing chloride group does not have a significant influence on the geometrical parameters of [Rh(N,O-Bid)(CO)(PPh₃)] complexes; these parameters are instead manipulated

Chapter 8

by the position of the substituents on the phenyl ring. For [Rh(4-Cl-Phony)(CO)(PPh₃)] the N₁₁-C₂-C₄-O₁₂ torsion angle is significantly smaller than the largest {0.4(3)^o *versus* 4.1(2)^o for [Rh(2,3-Me₂-Phony)(CO)(PPh₃)]}, and the P₁₃-Rh₁-C₁₄ angle for this complex is also significantly smaller than in the other complexes [86.76(9) Å *versus* 90.1(2) Å, 91.60(8) Å and 91.87(7) Å]. In these complexes the one-dimensional polymerism displayed by the [Rh(N,O-Bid)(CO)₂] complexes discussed in Chapter 6 is absent due to the steric influence of the PPh₃ ligands.

Crystal structures of complexes of the type [Rh(L,L'-Bid)(CO)(PX₃)] (where L is either N or O and L' is O) are surprisingly limited⁴. The presence of an electron rich moiety on the bidentate ligand plays a definite role in the geometrical parameters of [Rh(L,L'-Bid)(CO)(PX₃)] complexes found in literature (illustrated in Figure 8.18) as shown in Table 8.13.

⁴ Allen, F.H. The Cambridge Structural Database Version 1.9, *Acta Cryst.* **2002**, B58, 380-388.

Chapter 8

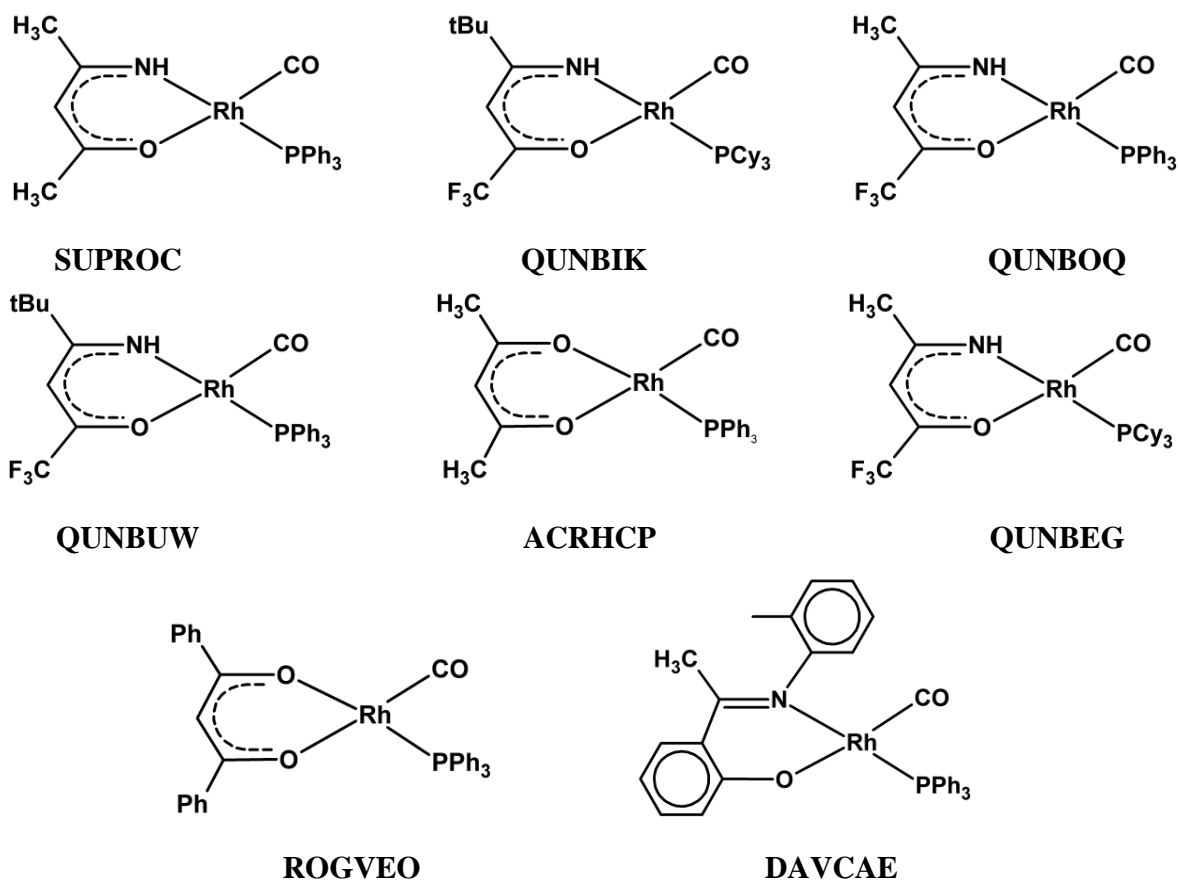


Figure 8.18. Illustrations of comparative $[\text{Rh}(\text{L}',\text{L}'\text{-bid})(\text{CO})(\text{PPh}_3)]$ complexes found in literature, ordered according to ascending $\text{N}\cdots\text{O}$ distance. ACRHCP = Acetylacetonato-carbonyl-(triphenylphosphine)-rhodium(I); DAVCAE = Carbonyl-(*N*-(*o*-tolyl)-salicylaldiminato)-triphenylphosphine-rhodium(I); QUNBEG = Carbonyl-(4-amino-1,1,1-trifluoro-3-penten-2-onato-*N,O*)-(tricyclohexylphosphine)-rhodium(I); QUNBIK = Carbonyl-(4-amino-5,5-dimethyl-1,1,1-trifluoro-3-hepten-2-onato-*N,O*)-(tricyclohexylphosphine)-rhodium(I); QUNBOQ = Carbonyl-(4-amino-1,1,1-trifluoro-3-penten-2-onato-*N,O*)-(triphenyl-phosphine)-rhodium(I); QUNBUW = Carbonyl-(4-amino-5,5-dimethyl-1,1,1-trifluoro-3-hepten-2-onato-*N,O*)-(triphenyl-phosphine)-rhodium(I); ROGVEO = Carbonyl-(1,3-diphenyl-1,3-propanedionato-*O,O'*)-(triphenylphosphine)-rhodium(I); SUPROC = (2-Imino-4-pentanonato-*N,O*)-carbonyl-triphenylphosphine-rhodium(I). References are given in Table 8.13.

Chapter 8

Table 8.13. Comparison of selected parameters of [Rh(N,O-Bid)(CO)(PPh₃)] complexes with [Rh(L,L'-Bid)(CO)(PX₃)] complexes.

	CSD ⁴ Reference code ^e	L,L' Type	<i>d</i> (N···O) ^f (Å)	<i>d</i> (Rh ₁ - P ₁₃) ^f (Å)	<i>d</i> (C ₁₄ - O ₁₄) ^f (Å)	N ₁₁ -Rh- O ₁₂ ^f (°)	P ₁₃ -Rh- C ₁₄ ^f (°)	N ₁₁ -C ₂ ··· C ₄ -O ₁₂ ^f (°)
1	SUPROK ⁵	N,O	2.826(6)	2.275(1)	1.142(7)	87.4(1)	90.3(2)	1.2(4)
2	QUNBIK ⁶	N,O	2.839(3)	2.282(1)	1.162(3)	87.80(5)	90.14(8)	-0.6(2)
3	QUNBOQ ⁶	N,O	2.841(3)	2.281(1)	1.148(4)	87.95(8)	89.49(8)	1.5(2)
4	QUNBUW ⁶	N,O	2.843(7)	2.278(2)	1.151(8)	87.9(2)	88.6(2)	-3.7(5)
5	ACRHCP ⁷	O,O	2.8569	2.2428	1.1520	87.916	87.790	-0.574
6	QUNBEG ⁶	N,O	2.860(3)	2.290(2)	1.150(3)	88.29(8)	89.26(8)	-2.0(2)
7	ROGVEO ⁸	O,O	2.87(1)	2.241(8)	1.16(1)	88.8(4)	91.5(4)	5.0(0)
II ^g		N,O	2.871(8)	2.268(2)	1.13(1)	88.7(2)	90.1(2)	-1.0(7)
8	DAVCAE ⁹	N,O	2.879(9)	2.281(2)	1.18(1)	88.7(3)	90.1(3)	-0.0(8)
III ^g		N,O	2.879(3)	2.2688(7)	1.150(4)	88.61(9)	91.60(8)	3.4(2)
I ^g		N,O	2.885(4)	2.2627(8)	1.146(4)	89.04(9)	90.75(6)	0.4(3)
IV ^g		N,O	2.885(3)	2.2634(6)	1.152(3)	88.61(8)	91.87(7)	4.1(2)
V ^g		N,O	2.886(3)	2.2701(6)	1.151(4)	89.43(8)	91.60(8)	-2.6(2)
Average			2.86(2)	2.269(9)	1.15(2)	88.4(6)	90.2(6)	2(1) ^h

^e ACRHCP = Acetylacetonato-carbonyl-(triphenylphosphine)-rhodium(I); DAVCAE = Carbonyl-(N-(*o*-tolyl)-salicylaldiminato)-triphenylphosphine-rhodium(I); QUNBEG = Carbonyl-(4-amino-1,1,1-trifluoro-3-penten-2-onato-N,O)-(tricyclohexylphosphine)-rhodium(I); QUNBIK = Carbonyl-(4-amino-5,5-dimethyl-1,1,1-trifluoro-3-hepten-2-onato-N,O)-(tricyclohexylphosphine)-rhodium(I); QUNBOQ = Carbonyl-(4-amino-1,1,1-trifluoro-3-penten-2-onato-N,O)-(triphenyl-phosphine)-rhodium(I); QUNBUW = Carbonyl-(4-amino-5,5-dimethyl-1,1,1-trifluoro-3-hepten-2-onato-N,O)-(triphenyl-phosphine)-rhodium(I); ROGVEO = Carbonyl-(1,3-diphenyl-1,3-propanedionato-O,O')-(triphenylphosphine)-rhodium(I); SUPROK = (2-Imino-4-pentanonato-N,O)-carbonyl-triphenylphosphine-rhodium(I).

^f Average values are used for complexes with more than one independent molecule in the asymmetric unit.

^g **I** = [Rh(4-Cl-Phony)(CO)(PPh₃)]; **II** = [Rh(2,4-Cl₂-Phony)(CO)(PPh₃)]; **III** = [Rh(2,6-Cl₂-Phony)(CO)(PPh₃)]; **IV** = [Rh(2,3-Me₂-Phony)(CO)(PPh₃)]; **V** = [Rh(2,6-Me₂-Phony)(CO)(PPh₃)].

^h Average calculated for absolute values of angles.

⁵ Damoense, L.J.; Purcell, W.; Roodt, A.; Leipoldt, J.G. *Rhodium Express* **1994**, 10-5.

⁶ Varshavsky, Y.S.; Galding, M.R.; Cherkasova, T.G.; Podkorytov, I.S.; Nikol'skii, A.B.; Trzeciak, A.M.; Olejnik, Z.; Lis, T.; Ziolkowski, J.J. *J. Organomet. Chem.* **2001**, 628, 195.

⁷ Leipoldt, J.G.; Basson, S.S.; Bok, L.D.C.; Gerber T.I.A. *Inorg. Chim. Acta* **1978**, 26, L35.

⁸ Lamprecht, D.; Lamprecht, G.J.; Botha, J.M.; Umakoshi, K.; Sasaki, Y. *Acta Cryst.* **1997**, C53, 1403.

⁹ Leipoldt, J.G.; Basson, S.S.; Grobler, E.C.; Roodt, A. *Inorg. Chim. Acta* **1985**, 99, 13.

Chapter 8

As with $[\text{Rh}(\text{L},\text{L}'\text{-Bid})(\text{CO})_2]$ complexes, the occurrence of complexes of the type $[\text{Rh}(\text{L},\text{L}'\text{-Bid})(\text{CO})(\text{PPh}_3)]$ in literature, where L is nitrogen and L' is oxygen, are very restricted⁴. The presence of a bulky phenyl ring makes a significant contribution to the bite angle of the bidentate ligand with the $\text{N}_{11}\text{-Rh}_1\text{-O}_{12}$ bite angles and $\text{N}_{11}\cdots\text{O}_{12}$ distances increasing for more bulky substituents on the pentane backbone. Even more significant is the presence of the phenyl ring on the nitrogen atom; these complexes, which largely comprise the Phony⁻ ligand group discussed in this chapter, display the largest bite angles. The steric bulk of the bidentate ligand does not have an influence on either the rhodium-phosphine or rhodium-carbonyl bond distances, and the $\text{P}_{13}\text{-Rh}_1\text{-C}_{14}$ angle is likewise unaffected by variations in the bidentate $\text{N}_{11}\text{-Rh}_1\text{-O}_{12}$ bite angle. Similarly, the $\text{N}_{11}\text{-C}_2\cdots\text{C}_4\text{-O}_{12}$ torsion angles are independent of the electronic properties of substituents on the ligand and do not follow a clear trend when compared with the $\text{N}_{11}\text{-Rh}_1\text{-O}_{12}$ bite angles, displaying angles of 5° or less. In complex 8 an unsaturated $\text{N}=\text{C}$ bond increases the *trans* influence of nitrogen significantly, leading to an abnormally long $\text{C}_{14}\text{-O}_{14}$ bond. As expected when considering the *trans* influence of nitrogen *versus* the *trans* influence of oxygen, the $\text{Rh}_1\text{-P}_{13}$ distance is shorter in complexes 5 and 7 where both L and L' are oxygen instead of L being nitrogen and L' oxygen. This phenomenon does not however have an influence on the bite angle of the ligand.

Since the phosphine group rotates in the gas phase, the calculations of the optimized structures of $[\text{Rh}(\text{N},\text{O-Bid})(\text{CO})(\text{PPh}_3)]$ complexes are labor and time intensive. No DFT calculations were performed.

8.4. Conclusion

A range of $[\text{Rh}(\text{N},\text{O-Bid})(\text{CO})(\text{PPh}_3)]$ complexes were synthesized and characterized, containing both electron withdrawing chloride atoms and electron donating methyl groups. These complexes are stable in solution and solid state, possibly due to the steric influence of the N-substituted phenyl ring in the bidentate ligand which hinders access to the metal center. Unlike the N,O-BidH ligand compounds and the $[\text{Rh}(\text{N},\text{O-Bid})(\text{CO})_2]$ complexes, some conformity of the crystal systems and space groups exist in these complexes, with three of the five complexes crystallizing in the monoclinic space group $P2_1/c$. Isomorphism was observed between $[\text{Rh}(2,6\text{-Cl}_2\text{-Phony})(\text{CO})(\text{PPh}_3)]$ and $[\text{Rh}(2,6\text{-Me}_2\text{-Phony})(\text{CO})(\text{PPh}_3)]$, both of which crystallizes in the

Chapter 8

above-mentioned space group. The $[\text{Rh}(\text{N},\text{O}\text{-Bid})(\text{CO})(\text{PPh}_3)]$ complexes display a surprising lack of intermolecular interactions, and very few intramolecular interactions were observed. Large differences in bond distances were observed, especially between complexes containing chloride substituents and methyl-containing complexes. Differences in the bonding angles are influenced by the position of the substituent on the phenyl ring rather than the substituent type.

The influence of the steric effect of the bidentate ligands with respect to ligand exchange will be discussed in the next chapter.

9 Mechanistic Study of the Phosphine Exchange in Carbonyl-[4-(phenylamino)pent-3-en-2-onato]-triphenylphosphine-rhodium(I) Complexes

9.1 Introduction

Investigations concerning the oxidative addition of methyl iodide (MeI) to square planar rhodium(I) complexes are not a new concept, and various studies have been conducted in this regard on complexes of the type $[\text{Rh}(\text{L},\text{L}'\text{-Bid})(\text{CO})(\text{PR}_3)]$, where L,L'-Bid = mono-anionic bidentate ligand and PR_3 = tertiary phosphine ligand¹. The mechanism of oxidative addition is explored with techniques such as X-ray crystallography as well as infrared, ultraviolet/visible and ¹H and ³¹P NMR spectroscopy. The current study focuses on the mechanisms involved in the exchange of uncoordinated triphenylphosphine with triphenylphosphine coordinated in complexes of the type $[\text{Rh}(\text{N},\text{O-Bid})(\text{CO})(\text{PPh}_3)]$ (where N,O-Bid is a bidentate ligand and derivative of 4-(phenylamino)pent-3-en-2-onate, PhonyH) which were discussed in Chapter 8.

Exchange reactions fulfill a fundamental role in quantifying catalytic processes and synthetic routes, justifying the investigation of these reactions as a means of understanding and improving downfield processes such as those involved in catalysis. While the exchange between free

¹ a) Roodt, A.; Visser, H.G.; Brink, A. *Crystallogr. Rev.* **2011**, *17*, 241.

b) Roodt, A.; Steyn, G.J.J. *Recent Res. Devel. Inorg. Chem.* **2000**, *2*, 1.

c) Basson, S.S.; Leipoldt, J.G.; Nel, J.T. *Inorg. Chim. Acta.* **1984**, *86*, 167.

d) Basson, S.S.; Leipoldt, J.G.; Roodt, A.; Venter, J.A. *Inorg. Chim. Acta.* **1987**, *128*, 31.

e) Leipoldt, J.G.; Steynberg, E.C.; Van Eldik, R. *Inorg. Chem.* **1987**, *26*, 3068.

Chapter 9

triphenylphosphine and coordinated $[\text{Rh}(\text{acac})(\text{CO})(\text{PPh}_3)]$ has been studied in the past² using several available techniques, the use of magnetization spin transfer allows for an accurate and user-friendly means of investigating the mechanism and rate of exchange provided that the rates are within certain limits. A correlation exists between the kinetic parameters of an exchange reaction and the corresponding observed NMR spectra, and the chemical exchange in magnetic resonance can be defined as follows:³ “It means that a chemical system is at macroscopic equilibrium, but at the microscopic level, an individual nucleus is exchanging its environment with another nucleus. The process causes no net change in the sample, but from the point of view of a particular nucleus, a chemical reaction has occurred.” This can be referred to as dynamic NMR since the molecules exhibit constant motion. Although the exchange process and other reactions in equilibrium have been studied using dynamic NMR⁴, literature concerning phosphine exchange reactions in metal complexes are scarce⁵.

Considering the lack of information regarding phosphine exchange in rhodium complexes, and the possible impact of exchange reactions on the studies in catalysis, the study thereof is imperative and this chapter therefore focuses on studying the exchange of free triphenylphosphine with triphenylphosphine coordinated in complexes of the type $[\text{Rh}(\text{N},\text{O}-\text{Bid})(\text{CO})(\text{PPh}_3)]$. Two complexes were chosen as study subjects: $[\text{Rh}(2,6-\text{Cl}_2\text{-Phony})(\text{CO})(\text{PPh}_3)]$ and $[\text{Rh}(2,6-\text{Me}_2\text{-Phony})(\text{CO})(\text{PPh}_3)]$, allowing for a comparison of the influence of the electron withdrawing properties of the chloride substituent *versus* the electron donating properties of the methyl groups in these Phony-type ligand systems on the rate of exchange.

² Trzeciak, A.M.; Jon, M.; Ziólkowski, J.J. *React. Kinet. Catal. Lett.* **1982**, *20*, 383.

³ Bain, A.D. *Chemical Exchange*, in *Modern Magnetic Resonance* edited by Webb, G.A. Springer, Dordrecht. **2008**.

⁴ a) Bain, A.D.; Bell, R.A.; Fletcher, D.A.; Hazendonk, P.; Maharajh, R.A.; Rigby, S.; Valliant, J.F. *J. Chem. Soc., Perkin Trans. 2*, **1999**, 1447.

b) Hasha, D.L.; Eguchi, T.; Jonas, J. *J. Am. Chem. Soc.* **1982**, *104*, 2290.

c) Perrin, C.L.; Dwyer, T.J. *Chem. Rev.* **1990**, *90*, 935.

⁵ a) Kotzé, P.D.R. *Methanol carbonylation via platinum group metal complexes*. Ph.D. Thesis, University of the Free State, Bloemfontein. **2010**.

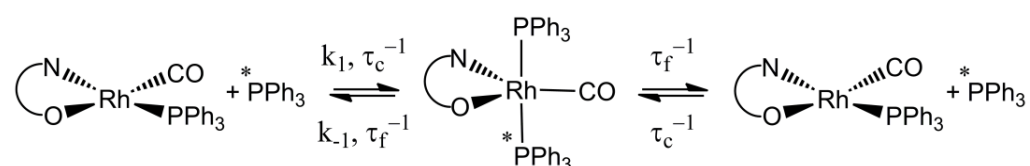
b) Fackler, J.P., Jr. *Inorg. Chem.* **1970**, *9*, 2625.

9.2 Magnetization Transfer Study on the Exchange Reaction of [Rh(N,O-Bid)(CO)(PPh₃)] Complexes with PPh₃

9.2.1 Theoretical Background

Magnetization transfer is an NMR technique where the magnetization of nuclei at a particular site or sites is perturbed, allowing for the determination of the kinetics of the exchange by following the rate at which magnetic equilibrium is restored⁶. This technique is applied for systems in which the exchange reactions are in equilibrium, with certain requirements.

Firstly, the investigated nuclear sites must have separate resonances. Consider the exchange reaction in Scheme 9.1:



Scheme 9.1. Phosphine exchange in rhodium complexes pertinent to this study.

The free and coordinated sites are given by f and c , respectively, and τ_c and τ_f are the mean lifetimes of the nuclei at each site. k_1 is the rate constant of the forward reaction and k_{-1} the rate constant of the backward reaction. In fulfillment of the abovementioned requirement, Equation 9.1 follows:

$$\Delta\nu_{cf} \gg \tau_c^{-1}, \tau_f^{-1} \quad \text{Eq. 9.1}$$

where $\Delta\nu_{cf}$ is the difference in the chemical shifts between a pair of resonances for the different nuclear sites under study⁷.

The second requirement entails that the spin-lattice relaxation times (T_{1c} and T_{1f} in the absence of exchange) are significant relative to the mean lifetime of the sites (τ_{cf}). The exchange rate for the reaction is then given by Equation 9.2:

⁶ Muller, P. *Pure Appl. Chem.* **1994**, 66, 1077.

⁷ McLaughlin, A.C.; Leigh, J.S., Jr. *J. Magn. Reson.* **1973**, 9, 296.

Chapter 9

$$\frac{-d[M-L_n]}{dt} = \frac{n[M-L_n]}{\tau_c} \text{ and } \frac{-d[M-L_{n-1}L^*]}{dt} = \frac{n[M-L_{n-1}L^*]}{\tau_f} \quad \text{Eq. 9.2}$$

In Equation 9.2, $[M-L_n]$ refers to the initial complex, L^* is the uncoordinated ligand [(PPh₃) in this study] and $[M-L_{n-1}L^*]$ refers to the complex after exchange had taken place. The dependence of reaction rate, k_{obs} , on temperature, T , was described by Arrhenius⁸ in Equation 9.3:

$$k_{obs} = Ae^{(-\Delta E^\ddagger/RT)} \quad \text{Eq. 9.3}$$

where A is the pre-exponential factor, R is the gas constant and ΔE^\ddagger is the energy of activation. Eyring's equation describes the rate constant, k_{obs} , as shown by Equation 9.4:

$$k_{obs} = k_1[L^*] + k_{-1} = \frac{1}{\tau_c} = \frac{rate}{n[M-L_n]} = \left(\frac{k_B T}{h}\right) \left(e^{\Delta S^\ddagger/R - \Delta H^\ddagger/RT}\right) \quad \text{Eq. 9.4}$$

where k_B is Boltzmann's constant and h is Planck's constant. The activation parameters can be calculated to describe the intrinsic properties of the mechanistic type for these reactions. The standard activation enthalpy change (ΔH^\ddagger) and the standard activation entropy change (ΔS^\ddagger) are often determined by using the logarithmic form of the Eyring equation (Equation 9.5), although the least squares fitting of the rate data to Equation 9.4 is also often utilized.

$$\ln\left(\frac{k_1}{T}\right) = \ln\left(\frac{k_B}{h}\right) - \frac{\Delta H^\ddagger}{RT} + \frac{\Delta S^\ddagger}{R} \quad \text{Eq. 9.5}$$

By plotting $\ln\left(\frac{k_1}{T}\right)$ versus $\frac{1}{T}$, a straight line with slope $-\frac{\Delta H^\ddagger}{R}$ and intercept $\ln\left(\frac{k_B}{h}\right) + \frac{\Delta S^\ddagger}{R}$ is obtained from which ΔH^\ddagger and ΔS^\ddagger can be derived.

Magnetization transfer experiments may utilize several methods, but since this study involves inversion-transfer only this method will be described. This method was developed from equations designed by Bloch⁹ that were modified to suit magnetization transfer by chemical exchange¹⁰. These equations describe the time dependence of the z component of nuclear

⁸ Laidler, K.J. *Chemical Kinetics*, McGraw-Hill, New York. **1965**.

⁹ Bloch, F. *Phys. Rev.* **1946**, 70, 460.

¹⁰ a) McConnell, H.M. *J. Chem. Phys.* **1958**, 28, 430.

b) Alexander, S. *J. Chem. Phys.* **1962**, 37, 967.

c) Binsch, G. *J. Am. Chem. Soc.* **1969**, 91, 1304.

d) Robinson, G., Chapman, B.E., Kuchel, P. W. *Eur. J. Biochem.* **1984**, 143, 643.

Chapter 9

magnetization at different sites with regard to, amongst others, their lifetimes and spin-lattice relaxation times and are shown in Equations 9.5 and 9.6:

$$\frac{dM_Z^c}{dt} = -\left(\frac{M_Z^c - M_e^c}{T_{1c}}\right) - \frac{M_Z^c}{\tau_c} + \frac{M_Z^f}{\tau_f} \quad \text{Eq. 9.6}$$

$$\frac{dM_Z^f}{dt} = -\left(\frac{M_Z^f - M_e^f}{T_{1f}}\right) + \frac{M_Z^c}{\tau_c} - \frac{M_Z^f}{\tau_f} \quad \text{Eq. 9.7}$$

Here M_Z^c and M_Z^f are the nuclear magnetization and M_e^c and M_e^f the equilibrium magnetizations of the different sites. The solutions of these equations with regard to magnetization transfer, as performed by an inversion of the resonance at site f are given in Equations 9.7 and 9.8:

$$M^c(t) = c_1 \tau_c \left(\lambda_1 + \frac{1}{\tau_{1c}}\right) e^{(\lambda_1 t)} + c_2 \tau_f \left(\lambda_2 + \frac{1}{\tau_{1f}}\right) e^{(\lambda_2 t)} + M_e^c \quad \text{Eq. 9.8}$$

$$M^f(t) = c_1 e^{(\lambda_1 t)} + c_2 e^{(\lambda_2 t)} + M_e^f \quad \text{Eq. 9.9}$$

$M^c(t)$ and $M^f(t)$ represent the time-dependent magnetizations, τ_{1c} and τ_{1f} represent the effective relaxation times of the different sites and t is the length of time in the pulse sequence during which inversion transfer takes place by chemical exchange. λ_1 , λ_2 , c_1 and c_2 are functions of the fundamental time constants, the equilibrium magnetizations and the magnetizations at $t \approx 0$ (M_0^c and M_0^f), respectively. The effective relaxation times, τ_{1c} and τ_{1f} , are described by Equations 9.10 and 9.11:

$$\frac{1}{\tau_{1c}} = \frac{1}{T_{1c}} + \frac{1}{\tau_c} \quad \text{Eq. 9.10}$$

$$\frac{1}{\tau_{1f}} = \frac{1}{T_{1f}} + \frac{1}{\tau_f} \quad \text{Eq. 9.11}$$

From inversion-transfer, the method applied in this study for the determination of kinetic values, the data for a set of inversion-transfer times is fitted to Equation 9.4¹¹. From this fit, estimates of T_{1c} , T_{1f} , τ_f , M_0^c and M_0^f can be calculated. During the fitting process τ_{1c} and τ_{1f} are eliminated from Equation 9.4 using Equations 9.6 and 9.7, and τ_c is eliminated using the equation $K_e = \tau_f/\tau_c$,

¹¹ Alger, J.R.; Prestegard, J.H. *J. Magn. Reson.* **1977**, *27*, 137.

Chapter 9

where $K_e = M_e^f/M_e^c$. Intensities that are measured when $t > 5T_1$ are used for M_e^f and M_e^c . The thermodynamic values can then be calculated as shown in Equation 9.2.

9.2.2 Experimental Procedure

As reported in Chapters 3 and 8, a series of complexes of the type $[\text{Rh}(\text{N,O-Bid})(\text{CO})(\text{PPh}_3)]$ have been synthesized and characterized in this study, with the electronic properties of the complexes represented by the carbonyl stretching frequencies, ν_{CO} , obtained from the infrared spectra. Both $[\text{Rh}(2,6\text{-Cl}_2\text{-Phony})(\text{CO})(\text{PPh}_3)]$ and $[\text{Rh}(2,6\text{-Me}_2\text{-Phony})(\text{CO})(\text{PPh}_3)]$ show good solubility in dichloromethane and are very stable in solution over a period of several months. These square planar complexes proceed to the exchange reaction product *via* a five-coordinate trigonal bipyramidal transition state, which is a well-known occurrence in rhodium complexes¹². To investigate the exchange of uncoordinated triphenylphosphine $[(\text{PPh}_3)_{\text{Free}}]$ and triphenylphosphine coordinated in the complexes $[(\text{PPh}_3)_{\text{Coord}}]$, the complexes were dissolved in CD_2Cl_2 in a 5mm NMR tube at a concentration of 0.06M for $(\text{PPh}_3)_{\text{Coord}}$ and a range of concentrations for $(\text{PPh}_3)_{\text{Free}}$ (0.06M, 0.12M, 0.30M and 0.60M). The ^{31}P NMR spectra were collected on a Bruker AXS600 spectrometer at the chosen temperature. Two sets of peaks could be observed for the different solutions; -6.63 for $(\text{PPh}_3)_{\text{Free}}$, 42.38 (d, $J_{\text{Rh-P}}$ 157.21 Hz) corresponding to $[\text{Rh}(2,6\text{-Cl}_2\text{-Phony})(\text{CO})(\text{PPh}_3)]$ and 43.73 ppm (d, $J_{\text{Rh-P}}$ 154.54 Hz) for $[\text{Rh}(2,6\text{-Me}_2\text{-Phony})(\text{CO})(\text{PPh}_3)]$. The magnetization transfer pulse program was applied.

The inversion-transfer method was chosen since the rate of exchange of phosphine in the complex falls within the time-frame of the method in terms of half-life. The method involves a pulse program where a non-selective 90° pulse and a $(\text{PPh}_3)_{\text{Coord}}$ selective 180° pulse were applied on the sample using variable delay times between consecutive pulses, as well as calculated coarse power and pulse width (see Figure 9.1).

¹² Allen, F.H. The Cambridge Structural Database Version 1.9, *Acta Cryst.* **2002**, B58, 380.

Chapter 9

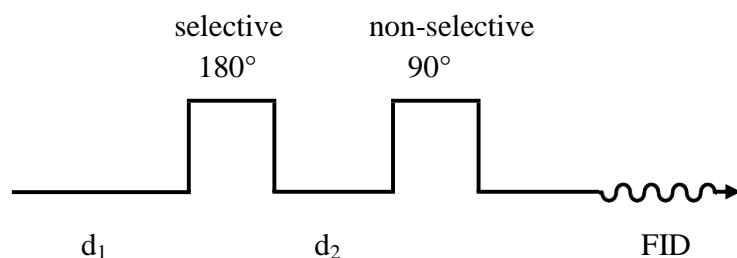


Figure 9.1. Pulse sequence for an inversion magnetization transfer experiment.

The result was the inversion of the peak representing the coordinated phosphine on the ^{31}P NMR spectrum. This peak underwent relaxation over a specified period and substitution of $(\text{PPh}_3)_{\text{Coord}}$ by $(\text{PPh}_3)_{\text{Free}}$ was observed by following the progress of this relaxation.

A series of samples were prepared where the concentration of $(\text{PPh}_3)_{\text{Coord}}$ was kept constant at approximately 0.06M, and the concentration of $(\text{PPh}_3)_{\text{Free}}$ was varied with values of 0.06M (1 eq), 0.12M (2 eq), 0.3M (5 eq) and 0.6M (10 eq). Magnetization transfer was performed on each sample at 18°C, 25°C, 35°C and 45 °C by collecting ^{31}P NMR spectra and applying the pulse program. The data obtained from these experiments were evaluated using the CIFIT2 kinetic modelling software package¹³ which calculated the observed rate constants for each sample at different temperatures. The software utilizes Equation 9.11 to fit the experimental data as a simple two-site exchange.

$$\frac{d}{dt} \begin{pmatrix} M_1(\infty) - M_1(t) \\ M_2(\infty) - M_2(t) \end{pmatrix} = -k \begin{pmatrix} K & -1 \\ -K & 1 \end{pmatrix} \begin{pmatrix} M_1(\infty) - M_1(t) \\ M_2(\infty) - M_2(t) \end{pmatrix} \quad \text{Eq. 9.12}$$

From the NMR and ν_{CO} values mentioned in Chapter 3 it is clear that monocarbonyl triphenylphosphine complexes are electron rich, though sterically congested. This leads to stabilization of the π -orbitals of the rhodium atom, from which it follows that exchange of the phosphine ligand will be slower than substitution of a carbonyl ligand by, for example, triphenylphosphine from a dicarbonyl complex¹⁴.

¹³ Bain, A.D. *Prog. Nucl. Mag. Res. Sp.* **2003**, 43, 63.

¹⁴ Ebenebe, P.N. *A mechanistic and structural study of carbonyl substitution in square-planar Rh(I)-beta-diketone complexes*. Ph.D. Thesis, University of the Free State, Bloemfontein. **1998**.

9.2.3 Results

A representation of the set of spectra obtained from an inversion-transfer experiment is illustrated in Figure 9.2, where $[\text{Rh}(2,6\text{-Me}_2\text{-Phony})(\text{CO})(\text{PP}_3)]$ was used as example complex. The integrated values of the peaks as a function of the delay time (d_2) are expressed in Figure 9.3.

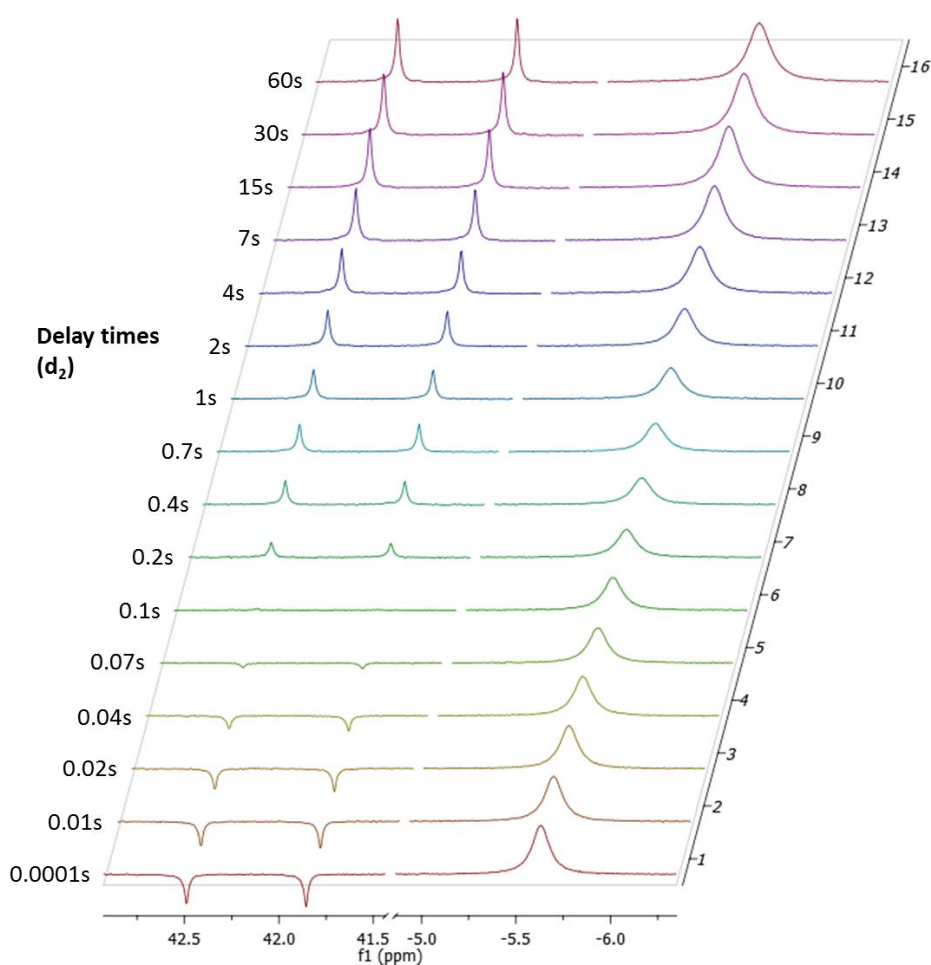


Figure 9.2. General profile of inversion-transfer spectra as from a solution containing 0.12M PPh_3 and 0.06M $[\text{Rh}(2,6\text{-Me}_2\text{-Phony})(\text{CO})(\text{PPh}_3)]$ in CD_2Cl_2 at 18 °C. The delay times (d_2) are indicated on the spectra.

Chapter 9

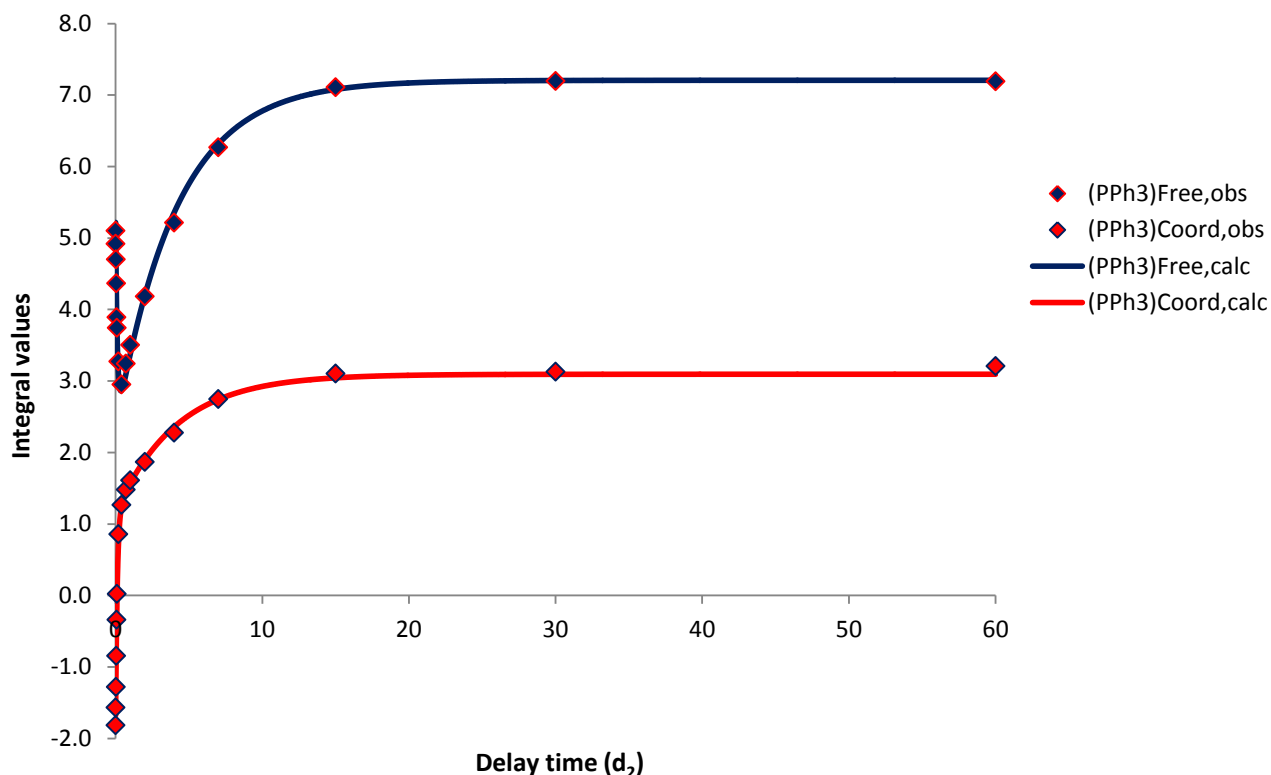
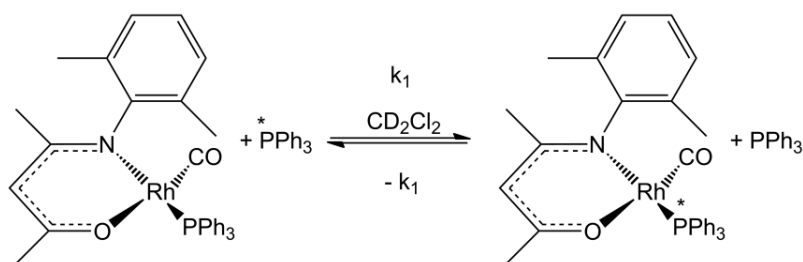


Figure 9.3. A general plot obtained from an inversion-transfer experiment for the exchange reaction of $(PPh_3)_{Free}$ and $(PPh_3)_{Coord}$ in a solution containing 0.12M PPh_3 and 0.06M $[Rh(2,6-Me_2-Phony)(CO)(PPh_3)]$ in CD_2Cl_2 at 18°C, illustrating the relation between the experimental (diamonds) and fitted (solid lines) data. Data for $(PPh_3)_{Free}$ is shown in blue and $(PPh_3)_{Coord}$ in red, while the diamonds (\blacklozenge and \blacklozenge) indicate experimental values and the lines indicate the fitted values based on Equation 9.12.

After application of the selective 180° pulse, the inverted peaks representing the coordinated phosphine $(PPh_3)_{Coord}$ (as $[Rh(2,6-Me_2-Phony)(CO)(PPh_3)]$ in this case) relax and are observed at various delay times (d_2) as indicated in the Figure 9.2. The peaks eventually relax back to their original position while the second peak, representing the uncoordinated phosphine $(PPh_3)_{Free}$, reduces over time and then returns back to its original intensity as observed from a 90° pulse. This suggests that phosphine exchange took place between the two species where $(PPh_3)_{Free}$ substituted one of the phosphine ligands on $[Rh(2,6-Me_2-Phony)(CO)(PPh_3)]$ [$(PPh_3)_{Coord}$] to reproduce the same complex, see Scheme 9.2. The rate expressions for the exchange reaction are similar to those described in § 9.2.1.

Chapter 9



Scheme 9.2. Phosphine exchange in $[\text{Rh}(\text{2,6-Me}_2\text{-Phony})(\text{CO})(\text{PPh}_3)]$.

The data obtained from spectra such as those illustrated in Figure 9.2 were fitted to Equation 9.12 with the kinetic modelling software CIFIT2 by varying values of the spin-lattice relaxation times and the magnetizations of the different species, as well as the rate constant of the exchange reaction. The correctly fitted values typically display plots similar to Figure 9.3, with the plot containing the calculated data conforming to that of the experimental data. From these fits the rate constants, k_{obs} , were calculated for different phosphine concentrations and at a range of temperatures. These values are represented in Figure 9.4 and Figure 9.5 for $[\text{Rh-2,6-dichloro-Phony})(\text{CO})(\text{PPh}_3)]$ and $[\text{Rh-2,6-dimethyl-Phony})(\text{CO})(\text{PPh}_3)]$, respectively. The kinetic data obtained from these figures according to Equation 9.4 are reflected in Table 9.1 and Table 9.2. The data was also fitted to the Eyring equation (Equation 9.5) which is illustrated in Figure 9.6.

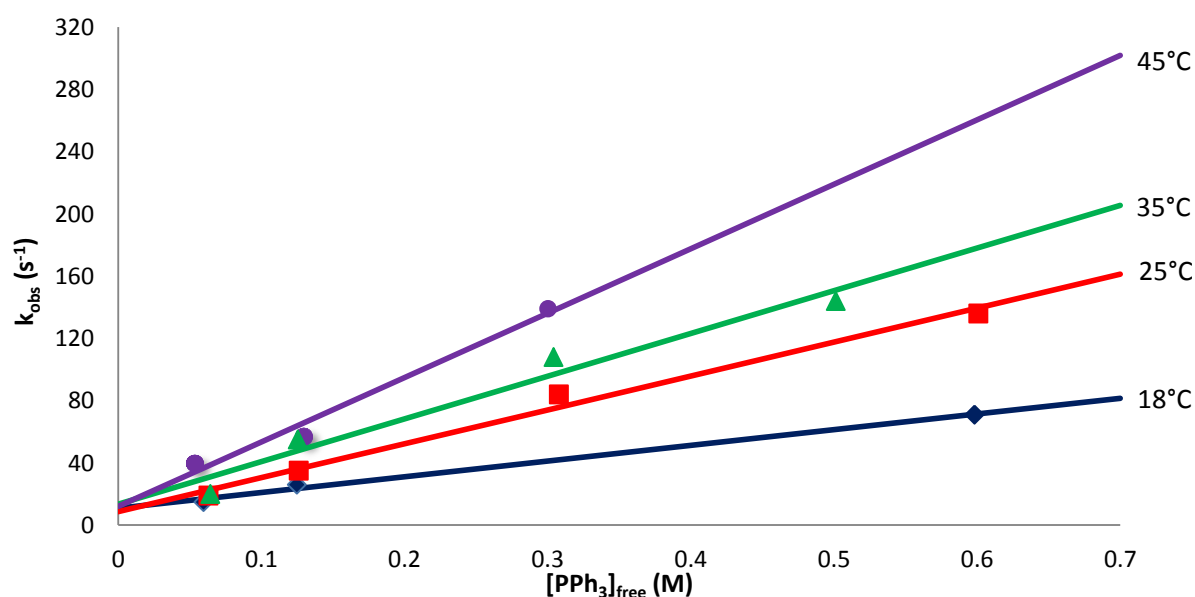


Figure 9.4. Plot of k_{obs} versus $[\text{PPh}_3]_{\text{Free}}$ for the exchange reaction between triphenylphosphine coordinated in $[\text{Rh}(\text{2,6-Cl}_2\text{-Phony})(\text{CO})(\text{PPh}_3)]$ and free triphenylphosphine in CD_2Cl_2 at different temperatures. $[\text{PPh}_3]_{\text{Coord}} = 0.06\text{M}$, $[\text{PPh}_3]_{\text{Free}} = 0.06\text{M}$, 0.12M , 0.30M and 0.60M .

Chapter 9

Table 9.1. Summary of the kinetic data obtained from Figure 9.4 for the exchange reaction between triphenylphosphine coordinated in $[\text{Rh}(2,6\text{-Cl}_2\text{-Phony})(\text{CO})(\text{PPh}_3)]$ and free triphenylphosphine.

	18 °C	25 °C	35 °C	45 °C
$k_1 (\text{M}^{-1} \cdot \text{s}^{-1})$	150(8)	218(16)	274(39)	414(61)
$k_{-1} (\text{s}^{-1})$	11(8)	9(6)	13(11)	12(12)
$K_1 (\text{M}^{-1})$	14(10)	24(16)	21(18)	35(35)

^a Although values for K_1 are reported, they are nearly negligible within experimental error.

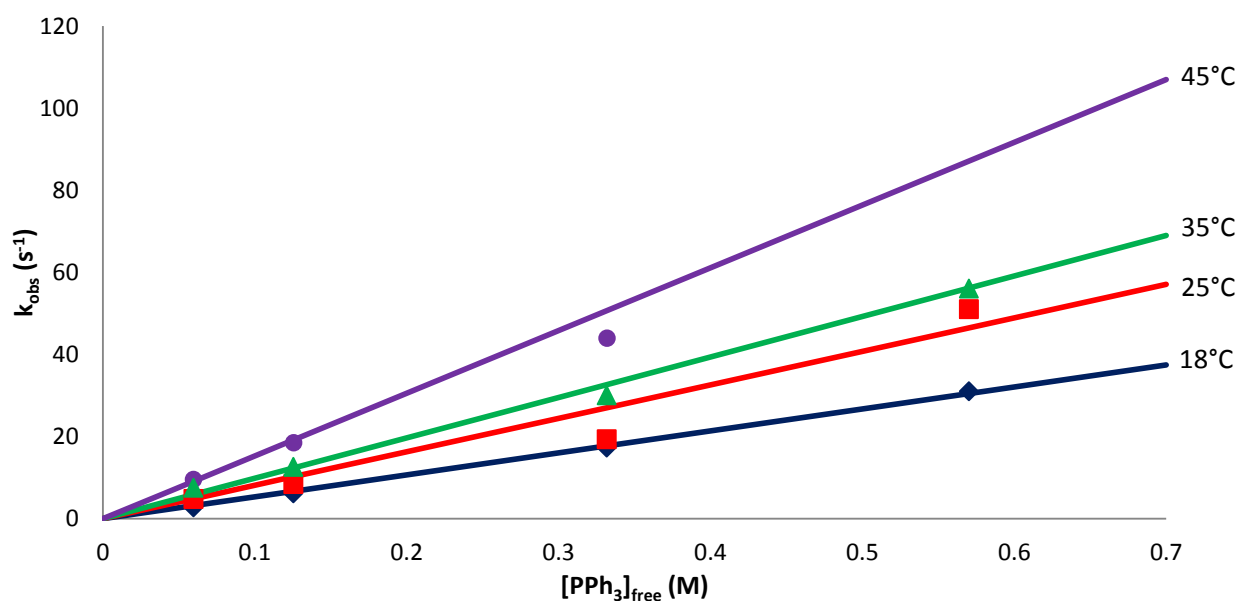


Figure 9.5. Plot of k_{obs} versus $[\text{PPh}_3]_{\text{Free}}$ for the exchange reaction between triphenylphosphine coordinated in $[\text{Rh}(2,6\text{-Me}_2\text{-Phony})(\text{CO})(\text{PPh}_3)]$ and free triphenylphosphine in CD_2Cl_2 at different temperatures. $[\text{PPh}_3]_{\text{Coord}} = 0.06\text{M}$, $[\text{PPh}_3]_{\text{Free}} = 0.06\text{M}, 0.12\text{M}, 0.30\text{M}$ and 0.60M .

Table 9.2. Summary of the kinetic data obtained from Figure 9.5 for the exchange reaction between triphenylphosphine coordinated in $[\text{Rh}(2,6\text{-Me}_2\text{-Phony})(\text{CO})(\text{PPh}_3)]$ and free triphenylphosphine.

	18 °C	25 °C	35 °C	45 °C
$k_1 (\text{M}^{-1} \cdot \text{s}^{-1})$	53.6(9)	82(7)	98.6(8)	153(6)
$k_{-1} (\text{s}^{-1})$	0	0	0	0

^b Since values for k_{-1} are extremely small and negligible within experimental error, these values were constrained to the value of 0 during the fitting process. From this follows that $K_1 \gg k_1$.

Chapter 9

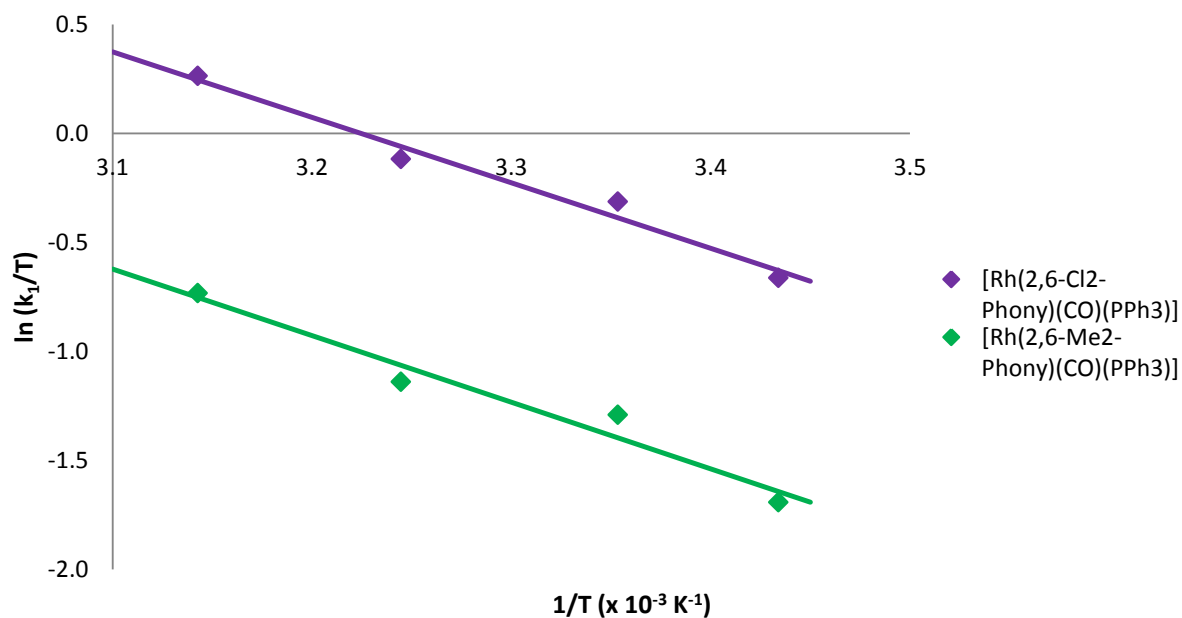


Figure 9.6. Eyring plot of $\ln\left(\frac{k_1}{T}\right)$ versus $\frac{1}{T}$ for the exchange reactions between $[\text{Rh}(2,6\text{-Cl}_2\text{-Phony})(\text{CO})(\text{PPh}_3)]$ (purple) and $[\text{Rh}(2,6\text{-Me}_2\text{-Phony})(\text{CO})(\text{PPh}_3)]$ (green) complexes and free triphenylphosphine for a temperature range of 18 °C to 45 °C.

From the Eyring plot (Figure 9.6) and the Eyring equation (Equation 9.5) the ΔH^\ddagger and ΔS^\ddagger activation parameters for the two different sets of exchange reactions were obtained, as well as the value for ΔG^\ddagger calculated from Equation 9.6. These values are shown in Table 9.3.

Table 9.3. Activation parameters for the exchange reaction between triphenylphosphine coordinated in $[\text{Rh}(2,6\text{-Cl}_2\text{-Phony})(\text{CO})(\text{PPh}_3)]$ and $[\text{Rh}(2,6\text{-Me}_2\text{-Phony})(\text{CO})(\text{PPh}_3)]$ complexes and free triphenylphosphine.

	[Rh(2,6-Cl₂-Phony)(CO)(PPh₃)]	[Rh(2,6-Me₂-Phony)(CO)(PPh₃)]
k_1 at 25°C (M ⁻¹ .s ⁻¹)	218(16)	82(7)
ΔH^\ddagger (kJ.mol ⁻¹)	25(3)	24(4)
ΔS^\ddagger (J.K ⁻¹ .mol ⁻¹)	-117(9)	-124(12)
ΔG^\ddagger at 18°C (kJ.mol ⁻¹)	59(3)	60(4)
ΔG^\ddagger at 25°C (kJ.mol ⁻¹)	60(3)	61(4)
ΔG^\ddagger at 35°C (kJ.mol ⁻¹)	61(3)	62(4)
ΔG^\ddagger at 45°C (kJ.mol ⁻¹)	62(3)	63(4)

9.3 Discussion and Conclusion

One of the main aims for this project was the investigation of the electronic properties of ligands on the rate of reactions in selected rhodium complexes. Since the exchange rates of ligands play a vital role in determining the activity of complexes, it was imperative that the exchange reaction in complexes of the type $[\text{Rh}(\text{N,O-Bid})(\text{CO})(\text{PPh}_3)]$ was investigated as part of this study. These complexes proved to be soluble in very few solvents, which limited the investigation. Once dissolved, the complexes were stable over a period of several months, with exchange reactions proceeding in the presence of excess triphenylphosphine. To simplify the investigation, the exchange reaction was limited to one ligand, although the exchange of triphenylphosphine with another type of phosphine could be an interesting topic for future investigations. Two $[\text{Rh}(\text{N,O-Bid})(\text{CO})(\text{PPh}_3)]$ complexes were chosen as subjects for these experiments; $[\text{Rh}(2,6\text{-Cl}_2\text{-Phony})(\text{CO})(\text{PPh}_3)]$ and $[\text{Rh}(2,6\text{-Me}_2\text{-Phony})(\text{CO})(\text{PPh}_3)]$. This allowed for the comparison of the electronic effect of the substituents on the phenyl rings, since the two complexes display similar steric properties while chloride substituents are electron withdrawing and methyl groups are electron donating.

According to the data in Table 9.1 and Table 9.2, the rate of reaction, k_1 , for phosphine exchange in $[\text{Rh}(2,6\text{-Cl}_2\text{-Phony})(\text{CO})(\text{PPh}_3)]$ is approximately three times faster than the rate of reaction for phosphine exchange in $[\text{Rh}(2,6\text{-Me}_2\text{-Phony})(\text{CO})(\text{PPh}_3)]$. This can be explained by the electron donating properties of the methyl substituents, which increases the electron density of the d -orbitals of the rhodium atom (also manifested in the ν_{CO} stretching frequencies, see § 3.5) and is therefore stabilizing the five-coordinate trigonal bipyramidal intermediate. The opposite is true for the chloride-containing complex. This phenomenon correlates with the difference in *trans* influence of the two complexes predicted by the ^{31}P NMR data, with $J_{\text{Rh-P}}$ values of 157.21 Hz and 154.54 Hz for $[\text{Rh}(2,6\text{-Cl}_2\text{-Phony})(\text{CO})(\text{PPh}_3)]$ and $[\text{Rh}(2,6\text{-Me}_2\text{-Phony})(\text{CO})(\text{PPh}_3)]$, respectively. The larger value for $J_{\text{Rh-P}}$ signifies a shorter Rh-P distance in $[\text{Rh}(2,6\text{-Cl}_2\text{-Phony})(\text{CO})(\text{PPh}_3)]$ than in $[\text{Rh}(2,6\text{-Me}_2\text{-Phony})(\text{CO})(\text{PPh}_3)]$, which was confirmed by the crystal data discussed in Chapter 8, with respective Rh-P distances of 2.2688(7) Å and 2.2701(6) Å. The decreased electron density surrounding the rhodium atom in $[\text{Rh}(2,6\text{-Cl}_2\text{-Phony})(\text{CO})(\text{PPh}_3)]$ also allows for the apparently more efficient reversal of the reaction as

Chapter 9

indicated by the k_1 values calculated from the [Rh(2,6-Cl₂-Phony)(CO)(PPh₃)] exchange reaction. This value is virtually absent in the reaction of the [Rh(2,6-Me₂-Phony)(CO)(PPh₃)] complex.

The activation parameters of the exchange reaction in [Rh(2,6-Cl₂-Phony)(CO)(PPh₃)] ($\Delta H^\ddagger = 25(3) \text{ kJ.mol}^{-1}$ and $\Delta S^\ddagger = -117(9) \text{ J.K}^{-1}.\text{mol}^{-1}$) correlate well with the parameters of the exchange reaction in [Rh(2,6-Me₂-Phony)(CO)(PPh₃)] ($\Delta H^\ddagger = 24(4) \text{ kJ.mol}^{-1}$ and $\Delta S^\ddagger = -124(12) \text{ J.K}^{-1}.\text{mol}^{-1}$). In both cases the value for entropy, ΔS^\ddagger , is significantly negative, indicating an associative mechanism. The relative contribution of $T\Delta S^\ddagger$ to ΔG^\ddagger is approximately 58 % and 61 % at 25°C for the respective complexes, whereas the enthalpy (ΔH^\ddagger) terms are correspondingly small. This indicates that the activation process is primarily controlled by entropy and involves the formation of a stable, well-ordered transition state while bond weakening is less important. This situation corresponds to the view that phosphines exert their high π -*trans* effect through stabilization of the transition state, while ground state destabilization is of lesser importance, and has been observed in other cases of substitution or exchange reactions taking place¹⁵. The relatively constant values for ΔG^\ddagger regardless of temperature, as seen in Table 9.3, also imply that the exchange reaction is not very sensitive to changes in temperature. The choice in technique is hereby ratified; for the proper application of magnetization spin transfer the rate constant needs to stay within a certain range in order to be observed.

The well-defined exchange reactions investigated in this study are an indication of further reaction possibilities, with the electronic properties of the ligands significantly influencing the rate of the reaction.

¹⁵ a) Plutino, M.R.; Otto, S.; Roodt, A.; Elding, L.I. *Inorg. Chem.* **1999**, 38, 1233.
b) Chatt, J.; Duncanson, L.A. *J. Chem. Soc.* **1953**, 2939.
c) Holloway, C.E.; Fogelman, J. *Can. J. Chem.* **1970**, 48, 3802.
d) Guillot-Edelheit, F.; Chottard, J.-C. *J. Chem. Soc., Dalton Trans.* **1984**, 169.

10 Evaluation of Study

10.1 Evaluation of Study

10.1.1 4-(Phenylamino)pent-3-en-2-one Derivatives

A range of potential ligand derivatives of 4-(Phenylamino)pent-3-en-2-one (PhonyH), with chloride substituents on different positions on the phenyl ring (N,O-BidH), were synthesized and characterized through X-ray crystallography as well as infrared and NMR spectroscopy. The gas-phase optimized structures of these compounds were also calculated using DFT methods and compared to the solid state data. The compounds crystallize in a range of space groups and varying crystal systems, and are stable in air over a period of several years and soluble in most solvents. The bond parameters were discussed in terms of distances and angles, with emphasis on the influences of intra- and intermolecular hydrogen and π - π interactions as well as chloride-chloride short contacts on the packing modes of the solid state compounds. The influence of the position of the chloride moiety on the phenyl ring with regard to bond parameters and packing modes was also discussed. Observations are supported by information from the calculated and literature structures, where the electronic properties of substituents on the phenyl ring impacts the geometrical parameters of the respective compounds. The calculated geometric parameters differ significantly from the observed solid state parameters, supporting the postulated influence of different chloride substitutions on packing modes and bond lengths, where seemingly small differences in substitution causes large variations in packing modes. The relative energies of the optimized structures adopt a cumulative nature – the relative energy of 2,4-Cl₂-PhonyH with regard to unsubstituted PhonyH is roughly equal to the sum of the relative energies of 2-Cl-PhonyH and 4-Cl-PhonyH, while the relative energy of 2,6-Cl₂-PhonyH equals twice the relative energy of 2-Cl-PhonyH. The distortion of the phenyl ring from the ideal planar position presented in the calculated structures corresponds to the distortion observed in the solid state.

The influence of the substituents allow for the tailoring of enaminoketone compounds to suit different criteria for their utilization as ligand systems.

10.1.2 Dicarbonyl-[4-(phenylamino)pent-3-en-2-onato]-rhodium(I) Complexes

A range of substituted dicarbonyl-[4-(phenylamino)pent-3-en-2-onato]-rhodium(I) {[Rh(N,O-Bid)(CO)₂]} complexes were synthesized and characterized, where the bidentate ligands were those discussed in earlier chapters. The optimized structures of these compounds were calculated using DFT methods. Slight differences were observed regarding bond distances and angles between the separate complexes, confirmed through both X-ray diffraction and NMR techniques. The *trans* influence of nitrogen was confirmed through the elongation of the Rh₁-C₁₃ bond with respect to the Rh₁-C₁₄ bond. The impact of the chloride substituents was observed from differences in geometrical parameters and is supported by information from the calculated structures and literature. This property allows for the tailoring of [Rh(N,O-bid)(CO)₂] complexes to suit different criteria for their potential utilization as future catalysts. Large differences between infrared stretching frequencies (ν_{CO}) of the solid state complexes can be explained by the influences of intra- and intermolecular hydrogen, rhodium-rhodium and π - π interactions on the packing modes. The position of the chloride atoms on the ring, and the subsequent influence on the packing modes, are also clearly signified in the variation in crystal systems and space groups as the position and number of the chloride atoms on the phenyl ring changes. The cumulative nature of the energies as displayed in the free ligands is repeated in the [Rh(N,O-Bid)(CO)₂] complexes: the relative energy of [Rh(2,4-Cl₂-Phony)(CO)₂] with regard to unsubstituted [Rh(Phony)(CO)₂] is roughly equal to the sum of the relative energies of [Rh(2-Cl-Phony)(CO)₂] and [Rh(4-Cl-Phony)(CO)₂], while the relative energy of [Rh(2,6-Cl₂-Phony)(CO)₂] is approximately the relative energy of [Rh(2-Cl-Phony)(CO)₂].

10.1.3 Carbonyl-[4-(phenylamino)pent-3-en-2-onato]-triphenylphosphine-rhodium(I) Complexes

A range of carbonyl-[4-(phenylamino)pent-3-en-2-onato]-triphenylphosphine-rhodium(I) {[Rh(N,O-Bid)(CO)(PPh₃)]} complexes were synthesized and characterized, containing both electron withdrawing chloride atoms and electron donating methyl groups. These complexes

Chapter 10

proved to be soluble in very few solvents, but once dissolved, were stable over a period of several months. Unlike the N,O-BidH ligand compounds and the $[\text{Rh}(\text{N,O-Bid})(\text{CO})_2]$ complexes, some conformity of the crystal systems and space groups exist in these complexes, with three of the five complexes crystallizing in the Monoclinic space group $P2_1/c$. Isomorphism was observed between $[\text{Rh}(2,6\text{-Cl}_2\text{-Phony})(\text{CO})(\text{PPh}_3)]$ and $[\text{Rh}(2,6\text{-Me}_2\text{-Phony})(\text{CO})(\text{PPh}_3)]$, both of which crystallizes in the above-mentioned space group. The $[\text{Rh}(\text{N,O-Bid})(\text{CO})(\text{PPh}_3)]$ complexes display a lack of intermolecular interactions, and very few intramolecular interactions were observed. Large differences in bond distances were observed, especially between complexes containing chloride substituents and methyl-containing complexes. Differences in the bonding angles are influenced by the position of the substituent on the phenyl ring rather than the substituent type. The overarching steric effect of the Phony-type ligand has been demonstrated by this study.

10.1.4 Phosphine Exchange Reactions

One of the main aims for this project was the investigation of the electronic properties of ligands on the rate of reactions in selected rhodium complexes. The focus in this study was the exchange reactions of coordinated phosphine with free phosphine, which occurs in the presence of excess triphenylphosphine. To simplify the investigation, the exchange reaction was limited to one ligand. Two $[\text{Rh}(\text{N,O-Bid})(\text{CO})(\text{PPh}_3)]$ complexes were chosen as subjects for these experiments; $[\text{Rh}(2,6\text{-Cl}_2\text{-Phony})(\text{CO})(\text{PPh}_3)]$ and $[\text{Rh}(2,6\text{-Me}_2\text{-Phony})(\text{CO})(\text{PPh}_3)]$. This allowed for the comparison of the electronic effect of the substituents on the phenyl rings, since the two complexes display similar steric properties while chloride substituents are electron withdrawing and methyl groups are electron donating. The method chosen for the investigation was magnetization spin transfer, an NMR technique which utilizes the magnetic properties of nuclei and determines the kinetic properties of the exchange by following the rate at which magnetic equilibrium is restored.

The rate of the phosphine exchange reaction in $[\text{Rh}(2,6\text{-Cl}_2\text{-Phony})(\text{CO})(\text{PPh}_3)]$ was found to be approximately one order of magnitude faster than the rate of reaction for phosphine exchange in $[\text{Rh}(2,6\text{-Me}_2\text{-Phony})(\text{CO})(\text{PPh}_3)]$. This can be explained by the electron donating properties of the methyl substituents, which increases the electron density of the d-orbitals of the rhodium

Chapter 10

atom and is therefore stabilizing the five-coordinate trigonal bipyramidal intermediate. The opposite is true for the chloride-containing complex. The decrease in electron density at the rhodium atom in $[\text{Rh}(2,6\text{-Cl}_2\text{-Phony})(\text{CO})(\text{PPh}_3)]$ also allows for the apparently more favoured reversal of the reaction as indicated by the k_{-1} values calculated from the $[\text{Rh}(2,6\text{-Cl}_2\text{-Phony})(\text{CO})(\text{PPh}_3)]$ exchange reaction. This value is absent in the reaction of the $[\text{Rh}(2,6\text{-Me}_2\text{-Phony})(\text{CO})(\text{PPh}_3)]$ complex. The activation parameters of the exchange reaction in $[\text{Rh}(2,6\text{-Cl}_2\text{-Phony})(\text{CO})(\text{PPh}_3)]$ correlate well with the parameters of the exchange reaction in $[\text{Rh}(2,6\text{-Me}_2\text{-Phony})(\text{CO})(\text{PPh}_3)]$. In both cases the value for the activation entropy, ΔS^\ddagger , is significantly negative, indicating an associative mechanism. Large contributions of ΔS^\ddagger to ΔG^\ddagger were also observed, indicating the significant π -*trans* effect of the PPh_3 ligand.

10.1.5 Oxidative Addition Reactions

The oxidative addition of methyl iodide to $[\text{Rh}(\text{N},\text{O}\text{-Bid})(\text{CO})(\text{PPh}_3)]$ complexes was attempted using UV/Vis, infrared and NMR spectroscopy, but the process doesn't follow the mechanism predicted by previous studies and was so convoluted that the exact mechanism evades elucidation at the moment. A crystalline product was obtained from the reaction of $[\text{Rh}(2,6\text{-Cl}_2\text{-Phony})(\text{CO})(\text{PPh}_3)]$ with methyl iodide with a basic structure unlike any other products for oxidative addition studies reported in literature. This complex contains both a methyl and a carbonyl ligand, which suggests that carbonylation might still be possible. This possibility was however not explored in the absence of information regarding the oxidative addition reaction mechanism.

10.2 Future Research

One of the main aims for this project was the investigation of the electronic properties of ligands on the rate of reactions in selected rhodium complexes. Since the results obtained covered only the influence of chloride and methyl substituents in two positions on the phenyl ring, this study can be significantly expanded by varying the position of the substituents on the phenyl ring as well as the nature of the substituents; bromide substituents will provide more electron withdrawing ligands while methoxide substituents are more electron donating than methyl groups. The steric influence of the substituents on the nitrogen atom can be evaluated by varying

Chapter 10

the phenyl ring with more bulky cyclohexyl or less bulky ethyl groups, to name only two examples.

The exchange of different types of phosphines (containing a combination of methoxy, ethyl tertiary butyl or cyclohexyl substituents, among other) will provide an insight into the influence of the steric and electronic properties of the exchanging ligands on the reaction rate. This study can be expanded further by including arsines and stibines as well.

The well-defined exchange reactions investigated in this study are an indication of further reaction possibilities, with the electronic properties of the ligands significantly influencing the rate of the reaction. This study on phosphine exchange should be expanded to include mechanistic investigations on oxidative addition reactions of methyl iodide and ligand influence on the formation rate, as well as the activity of these complexes under catalytic conditions for carbonylation reactions.

The activity of these ligands in complexes with different metal centres, for example iridium and cobalt, will provide further insight into the influence of π -electrons on these systems.

DFT calculations of the transition states will provide a model of how the reactions proceed and improve the understanding of the process. The calculations may also facilitate understanding of the oxidative addition reaction and offer possible explanations for the difficulties that have been experienced.

Chapter 10

A Appendix: Crystal Data of 4-(Phenylamino)pent-3-en-2-one Derivatives

A.1. 4-(2-Chlorophenylamino)pent-3-en-2-one (2-Cl-PhonyH)

Table A.1. Atomic coordinates ($\times 10^4$) and equivalent isotropic displacement parameters ($\text{\AA}^2 \times 10^3$) for 2-Cl-PhonyH. $U(\text{eq})$ is defined as one third of the trace of the orthogonalized U_{ij} tensor.

	x	y	z	U(eq)
Cl(12)	24(1)	2052(1)	5316(1)	23(1)
N(11)	2180(2)	2887(1)	6790(1)	17(1)
O(12)	3300(1)	17(1)	6837(1)	21(1)
C(3)	2468(2)	1443(2)	8015(1)	18(1)
C(2)	2091(2)	2809(2)	7621(1)	17(1)
C(111)	1805(2)	4134(2)	6266(1)	17(1)
C(116)	2464(2)	5609(2)	6416(1)	20(1)
C(4)	3006(2)	74(2)	7598(1)	21(1)
C(113)	420(2)	5072(2)	4998(1)	23(1)
C(5)	3168(2)	-1385(2)	8094(1)	23(1)
C(112)	804(2)	3893(2)	5542(1)	18(1)
C(115)	2072(2)	6807(2)	5879(1)	23(1)
C(1)	1554(2)	4197(2)	8114(1)	20(1)
C(114)	1048(2)	6539(2)	5173(1)	24(1)

Appendix A

Table A.2. Bond lengths [Å] and angles [°] for 2-Cl-PhonyH

Atoms	Bond lengths (Å)	Atoms	Bond angles (°)
Cl(12)-C(112)	1.7413(15)	C(2)-N(11)-C(111)	129.12(13)
N(11)-C(2)	1.3497(18)	C(2)-N(11)-H(11)	115.4
N(11)-C(111)	1.4048(18)	C(111)-N(11)-H(11)	115.4
N(11)-H(11)	0.8253	C(2)-C(3)-C(4)	123.97(13)
O(12)-C(4)	1.2525(18)	C(2)-C(3)-H(3)	118.0
C(3)-C(2)	1.3785(19)	C(4)-C(3)-H(3)	118.0
C(3)-C(4)	1.425(2)	N(11)-C(2)-C(3)	119.67(13)
C(3)-H(3)	0.9500	N(11)-C(2)-C(1)	120.20(13)
C(2)-C(1)	1.5004(19)	C(3)-C(2)-C(1)	120.13(12)
C(111)-C(116)	1.3942(19)	C(116)-C(111)-C(112)	117.73(13)
C(111)-C(112)	1.3993(19)	C(116)-C(111)-N(11)	122.70(12)
C(116)-C(115)	1.388(2)	C(112)-C(111)-N(11)	119.50(12)
C(116)-H(116)	0.9500	C(115)-C(116)-C(111)	120.83(13)
C(4)-C(5)	1.507(2)	C(115)-C(116)-H(116)	119.6
C(113)-C(112)	1.383(2)	C(111)-C(116)-H(116)	119.6
C(113)-C(114)	1.387(2)	O(12)-C(4)-C(3)	123.12(14)
C(113)-H(113)	0.9500	O(12)-C(4)-C(5)	118.48(14)
C(5)-H(5A)	0.9800	C(3)-C(4)-C(5)	118.37(13)
C(5)-H(5B)	0.9800	C(112)-C(113)-C(114)	119.11(14)
C(5)-H(5C)	0.9800	C(112)-C(113)-H(113)	120.4
C(115)-C(114)	1.388(2)	C(114)-C(113)-H(113)	120.4
C(115)-H(115)	0.9500	C(4)-C(5)-H(5A)	109.5
C(1)-H(1A)	0.9800	C(4)-C(5)-H(5B)	109.5
C(1)-H(1B)	0.9800	H(5A)-C(5)-H(5B)	109.5
C(1)-H(1C)	0.9800	C(4)-C(5)-H(5C)	109.5
C(114)-H(114)	0.9500	H(5A)-C(5)-H(5C)	109.5
		H(5B)-C(5)-H(5C)	109.5
		C(113)-C(112)-C(111)	121.99(13)
		C(113)-C(112)-Cl(12)	118.89(11)
		C(111)-C(112)-Cl(12)	119.12(11)
		C(114)-C(115)-C(116)	120.11(14)
		C(114)-C(115)-H(115)	119.9
		C(116)-C(115)-H(115)	119.9
		C(2)-C(1)-H(1A)	109.5
		C(2)-C(1)-H(1B)	109.5

Appendix A

H(1A)-C(1)-H(1B)	109.5
C(2)-C(1)-H(1C)	109.5
H(1A)-C(1)-H(1C)	109.5
H(1B)-C(1)-H(1C)	109.5
C(113)-C(114)-C(115)	120.18(14)
C(113)-C(114)-H(114)	119.9
C(115)-C(114)-H(114)	119.9

Table A.3. Anisotropic displacement parameters ($\text{\AA}^2 \times 10^3$) for 2-Cl-PhonyH. The anisotropic displacement factor exponent takes the form: $-2\pi^2 [h^2 a^{*2} U^{11} + \dots + 2 h k a^* b^* U^{12}]$

	U^{11}	U^{22}	U^{33}	U^{23}	U^{13}	U^{12}
Cl(12)	25(1)	27(1)	18(1)	-5(1)	-2(1)	-6(1)
N(11)	19(1)	18(1)	15(1)	-2(1)	0(1)	2(1)
O(12)	23(1)	23(1)	18(1)	0(1)	3(1)	-1(1)
C(3)	16(1)	24(1)	14(1)	-1(1)	-1(1)	-1(1)
C(2)	12(1)	22(1)	17(1)	-3(1)	-1(1)	-1(1)
C(111)	14(1)	22(1)	14(1)	-1(1)	2(1)	1(1)
C(116)	17(1)	22(1)	20(1)	-3(1)	1(1)	-1(1)
C(4)	23(1)	23(1)	18(1)	0(1)	3(1)	-1(1)
C(113)	20(1)	33(1)	15(1)	2(1)	0(1)	2(1)
C(5)	21(1)	23(1)	24(1)	2(1)	1(1)	2(1)
C(112)	15(1)	24(1)	16(1)	-3(1)	3(1)	-2(1)
C(115)	21(1)	22(1)	24(1)	1(1)	6(1)	-1(1)
C(1)	21(1)	22(1)	18(1)	-3(1)	1(1)	2(1)
C(114)	23(1)	28(1)	22(1)	8(1)	4(1)	3(1)

Appendix A

Table A.4. Hydrogen coordinates ($\times 10^4$) and isotropic displacement parameters ($\text{\AA}^2 \times 10^3$) for 2-Cl-PhonyH.

	x	y	z	U(eq)
H(11)	2500(8)	2090(20)	6556(6)	27(5)
H(3)	2362	1411	8599	21
H(116)	3191	5797	6891	24
H(113)	-264	4881	4510	27
H(5A)	2032	-1973	8047	34
H(5B)	3391	-1131	8674	34
H(5C)	4185	-2000	7881	34
H(115)	2505	7812	5996	27
H(1A)	2629	4844	8205	30
H(1B)	1055	3871	8647	30
H(1C)	628	4781	7810	30
H(114)	776	7363	4808	29

Table A.5. Torsion angles [$^\circ$] for 2-Cl-PhonyH.

Atoms	Angles ($^\circ$)
C(111)-N(11)-C(2)-C(3)	177.99(12)
C(111)-N(11)-C(2)-C(1)	-0.9(2)
C(4)-C(3)-C(2)-N(11)	1.7(2)
C(4)-C(3)-C(2)-C(1)	-179.31(13)
C(2)-N(11)-C(111)-C(116)	46.2(2)
C(2)-N(11)-C(111)-C(112)	-136.84(15)
C(112)-C(111)-C(116)-C(115)	2.6(2)
N(11)-C(111)-C(116)-C(115)	179.53(13)
C(2)-C(3)-C(4)-O(12)	4.8(2)
C(2)-C(3)-C(4)-C(5)	-173.14(13)
C(114)-C(113)-C(112)-C(111)	0.1(2)
C(114)-C(113)-C(112)-Cl(12)	-179.62(11)
C(116)-C(111)-C(112)-C(113)	-1.8(2)
N(11)-C(111)-C(112)-C(113)	-178.91(12)
C(116)-C(111)-C(112)-Cl(12)	177.83(10)
N(11)-C(111)-C(112)-Cl(12)	0.77(18)
C(111)-C(116)-C(115)-C(114)	-1.5(2)
C(112)-C(113)-C(114)-C(115)	1.1(2)
C(116)-C(115)-C(114)-C(113)	-0.3(2)

Appendix A

Table A.6. Hydrogen bonds for 2-Cl-PhonyH [\AA and $^\circ$].

D-H...A	d(D-H)	d(H...A)	d(D...A)	$\angle(\text{DHA})$
N(11)-H(11)...O(12)	0.83	1.95	2.6317(16)	139.2
C(113)-H(113)...O(12) ⁱ	0.95	2.42	3.3537(18)	166.1
C(115)-H(115)...O(12) ⁱⁱ	0.95	2.43	3.3219(19)	157.1

Symmetry operators: i) $x - \frac{1}{2}, -y + \frac{1}{2}, -z + 1$ ii) $x, y + 1, z$

A.2. 4-(4-Chlorophenylamino)pent-3-en-2-one (4-Cl-PhonyH)

Table A.7. Atomic coordinates ($\times 10^4$) and equivalent isotropic displacement parameters ($\text{\AA}^2 \times 10^3$) for 4-Cl-PhonyH. $U(\text{eq})$ is defined as one third of the trace of the orthogonalized U^{ij} tensor.

	x	y	z	U(eq)
C(1)	9300(2)	-213(2)	4499(1)	21(1)
C(2)	8412(2)	-406(2)	4768(1)	16(1)
C(3)	8244(2)	51(2)	5323(1)	18(1)
C(4)	7389(2)	-28(2)	5594(1)	19(1)
C(5)	7295(2)	571(2)	6182(1)	24(1)
C(6)	5129(2)	461(2)	4176(1)	23(1)
C(7)	5417(2)	1350(2)	4528(1)	18(1)
C(8)	5088(2)	1561(2)	5103(1)	20(1)
C(9)	5311(2)	2394(2)	5464(1)	19(1)
C(10)	4939(2)	2531(2)	6104(1)	26(1)
C(11)	7313(2)	7057(2)	5407(1)	24(1)
C(12)	7021(2)	6166(2)	5063(1)	18(1)
C(13)	7325(2)	5958(2)	4475(1)	20(1)
C(14)	7100(2)	5126(2)	4119(1)	20(1)
C(15)	7434(2)	5008(2)	3460(1)	31(1)
C(16)	3129(2)	7710(2)	5193(1)	23(1)
C(17)	4028(2)	7910(2)	4930(1)	17(1)
C(18)	4208(2)	7451(2)	4379(1)	20(1)
C(19)	5056(2)	7569(2)	4096(1)	18(1)
C(20)	5152(2)	6972(2)	3504(1)	23(1)
C(111)	7828(2)	-1496(2)	3851(1)	15(1)
C(112)	7069(2)	-1451(2)	3316(1)	19(1)
C(113)	7095(2)	-1945(2)	2743(1)	20(1)

Appendix A

C(114)	7891(2)	-2491(2)	2715(1)	20(1)
C(115)	8654(2)	-2546(2)	3241(1)	21(1)
C(116)	8614(2)	-2048(2)	3813(1)	17(1)
C(211)	6450(2)	1856(2)	3724(1)	17(1)
C(212)	6917(2)	1043(2)	3609(1)	18(1)
C(213)	7417(2)	986(2)	3083(1)	20(1)
C(214)	7457(2)	1745(2)	2687(1)	20(1)
C(215)	7021(2)	2566(2)	2811(1)	23(1)
C(216)	6516(2)	2613(2)	3324(1)	22(1)
C(311)	6043(2)	5625(2)	5888(1)	17(1)
C(312)	6000(2)	4825(2)	6259(1)	21(1)
C(313)	5547(2)	4829(2)	6805(1)	24(1)
C(314)	5134(2)	5633(2)	6978(1)	21(1)
C(315)	5160(2)	6429(2)	6617(1)	22(1)
C(316)	5608(2)	6425(2)	6064(1)	22(1)
C(411)	4557(2)	9051(2)	5821(1)	16(1)
C(412)	3745(2)	9590(2)	5827(1)	18(1)
C(413)	3671(2)	10129(2)	6371(1)	18(1)
C(414)	4427(2)	10141(2)	6909(1)	19(1)
C(415)	5238(2)	9613(2)	6915(1)	21(1)
C(416)	5300(2)	9065(2)	6368(1)	21(1)
N(11)	7753(2)	-998(1)	4438(1)	16(1)
N(21)	5961(1)	1960(2)	4267(1)	18(1)
N(31)	6477(1)	5555(2)	5325(1)	18(1)
N(41)	4666(2)	8522(1)	5257(1)	18(1)
O(12)	6717(1)	-559(1)	5364(1)	22(1)
O(22)	5785(1)	3029(1)	5268(1)	22(1)
O(32)	6642(1)	4478(1)	4317(1)	24(1)
O(42)	5704(1)	8122(1)	4322(1)	22(1)
Cl(14)	7938(1)	-3120(1)	1998(1)	31(1)
Cl(24)	8074(1)	1677(1)	2025(1)	27(1)
Cl(34)	4581(1)	5633(1)	7669(1)	30(1)
Cl(44)	4356(1)	10852(1)	7584(1)	26(1)

Appendix A

Table A.8. Bond lengths [Å] and angles [°] for 4-Cl-PhonyH.

Atoms	Bond lengths (Å)	Atoms	Angles (°)
C(1)-C(2)	1.487(4)	C(2)-C(1)-H(1A)	109.5
C(1)-H(1A)	0.9800	C(2)-C(1)-H(1B)	109.5
C(1)-H(1B)	0.9800	H(1A)-C(1)-H(1B)	109.5
C(1)-H(1C)	0.9800	C(2)-C(1)-H(1C)	109.5
C(1)-H(1D)	0.9800	H(1A)-C(1)-H(1C)	109.5
C(1)-H(1E)	0.9800	H(1B)-C(1)-H(1C)	109.5
C(1)-H(1F)	0.9800	C(2)-C(1)-H(1D)	109.5
C(2)-N(11)	1.354(3)	H(1A)-C(1)-H(1D)	141.1
C(2)-C(3)	1.373(3)	H(1B)-C(1)-H(1D)	56.3
C(3)-C(4)	1.424(4)	H(1C)-C(1)-H(1D)	56.3
C(3)-H(3)	0.9500	C(2)-C(1)-H(1E)	109.5
C(4)-O(12)	1.248(3)	H(1A)-C(1)-H(1E)	56.3
C(4)-C(5)	1.511(3)	H(1B)-C(1)-H(1E)	141.1
C(5)-H(5A)	0.9800	H(1C)-C(1)-H(1E)	56.3
C(5)-H(5B)	0.9800	H(1D)-C(1)-H(1E)	109.5
C(5)-H(5C)	0.9800	C(2)-C(1)-H(1F)	109.5
C(6)-C(7)	1.499(4)	H(1A)-C(1)-H(1F)	56.3
C(6)-H(6A)	0.9800	H(1B)-C(1)-H(1F)	56.3
C(6)-H(6B)	0.9800	H(1C)-C(1)-H(1F)	141.1
C(6)-H(6C)	0.9800	H(1D)-C(1)-H(1F)	109.5
C(6)-H(6D)	0.9800	H(1E)-C(1)-H(1F)	109.5
C(6)-H(6E)	0.9800	N(11)-C(2)-C(3)	120.9(2)
C(6)-H(6F)	0.9800	N(11)-C(2)-C(1)	119.0(2)
C(7)-N(21)	1.347(3)	C(3)-C(2)-C(1)	120.0(2)
C(7)-C(8)	1.376(3)	C(2)-C(3)-C(4)	124.8(2)
C(8)-C(9)	1.423(4)	C(2)-C(3)-H(3)	117.6
C(8)-H(8)	0.9500	C(4)-C(3)-H(3)	117.6
C(9)-O(22)	1.250(3)	O(12)-C(4)-C(3)	123.0(2)
C(9)-C(10)	1.512(4)	O(12)-C(4)-C(5)	119.1(2)
C(10)-H(10A)	0.9800	C(3)-C(4)-C(5)	118.0(2)
C(10)-H(10B)	0.9800	C(4)-C(5)-H(5A)	109.5
C(10)-H(10C)	0.9800	C(4)-C(5)-H(5B)	109.5
C(10)-H(10D)	0.9800	H(5A)-C(5)-H(5B)	109.5
C(10)-H(10E)	0.9800	C(4)-C(5)-H(5C)	109.5

Appendix A

C(10)-H(10F)	0.9800	H(5A)-C(5)-H(5C)	109.5
C(11)-C(12)	1.495(4)	H(5B)-C(5)-H(5C)	109.5
C(11)-H(11A)	0.9800	C(7)-C(6)-H(6A)	109.5
C(11)-H(11B)	0.9800	C(7)-C(6)-H(6B)	109.5
C(11)-H(11C)	0.9800	H(6A)-C(6)-H(6B)	109.5
C(11)-H(11D)	0.9800	C(7)-C(6)-H(6C)	109.5
C(11)-H(11E)	0.9800	H(6A)-C(6)-H(6C)	109.5
C(11)-H(11F)	0.9800	H(6B)-C(6)-H(6C)	109.5
C(12)-N(31)	1.349(3)	C(7)-C(6)-H(6D)	109.5
C(12)-C(13)	1.384(3)	H(6A)-C(6)-H(6D)	141.1
C(13)-C(14)	1.418(4)	H(6B)-C(6)-H(6D)	56.3
C(13)-H(13)	0.9500	H(6C)-C(6)-H(6D)	56.3
C(14)-O(32)	1.252(3)	C(7)-C(6)-H(6E)	109.5
C(14)-C(15)	1.518(3)	H(6A)-C(6)-H(6E)	56.3
C(15)-H(15A)	0.9800	H(6B)-C(6)-H(6E)	141.1
C(15)-H(15B)	0.9800	H(6C)-C(6)-H(6E)	56.3
C(15)-H(15C)	0.9800	H(6D)-C(6)-H(6E)	109.5
C(15)-H(15D)	0.9800	C(7)-C(6)-H(6F)	109.5
C(15)-H(15E)	0.9800	H(6A)-C(6)-H(6F)	56.3
C(15)-H(15F)	0.9800	H(6B)-C(6)-H(6F)	56.3
C(16)-C(17)	1.498(3)	H(6C)-C(6)-H(6F)	141.1
C(16)-H(16A)	0.9800	H(6D)-C(6)-H(6F)	109.5
C(16)-H(16B)	0.9800	H(6E)-C(6)-H(6F)	109.5
C(16)-H(16C)	0.9800	N(21)-C(7)-C(8)	120.0(2)
C(16)-H(16D)	0.9800	N(21)-C(7)-C(6)	120.1(2)
C(16)-H(16E)	0.9800	C(8)-C(7)-C(6)	119.9(2)
C(16)-H(16F)	0.9800	C(7)-C(8)-C(9)	123.8(2)
C(17)-N(41)	1.353(3)	C(7)-C(8)-H(8)	118.1
C(17)-C(18)	1.373(3)	C(9)-C(8)-H(8)	118.1
C(18)-C(19)	1.435(4)	O(22)-C(9)-C(8)	122.8(2)
C(18)-H(18)	0.9500	O(22)-C(9)-C(10)	118.2(2)
C(19)-O(42)	1.244(3)	C(8)-C(9)-C(10)	118.9(2)
C(19)-C(20)	1.515(3)	C(9)-C(10)-H(10A)	109.5
C(20)-H(20A)	0.9800	C(9)-C(10)-H(10B)	109.5
C(20)-H(20B)	0.9800	H(10A)-C(10)-H(10B)	109.5
C(20)-H(20C)	0.9800	C(9)-C(10)-H(10C)	109.5
C(111)-C(116)	1.386(3)	H(10A)-C(10)-H(10C)	109.5
C(111)-C(112)	1.387(3)	H(10B)-C(10)-H(10C)	109.5

Appendix A

C(111)-N(11)	1.423(3)	C(9)-C(10)-H(10D)	109.5
C(112)-C(113)	1.383(3)	H(10A)-C(10)-H(10D)	141.1
C(112)-H(112)	0.9500	H(10B)-C(10)-H(10D)	56.3
C(113)-C(114)	1.388(4)	H(10C)-C(10)-H(10D)	56.3
C(113)-H(113)	0.9500	C(9)-C(10)-H(10E)	109.5
C(114)-C(115)	1.381(4)	H(10A)-C(10)-H(10E)	56.3
C(114)-Cl(14)	1.740(2)	H(10B)-C(10)-H(10E)	141.1
C(115)-C(116)	1.387(3)	H(10C)-C(10)-H(10E)	56.3
C(115)-H(115)	0.9500	H(10D)-C(10)-H(10E)	109.5
C(116)-H(116)	0.9500	C(9)-C(10)-H(10F)	109.5
C(211)-C(216)	1.385(4)	H(10A)-C(10)-H(10F)	56.3
C(211)-C(212)	1.395(3)	H(10B)-C(10)-H(10F)	56.3
C(211)-N(21)	1.419(3)	H(10C)-C(10)-H(10F)	141.1
C(212)-C(213)	1.395(3)	H(10D)-C(10)-H(10F)	109.5
C(212)-H(212)	0.9500	H(10E)-C(10)-H(10F)	109.5
C(213)-C(214)	1.376(4)	C(12)-C(11)-H(11A)	109.5
C(213)-H(213)	0.9500	C(12)-C(11)-H(11B)	109.5
C(214)-C(215)	1.388(4)	H(11A)-C(11)-H(11B)	109.5
C(214)-Cl(24)	1.744(3)	C(12)-C(11)-H(11C)	109.5
C(215)-C(216)	1.375(4)	H(11A)-C(11)-H(11C)	109.5
C(215)-H(215)	0.9500	H(11B)-C(11)-H(11C)	109.5
C(216)-H(216)	0.9500	C(12)-C(11)-H(11D)	109.5
C(311)-C(316)	1.394(3)	H(11A)-C(11)-H(11D)	141.1
C(311)-C(312)	1.397(3)	H(11B)-C(11)-H(11D)	56.3
C(311)-N(31)	1.407(3)	H(11C)-C(11)-H(11D)	56.3
C(312)-C(313)	1.387(4)	C(12)-C(11)-H(11E)	109.5
C(312)-H(312)	0.9500	H(11A)-C(11)-H(11E)	56.3
C(313)-C(314)	1.381(4)	H(11B)-C(11)-H(11E)	141.1
C(313)-H(313)	0.9500	H(11C)-C(11)-H(11E)	56.3
C(314)-C(315)	1.377(4)	H(11D)-C(11)-H(11E)	109.5
C(314)-Cl(34)	1.738(3)	C(12)-C(11)-H(11F)	109.5
C(315)-C(316)	1.394(4)	H(11A)-C(11)-H(11F)	56.3
C(315)-H(315)	0.9500	H(11B)-C(11)-H(11F)	56.3
C(316)-H(316)	0.9500	H(11C)-C(11)-H(11F)	141.1
C(411)-C(416)	1.389(3)	H(11D)-C(11)-H(11F)	109.5
C(411)-C(412)	1.392(3)	H(11E)-C(11)-H(11F)	109.5
C(411)-N(41)	1.421(3)	N(31)-C(12)-C(13)	119.4(2)
C(412)-C(413)	1.381(3)	N(31)-C(12)-C(11)	120.8(2)

Appendix A

C(412)-H(412)	0.9500	C(13)-C(12)-C(11)	119.8(2)
C(413)-C(414)	1.389(4)	C(12)-C(13)-C(14)	124.0(2)
C(413)-H(413)	0.9500	C(12)-C(13)-H(13)	118.0
C(414)-C(415)	1.377(4)	C(14)-C(13)-H(13)	118.0
C(414)-Cl(44)	1.742(2)	O(32)-C(14)-C(13)	123.7(2)
C(415)-C(416)	1.390(4)	O(32)-C(14)-C(15)	117.8(2)
C(415)-H(415)	0.9500	C(13)-C(14)-C(15)	118.5(2)
C(416)-H(416)	0.9500	C(14)-C(15)-H(15A)	109.5
N(11)-H(11)	0.8800	C(14)-C(15)-H(15B)	109.5
N(21)-H(12)	0.8800	H(15A)-C(15)-H(15B)	109.5
N(31)-H(31)	0.8800	C(14)-C(15)-H(15C)	109.5
N(41)-H(41)	0.8800	H(15A)-C(15)-H(15C)	109.5
		H(15B)-C(15)-H(15C)	109.5
		C(14)-C(15)-H(15D)	109.5
		H(15A)-C(15)-H(15D)	141.1
		H(15B)-C(15)-H(15D)	56.3
		H(15C)-C(15)-H(15D)	56.3
		C(14)-C(15)-H(15E)	109.5
		H(15A)-C(15)-H(15E)	56.3
		H(15B)-C(15)-H(15E)	141.1
		H(15C)-C(15)-H(15E)	56.3
		H(15D)-C(15)-H(15E)	109.5
		C(14)-C(15)-H(15F)	109.5
		H(15A)-C(15)-H(15F)	56.3
		H(15B)-C(15)-H(15F)	56.3
		H(15C)-C(15)-H(15F)	141.1
		H(15D)-C(15)-H(15F)	109.5
		H(15E)-C(15)-H(15F)	109.5
		C(17)-C(16)-H(16A)	109.5
		C(17)-C(16)-H(16B)	109.5
		H(16A)-C(16)-H(16B)	109.5
		C(17)-C(16)-H(16C)	109.5
		H(16A)-C(16)-H(16C)	109.5
		H(16B)-C(16)-H(16C)	109.5
		C(17)-C(16)-H(16D)	109.5
		H(16A)-C(16)-H(16D)	141.1
		H(16B)-C(16)-H(16D)	56.3
		H(16C)-C(16)-H(16D)	56.3

Appendix A

C(17)-C(16)-H(16E)	109.5
H(16A)-C(16)-H(16E)	56.3
H(16B)-C(16)-H(16E)	141.1
H(16C)-C(16)-H(16E)	56.3
H(16D)-C(16)-H(16E)	109.5
C(17)-C(16)-H(16F)	109.5
H(16A)-C(16)-H(16F)	56.3
H(16B)-C(16)-H(16F)	56.3
H(16C)-C(16)-H(16F)	141.1
H(16D)-C(16)-H(16F)	109.5
H(16E)-C(16)-H(16F)	109.5
N(41)-C(17)-C(18)	121.3(2)
N(41)-C(17)-C(16)	118.9(2)
C(18)-C(17)-C(16)	119.8(2)
C(17)-C(18)-C(19)	124.6(2)
C(17)-C(18)-H(18)	117.7
C(19)-C(18)-H(18)	117.7
O(42)-C(19)-C(18)	122.6(2)
O(42)-C(19)-C(20)	120.1(2)
C(18)-C(19)-C(20)	117.3(2)
C(19)-C(20)-H(20A)	109.5
C(19)-C(20)-H(20B)	109.5
H(20A)-C(20)-H(20B)	109.5
C(19)-C(20)-H(20C)	109.5
H(20A)-C(20)-H(20C)	109.5
H(20B)-C(20)-H(20C)	109.5
C(116)-C(111)-C(112)	119.7(2)
C(116)-C(111)-N(11)	121.7(2)
C(112)-C(111)-N(11)	118.5(2)
C(113)-C(112)-C(111)	120.7(2)
C(113)-C(112)-H(112)	119.7
C(111)-C(112)-H(112)	119.7
C(112)-C(113)-C(114)	118.7(2)
C(112)-C(113)-H(113)	120.7
C(114)-C(113)-H(113)	120.7
C(115)-C(114)-C(113)	121.6(2)
C(115)-C(114)-Cl(14)	118.9(2)
C(113)-C(114)-Cl(14)	119.4(2)

Appendix A

C(114)-C(115)-C(116)	118.9(2)
C(114)-C(115)-H(115)	120.5
C(116)-C(115)-H(115)	120.5
C(111)-C(116)-C(115)	120.4(2)
C(111)-C(116)-H(116)	119.8
C(115)-C(116)-H(116)	119.8
C(216)-C(211)-C(212)	119.2(2)
C(216)-C(211)-N(21)	118.2(2)
C(212)-C(211)-N(21)	122.4(2)
C(213)-C(212)-C(211)	120.1(2)
C(213)-C(212)-H(212)	119.9
C(211)-C(212)-H(212)	119.9
C(214)-C(213)-C(212)	119.3(2)
C(214)-C(213)-H(213)	120.3
C(212)-C(213)-H(213)	120.3
C(213)-C(214)-C(215)	120.9(2)
C(213)-C(214)-Cl(24)	119.55(19)
C(215)-C(214)-Cl(24)	119.6(2)
C(216)-C(215)-C(214)	119.5(2)
C(216)-C(215)-H(215)	120.2
C(214)-C(215)-H(215)	120.2
C(215)-C(216)-C(211)	120.8(2)
C(215)-C(216)-H(216)	119.6
C(211)-C(216)-H(216)	119.6
C(316)-C(311)-C(312)	119.3(2)
C(316)-C(311)-N(31)	123.5(2)
C(312)-C(311)-N(31)	117.0(2)
C(313)-C(312)-C(311)	120.5(2)
C(313)-C(312)-H(312)	119.8
C(311)-C(312)-H(312)	119.8
C(314)-C(313)-C(312)	119.3(2)
C(314)-C(313)-H(313)	120.4
C(312)-C(313)-H(313)	120.4
C(315)-C(314)-C(313)	121.3(2)
C(315)-C(314)-Cl(34)	119.9(2)
C(313)-C(314)-Cl(34)	118.8(2)
C(314)-C(315)-C(316)	119.6(2)
C(314)-C(315)-H(315)	120.2

Appendix A

C(316)-C(315)-H(315)	120.2
C(311)-C(316)-C(315)	120.0(2)
C(311)-C(316)-H(316)	120.0
C(315)-C(316)-H(316)	120.0
C(416)-C(411)-C(412)	119.3(2)
C(416)-C(411)-N(41)	119.0(2)
C(412)-C(411)-N(41)	121.6(2)
C(413)-C(412)-C(411)	120.7(2)
C(413)-C(412)-H(412)	119.7
C(411)-C(412)-H(412)	119.7
C(412)-C(413)-C(414)	119.1(2)
C(412)-C(413)-H(413)	120.4
C(414)-C(413)-H(413)	120.4
C(415)-C(414)-C(413)	121.2(2)
C(415)-C(414)-Cl(44)	119.5(2)
C(413)-C(414)-Cl(44)	119.31(19)
C(414)-C(415)-C(416)	119.2(2)
C(414)-C(415)-H(415)	120.4
C(416)-C(415)-H(415)	120.4
C(411)-C(416)-C(415)	120.5(2)
C(411)-C(416)-H(416)	119.8
C(415)-C(416)-H(416)	119.8
C(2)-N(11)-C(111)	126.4(2)
C(2)-N(11)-H(11)	116.8
C(111)-N(11)-H(11)	116.8
C(7)-N(21)-C(211)	129.4(2)
C(7)-N(21)-H(12)	115.3
C(211)-N(21)-H(12)	115.3
C(12)-N(31)-C(311)	130.0(2)
C(12)-N(31)-H(31)	115.0
C(311)-N(31)-H(31)	115.0
C(17)-N(41)-C(411)	126.6(2)
C(17)-N(41)-H(41)	116.7
C(411)-N(41)-H(41)	116.7

Appendix A

Table A.9. Anisotropic displacement parameters ($\text{\AA}^2 \times 10^3$) for 4-Cl-PhonyH. The anisotropic displacement factor exponent takes the form: $-2\pi^2 [h^2 a^{*2} U^{11} + \dots + 2 h k a^* b^* U^{12}]$.

	U^{11}	U^{22}	U^{33}	U^{23}	U^{13}	U^{12}
C(1)	21(1)	21(1)	23(1)	-3(1)	4(1)	-2(1)
C(2)	16(1)	13(1)	18(1)	4(1)	1(1)	0(1)
C(3)	20(1)	15(1)	18(1)	-3(1)	-1(1)	-3(1)
C(4)	22(1)	15(1)	19(1)	1(1)	1(1)	2(1)
C(5)	29(1)	24(1)	21(1)	-8(1)	8(1)	-3(1)
C(6)	24(1)	18(1)	27(1)	-1(1)	4(1)	-4(1)
C(7)	15(1)	14(1)	22(1)	2(1)	-1(1)	2(1)
C(8)	22(1)	16(1)	22(1)	4(1)	3(1)	-1(1)
C(9)	16(1)	21(1)	21(1)	1(1)	3(1)	0(1)
C(10)	34(2)	25(1)	21(1)	-1(1)	7(1)	-7(1)
C(11)	27(1)	18(1)	26(1)	1(1)	2(1)	-2(1)
C(12)	15(1)	18(1)	20(1)	5(1)	-2(1)	2(1)
C(13)	18(1)	21(1)	21(1)	4(1)	3(1)	-3(1)
C(14)	16(1)	22(1)	21(1)	1(1)	4(1)	1(1)
C(15)	38(2)	36(2)	22(1)	0(1)	13(1)	-7(1)
C(16)	21(1)	23(1)	27(1)	-5(1)	8(1)	-9(1)
C(17)	18(1)	16(1)	16(1)	3(1)	-1(1)	1(1)
C(18)	17(1)	19(1)	24(1)	0(1)	4(1)	-3(1)
C(19)	20(1)	15(1)	18(1)	3(1)	2(1)	1(1)
C(20)	24(1)	22(1)	23(1)	-1(1)	5(1)	-2(1)
C(111)	18(1)	11(1)	16(1)	1(1)	4(1)	-3(1)
C(112)	19(1)	16(1)	22(1)	-2(1)	6(1)	-2(1)
C(113)	20(1)	22(1)	19(1)	-3(1)	3(1)	-3(1)
C(114)	29(1)	16(1)	17(1)	-5(1)	10(1)	-8(1)
C(115)	24(1)	15(1)	27(1)	1(1)	11(1)	2(1)
C(116)	18(1)	16(1)	16(1)	2(1)	3(1)	-1(1)
C(211)	15(1)	18(1)	17(1)	-2(1)	1(1)	-1(1)
C(212)	18(1)	17(1)	18(1)	3(1)	2(1)	1(1)
C(213)	21(1)	18(1)	21(1)	-1(1)	2(1)	4(1)
C(214)	18(1)	26(1)	16(1)	-3(1)	3(1)	-3(1)
C(215)	23(1)	21(1)	25(1)	5(1)	5(1)	0(1)
C(216)	22(1)	14(1)	30(1)	-1(1)	5(1)	2(1)
C(311)	14(1)	18(1)	16(1)	-2(1)	-1(1)	-1(1)
C(312)	22(1)	16(1)	25(1)	-3(1)	6(1)	-1(1)

Appendix A

C(313)	30(2)	15(1)	27(1)	-2(1)	6(1)	-2(1)
C(314)	18(1)	25(1)	20(1)	-7(1)	6(1)	-5(1)
C(315)	20(1)	18(1)	26(1)	-6(1)	2(1)	2(1)
C(316)	21(1)	17(1)	26(1)	2(1)	-1(1)	4(1)
C(411)	18(1)	13(1)	19(1)	0(1)	6(1)	-5(1)
C(412)	15(1)	17(1)	21(1)	5(1)	1(1)	0(1)
C(413)	20(1)	15(1)	19(1)	5(1)	3(1)	1(1)
C(414)	24(1)	20(1)	16(1)	-1(1)	8(1)	-4(1)
C(415)	19(1)	27(2)	16(1)	-1(1)	0(1)	1(1)
C(416)	14(1)	24(1)	24(1)	1(1)	3(1)	3(1)
N(11)	16(1)	17(1)	16(1)	-2(1)	5(1)	0(1)
N(21)	19(1)	14(1)	24(1)	-3(1)	6(1)	-1(1)
N(31)	18(1)	16(1)	21(1)	-4(1)	2(1)	0(1)
N(41)	17(1)	17(1)	20(1)	0(1)	5(1)	-3(1)
O(12)	23(1)	23(1)	21(1)	-5(1)	5(1)	-5(1)
O(22)	25(1)	18(1)	26(1)	-3(1)	10(1)	-5(1)
O(32)	28(1)	21(1)	26(1)	-3(1)	11(1)	-4(1)
O(42)	19(1)	22(1)	24(1)	-4(1)	5(1)	-5(1)
Cl(14)	42(1)	29(1)	24(1)	-11(1)	13(1)	-3(1)
Cl(24)	30(1)	33(1)	21(1)	-1(1)	9(1)	-1(1)
Cl(34)	34(1)	33(1)	27(1)	-9(1)	16(1)	-3(1)
Cl(44)	31(1)	29(1)	20(1)	-5(1)	7(1)	2(1)

Appendix A

Table A.10. Hydrogen coordinates ($\times 10^4$) and isotropic displacement parameters ($\text{\AA}^2 \times 10^3$) for 4-Cl-PhonyH.

	x	y	z	U(eq)
H(1A)	9307	-594	4105	32
H(1B)	9866	-354	4837	32
H(1C)	9312	438	4376	32
H(1D)	9683	254	4774	32
H(1E)	9124	14	4042	32
H(1F)	9678	-778	4503	32
H(3)	8734	450	5541	22
H(5A)	7236	180	6562	36
H(5B)	6722	958	6069	36
H(5C)	7867	961	6295	36
H(6A)	5423	419	3779	34
H(6B)	4427	439	4045	34
H(6C)	5348	-54	4474	34
H(6D)	4709	117	4420	34
H(6E)	5705	97	4154	34
H(6F)	4784	590	3725	34
H(8)	4689	1126	5267	24
H(10A)	5149	3132	6294	39
H(10B)	5193	2045	6419	39
H(10C)	4234	2504	6014	39
H(10D)	4568	1989	6191	39
H(10E)	4525	3076	6065	39
H(10F)	5483	2616	6471	39
H(11A)	7040	7097	5813	36
H(11B)	7074	7569	5112	36
H(11C)	8016	7088	5522	36
H(11D)	7714	7406	5152	36
H(11E)	7680	6933	5853	36
H(11F)	6737	7415	5443	36
H(13)	7707	6398	4299	24
H(15A)	7227	4406	3271	47
H(15B)	8137	5049	3531	47
H(15C)	7152	5493	3153	47
H(15D)	7784	5559	3365	47

Appendix A

H(15E)	6874	4916	3106	47
H(15F)	7859	4472	3483	47
H(16A)	3111	8094	5584	35
H(16B)	3119	7060	5317	35
H(16C)	2567	7847	4849	35
H(16D)	2753	7240	4916	35
H(16E)	2746	8274	5183	35
H(16F)	3298	7486	5651	35
H(18)	3737	7025	4172	24
H(20A)	4710	7194	3110	35
H(20B)	4993	6334	3595	35
H(20C)	5814	7003	3426	35
H(112)	6527	-1078	3344	22
H(113)	6578	-1911	2375	24
H(115)	9197	-2919	3212	25
H(116)	9130	-2086	4181	21
H(212)	6895	526	3890	22
H(213)	7726	430	2998	24
H(215)	7072	3092	2545	27
H(216)	6207	3171	3404	26
H(312)	6283	4273	6136	25
H(313)	5521	4285	7058	29
H(315)	4874	6977	6743	26
H(316)	5618	6969	5808	26
H(412)	3236	9587	5453	21
H(413)	3110	10487	6376	22
H(415)	5748	9624	7287	25
H(416)	5855	8696	6368	25
H(11)	7227	-1084	4603	24
H(12)	6023	2503	4461	28
H(31)	6378	5030	5109	27
H(41)	5204	8600	5104	27

Appendix A

Table A.11. Torsion angles [°] for 4-Cl-PhonyH.

Atoms	Angles (°)
N(11)-C(2)-C(3)-C(4)	-1.2(4)
C(1)-C(2)-C(3)-C(4)	175.1(2)
C(2)-C(3)-C(4)-O(12)	3.0(4)
C(2)-C(3)-C(4)-C(5)	-176.2(2)
N(21)-C(7)-C(8)-C(9)	-2.0(4)
C(6)-C(7)-C(8)-C(9)	-178.9(2)
C(7)-C(8)-C(9)-O(22)	4.0(4)
C(7)-C(8)-C(9)-C(10)	-177.5(2)
N(31)-C(12)-C(13)-C(14)	-0.1(4)
C(11)-C(12)-C(13)-C(14)	178.9(2)
C(12)-C(13)-C(14)-O(32)	-3.5(4)
C(12)-C(13)-C(14)-C(15)	176.7(2)
N(41)-C(17)-C(18)-C(19)	-0.6(4)
C(16)-C(17)-C(18)-C(19)	-178.3(2)
C(17)-C(18)-C(19)-O(42)	-1.4(4)
C(17)-C(18)-C(19)-C(20)	177.4(2)
C(116)-C(111)-C(112)-C(113)	-0.7(4)
N(11)-C(111)-C(112)-C(113)	-178.0(2)
C(111)-C(112)-C(113)-C(114)	0.5(4)
C(112)-C(113)-C(114)-C(115)	-0.4(4)
C(112)-C(113)-C(114)-Cl(14)	179.9(2)
C(113)-C(114)-C(115)-C(116)	0.6(4)
Cl(14)-C(114)-C(115)-C(116)	-179.71(19)
C(112)-C(111)-C(116)-C(115)	0.9(4)
N(11)-C(111)-C(116)-C(115)	178.1(2)
C(114)-C(115)-C(116)-C(111)	-0.8(4)
C(216)-C(211)-C(212)-C(213)	-2.2(4)
N(21)-C(211)-C(212)-C(213)	-177.7(2)
C(211)-C(212)-C(213)-C(214)	1.1(4)
C(212)-C(213)-C(214)-C(215)	1.1(4)
C(212)-C(213)-C(214)-Cl(24)	-179.62(19)
C(213)-C(214)-C(215)-C(216)	-2.2(4)
Cl(24)-C(214)-C(215)-C(216)	178.5(2)
C(214)-C(215)-C(216)-C(211)	1.1(4)
C(212)-C(211)-C(216)-C(215)	1.0(4)

Appendix A

N(21)-C(211)-C(216)-C(215)	176.7(2)
C(316)-C(311)-C(312)-C(313)	-1.3(4)
N(31)-C(311)-C(312)-C(313)	-177.3(2)
C(311)-C(312)-C(313)-C(314)	0.3(4)
C(312)-C(313)-C(314)-C(315)	0.2(4)
C(312)-C(313)-C(314)-Cl(34)	-179.2(2)
C(313)-C(314)-C(315)-C(316)	0.3(4)
Cl(34)-C(314)-C(315)-C(316)	179.70(19)
C(312)-C(311)-C(316)-C(315)	1.8(4)
N(31)-C(311)-C(316)-C(315)	177.5(2)
C(314)-C(315)-C(316)-C(311)	-1.2(4)
C(416)-C(411)-C(412)-C(413)	-0.5(4)
N(41)-C(411)-C(412)-C(413)	-177.2(2)
C(411)-C(412)-C(413)-C(414)	1.1(4)
C(412)-C(413)-C(414)-C(415)	-1.1(4)
C(412)-C(413)-C(414)-Cl(44)	177.64(18)
C(413)-C(414)-C(415)-C(416)	0.4(4)
Cl(44)-C(414)-C(415)-C(416)	-178.4(2)
C(412)-C(411)-C(416)-C(415)	-0.3(4)
N(41)-C(411)-C(416)-C(415)	176.6(2)
C(414)-C(415)-C(416)-C(411)	0.3(4)
C(3)-C(2)-N(11)-C(111)	178.3(2)
C(1)-C(2)-N(11)-C(111)	2.0(3)
C(116)-C(111)-N(11)-C(2)	54.0(3)
C(112)-C(111)-N(11)-C(2)	-128.8(3)
C(8)-C(7)-N(21)-C(211)	173.2(2)
C(6)-C(7)-N(21)-C(211)	-9.9(4)
C(216)-C(211)-N(21)-C(7)	145.7(3)
C(212)-C(211)-N(21)-C(7)	-38.7(4)
C(13)-C(12)-N(31)-C(311)	-176.2(2)
C(11)-C(12)-N(31)-C(311)	4.8(4)
C(316)-C(311)-N(31)-C(12)	39.5(4)
C(312)-C(311)-N(31)-C(12)	-144.8(3)
C(18)-C(17)-N(41)-C(411)	178.7(2)
C(16)-C(17)-N(41)-C(411)	-3.5(4)
C(416)-C(411)-N(41)-C(17)	130.6(3)
C(412)-C(411)-N(41)-C(17)	-52.6(4)

Appendix A

Table A.12. Hydrogen bonds for 4-Cl-PhonyH [\AA and $^\circ$].

D-H...A	d(D-H)	d(H...A)	d(D...A)	<(DHA)
N(11)-H(11)...O(12)	0.88	1.98	2.675(3)	134.5
N(21)-H(12)...O(22)	0.88	1.91	2.620(3)	137.1
N(31)-H(31)...O(32)	0.88	1.91	2.634(3)	139.0
N(41)-H(41)...O(42)	0.88	1.99	2.678(3)	134.2
C(6)-H(6C)...O(12)	0.98	2.51	3.341(3)	142.0
C(11)-H(11B)...O(42)	0.98	2.42	3.266(3)	143.9
C(312)-H(312)...O(22)	0.95	2.54	3.287(3)	135.2
N(11)-H(11)...O(42) ⁱⁱⁱ	0.88	2.42	3.136(3)	139.0
N(41)-H(41)...O(12) ^{iv}	0.88	2.44	3.164(3)	140.1

Symmetry operators: iii) $x, y - 1, z$ iv) $x, y + 1, z$

A.3. 4-(2,4-Dichlorophenylamino)pent-3-en-2-one (2,4-Cl₂-PhonyH)

Table A.13. Atomic coordinates ($\times 10^4$) and equivalent isotropic displacement parameters ($\text{\AA}^2 \times 10^3$) for 2,4-Cl₂-PhonyH. $U(\text{eq})$ is defined as one third of the trace of the orthogonalized U_{ij} tensor.

	x	y	z	U(eq)
C(5)	6543(3)	6750(2)	10868(1)	24(1)
C(4)	6424(3)	6959(2)	9786(1)	18(1)
C(3)	6032(3)	8123(2)	9430(1)	17(1)
C(2)	5790(3)	8400(2)	8462(1)	16(1)
C(1)	5262(3)	9621(2)	8157(1)	20(1)
C(10)	240(3)	8122(2)	4131(1)	25(1)
C(9)	516(3)	7937(2)	5216(1)	19(1)
C(8)	-204(3)	6767(2)	5607(1)	18(1)
C(7)	-89(3)	6510(2)	6584(1)	16(1)
C(6)	-977(3)	5282(2)	6946(1)	21(1)
C(111)	5765(3)	7661(2)	6755(1)	15(1)
C(112)	4855(3)	6654(2)	6187(1)	17(1)
C(113)	4650(3)	6694(2)	5183(1)	18(1)
C(114)	5373(3)	7770(2)	4732(1)	19(1)
C(115)	6310(3)	8783(2)	5260(1)	18(1)
C(116)	6519(3)	8715(2)	6270(1)	18(1)
C(211)	1009(3)	7340(2)	8249(1)	15(1)
C(212)	879(3)	8389(2)	8807(1)	16(1)

Appendix A

C(213)	1116(3)	8400(2)	9815(1)	17(1)
C(214)	1488(3)	7337(2)	10276(1)	17(1)
C(215)	1690(3)	6292(2)	9760(1)	18(1)
C(216)	1468(3)	6309(2)	8750(1)	17(1)
N(11)	5973(2)	7557(1)	7772(1)	17(1)
N(21)	779(2)	7387(1)	7231(1)	17(1)
O(12)	6652(2)	6099(1)	9229(1)	22(1)
O(22)	1344(2)	8821(1)	5737(1)	22(1)
Cl(12)	3992(1)	5278(1)	6743(1)	20(1)
Cl(14)	5118(1)	7838(1)	3464(1)	25(1)
Cl(22)	435(1)	9733(1)	8225(1)	19(1)
Cl(24)	1754(1)	7328(1)	11547(1)	23(1)

Table A.14. Bond lengths [\AA] and angles [$^\circ$] for 2,4-Cl₂-PhonyH.

Atoms	Bond lengths (\AA)	Atoms	Angles ($^\circ$)
C(5)-C(4)	1.505(3)	C(4)-C(5)-H(5A)	109.5
C(5)-H(5A)	0.9800	C(4)-C(5)-H(5B)	109.5
C(5)-H(5B)	0.9800	H(5A)-C(5)-H(5B)	109.5
C(5)-H(5C)	0.9800	C(4)-C(5)-H(5C)	109.5
C(4)-O(12)	1.253(2)	H(5A)-C(5)-H(5C)	109.5
C(4)-C(3)	1.428(2)	H(5B)-C(5)-H(5C)	109.5
C(3)-C(2)	1.371(3)	O(12)-C(4)-C(3)	122.42(17)
C(3)-H(3)	0.9500	O(12)-C(4)-C(5)	118.79(17)
C(2)-N(11)	1.352(2)	C(3)-C(4)-C(5)	118.79(17)
C(2)-C(1)	1.500(2)	C(2)-C(3)-C(4)	124.28(18)
C(1)-H(1A)	0.9800	C(2)-C(3)-H(3)	117.9
C(1)-H(1B)	0.9800	C(4)-C(3)-H(3)	117.9
C(1)-H(1C)	0.9800	N(11)-C(2)-C(3)	120.05(17)
C(10)-C(9)	1.508(3)	N(11)-C(2)-C(1)	119.42(17)
C(10)-H(10A)	0.9800	C(3)-C(2)-C(1)	120.50(17)
C(10)-H(10B)	0.9800	C(2)-C(1)-H(1A)	109.5
C(10)-H(10C)	0.9800	C(2)-C(1)-H(1B)	109.5
C(9)-O(22)	1.249(2)	H(1A)-C(1)-H(1B)	109.5
C(9)-C(8)	1.427(3)	C(2)-C(1)-H(1C)	109.5
C(8)-C(7)	1.372(3)	H(1A)-C(1)-H(1C)	109.5
C(8)-H(8)	0.9500	H(1B)-C(1)-H(1C)	109.5

Appendix A

C(7)-N(21)	1.353(2)	C(9)-C(10)-H(10A)	109.5
C(7)-C(6)	1.501(2)	C(9)-C(10)-H(10B)	109.5
C(6)-H(6A)	0.9800	H(10A)-C(10)-H(10B)	109.5
C(6)-H(6B)	0.9800	C(9)-C(10)-H(10C)	109.5
C(6)-H(6C)	0.9800	H(10A)-C(10)-H(10C)	109.5
C(111)-C(116)	1.392(2)	H(10B)-C(10)-H(10C)	109.5
C(111)-C(112)	1.396(3)	O(22)-C(9)-C(8)	122.66(17)
C(111)-N(11)	1.403(2)	O(22)-C(9)-C(10)	118.52(17)
C(112)-C(113)	1.379(3)	C(8)-C(9)-C(10)	118.81(18)
C(112)-Cl(12)	1.7409(18)	C(7)-C(8)-C(9)	123.77(18)
C(113)-C(114)	1.382(2)	C(7)-C(8)-H(8)	118.1
C(113)-H(113)	0.9500	C(9)-C(8)-H(8)	118.1
C(114)-C(115)	1.380(3)	N(21)-C(7)-C(8)	119.70(17)
C(114)-Cl(14)	1.7427(19)	N(21)-C(7)-C(6)	119.57(17)
C(115)-C(116)	1.388(3)	C(8)-C(7)-C(6)	120.70(18)
C(115)-H(115)	0.9500	C(7)-C(6)-H(6A)	109.5
C(116)-H(116)	0.9500	C(7)-C(6)-H(6B)	109.5
C(211)-C(216)	1.396(2)	H(6A)-C(6)-H(6B)	109.5
C(211)-N(21)	1.399(2)	C(7)-C(6)-H(6C)	109.5
C(211)-C(212)	1.400(3)	H(6A)-C(6)-H(6C)	109.5
C(212)-C(213)	1.384(3)	H(6B)-C(6)-H(6C)	109.5
C(212)-Cl(22)	1.7378(18)	C(116)-C(111)-C(112)	117.54(17)
C(213)-C(214)	1.380(2)	C(116)-C(111)-N(11)	122.73(17)
C(213)-H(213)	0.9500	C(112)-C(111)-N(11)	119.64(16)
C(214)-C(215)	1.380(3)	C(113)-C(112)-C(111)	122.14(17)
C(214)-Cl(24)	1.7433(19)	C(113)-C(112)-Cl(12)	117.90(15)
C(215)-C(216)	1.386(3)	C(111)-C(112)-Cl(12)	119.94(14)
C(215)-H(215)	0.9500	C(112)-C(113)-C(114)	118.44(18)
C(216)-H(216)	0.9500	C(112)-C(113)-H(113)	120.8
N(11)-H(11)	0.86(2)	C(114)-C(113)-H(113)	120.8
N(21)-H(21)	0.90(2)	C(113)-C(114)-C(115)	121.56(18)
		C(113)-C(114)-Cl(14)	119.04(16)
		C(115)-C(114)-Cl(14)	119.40(14)
		C(114)-C(115)-C(116)	118.89(17)
		C(114)-C(115)-H(115)	120.6
		C(116)-C(115)-H(115)	120.6
		C(115)-C(116)-C(111)	121.38(18)
		C(115)-C(116)-H(116)	119.3

Appendix A

C(111)-C(116)-H(116)	119.3
C(216)-C(211)-N(21)	123.19(17)
C(216)-C(211)-C(212)	117.10(17)
N(21)-C(211)-C(212)	119.61(16)
C(213)-C(212)-C(211)	122.10(16)
C(213)-C(212)-Cl(22)	118.37(14)
C(211)-C(212)-Cl(22)	119.52(14)
C(214)-C(213)-C(212)	118.35(17)
C(214)-C(213)-H(213)	120.8
C(212)-C(213)-H(213)	120.8
C(213)-C(214)-C(215)	121.84(17)
C(213)-C(214)-Cl(24)	118.92(15)
C(215)-C(214)-Cl(24)	119.23(14)
C(214)-C(215)-C(216)	118.65(17)
C(214)-C(215)-H(215)	120.7
C(216)-C(215)-H(215)	120.7
C(215)-C(216)-C(211)	121.85(18)
C(215)-C(216)-H(216)	119.1
C(211)-C(216)-H(216)	119.1
C(2)-N(11)-C(111)	128.50(16)
C(2)-N(11)-H(11)	111.9(16)
C(111)-N(11)-H(11)	119.6(16)
C(7)-N(21)-C(211)	129.29(16)
C(7)-N(21)-H(21)	113.1(15)
C(211)-N(21)-H(21)	117.4(15)

Appendix A

Table A.15. Anisotropic displacement parameters ($\text{\AA}^2 \times 10^3$) for 2,4-Cl₂-PhonyH. The anisotropic displacement factor exponent takes the form: $-2\pi^2 [h^2 a^{*2} U^{11} + \dots + 2 h k a^* b^* U^{12}]$

	U ¹¹	U ²²	U ³³	U ²³	U ¹³	U ¹²
C(5)	29(1)	29(1)	16(1)	7(1)	1(1)	5(1)
C(4)	14(1)	23(1)	15(1)	6(1)	0(1)	0(1)
C(3)	19(1)	17(1)	15(1)	0(1)	1(1)	1(1)
C(2)	14(1)	17(1)	17(1)	3(1)	2(1)	1(1)
C(1)	22(1)	19(1)	20(1)	4(1)	4(1)	6(1)
C(10)	30(1)	30(1)	16(1)	7(1)	3(1)	8(1)
C(9)	20(1)	23(1)	15(1)	4(1)	2(1)	8(1)
C(8)	18(1)	20(1)	17(1)	1(1)	-1(1)	4(1)
C(7)	17(1)	17(1)	17(1)	3(1)	2(1)	6(1)
C(6)	20(1)	19(1)	21(1)	4(1)	-2(1)	-1(1)
C(111)	16(1)	18(1)	12(1)	4(1)	0(1)	5(1)
C(112)	16(1)	16(1)	19(1)	7(1)	4(1)	5(1)
C(113)	16(1)	20(1)	17(1)	2(1)	0(1)	4(1)
C(114)	19(1)	26(1)	12(1)	5(1)	-1(1)	7(1)
C(115)	19(1)	19(1)	18(1)	8(1)	3(1)	4(1)
C(116)	19(1)	16(1)	18(1)	3(1)	1(1)	3(1)
C(211)	15(1)	19(1)	11(1)	3(1)	2(1)	1(1)
C(212)	15(1)	16(1)	17(1)	7(1)	2(1)	3(1)
C(213)	16(1)	18(1)	16(1)	1(1)	1(1)	2(1)
C(214)	16(1)	22(1)	12(1)	6(1)	0(1)	1(1)
C(215)	19(1)	18(1)	17(1)	7(1)	0(1)	1(1)
C(216)	20(1)	16(1)	15(1)	3(1)	1(1)	3(1)
N(11)	22(1)	15(1)	13(1)	5(1)	-1(1)	4(1)
N(21)	21(1)	16(1)	13(1)	5(1)	2(1)	2(1)
O(12)	30(1)	21(1)	17(1)	5(1)	2(1)	7(1)
O(22)	28(1)	20(1)	17(1)	6(1)	2(1)	2(1)
Cl(12)	26(1)	16(1)	18(1)	5(1)	5(1)	1(1)
Cl(14)	33(1)	29(1)	12(1)	6(1)	-2(1)	7(1)
Cl(22)	25(1)	17(1)	16(1)	5(1)	0(1)	6(1)
Cl(24)	32(1)	24(1)	13(1)	6(1)	-2(1)	2(1)

Appendix A

Table A.16. Hydrogen coordinates ($\times 10^4$) and isotropic displacement parameters ($\text{\AA}^2 \times 10^3$) for 2,4-Cl₂-PhonyH.

	x	y	z	U(eq)
H(11)	6200(30)	6870(20)	8026(17)	36(7)
H(21)	1180(30)	8110(20)	6952(17)	32(6)
H(5A)	5694	6000	11012	37
H(5B)	6210	7464	11202	37
H(5C)	7803	6651	11096	37
H(3)	5933	8746	9895	21
H(1A)	6359	10186	7992	30
H(1B)	4716	9979	8693	30
H(1C)	4365	9494	7585	30
H(10A)	-159	8925	4007	38
H(10B)	-702	7458	3843	38
H(10C)	1400	8104	3838	38
H(8)	-797	6130	5166	22
H(6A)	-43	4747	7076	31
H(6B)	-1920	4889	6450	31
H(6C)	-1548	5409	7548	31
H(113)	4025	5998	4810	21
H(115)	6804	9515	4939	22
H(116)	7192	9400	6637	21
H(213)	1025	9122	10181	20
H(215)	1976	5575	10089	22
H(216)	1633	5600	8390	21

Appendix A

Table A.17. Torsion angles [°] for 2,4-Cl₂-PhonyH.

Atoms	Angles (°)
O(12)-C(4)-C(3)-C(2)	2.9(3)
C(5)-C(4)-C(3)-C(2)	-176.27(18)
C(4)-C(3)-C(2)-N(11)	-2.0(3)
C(4)-C(3)-C(2)-C(1)	176.04(17)
O(22)-C(9)-C(8)-C(7)	1.3(3)
C(10)-C(9)-C(8)-C(7)	-177.67(17)
C(9)-C(8)-C(7)-N(21)	-1.4(3)
C(9)-C(8)-C(7)-C(6)	176.35(18)
C(116)-C(111)-C(112)-C(113)	-1.9(3)
N(11)-C(111)-C(112)-C(113)	-178.44(16)
C(116)-C(111)-C(112)-Cl(12)	176.41(14)
N(11)-C(111)-C(112)-Cl(12)	-0.2(2)
C(111)-C(112)-C(113)-C(114)	0.0(3)
Cl(12)-C(112)-C(113)-C(114)	-178.26(15)
C(112)-C(113)-C(114)-C(115)	1.0(3)
C(112)-C(113)-C(114)-Cl(14)	-179.76(14)
C(113)-C(114)-C(115)-C(116)	-0.2(3)
Cl(14)-C(114)-C(115)-C(116)	-179.43(14)
C(114)-C(115)-C(116)-C(111)	-1.7(3)
C(112)-C(111)-C(116)-C(115)	2.7(3)
N(11)-C(111)-C(116)-C(115)	179.16(16)
C(216)-C(211)-C(212)-C(213)	-2.7(3)
N(21)-C(211)-C(212)-C(213)	-179.21(17)
C(216)-C(211)-C(212)-Cl(22)	176.53(14)
N(21)-C(211)-C(212)-Cl(22)	0.0(2)
C(211)-C(212)-C(213)-C(214)	-0.1(3)
Cl(22)-C(212)-C(213)-C(214)	-179.33(14)
C(212)-C(213)-C(214)-C(215)	2.3(3)
C(212)-C(213)-C(214)-Cl(24)	-179.02(14)
C(213)-C(214)-C(215)-C(216)	-1.6(3)
Cl(24)-C(214)-C(215)-C(216)	179.77(14)
C(214)-C(215)-C(216)-C(211)	-1.4(3)
N(21)-C(211)-C(216)-C(215)	179.85(17)
C(212)-C(211)-C(216)-C(215)	3.5(3)

Appendix A

C(3)-C(2)-N(11)-C(111)	179.40(18)
C(1)-C(2)-N(11)-C(111)	1.4(3)
C(116)-C(111)-N(11)-C(2)	45.0(3)
C(112)-C(111)-N(11)-C(2)	-138.6(2)
C(8)-C(7)-N(21)-C(211)	177.89(17)
C(6)-C(7)-N(21)-C(211)	0.1(3)
C(216)-C(211)-N(21)-C(7)	42.7(3)
C(212)-C(211)-N(21)-C(7)	-141.0(2)

Table A.18. Hydrogen bonds for 2,4-Cl₂-PhonyH [\AA and $^\circ$].

D-H...A	d(D-H)	d(H...A)	d(D...A)	$\angle(\text{DHA})$
N(21)-H(21)...Cl(22)	0.90(2)	2.64(2)	2.9626(17)	102.0(16)
N(21)-H(21)...O(22)	0.90(2)	1.85(2)	2.6073(19)	141(2)
C(115)-H(115)...O(22) ^v	0.95	2.34	3.269(2)	167.0
C(215)-H(215)...O(12) ^{vi}	0.95	2.39	3.320(2)	167.1

Symmetry operators: v) $-x + 1, -y + 2, -z + 1$ vi) $-x + 1, -y + 1, -z + 2$

A.4. 4-(2,6-Dichlorophenylamino)pent-3-en-2-one (2,6-Cl₂-PhonyH)

Table A.19. Atomic coordinates ($\times 10^4$) and equivalent isotropic displacement parameters ($\text{\AA}^2 \times 10^3$) for 2,6-Cl₂-PhonyH. $U(\text{eq})$ is defined as one third of the trace of the orthogonalized U_{ij} tensor.

	x	y	z	U(eq)
C(1)	2999(1)	10652(2)	1072(1)	32(1)
C(2)	2287(1)	10124(2)	1355(1)	22(1)
C(3)	2433(1)	9964(2)	1967(1)	26(1)
C(4)	1779(1)	9464(1)	2254(1)	21(1)
C(5)	2027(1)	9341(2)	2931(1)	34(1)
C(111)	1271(1)	9907(1)	352(1)	17(1)
C(112)	1024(1)	11297(1)	55(1)	21(1)
C(113)	763(1)	11382(2)	-569(1)	25(1)
C(114)	751(1)	10063(2)	-905(1)	27(1)
C(115)	997(1)	8666(2)	-626(1)	26(1)
C(116)	1252(1)	8604(1)	-3(1)	20(1)
C(211)	0	5342(2)	2500	18(1)
C(212)	288(1)	4470(1)	2070(1)	18(1)

Appendix A

C(213)	304(1)	2884(1)	2072(1)	22(1)
C(214)	0	2083(2)	2500	24(1)
N(11)	1493(1)	9803(1)	987(1)	20(1)
N(21)	0	6898(2)	2500	27(1)
O(12)	1009(1)	9146(1)	1969(1)	21(1)
Cl(12)	1026(1)	12945(1)	475(1)	33(1)
Cl(16)	1550(1)	6855(1)	346(1)	31(1)
Cl(22)	634(1)	5471(1)	1515(1)	23(1)

Table A.20. Bond lengths [\AA] and angles [$^\circ$] for 2,6-Cl₂-PhonyH.

Atoms	Bond lengths (\AA)	Atoms	Angles ($^\circ$)
C(1)-C(2)	1.5028(18)	C(2)-C(1)-H(1A)	109.5
C(1)-H(1A)	0.9800	C(2)-C(1)-H(1B)	109.5
C(1)-H(1B)	0.9800	H(1A)-C(1)-H(1B)	109.5
C(1)-H(1C)	0.9800	C(2)-C(1)-H(1C)	109.5
C(2)-N(11)	1.3459(16)	H(1A)-C(1)-H(1C)	109.5
C(2)-C(3)	1.3745(17)	H(1B)-C(1)-H(1C)	109.5
C(3)-C(4)	1.4248(18)	N(11)-C(2)-C(3)	120.52(12)
C(3)-H(3)	0.9500	N(11)-C(2)-C(1)	117.71(11)
C(4)-O(12)	1.2501(15)	C(3)-C(2)-C(1)	121.77(12)
C(4)-C(5)	1.5083(18)	C(2)-C(3)-C(4)	123.63(12)
C(5)-H(5A)	0.9800	C(2)-C(3)-H(3)	118.2
C(5)-H(5B)	0.9800	C(4)-C(3)-H(3)	118.2
C(5)-H(5C)	0.9800	O(12)-C(4)-C(3)	122.73(11)
C(111)-C(116)	1.3948(17)	O(12)-C(4)-C(5)	119.08(12)
C(111)-C(112)	1.3960(17)	C(3)-C(4)-C(5)	118.18(11)
C(111)-N(11)	1.4163(15)	C(4)-C(5)-H(5A)	109.5
C(112)-C(113)	1.3888(18)	C(4)-C(5)-H(5B)	109.5
C(112)-Cl(12)	1.7316(13)	H(5A)-C(5)-H(5B)	109.5
C(113)-C(114)	1.383(2)	C(4)-C(5)-H(5C)	109.5
C(113)-H(113)	0.9500	H(5A)-C(5)-H(5C)	109.5
C(114)-C(115)	1.385(2)	H(5B)-C(5)-H(5C)	109.5
C(114)-H(114)	0.9500	C(116)-C(111)-C(112)	117.33(11)
C(115)-C(116)	1.3867(17)	C(116)-C(111)-N(11)	120.94(11)
C(115)-H(115)	0.9500	C(112)-C(111)-N(11)	121.67(11)
C(116)-Cl(16)	1.7322(12)	C(113)-C(112)-C(111)	121.56(12)

Appendix A

C(211)-N(21)	1.357(2)	C(113)-C(112)-Cl(12)	119.29(10)
C(211)-C(212) ^{viii}	1.4105(15)	C(111)-C(112)-Cl(12)	119.15(10)
C(211)-C(212)	1.4105(15)	C(114)-C(113)-C(112)	119.37(12)
C(212)-C(213)	1.3835(17)	C(114)-C(113)-H(113)	120.3
C(212)-Cl(22)	1.7437(12)	C(112)-C(113)-H(113)	120.3
C(213)-C(214)	1.3880(16)	C(113)-C(114)-C(115)	120.73(12)
C(213)-H(213)	0.9500	C(113)-C(114)-H(114)	119.6
C(214)-C(213) ^{viii}	1.3880(16)	C(115)-C(114)-H(114)	119.6
C(214)-H(214)	0.9500	C(114)-C(115)-C(116)	119.01(12)
N(11)-H(11)	0.827(17)	C(114)-C(115)-H(115)	120.5
N(21)-H(21)	0.846(16)	C(116)-C(115)-H(115)	120.5
		C(115)-C(116)-C(111)	122.00(11)
		C(115)-C(116)-Cl(16)	119.05(10)
		C(111)-C(116)-Cl(16)	118.95(9)
		N(21)-C(211)-C(212) ^{viii}	122.62(7)
		N(21)-C(211)-C(212)	122.62(8)
		C(212) ^{viii} -C(211)-C(212)	114.77(15)
		C(213)-C(212)-C(211)	123.07(12)
		C(213)-C(212)-Cl(22)	119.58(10)
		C(211)-C(212)-Cl(22)	117.35(9)
		C(212)-C(213)-C(214)	119.74(12)
		C(212)-C(213)-H(213)	120.1
		C(214)-C(213)-H(213)	120.1
		C(213) ^{viii} -C(214)-C(213)	119.55(16)
		C(213) ^{viii} -C(214)-H(214)	120.2
		C(213)-C(214)-H(214)	120.2
		C(2)-N(11)-C(111)	125.41(11)
		C(2)-N(11)-H(11)	113.8(11)
		C(111)-N(11)-H(11)	120.8(11)
		C(211)-N(21)-H(21)	119.1(11)

Symmetry operator: viii) $-x, y, -z + \frac{1}{2}$

Appendix A

Table A.21. Anisotropic displacement parameters ($\text{\AA}^2 \times 10^3$) for 2,6-Cl₂-PhonyH. The anisotropic displacement factor exponent takes the form: $-2\pi^2[h^2 a^{*2} U^{11} + \dots + 2 h k a^* b^* U^{12}]$.

	U¹¹	U²²	U³³	U²³	U¹³	U¹²
C(1)	18(1)	56(1)	22(1)	3(1)	4(1)	-8(1)
C(2)	17(1)	30(1)	20(1)	0(1)	4(1)	-3(1)
C(3)	18(1)	40(1)	18(1)	1(1)	2(1)	-5(1)
C(4)	23(1)	22(1)	18(1)	1(1)	4(1)	0(1)
C(5)	30(1)	55(1)	18(1)	4(1)	5(1)	-7(1)
C(111)	14(1)	22(1)	17(1)	1(1)	4(1)	-2(1)
C(112)	17(1)	21(1)	26(1)	1(1)	7(1)	-2(1)
C(113)	17(1)	31(1)	27(1)	12(1)	5(1)	-1(1)
C(114)	20(1)	45(1)	17(1)	5(1)	5(1)	-2(1)
C(115)	23(1)	33(1)	21(1)	-6(1)	7(1)	-2(1)
C(116)	18(1)	21(1)	21(1)	2(1)	5(1)	0(1)
C(211)	15(1)	18(1)	20(1)	0	1(1)	0
C(212)	18(1)	20(1)	16(1)	2(1)	2(1)	1(1)
C(213)	25(1)	20(1)	18(1)	-2(1)	1(1)	3(1)
C(214)	32(1)	16(1)	23(1)	0	1(1)	0
N(11)	17(1)	28(1)	15(1)	0(1)	5(1)	-5(1)
N(21)	38(1)	16(1)	37(1)	0	26(1)	0
O(12)	20(1)	24(1)	20(1)	2(1)	5(1)	-3(1)
Cl(12)	35(1)	19(1)	45(1)	-5(1)	12(1)	-2(1)
Cl(16)	40(1)	21(1)	34(1)	4(1)	13(1)	5(1)
Cl(22)	29(1)	22(1)	22(1)	3(1)	11(1)	5(1)

Appendix A

Table A.22. Hydrogen coordinates ($\times 10^4$) and isotropic displacement parameters ($\text{\AA}^2 \times 10^3$) for 2,6-Cl₂-PhonyH.

	x	y	z	U(eq)
H(1A)	3066	9907	768	48
H(1B)	3555	10741	1382	48
H(1C)	2840	11653	881	48
H(3)	3002	10201	2213	31
H(5A)	2077	10371	3107	52
H(5B)	2593	8809	3065	52
H(5C)	1573	8763	3060	52
H(113)	594	12337	-762	30
H(114)	572	10116	-1331	32
H(115)	991	7764	-858	31
H(213)	523	2345	1781	26
H(214)	0	993	2500	29
H(11)	1129(11)	9498(19)	1165(7)	26(4)
H(21)	252(10)	7370(18)	2269(7)	26(4)

Table A.23. Torsion angles [$^\circ$] for 2,6-Cl₂-PhonyH.

Atoms	Angles ($^\circ$)
N(11)-C(2)-C(3)-C(4)	0.0(2)
C(1)-C(2)-C(3)-C(4)	-179.83(14)
C(2)-C(3)-C(4)-O(12)	-1.0(2)
C(2)-C(3)-C(4)-C(5)	-179.93(14)
C(116)-C(111)-C(112)-C(113)	0.53(18)
N(11)-C(111)-C(112)-C(113)	-176.62(11)
C(116)-C(111)-C(112)-Cl(12)	179.39(9)
N(11)-C(111)-C(112)-Cl(12)	2.24(16)
C(111)-C(112)-C(113)-C(114)	-0.40(19)
Cl(12)-C(112)-C(113)-C(114)	-179.26(10)
C(112)-C(113)-C(114)-C(115)	-0.05(19)
C(113)-C(114)-C(115)-C(116)	0.35(19)
C(114)-C(115)-C(116)-C(111)	-0.20(19)
C(114)-C(115)-C(116)-Cl(16)	179.47(10)
C(112)-C(111)-C(116)-C(115)	-0.23(18)
N(11)-C(111)-C(116)-C(115)	176.94(11)
C(112)-C(111)-C(116)-Cl(16)	-179.90(9)

Appendix A

N(11)-C(111)-C(116)-Cl(16)	-2.73(16)
N(21)-C(211)-C(212)-C(213)	178.87(9)
C(212) ^{viii} -C(211)-C(212)-C(213)	-1.13(9)
N(21)-C(211)-C(212)-Cl(22)	-1.16(10)
C(212) ^{viii} -C(211)-C(212)-Cl(22)	178.84(10)
C(211)-C(212)-C(213)-C(214)	2.24(17)
Cl(22)-C(212)-C(213)-C(214)	-177.72(7)
C(212)-C(213)-C(214)-C(213) ^{viii}	-1.08(8)
C(3)-C(2)-N(11)-C(111)	-179.21(12)
C(1)-C(2)-N(11)-C(111)	0.7(2)
C(116)-C(111)-N(11)-C(2)	99.59(15)
C(112)-C(111)-N(11)-C(2)	-83.36(16)

Symmetry operator: viii) -x, y, -z + ½

Table A.24. Hydrogen bonds for 2,6-Cl₂-PhonyH [Å and °].

D-H...A	d(D-H)	d(H...A)	d(D...A)	<(DHA)
N(11)-H(11)...O(12)	0.827(17)	1.930(16)	2.6222(13)	140.7(15)
N(21)-H(21)...Cl(22)	0.846(16)	2.578(15)	2.9709(7)	109.6(12)
N(21)-H(21)...O(12)	0.846(16)	2.170(16)	2.9733(13)	158.4(14)

Symmetry operator: viii) -x, y, -z + ½

B Appendix: DFT Calculated Data of 4-(Phenylamino)pent-3-en-2-one Derivatives

B.1. 4-(Phenylamino)pent-3-en-2-one (PhonyH)

Table B.1. Calculated atomic coordinates ($\times 10^4$) PhonyH.

	x	y	z
N	-0.204633	-0.069969	-0.018962
C	-0.503249	2.333243	0.546899
H	0.373187	2.265217	1.197348
H	-1.274427	2.917228	1.052449
H	-0.207231	2.883748	-0.352595
O	-2.368923	-1.549710	-0.335837
C	1.205286	-0.127969	-0.029687
C	-2.419394	0.765646	0.155720
C	-1.047298	0.969552	0.206316
C	-3.031158	-0.505875	-0.126982
C	1.810486	-1.285048	0.492188
C	3.405974	0.721610	-0.599689
C	4.004480	-0.423841	-0.070134
C	2.017157	0.868962	-0.594178
C	3.196383	-1.430765	0.467099
C	-4.546864	-0.591956	-0.169590
H	-4.856766	-0.928063	-1.164923
H	-5.035467	0.359687	0.054667
H	-4.883905	-1.349133	0.545904
H	1.570759	1.740957	-1.055849
H	-3.061386	1.613877	0.360159
H	1.183800	-2.061790	0.920857

Appendix B

H	3.645451	-2.331232	0.875850
H	5.084226	-0.535145	-0.084302
H	4.019647	1.502248	-1.040069
H	-0.724881	-0.951476	-0.157835

B.2. 4-(2-Chlorophenylamino)pent-3-en-2-one (2-Cl-PhonyH)

Table B.2. Calculated atomic coordinates ($\times 10^4$) for 2-Cl-PhonyH.

	x	y	z
Cl	1.095343	2.301128	0.620251
N	-0.381980	-0.218019	-0.091091
H	-0.851950	0.611067	-0.489624
O	-2.498579	1.151383	-0.888414
C	-2.628556	-0.861708	0.347803
H	-3.298076	-1.564658	0.828745
C	-1.267876	-1.093970	0.455251
C	1.017709	-0.322791	-0.180453
C	1.654145	-1.498779	-0.613222
H	1.045072	-2.349870	-0.894623
C	-3.197438	0.264641	-0.349936
C	3.217301	0.731372	-0.021689
H	3.808517	1.611564	0.205973
C	-4.709557	0.380367	-0.433597
H	-5.010570	0.355719	-1.486504
H	-5.017969	1.351042	-0.032240
H	-5.229578	-0.415999	0.104959
C	1.829617	0.794784	0.101535
C	3.041746	-1.572669	-0.719681
H	3.504092	-2.495696	-1.055559
C	-0.766190	-2.294327	1.218390
H	-1.538077	-2.630829	1.912914
H	0.140524	-2.060791	1.783208
H	-0.534704	-3.131767	0.551990
C	3.828325	-0.457020	-0.423675
H	4.909010	-0.503293	-0.512921

Appendix B

B.3. 4-(4-Chlorophenylamino)pent-3-en-2-one (4-Cl-PhonyH)

Table B.3. Calculated atomic coordinates ($\times 10^4$) for 4-Cl-PhonyH.

	x	y	z
C	1.467081	2.365022	0.530062
H	2.273725	2.917005	1.015575
H	0.600557	2.347430	1.197166
H	1.182828	2.919652	-0.370842
C	1.939684	0.973163	0.197774
C	3.298118	0.699205	0.139706
H	3.984002	1.515368	0.331578
C	3.842405	-0.605690	-0.133992
C	5.350704	-0.771279	-0.181482
H	5.635245	-1.166933	-1.162139
H	5.653958	-1.512295	0.565609
H	5.888812	0.162668	-0.001074
C	-0.363789	-0.018727	-0.014943
C	-1.020945	-1.152098	0.496307
H	-0.432683	-1.965018	0.911456
C	-2.410648	-1.241359	0.484275
H	-2.906581	-2.119248	0.883367
C	-3.161063	-0.185332	-0.035067
C	-2.530560	0.942446	-0.558260
H	-3.120115	1.748420	-0.981438
C	-1.137033	1.019063	-0.559396
H	-0.660975	1.878046	-1.014682
N	1.044584	-0.026950	-0.013370
H	1.522591	-0.933525	-0.148414
O	3.124710	-1.614873	-0.327956
Cl	-4.916168	-0.284143	-0.041107

Appendix B

B.4. 4-(2,4-Dichlorophenylamino)pent-3-en-2-one (2,4-Cl₂-PhonyH)

Table B.4. Calculated atomic coordinates ($\times 10^4$) for 2,4-Cl₂-PhonyH.

	x	y	z
H	-1.575939	0.601458	-0.477100
C	-5.413050	0.211223	-0.573060
H	-5.776199	1.168688	-0.186112
H	-5.921107	-0.605547	-0.054185
H	-5.670954	0.174288	-1.637003
C	-3.902584	0.157141	-0.429414
C	-3.315057	-0.947795	0.288695
H	-3.973283	-1.679611	0.741215
C	-1.952137	-1.122368	0.451402
C	-1.430121	-2.300973	1.234153
H	-1.130397	-3.124900	0.578068
H	-2.216074	-2.675686	1.892253
H	-0.562420	-2.028066	1.841229
C	0.319474	-0.244820	-0.091445
C	1.066375	0.914545	0.203525
C	2.459202	0.922606	0.139375
H	3.006853	1.827048	0.374782
C	3.129783	-0.245698	-0.217507
C	2.424548	-1.407587	-0.529189
H	2.952873	-2.305007	-0.830428
C	1.032835	-1.391659	-0.478529
H	0.483886	-2.278270	-0.772295
N	-1.083823	-0.206078	-0.059714
O	-3.219072	1.073358	-0.936933
Cl	0.246451	2.390966	0.665901
Cl	4.883342	-0.243107	-0.286194

Appendix B

B.5. 4-(2,6-Dichlorophenylamino)pent-3-en-2-one (2,6-Cl₂-PhonyH)

Table B.5. Calculated atomic coordinates ($\times 10^4$) for 2,6-Cl₂-PhonyH.

	x	y	z
C	0.641328	-0.453969	2.281876
H	0.367437	2.545754	
H	1.396788	-0.548480	3.063006
H	0.048840	-1.374942	2.259579
C	1.294798	-0.203441	0.950443
C	2.671306	-0.185160	0.814069
H	3.271436	-0.358545	1.698713
C	3.335533	0.060590	-0.440153
C	4.853601	0.061167	-0.474777
H	5.194550	-0.644695	-1.238832
H	5.302386	-0.200834	0.486761
H	5.203599	1.055210	-0.773731
C	-0.914847	0.031395	-0.134287
C	-1.672854	-1.151959	-0.235401
C	-3.066527	-1.131914	-0.287794
H	-3.612726	-2.064917	-0.365425
C	-3.734847	0.091389	-0.252265
H	-4.819076	0.114124	-0.297869
C	-3.020834	1.285733	-0.163339
H	-3.531172	2.241673	-0.137821
C	-1.627867	1.246408	-0.104109
N	0.497100	0.014271	-0.126919
O	2.714606	0.281225	-1.505377
Cl	-0.853464	-2.698184	-0.311794
Cl	-0.746752	2.754211	0.015063
H	1.033583	0.210378	-0.989842

Appendix B

C Appendix: Crystal Data of Dicarbonyl-[4-(Phenylamino)pent-3-en-2-onato]-Rhodium(I) Derivatives

C.1. Dicarbonyl-[4-(phenylamino)pent-3-en-2-onato]-Rhodium(I) [Rh(Phony)(CO)₂]

Table C.1. Atomic coordinates ($\times 10^4$) and equivalent isotropic displacement parameters ($\text{\AA}^2 \times 10^3$) for [Rh(Phony)(CO)₂]. U(eq) is defined as one third of the trace of the orthogonalized U^{ij} tensor.

	x	y	z	U(eq)
Rh(1)	1229(1)	-274(1)	57(1)	16(1)
O(14)	1390(1)	-2941(2)	844(1)	31(1)
O(13)	1169(1)	-2298(2)	-1053(1)	28(1)
O(12)	1172(1)	1440(2)	-540(1)	20(1)
N(11)	1301(1)	1085(2)	826(1)	16(1)
C(113)	2709(2)	-316(3)	2306(1)	25(1)
C(1)	1245(2)	3353(2)	1407(1)	24(1)
C(112)	2497(2)	347(2)	1720(1)	19(1)
C(111)	1509(2)	438(2)	1447(1)	19(1)
C(14)	1313(2)	-1902(3)	554(1)	23(1)
C(116)	742(2)	-154(3)	1754(1)	29(1)
C(5)	1040(2)	3810(3)	-928(1)	28(1)
C(2)	1214(2)	2498(2)	799(1)	18(1)
C(13)	1188(2)	-1514(2)	-637(1)	21(1)
C(3)	1081(2)	3287(2)	229(1)	20(1)
C(114)	1948(2)	-877(3)	2620(1)	31(1)
C(4)	1099(2)	2777(2)	-381(1)	20(1)
C(115)	968(2)	-801(3)	2342(1)	35(1)

Appendix C

Table C.2. Bond lengths [Å] and angles [°] for [Rh(Phony)(CO)₂].

Atoms	Bond lengths (Å)	Atoms	Angles (°)
Rh(1)-C(14)	1.841(3)	C(14)-Rh(1)-C(13)	86.53(10)
Rh(1)-C(13)	1.866(2)	C(14)-Rh(1)-O(12)	175.99(8)
Rh(1)-O(12)	2.0315(15)	C(13)-Rh(1)-O(12)	89.76(8)
Rh(1)-N(11)	2.0581(17)	C(14)-Rh(1)-N(11)	93.13(9)
O(14)-C(14)	1.144(3)	C(13)-Rh(1)-N(11)	178.94(8)
O(13)-C(13)	1.142(3)	O(12)-Rh(1)-N(11)	90.55(7)
O(12)-C(4)	1.294(3)	C(4)-O(12)-Rh(1)	126.04(14)
N(11)-C(2)	1.318(3)	C(2)-N(11)-C(111)	117.42(18)
N(11)-C(111)	1.447(3)	C(2)-N(11)-Rh(1)	125.43(15)
C(113)-C(114)	1.378(3)	C(111)-N(11)-Rh(1)	117.08(14)
C(113)-C(112)	1.389(3)	C(114)-C(113)-C(112)	120.7(2)
C(113)-H(113)	0.9500	C(114)-C(113)-H(113)	119.6
C(1)-C(2)	1.511(3)	C(112)-C(113)-H(113)	119.6
C(1)-H(1A)	0.9800	C(2)-C(1)-H(1A)	109.5
C(1)-H(1B)	0.9800	C(2)-C(1)-H(1B)	109.5
C(1)-H(1C)	0.9800	H(1A)-C(1)-H(1B)	109.5
C(112)-C(111)	1.388(3)	C(2)-C(1)-H(1C)	109.5
C(112)-H(112)	0.9500	H(1A)-C(1)-H(1C)	109.5
C(111)-C(116)	1.387(3)	H(1B)-C(1)-H(1C)	109.5
C(116)-C(115)	1.387(3)	C(111)-C(112)-C(113)	119.6(2)
C(116)-H(116)	0.9500	C(111)-C(112)-H(112)	120.2
C(5)-C(4)	1.501(3)	C(113)-C(112)-H(112)	120.2
C(5)-H(5A)	0.9800	C(116)-C(111)-C(112)	120.0(2)
C(5)-H(5B)	0.9800	C(116)-C(111)-N(11)	120.9(2)
C(5)-H(5C)	0.9800	C(112)-C(111)-N(11)	119.08(19)
C(2)-C(3)	1.410(3)	O(14)-C(14)-Rh(1)	177.0(2)
C(3)-C(4)	1.381(3)	C(111)-C(116)-C(115)	119.5(2)
C(3)-H(3)	0.9500	C(111)-C(116)-H(116)	120.2
C(114)-C(115)	1.381(3)	C(115)-C(116)-H(116)	120.2
C(114)-H(114)	0.9500	C(4)-C(5)-H(5A)	109.5
C(115)-H(115)	0.9500	C(4)-C(5)-H(5B)	109.5
		H(5A)-C(5)-H(5B)	109.5
		C(4)-C(5)-H(5C)	109.5
		H(5A)-C(5)-H(5C)	109.5
		H(5B)-C(5)-H(5C)	109.5

Appendix C

N(11)-C(2)-C(3)	123.9(2)
N(11)-C(2)-C(1)	119.5(2)
C(3)-C(2)-C(1)	116.6(2)
O(13)-C(13)-Rh(1)	178.5(2)
C(4)-C(3)-C(2)	127.8(2)
C(4)-C(3)-H(3)	116.1
C(2)-C(3)-H(3)	116.1
C(113)-C(114)-C(115)	119.4(2)
C(113)-C(114)-H(114)	120.3
C(115)-C(114)-H(114)	120.3
O(12)-C(4)-C(3)	125.7(2)
O(12)-C(4)-C(5)	114.3(2)
C(3)-C(4)-C(5)	120.0(2)
C(114)-C(115)-C(116)	120.8(2)
C(114)-C(115)-H(115)	119.6
C(116)-C(115)-H(115)	119.6

Table C.3. Anisotropic displacement parameters ($\text{\AA}^2 \times 10^3$) for $[\text{Rh}(\text{Phony})(\text{CO})_2]$. The anisotropic displacement factor exponent takes the form: $-2\pi^2[h^2 a^{*2} U^{11} + \dots + 2 h k a^* b^* U^{12}]$

	U^{11}	U^{22}	U^{33}	U^{23}	U^{13}	U^{12}
Rh(1)	17(1)	14(1)	18(1)	-1(1)	4(1)	0(1)
O(14)	39(1)	18(1)	35(1)	7(1)	-1(1)	1(1)
O(13)	32(1)	24(1)	30(1)	-11(1)	10(1)	-2(1)
O(12)	23(1)	19(1)	18(1)	1(1)	6(1)	2(1)
N(11)	15(1)	17(1)	18(1)	-1(1)	4(1)	0(1)
C(113)	35(1)	22(1)	19(1)	-3(1)	-1(1)	4(1)
C(1)	31(1)	17(1)	23(1)	-6(1)	4(1)	-1(1)
C(112)	23(1)	16(1)	18(1)	-4(1)	4(1)	-1(1)
C(111)	25(1)	15(1)	18(1)	-2(1)	5(1)	0(1)
C(14)	20(1)	21(1)	26(1)	-6(1)	1(1)	-1(1)
C(116)	25(1)	34(2)	30(1)	6(1)	9(1)	0(1)
C(5)	30(1)	26(2)	28(1)	7(1)	6(1)	3(1)
C(2)	14(1)	16(1)	24(1)	-4(1)	6(1)	-2(1)
C(13)	18(1)	18(1)	26(1)	4(1)	5(1)	1(1)
C(3)	24(1)	12(1)	25(1)	2(1)	5(1)	1(1)

Appendix C

C(114)	49(2)	25(1)	18(1)	1(1)	8(1)	6(1)
C(4)	17(1)	19(1)	24(1)	4(1)	6(1)	0(1)
C(115)	42(2)	36(2)	32(2)	8(1)	19(1)	-1(1)

Table C.4. Hydrogen coordinates ($\times 10^4$) and isotropic displacement parameters ($\text{\AA}^2 \times 10^3$) for $[\text{Rh}(\text{Phony})(\text{CO})_2]$.

	x	y	z	U(eq)
H(113)	3386	-383	2492	30
H(1A)	702	3034	1648	35
H(1B)	1160	4378	1306	35
H(1C)	1894	3203	1659	35
H(112)	3026	736	1507	23
H(116)	66	-118	1563	35
H(5A)	1711	3943	-1064	41
H(5B)	783	4739	-796	41
H(5C)	585	3424	-1281	41
H(3)	964	4289	269	24
H(114)	2097	-1312	3024	37
H(115)	442	-1195	2555	42

Table C.5. Torsion angles [$^\circ$] for $[\text{Rh}(\text{Phony})(\text{CO})_2]$.

Atoms	Angles ($^\circ$)
C(14)-Rh(1)-O(12)-C(4)	-163.4(11)
C(13)-Rh(1)-O(12)-C(4)	174.58(17)
N(11)-Rh(1)-O(12)-C(4)	-6.44(17)
C(14)-Rh(1)-N(11)-C(2)	-175.61(17)
C(13)-Rh(1)-N(11)-C(2)	113(5)
O(12)-Rh(1)-N(11)-C(2)	5.96(17)
C(14)-Rh(1)-N(11)-C(111)	7.36(15)
C(13)-Rh(1)-N(11)-C(111)	-64(5)
O(12)-Rh(1)-N(11)-C(111)	-171.07(14)
C(114)-C(113)-C(112)-C(111)	-0.3(4)
C(113)-C(112)-C(111)-C(116)	-1.2(3)
C(113)-C(112)-C(111)-N(11)	-177.8(2)
C(2)-N(11)-C(111)-C(116)	98.6(3)
Rh(1)-N(11)-C(111)-C(116)	-84.1(2)
C(2)-N(11)-C(111)-C(112)	-84.8(2)

Appendix C

Rh(1)-N(11)-C(111)-C(112)	92.4(2)
C(13)-Rh(1)-C(14)-O(14)	34(4)
O(12)-Rh(1)-C(14)-O(14)	12(5)
N(11)-Rh(1)-C(14)-O(14)	-145(4)
C(112)-C(111)-C(116)-C(115)	1.8(4)
N(11)-C(111)-C(116)-C(115)	178.3(2)
C(111)-N(11)-C(2)-C(3)	175.55(19)
Rh(1)-N(11)-C(2)-C(3)	-1.5(3)
C(111)-N(11)-C(2)-C(1)	-5.2(3)
Rh(1)-N(11)-C(2)-C(1)	177.76(14)
C(14)-Rh(1)-C(13)-O(13)	-9(7)
O(12)-Rh(1)-C(13)-O(13)	169(7)
N(11)-Rh(1)-C(13)-O(13)	62(10)
N(11)-C(2)-C(3)-C(4)	-5.8(4)
C(1)-C(2)-C(3)-C(4)	174.9(2)
C(112)-C(113)-C(114)-C(115)	1.2(4)
Rh(1)-O(12)-C(4)-C(3)	2.3(3)
Rh(1)-O(12)-C(4)-C(5)	-178.10(13)
C(2)-C(3)-C(4)-O(12)	5.4(4)
C(2)-C(3)-C(4)-C(5)	-174.1(2)
C(113)-C(114)-C(115)-C(116)	-0.6(4)
C(111)-C(116)-C(115)-C(114)	-0.9(4)

Table C.6. Hydrogen bonds for [Rh(Phony)(CO)₂] [Å and °].

D-H...A	d(D-H)	d(H...A)	d(D...A)	<(DHA)
C(112)-H(112)...O(12) ^{ix}	0.95	2.50	3.380(3)	153.6

Symmetry operation: ix) -x + ½, y, -z

Appendix C

C.2. Dicarbonyl-[4-(2-Chlorophenylamino)pent-3-en-2-onato]-Rhodium(I) [Rh(2-Cl-Phony)(CO)₂]

Table C.7. Atomic coordinates ($\times 10^4$) and equivalent isotropic displacement parameters ($\text{\AA}^2 \times 10^3$) for [Rh(2-Cl-Phony)(CO)₂]. U(eq) is defined as one third of the trace of the orthogonalized U^{ij} tensor.

	x	y	z	U(eq)
Rh(1)	4563(1)	8927(1)	4384(1)	19(1)
Cl(12)	3309(1)	9821(1)	2485(1)	34(1)
N(11)	4206(1)	10624(2)	3846(1)	21(1)
O(12)	3428(1)	9139(2)	5009(1)	24(1)
O(13)	5042(2)	6458(2)	5184(1)	34(1)
O(14)	6216(1)	8287(2)	3479(1)	32(1)
C(1)	3360(2)	12675(3)	3576(2)	30(1)
C(2)	3518(2)	11442(3)	4010(1)	24(1)
C(3)	2906(2)	11236(3)	4587(1)	26(1)
C(4)	2871(2)	10150(3)	5023(1)	24(1)
C(5)	2130(2)	10047(3)	5585(2)	34(1)
C(13)	4860(2)	7398(3)	4884(1)	24(1)
C(14)	5584(2)	8567(3)	3816(2)	25(1)
C(111)	4739(2)	10872(3)	3216(2)	24(1)
C(112)	4428(2)	10471(3)	2563(2)	28(1)
C(113)	4990(2)	10568(3)	1966(2)	38(1)
C(114)	5879(2)	11108(3)	2037(2)	42(1)
C(115)	6194(2)	11532(3)	2683(2)	38(1)
C(116)	5630(2)	11418(3)	3273(2)	32(1)

Table C.8. Bond lengths [\AA] and angles [$^\circ$] for [Rh(2-Cl-Phony)(CO)₂].

Atoms	Bond lengths (\AA)	Atoms	Angles ($^\circ$)
Rh(1)-C(14)	1.848(3)	C(14)-Rh(1)-C(13)	87.18(12)
Rh(1)-C(13)	1.858(3)	C(14)-Rh(1)-O(12)	174.73(10)
Rh(1)-O(12)	2.0193(18)	C(13)-Rh(1)-O(12)	88.54(10)
Rh(1)-N(11)	2.054(2)	C(14)-Rh(1)-N(11)	94.20(10)
Cl(12)-C(112)	1.737(3)	C(13)-Rh(1)-N(11)	178.62(10)
N(11)-C(2)	1.321(3)	O(12)-Rh(1)-N(11)	90.08(8)
N(11)-C(111)	1.436(3)	C(2)-N(11)-C(111)	118.8(2)
O(12)-C(4)	1.294(3)	C(2)-N(11)-Rh(1)	126.10(18)

Appendix C

O(13)-C(13)	1.135(3)	C(111)-N(11)-Rh(1)	115.02(16)
O(14)-C(14)	1.143(3)	C(4)-O(12)-Rh(1)	126.12(17)
C(1)-C(2)	1.507(4)	C(2)-C(1)-H(1A)	109.5
C(1)-H(1A)	0.9800	C(2)-C(1)-H(1B)	109.5
C(1)-H(1B)	0.9800	H(1A)-C(1)-H(1B)	109.5
C(1)-H(1C)	0.9800	C(2)-C(1)-H(1C)	109.5
C(2)-C(3)	1.413(4)	H(1A)-C(1)-H(1C)	109.5
C(3)-C(4)	1.371(4)	H(1B)-C(1)-H(1C)	109.5
C(3)-H(3)	0.9500	N(11)-C(2)-C(3)	123.4(2)
C(4)-C(5)	1.505(4)	N(11)-C(2)-C(1)	119.9(2)
C(5)-H(5A)	0.9800	C(3)-C(2)-C(1)	116.6(2)
C(5)-H(5B)	0.9800	C(4)-C(3)-C(2)	127.1(2)
C(5)-H(5C)	0.9800	C(4)-C(3)-H(3)	116.5
C(111)-C(112)	1.371(4)	C(2)-C(3)-H(3)	116.5
C(111)-C(116)	1.393(4)	O(12)-C(4)-C(3)	126.6(2)
C(112)-C(113)	1.388(4)	O(12)-C(4)-C(5)	113.2(2)
C(113)-C(114)	1.390(5)	C(3)-C(4)-C(5)	120.3(2)
C(113)-H(113)	0.9500	C(4)-C(5)-H(5A)	109.5
C(114)-C(115)	1.370(5)	C(4)-C(5)-H(5B)	109.5
C(114)-H(114)	0.9500	H(5A)-C(5)-H(5B)	109.5
C(115)-C(116)	1.381(4)	C(4)-C(5)-H(5C)	109.5
C(115)-H(115)	0.9500	H(5A)-C(5)-H(5C)	109.5
C(116)-H(116)	0.9500	H(5B)-C(5)-H(5C)	109.5
		O(13)-C(13)-Rh(1)	179.5(2)
		O(14)-C(14)-Rh(1)	176.8(2)
		C(112)-C(111)-C(116)	118.9(3)
		C(112)-C(111)-N(11)	121.5(2)
		C(116)-C(111)-N(11)	119.3(3)
		C(111)-C(112)-C(113)	121.5(3)
		C(111)-C(112)-Cl(12)	119.1(2)
		C(113)-C(112)-Cl(12)	119.4(2)
		C(112)-C(113)-C(114)	118.6(3)
		C(112)-C(113)-H(113)	120.7
		C(114)-C(113)-H(113)	120.7
		C(115)-C(114)-C(113)	120.6(3)
		C(115)-C(114)-H(114)	119.7
		C(113)-C(114)-H(114)	119.7
		C(114)-C(115)-C(116)	120.0(3)

Appendix C

C(114)-C(115)-H(115)	120.0
C(116)-C(115)-H(115)	120.0
C(115)-C(116)-C(111)	120.3(3)
C(115)-C(116)-H(116)	119.8
C(111)-C(116)-H(116)	119.8

Table C.9. Anisotropic displacement parameters ($\text{\AA}^2 \times 10^3$) for $[\text{Rh}(2\text{-Cl-Phony})(\text{CO})_2]$. The anisotropic displacement factor exponent takes the form: $-2\pi^2 [h^2 a^{*2} U^{11} + \dots + 2 h k a^* b^* U^{12}]$.

	U^{11}	U^{22}	U^{33}	U^{23}	U^{13}	U^{12}
Rh(1)	15(1)	18(1)	23(1)	-2(1)	0(1)	0(1)
Cl(12)	34(1)	37(1)	32(1)	-3(1)	-8(1)	4(1)
N(11)	17(1)	22(1)	24(1)	0(1)	0(1)	0(1)
O(12)	19(1)	24(1)	29(1)	-2(1)	2(1)	-2(1)
O(13)	34(1)	24(1)	43(1)	4(1)	2(1)	2(1)
O(14)	25(1)	31(1)	41(1)	-3(1)	9(1)	3(1)
C(1)	26(1)	27(1)	36(2)	0(1)	-2(1)	4(1)
C(2)	19(1)	23(1)	30(1)	-4(1)	-6(1)	0(1)
C(3)	17(1)	30(2)	31(1)	-7(1)	0(1)	4(1)
C(4)	16(1)	30(1)	26(1)	-7(1)	-3(1)	-2(1)
C(5)	23(1)	43(2)	36(2)	-3(1)	5(1)	2(1)
C(13)	20(1)	23(1)	30(1)	-5(1)	4(1)	-2(1)
C(14)	26(1)	19(1)	30(1)	0(1)	-2(1)	0(1)
C(111)	22(1)	19(1)	31(1)	4(1)	4(1)	5(1)
C(112)	28(1)	28(1)	30(1)	6(1)	1(1)	9(1)
C(113)	47(2)	39(2)	27(2)	9(1)	6(1)	19(2)
C(114)	41(2)	40(2)	45(2)	20(2)	22(2)	17(2)
C(115)	32(2)	29(2)	54(2)	8(1)	12(2)	4(1)
C(116)	26(2)	26(1)	44(2)	8(1)	10(1)	8(1)

Appendix C

Table C.10. Hydrogen coordinates ($\times 10^4$) and isotropic displacement parameters ($\text{\AA}^2 \times 10^3$) for $[\text{Rh}(\text{2-Cl-Phony})(\text{CO})_2]$.

	x	y	z	U(eq)
H(1A)	3943	13183	3548	44
H(1B)	2875	13219	3800	44
H(1C)	3160	12426	3098	44
H(3)	2472	11925	4684	31
H(5A)	1659	9397	5440	50
H(5B)	1833	10914	5650	50
H(5C)	2416	9764	6032	50
H(113)	4771	10272	1518	45
H(114)	6271	11183	1633	50
H(115)	6802	11904	2726	46
H(116)	5850	11715	3721	39

Table C.11. Torsion angles [$^\circ$] for $[\text{Rh}(\text{2-Cl-Phony})(\text{CO})_2]$.

Atoms	Angles ($^\circ$)
C(14)-Rh(1)-N(11)-C(2)	-176.9(2)
C(13)-Rh(1)-N(11)-C(2)	7(4)
O(12)-Rh(1)-N(11)-C(2)	6.2(2)
C(14)-Rh(1)-N(11)-C(111)	6.65(19)
C(13)-Rh(1)-N(11)-C(111)	-170(4)
O(12)-Rh(1)-N(11)-C(111)	-170.26(18)
C(14)-Rh(1)-O(12)-C(4)	-151.8(10)
C(13)-Rh(1)-O(12)-C(4)	172.3(2)
N(11)-Rh(1)-O(12)-C(4)	-7.7(2)
C(111)-N(11)-C(2)-C(3)	175.1(2)
Rh(1)-N(11)-C(2)-C(3)	-1.3(4)
C(111)-N(11)-C(2)-C(1)	-5.6(4)
Rh(1)-N(11)-C(2)-C(1)	178.09(18)
N(11)-C(2)-C(3)-C(4)	-5.6(4)
C(1)-C(2)-C(3)-C(4)	175.1(3)
Rh(1)-O(12)-C(4)-C(3)	4.4(4)
Rh(1)-O(12)-C(4)-C(5)	-175.80(16)
C(2)-C(3)-C(4)-O(12)	4.0(4)

Appendix C

C(2)-C(3)-C(4)-C(5)	-175.8(3)
C(14)-Rh(1)-C(13)-O(13)	-48(26)
O(12)-Rh(1)-C(13)-O(13)	129(26)
N(11)-Rh(1)-C(13)-O(13)	129(24)
C(13)-Rh(1)-C(14)-O(14)	12(4)
O(12)-Rh(1)-C(14)-O(14)	-24(5)
N(11)-Rh(1)-C(14)-O(14)	-168(4)
C(2)-N(11)-C(111)-C(112)	-82.4(3)
Rh(1)-N(11)-C(111)-C(112)	94.3(3)
C(2)-N(11)-C(111)-C(116)	103.7(3)
Rh(1)-N(11)-C(111)-C(116)	-79.5(3)
C(116)-C(111)-C(112)-C(113)	1.6(4)
N(11)-C(111)-C(112)-C(113)	-172.2(2)
C(116)-C(111)-C(112)-Cl(12)	-178.7(2)
N(11)-C(111)-C(112)-Cl(12)	7.4(4)
C(111)-C(112)-C(113)-C(114)	-1.2(4)
Cl(12)-C(112)-C(113)-C(114)	179.2(2)
C(112)-C(113)-C(114)-C(115)	0.1(4)
C(113)-C(114)-C(115)-C(116)	0.4(5)
C(114)-C(115)-C(116)-C(111)	0.1(4)
C(112)-C(111)-C(116)-C(115)	-1.1(4)
N(11)-C(111)-C(116)-C(115)	172.9(2)

C.3. Dicarbonyl-[4-(4-Chlorophenylamino)pent-3-en-2-onato]-Rhodium(I) [Rh(4-Cl-Phony)(CO)₂]

Table C.12. Atomic coordinates ($\times 10^4$) and equivalent isotropic displacement parameters ($\text{\AA}^2 \times 10^3$) for [Rh(4-Cl-Phony)(CO)₂]. $U(\text{eq})$ is defined as one third of the trace of the orthogonalized U_{ij} tensor.

	x	y	z	U(eq)
C(1)	12844(8)	2500	6125(8)	36(4)
C(2)	11905(9)	2500	5522(8)	29(3)
C(3)	12113(9)	2500	4588(8)	39(4)
C(4)	11426(9)	2500	3906(8)	30(3)
C(5)	11756(9)	2500	2936(8)	46(4)
C(13)	8470(9)	2500	4483(8)	32(2)
C(14)	8847(9)	2500	6150(8)	32(2)

Appendix C

C(111)	10903(11)	2500	6841(8)	31(1)
C(112)	10818(7)	765(14)	7305(6)	31(1)
C(113)	10711(7)	769(14)	8231(5)	31(1)
C(114)	10690(8)	2500	8685(7)	24(3)
N(11)	10992(6)	2500	5873(6)	12(2)
O(12)	10439(5)	2500	3979(5)	19(2)
O(13)	7733(7)	2500	4076(6)	57(4)
O(14)	8292(7)	2500	6748(6)	40(3)
Cl(14)	10602(2)	2500	9856(2)	32(1)
Rh	9660(1)	2500	5151(1)	18(1)

Table C.13. Bond lengths [\AA] and angles [$^\circ$] for $[\text{Rh}(4\text{-Cl-Phony})(\text{CO})_2]$.

Atoms	Bond lengths (\AA)	Atoms	Angles ($^\circ$)
C(1)-C(2)	1.531(15)	C(2)-C(1)-H(1A)	109.5
C(1)-H(1A)	0.9800	C(2)-C(1)-H(1B)	109.5
C(1)-H(1B)	0.9800	H(1A)-C(1)-H(1B)	109.5
C(1)-H(1C)	0.9800	C(2)-C(1)-H(1C)	109.5
C(1)-H(1D)	0.9800	H(1A)-C(1)-H(1C)	109.5
C(1)-H(1E)	0.9800	H(1B)-C(1)-H(1C)	109.5
C(1)-H(1F)	0.9800	C(2)-C(1)-H(1D)	109.5
C(2)-N(11)	1.312(14)	H(1A)-C(1)-H(1D)	141.1
C(2)-C(3)	1.424(17)	H(1B)-C(1)-H(1D)	56.3
C(3)-C(4)	1.364(17)	H(1C)-C(1)-H(1D)	56.3
C(3)-H(3)	0.9500	C(2)-C(1)-H(1E)	109.5
C(4)-O(12)	1.303(14)	H(1A)-C(1)-H(1E)	56.3
C(4)-C(5)	1.515(16)	H(1B)-C(1)-H(1E)	141.1
C(5)-H(5A)	0.9800	H(1C)-C(1)-H(1E)	56.3
C(5)-H(5B)	0.9800	H(1D)-C(1)-H(1E)	109.5
C(5)-H(5C)	0.9800	C(2)-C(1)-H(1F)	109.5
C(5)-H(5D)	0.9800	H(1A)-C(1)-H(1F)	56.3
C(5)-H(5E)	0.9800	H(1B)-C(1)-H(1F)	56.3
C(5)-H(5F)	0.9800	H(1C)-C(1)-H(1F)	141.1
C(13)-O(13)	1.146(15)	H(1D)-C(1)-H(1F)	109.5
C(13)-Rh	1.858(12)	H(1E)-C(1)-H(1F)	109.5
C(14)-O(14)	1.154(14)	N(11)-C(2)-C(3)	124.7(11)
C(14)-Rh	1.839(13)	N(11)-C(2)-C(1)	120.3(10)

Appendix C

C(111)-C(112) ^{xi}	1.374(11)	C(3)-C(2)-C(1)	115.0(10)
C(111)-C(112)	1.374(11)	C(4)-C(3)-C(2)	127.4(11)
C(111)-N(11)	1.454(15)	C(4)-C(3)-H(3)	116.3
C(112)-C(113)	1.393(11)	C(2)-C(3)-H(3)	116.3
C(112)-H(112)	0.9500	O(12)-C(4)-C(3)	126.7(11)
C(113)-C(114)	1.360(10)	O(12)-C(4)-C(5)	111.5(10)
C(113)-H(113)	0.9500	C(3)-C(4)-C(5)	121.8(11)
C(114)-C(113) ^{xi}	1.360(10)	C(4)-C(5)-H(5A)	109.5
C(114)-Cl(14)	1.756(11)	C(4)-C(5)-H(5B)	109.5
N(11)-Rh	2.059(8)	H(5A)-C(5)-H(5B)	109.5
O(12)-Rh	2.031(7)	C(4)-C(5)-H(5C)	109.5
		H(5A)-C(5)-H(5C)	109.5
		H(5B)-C(5)-H(5C)	109.5
		C(4)-C(5)-H(5D)	109.5
		H(5A)-C(5)-H(5D)	141.1
		H(5B)-C(5)-H(5D)	56.3
		H(5C)-C(5)-H(5D)	56.3
		C(4)-C(5)-H(5E)	109.5
		H(5A)-C(5)-H(5E)	56.3
		H(5B)-C(5)-H(5E)	141.1
		H(5C)-C(5)-H(5E)	56.3
		H(5D)-C(5)-H(5E)	109.5
		C(4)-C(5)-H(5F)	109.5
		H(5A)-C(5)-H(5F)	56.3
		H(5B)-C(5)-H(5F)	56.3
		H(5C)-C(5)-H(5F)	141.1
		H(5D)-C(5)-H(5F)	109.5
		H(5E)-C(5)-H(5F)	109.5
		O(13)-C(13)-Rh	179.6(11)
		O(14)-C(14)-Rh	176.4(11)
		C(112) ^{xi} -C(111)-C(112)	118.5(11)
		C(112) ^{xi} -C(111)-N(11)	120.7(6)
		C(112)-C(111)-N(11)	120.7(6)
		C(111)-C(112)-C(113)	120.6(9)
		C(111)-C(112)-H(112)	119.7
		C(113)-C(112)-H(112)	119.7
		C(114)-C(113)-C(112)	120.0(9)
		C(114)-C(113)-H(113)	120.0

Appendix C

C(112)-C(113)-H(113)	120.0
C(113)-C(114)-C(113) ^{xi}	120.1(11)
C(113)-C(114)-Cl(14)	120.0(5)
C(113) ^{xi} -C(114)-Cl(14)	120.0(5)
C(2)-N(11)-C(111)	118.2(10)
C(2)-N(11)-Rh	124.7(7)
C(111)-N(11)-Rh	117.0(7)
C(4)-O(12)-Rh	125.2(7)
C(14)-Rh-C(13)	86.9(5)
C(14)-Rh-O(12)	174.7(4)
C(13)-Rh-O(12)	87.8(4)
C(14)-Rh-N(11)	94.0(4)
C(13)-Rh-N(11)	179.1(4)
O(12)-Rh-N(11)	91.3(3)

Symmetry operator: xi) x, -y + 1/2, z.

Table C.14. Anisotropic displacement parameters ($\text{\AA}^2 \times 10^3$) for $[\text{Rh}(\text{4-Cl-Phony})(\text{CO})_2]$. The anisotropic displacement factor exponent takes the form: $-2\pi^2 [h^2 a^{*2} U^{11} + \dots + 2 h k a^* b^* U^{12}]$

	U^{11}	U^{22}	U^{33}	U^{23}	U^{13}	U^{12}
C(1)	10(6)	74(11)	24(6)	0	1(5)	0
C(2)	13(6)	55(9)	21(6)	0	-3(5)	0
C(3)	14(6)	79(12)	24(7)	0	-2(5)	0
C(4)	23(6)	48(9)	19(6)	0	8(5)	0
C(5)	13(6)	100(14)	24(7)	0	5(5)	0
C(13)	23(5)	51(7)	22(5)	0	-2(4)	0
C(14)	23(5)	51(7)	22(5)	0	-2(4)	0
C(111)	46(3)	21(3)	27(3)	0	3(2)	0
C(112)	46(3)	21(3)	27(3)	0	3(2)	0
C(113)	46(3)	21(3)	27(3)	0	3(2)	0
C(114)	14(6)	44(8)	15(6)	0	2(4)	0
N(11)	15(4)	6(4)	14(4)	0	-1(3)	0
O(12)	10(4)	25(5)	20(4)	0	-3(3)	0
O(13)	20(5)	129(11)	22(5)	0	-3(4)	0
O(14)	28(5)	70(8)	21(5)	0	5(4)	0
Cl(14)	29(2)	51(2)	15(1)	0	0(1)	0
Rh	14(1)	26(1)	13(1)	0	0(1)	0

Appendix C

Table C.15. Hydrogen coordinates ($\times 10^4$) and isotropic displacement parameters ($\text{\AA}^2 \times 10^3$) for $[\text{Rh}(4\text{-Cl-Phony})(\text{CO})_2]$.

	x	y	z	U(eq)
H(1A)	12631	2500	6753	54
H(1B)	13252	3676	6005	54
H(1C)	13252	1324	6005	54
H(1D)	13459	2500	5755	54
H(1E)	12838	1324	6503	54
H(1F)	12838	3676	6503	54
H(3)	12809	2500	4421	47
H(5A)	11154	2500	2550	69
H(5B)	12163	1324	2816	69
H(5C)	12163	3676	2816	69
H(5D)	12499	2500	2904	69
H(5E)	11491	3676	2638	69
H(5F)	11491	1324	2638	69
H(112)	10832	-448	6991	38
H(113)	10653	-438	8546	38

Table C.16. Torsion angles [$^\circ$] for $[\text{Rh}(4\text{-Cl-Phony})(\text{CO})_2]$.

Atoms	Angles ($^\circ$)
N(11)-C(2)-C(3)-C(4)	0.000(3)
C(1)-C(2)-C(3)-C(4)	180.000(2)
C(2)-C(3)-C(4)-O(12)	0.000(2)
C(2)-C(3)-C(4)-C(5)	180.000(2)
C(112) ^{xi} -C(111)-C(112)-C(113)	-4(2)
N(11)-C(111)-C(112)-C(113)	-178.6(10)
C(111)-C(112)-C(113)-C(114)	0.0(16)
C(112)-C(113)-C(114)-C(113) ^{xi}	4.0(18)
C(112)-C(113)-C(114)-Cl(14)	-177.7(7)
C(3)-C(2)-N(11)-C(111)	180.000(3)
C(1)-C(2)-N(11)-C(111)	0.000(3)
C(3)-C(2)-N(11)-Rh	0.000(2)
C(1)-C(2)-N(11)-Rh	180.000(2)
C(112) ^{xi} -C(111)-N(11)-C(2)	92.7(12)
C(112)-C(111)-N(11)-C(2)	-92.7(12)

Appendix C

C(112) ^{xi} -C(111)-N(11)-Rh	-87.3(12)
C(112)-C(111)-N(11)-Rh	87.3(12)
C(3)-C(4)-O(12)-Rh	0.000(2)
C(5)-C(4)-O(12)-Rh	180.0
O(14)-C(14)-Rh-C(13)	0.00(3)
O(14)-C(14)-Rh-O(12)	0.00(4)
O(14)-C(14)-Rh-N(11)	180.00(3)
O(13)-C(13)-Rh-C(14)	0.0(4)
O(13)-C(13)-Rh-O(12)	180.0(4)
O(13)-C(13)-Rh-N(11)	180.0(4)
C(4)-O(12)-Rh-C(14)	180.000(13)
C(4)-O(12)-Rh-C(13)	180.000(1)
C(4)-O(12)-Rh-N(11)	0.000(1)
C(2)-N(11)-Rh-C(14)	180.000(2)
C(111)-N(11)-Rh-C(14)	0.000(2)
C(2)-N(11)-Rh-C(13)	0.00(6)
C(111)-N(11)-Rh-C(13)	180.00(6)
C(2)-N(11)-Rh-O(12)	0.000(1)
C(111)-N(11)-Rh-O(12)	180.000(1)

Symmetry operator: xi) $x, -y + \frac{1}{2}, z$.

Table C.17. Hydrogen bonds for [Rh(4-Cl-Phony)(CO)₂] [\AA and $^\circ$].

D-H...A	d(D-H)	d(H...A)	d(D...A)	<(DHA)
C(1)-H(1A)...O(14) ^{xii}	0.98	2.41	3.236(15)	142.1

Symmetry operators: xi) $x, -y + \frac{1}{2}, z$ xii) $x + \frac{1}{2}, -y + \frac{1}{2}, -z + \frac{1}{2}$.

Appendix C

C.4. Dicarboxyl-[4-(2,4-Dichlorophenylamino)pent-3-en-2-onato]-Rhodium(I) [Rh(2,4-Cl₂-Phony)(CO)₂]

Table C.18. Atomic coordinates ($\times 10^4$) and equivalent isotropic displacement parameters ($\text{\AA}^2 \times 10^3$) for [Rh(2,4-Cl₂-Phony)(CO)₂]. U(eq) is defined as one third of the trace of the orthogonalized U_{ij} tensor.

	x	y	z	U(eq)
Rh(1)	2259(1)	733(1)	9725(1)	12(1)
Cl(2)	5304(1)	2753(1)	6331(1)	21(1)
Cl(4)	-567(1)	6725(1)	6260(1)	23(1)
O(12)	3109(2)	-1263(2)	9504(1)	15(1)
O(13)	2584(2)	280(2)	12492(2)	26(1)
O(14)	1283(2)	3660(2)	10221(2)	26(1)
C(14)	1628(3)	2538(2)	10016(2)	17(1)
C(13)	2482(3)	444(2)	11443(2)	17(1)
N(11)	2032(2)	1019(2)	7831(2)	12(1)
C(4)	3306(3)	-1893(2)	8477(2)	15(1)
C(3)	2997(3)	-1308(2)	7307(2)	15(1)
C(5)	3939(3)	-3390(2)	8634(2)	21(1)
C(111)	1423(3)	2375(2)	7392(2)	13(1)
C(2)	2404(3)	60(2)	6996(2)	14(1)
C(1)	2174(3)	431(2)	5635(2)	18(1)
C(114)	198(3)	5049(2)	6696(2)	16(1)
C(112)	2784(3)	3284(2)	6716(2)	15(1)
C(113)	2203(3)	4617(2)	6357(2)	16(1)
C(116)	-585(3)	2857(2)	7722(2)	16(1)
C(115)	-1200(3)	4183(2)	7374(2)	18(1)

Appendix C

Table C.19. Bond lengths [\AA] and angles [$^\circ$] for $[\text{Rh}(2,4\text{-Cl}_2\text{-Phony})(\text{CO})_2]$.

Atoms	Bond lengths (\AA)	Atoms	Angles ($^\circ$)
Rh(1)-C(14)	1.835(2)	C(14)-Rh(1)-C(13)	87.07(9)
Rh(1)-C(13)	1.872(2)	C(14)-Rh(1)-O(12)	175.00(7)
Rh(1)-O(12)	2.0212(15)	C(13)-Rh(1)-O(12)	88.76(7)
Rh(1)-N(11)	2.0574(17)	C(14)-Rh(1)-N(11)	93.83(8)
Cl(2)-C(112)	1.739(2)	C(13)-Rh(1)-N(11)	179.10(8)
Cl(4)-C(114)	1.742(2)	O(12)-Rh(1)-N(11)	90.35(6)
O(13)-C(13)	1.133(3)	C(4)-O(12)-Rh(1)	126.94(13)
O(12)-C(4)	1.287(2)	O(14)-C(14)-Rh(1)	177.61(18)
O(14)-C(14)	1.145(3)	O(13)-C(13)-Rh(1)	178.80(19)
N(11)-C(2)	1.328(3)	C(2)-N(11)-C(111)	118.08(16)
N(11)-C(111)	1.434(3)	C(2)-N(11)-Rh(1)	125.52(14)
C(4)-C(3)	1.382(3)	C(111)-N(11)-Rh(1)	116.40(12)
C(4)-C(5)	1.506(3)	O(12)-C(4)-C(3)	125.64(19)
C(3)-C(2)	1.405(3)	O(12)-C(4)-C(5)	113.97(18)
C(3)-H(3)	0.9500	C(3)-C(4)-C(5)	120.39(18)
C(5)-H(5A)	0.9800	C(4)-C(3)-C(2)	127.77(19)
C(5)-H(5B)	0.9800	C(4)-C(3)-H(3)	116.1
C(5)-H(5C)	0.9800	C(2)-C(3)-H(3)	116.1
C(111)-C(112)	1.390(3)	C(4)-C(5)-H(5A)	109.5
C(111)-C(116)	1.397(3)	C(4)-C(5)-H(5B)	109.5
C(2)-C(1)	1.507(3)	H(5A)-C(5)-H(5B)	109.5
C(1)-H(1A)	0.9800	C(4)-C(5)-H(5C)	109.5
C(1)-H(1B)	0.9800	H(5A)-C(5)-H(5C)	109.5
C(1)-H(1C)	0.9800	H(5B)-C(5)-H(5C)	109.5
C(114)-C(115)	1.379(3)	C(112)-C(111)-C(116)	117.65(19)
C(114)-C(113)	1.384(3)	C(112)-C(111)-N(11)	121.95(18)
C(112)-C(113)	1.384(3)	C(116)-C(111)-N(11)	120.23(18)
C(113)-H(113)	0.9500	N(11)-C(2)-C(3)	123.77(18)
C(116)-C(115)	1.382(3)	N(11)-C(2)-C(1)	119.29(18)
C(116)-H(116)	0.9500	C(3)-C(2)-C(1)	116.94(18)
C(115)-H(115)	0.9500	C(2)-C(1)-H(1A)	109.5
		C(2)-C(1)-H(1B)	109.5
		H(1A)-C(1)-H(1B)	109.5
		C(2)-C(1)-H(1C)	109.5
		H(1A)-C(1)-H(1C)	109.5

Appendix C

H(1B)-C(1)-H(1C)	109.5
C(115)-C(114)-C(113)	121.37(19)
C(115)-C(114)-Cl(4)	119.54(16)
C(113)-C(114)-Cl(4)	119.10(17)
C(113)-C(112)-C(111)	122.16(19)
C(113)-C(112)-Cl(2)	118.30(17)
C(111)-C(112)-Cl(2)	119.53(16)
C(114)-C(113)-C(112)	118.3(2)
C(114)-C(113)-H(113)	120.8
C(112)-C(113)-H(113)	120.8
C(115)-C(116)-C(111)	121.2(2)
C(115)-C(116)-H(116)	119.4
C(111)-C(116)-H(116)	119.4
C(114)-C(115)-C(116)	119.3(2)
C(114)-C(115)-H(115)	120.3
C(116)-C(115)-H(115)	120.3

Appendix C

Table C.20. Anisotropic displacement parameters ($\text{\AA}^2 \times 10^3$) for $[\text{Rh}(2,4\text{-Cl}_2\text{-Phony})(\text{CO})_2]$. The anisotropic displacement factor exponent takes the form: $-2\pi^2[h^2 a^{*2} U^{11} + \dots + 2 h k a^* b^* U^{12}]$.

	U^{11}	U^{22}	U^{33}	U^{23}	U^{13}	U^{12}
Rh(1)	14(1)	12(1)	9(1)	-1(1)	-4(1)	-1(1)
Cl(2)	15(1)	21(1)	26(1)	2(1)	-4(1)	-3(1)
Cl(4)	33(1)	12(1)	24(1)	1(1)	-11(1)	2(1)
O(13)	38(1)	21(1)	19(1)	-3(1)	-13(1)	1(1)
O(12)	17(1)	14(1)	14(1)	-1(1)	-6(1)	-1(1)
O(14)	38(1)	21(1)	19(1)	-3(1)	-13(1)	1(1)
C(14)	20(1)	16(1)	15(1)	-1(1)	-6(1)	-1(1)
C(13)	20(1)	16(1)	15(1)	-1(1)	-6(1)	-1(1)
N(11)	14(1)	12(1)	9(1)	1(1)	-4(1)	-2(1)
C(4)	11(1)	16(1)	17(1)	-3(1)	-2(1)	-1(1)
C(3)	17(1)	16(1)	13(1)	-4(1)	-3(1)	-2(1)
C(5)	26(1)	16(1)	21(1)	0(1)	-9(1)	1(1)
C(111)	19(1)	13(1)	8(1)	-1(1)	-5(1)	0(1)
C(2)	12(1)	17(1)	11(1)	-1(1)	-3(1)	-3(1)
C(1)	24(1)	18(1)	14(1)	-2(1)	-8(1)	-1(1)
C(114)	26(1)	11(1)	14(1)	-1(1)	-10(1)	1(1)
C(112)	15(1)	17(1)	12(1)	-1(1)	-5(1)	0(1)
C(113)	23(1)	14(1)	13(1)	1(1)	-6(1)	-6(1)
C(116)	18(1)	15(1)	15(1)	-1(1)	-5(1)	-3(1)
C(115)	19(1)	17(1)	18(1)	-4(1)	-8(1)	2(1)

Appendix C

Table C.21. Hydrogen coordinates ($\times 10^4$) and isotropic displacement parameters ($\text{\AA}^2 \times 10^3$) for $[\text{Rh}(2,4\text{-Cl}_2\text{-Phony})(\text{CO})_2]$.

	x	y	z	U(eq)
H(3)	3210	-1902	6630	18
H(5A)	5160	-3528	8885	32
H(5B)	4173	-3786	7792	32
H(5C)	2894	-3829	9326	32
H(1A)	837	878	5720	27
H(1B)	2384	-394	5171	27
H(1C)	3151	1048	5129	27
H(113)	3156	5220	5889	20
H(116)	-1546	2261	8194	19
H(115)	-2570	4496	7600	21

Table C.22. Torsion angles [$^\circ$] for $[\text{Rh}(2,4\text{-Cl}_2\text{-Phony})(\text{CO})_2]$.

Atoms	Angles ($^\circ$)
C(14)-Rh(1)-O(12)-C(4)	-147.3(8)
C(13)-Rh(1)-O(12)-C(4)	179.39(17)
N(11)-Rh(1)-O(12)-C(4)	-0.70(16)
C(13)-Rh(1)-C(14)-O(14)	38(5)
O(12)-Rh(1)-C(14)-O(14)	5(6)
N(11)-Rh(1)-C(14)-O(14)	-141(5)
C(14)-Rh(1)-C(13)-O(13)	56(10)
O(12)-Rh(1)-C(13)-O(13)	-126(10)
N(11)-Rh(1)-C(13)-O(13)	-132(8)
C(14)-Rh(1)-N(11)-C(2)	177.11(17)
C(13)-Rh(1)-N(11)-C(2)	6(5)
O(12)-Rh(1)-N(11)-C(2)	-0.13(16)
C(14)-Rh(1)-N(11)-C(111)	-2.72(15)
C(13)-Rh(1)-N(11)-C(111)	-174(5)
O(12)-Rh(1)-N(11)-C(111)	-179.96(14)
Rh(1)-O(12)-C(4)-C(3)	1.1(3)
Rh(1)-O(12)-C(4)-C(5)	-179.21(13)
O(12)-C(4)-C(3)-C(2)	-0.4(4)
C(5)-C(4)-C(3)-C(2)	179.8(2)
C(2)-N(11)-C(111)-C(112)	-88.0(2)

Appendix C

Rh(1)-N(11)-C(111)-C(112)	91.83(19)
C(2)-N(11)-C(111)-C(116)	96.8(2)
Rh(1)-N(11)-C(111)-C(116)	-83.3(2)
C(111)-N(11)-C(2)-C(3)	-179.51(18)
Rh(1)-N(11)-C(2)-C(3)	0.7(3)
C(111)-N(11)-C(2)-C(1)	-0.1(3)
Rh(1)-N(11)-C(2)-C(1)	-179.88(14)
C(4)-C(3)-C(2)-N(11)	-0.5(3)
C(4)-C(3)-C(2)-C(1)	-180.0(2)
C(116)-C(111)-C(112)-C(113)	-0.9(3)
N(11)-C(111)-C(112)-C(113)	-176.21(18)
C(116)-C(111)-C(112)-Cl(2)	177.82(15)
N(11)-C(111)-C(112)-Cl(2)	2.5(3)
C(115)-C(114)-C(113)-C(112)	0.0(3)
Cl(4)-C(114)-C(113)-C(112)	179.72(15)
C(111)-C(112)-C(113)-C(114)	0.5(3)
Cl(2)-C(112)-C(113)-C(114)	-178.25(15)
C(112)-C(111)-C(116)-C(115)	0.9(3)
N(11)-C(111)-C(116)-C(115)	176.25(18)
C(113)-C(114)-C(115)-C(116)	0.0(3)
Cl(4)-C(114)-C(115)-C(116)	-179.75(15)
C(111)-C(116)-C(115)-C(114)	-0.4(3)

Table C.23. Hydrogen bonds for [Rh(2,4-Cl₂-Phony)(CO)₂] [Å and °].

D-H...A	d(D-H)	d(H...A)	d(D...A)	<(DHA)
C(116)-H(116)...O(12) ^{xiv}	0.95	2.50	3.289(3)	140.7

Symmetry operator: xiv) -x, -y, -z + 2.

Appendix C

C.5. Dicarboxyl-[4-(2,6-Dichlorophenylamino)pent-3-en-2-onato]-Rhodium(I) [Rh(2,6-Cl₂-Phony)(CO)₂]

Table C.24. Atomic coordinates ($\times 10^4$) and equivalent isotropic displacement parameters ($\text{\AA}^2 \times 10^3$) for [Rh(2,6-Cl₂-Phony)(CO)₂]. U(eq) is defined as one third of the trace of the orthogonalized U_{ij} tensor.

	x	y	z	U(eq)
Rh(1)	4370(1)	9434(1)	3779(1)	14(1)
N(11)	5845(2)	10644(1)	4312(1)	13(1)
O(12)	3200(2)	10532(1)	2996(1)	17(1)
O(13)	2113(2)	7740(1)	2959(1)	31(1)
O(14)	5944(3)	7736(1)	4918(1)	49(1)
Cl(12)	4884(1)	10443(1)	6237(1)	24(1)
Cl(16)	9209(1)	10197(1)	3468(1)	24(1)
C(1)	6930(3)	12480(2)	4558(2)	25(1)
C(2)	5733(2)	11690(1)	4117(1)	15(1)
C(3)	4545(2)	12130(1)	3518(1)	17(1)
C(4)	3380(2)	11572(2)	3014(1)	16(1)
C(5)	2177(3)	12188(2)	2422(1)	23(1)
C(13)	2977(2)	8372(2)	3269(1)	20(1)
C(14)	5344(3)	8385(2)	4478(1)	26(1)
C(111)	7171(2)	10326(1)	4905(1)	13(1)
C(112)	6898(2)	10197(2)	5815(1)	15(1)
C(113)	8173(3)	9879(2)	6382(1)	19(1)
C(114)	9787(2)	9679(2)	6052(1)	18(1)
C(115)	8800(2)	10091(2)	4596(1)	14(1)
C(116)	10099(2)	9777(2)	5150(1)	18(1)

Appendix C

Table C.25. Bond lengths [\AA] and angles [$^\circ$] for $[\text{Rh}(\text{2,6-Cl}_2\text{-Phony})(\text{CO})_2]$.

Atoms	Bond lengths (\AA)	Atoms	Angles ($^\circ$)
Rh(1)-C(14)	1.834(2)	C(14)-Rh(1)-C(13)	89.45(9)
Rh(1)-C(13)	1.872(2)	C(14)-Rh(1)-O(12)	176.98(7)
Rh(1)-O(12)	2.0165(13)	C(13)-Rh(1)-O(12)	87.63(7)
Rh(1)-N(11)	2.0514(15)	C(14)-Rh(1)-N(11)	92.77(7)
N(11)-C(2)	1.323(2)	C(13)-Rh(1)-N(11)	177.76(8)
N(11)-C(111)	1.429(2)	O(12)-Rh(1)-N(11)	90.15(6)
O(12)-C(4)	1.287(2)	C(2)-N(11)-C(111)	116.93(15)
O(13)-C(13)	1.134(2)	C(2)-N(11)-Rh(1)	125.53(12)
O(14)-C(14)	1.140(3)	C(111)-N(11)-Rh(1)	117.43(11)
Cl(12)-C(112)	1.7367(19)	C(4)-O(12)-Rh(1)	127.08(12)
Cl(16)-C(115)	1.7356(18)	C(2)-C(1)-H(1A)	109.5
C(1)-C(2)	1.508(3)	C(2)-C(1)-H(1B)	109.5
C(1)-H(1A)	0.9800	H(1A)-C(1)-H(1B)	109.5
C(1)-H(1B)	0.9800	C(2)-C(1)-H(1C)	109.5
C(1)-H(1C)	0.9800	H(1A)-C(1)-H(1C)	109.5
C(2)-C(3)	1.409(3)	H(1B)-C(1)-H(1C)	109.5
C(3)-C(4)	1.376(3)	N(11)-C(2)-C(3)	124.05(17)
C(3)-H(3)	0.9500	N(11)-C(2)-C(1)	119.18(16)
C(4)-C(5)	1.507(3)	C(3)-C(2)-C(1)	116.77(16)
C(5)-H(5A)	0.9800	C(4)-C(3)-C(2)	127.28(17)
C(5)-H(5B)	0.9800	C(4)-C(3)-H(3)	116.4
C(5)-H(5C)	0.9800	C(2)-C(3)-H(3)	116.4
C(111)-C(115)	1.396(2)	O(12)-C(4)-C(3)	125.53(17)
C(111)-C(112)	1.398(2)	O(12)-C(4)-C(5)	114.73(17)
C(112)-C(113)	1.376(3)	C(3)-C(4)-C(5)	119.74(18)
C(113)-C(114)	1.387(3)	C(4)-C(5)-H(5A)	109.5
C(113)-H(113)	0.9500	C(4)-C(5)-H(5B)	109.5
C(114)-C(116)	1.388(3)	H(5A)-C(5)-H(5B)	109.5
C(114)-H(114)	0.9500	C(4)-C(5)-H(5C)	109.5
C(115)-C(116)	1.376(3)	H(5A)-C(5)-H(5C)	109.5
C(116)-H(116)	0.9500	H(5B)-C(5)-H(5C)	109.5
		O(13)-C(13)-Rh(1)	178.96(18)
		O(14)-C(14)-Rh(1)	179.6(2)
		C(115)-C(111)-C(112)	116.41(16)
		C(115)-C(111)-N(11)	121.38(15)

Appendix C

C(112)-C(111)-N(11)	122.18(16)
C(113)-C(112)-C(111)	122.02(17)
C(113)-C(112)-Cl(12)	119.31(14)
C(111)-C(112)-Cl(12)	118.67(14)
C(112)-C(113)-C(114)	119.81(18)
C(112)-C(113)-H(113)	120.1
C(114)-C(113)-H(113)	120.1
C(116)-C(114)-C(113)	119.89(17)
C(116)-C(114)-H(114)	120.1
C(113)-C(114)-H(114)	120.1
C(116)-C(115)-C(111)	122.69(16)
C(116)-C(115)-Cl(16)	118.50(14)
C(111)-C(115)-Cl(16)	118.81(14)
C(115)-C(116)-C(114)	119.15(17)
C(115)-C(116)-H(116)	120.4
C(114)-C(116)-H(116)	120.4

Table C.26. Anisotropic displacement parameters ($\text{\AA}^2 \times 10^3$) for $[\text{Rh}(2,6\text{-Cl}_2\text{-Phony})(\text{CO})_2]$. The anisotropic displacement factor exponent takes the form: $-2\pi^2 [h^2 a^{*2} U^{11} + \dots + 2 h k a^* b^* U^{12}]$.

	U^{11}	U^{22}	U^{33}	U^{23}	U^{13}	U^{12}
Rh(1)	13(1)	13(1)	15(1)	0(1)	-1(1)	0(1)
N(11)	13(1)	14(1)	11(1)	0(1)	-1(1)	-1(1)
O(12)	15(1)	19(1)	17(1)	1(1)	-2(1)	2(1)
O(13)	28(1)	27(1)	39(1)	-7(1)	-8(1)	-7(1)
O(14)	74(1)	17(1)	56(1)	7(1)	-38(1)	-4(1)
Cl(12)	19(1)	37(1)	17(1)	0(1)	5(1)	6(1)
Cl(16)	17(1)	42(1)	13(1)	3(1)	3(1)	2(1)
C(1)	26(1)	15(1)	33(1)	1(1)	-10(1)	-2(1)
C(2)	15(1)	16(1)	15(1)	0(1)	0(1)	-1(1)
C(3)	17(1)	14(1)	20(1)	4(1)	2(1)	1(1)
C(4)	14(1)	22(1)	13(1)	2(1)	3(1)	3(1)
C(5)	20(1)	24(1)	25(1)	3(1)	-6(1)	5(1)
C(13)	19(1)	19(1)	22(1)	2(1)	-1(1)	3(1)
C(14)	34(1)	14(1)	30(1)	-2(1)	-12(1)	-6(1)
C(111)	16(1)	11(1)	13(1)	-1(1)	-2(1)	-1(1)
C(112)	16(1)	15(1)	15(1)	-2(1)	4(1)	1(1)

Appendix C

C(113)	26(1)	18(1)	12(1)	1(1)	-1(1)	0(1)
C(114)	20(1)	18(1)	18(1)	2(1)	-5(1)	5(1)
C(115)	18(1)	14(1)	11(1)	1(1)	2(1)	0(1)
C(116)	16(1)	17(1)	21(1)	-1(1)	1(1)	2(1)

Table C.27. Hydrogen coordinates ($\times 10^4$) and isotropic displacement parameters ($\text{\AA}^2 \times 10^3$) for $[\text{Rh}(2,6\text{-Cl}_2\text{-Phony})(\text{CO})_2]$.

	x	y	z	U(eq)
H(1A)	6827	12415	5203	37
H(1B)	6643	13223	4376	37
H(1C)	8098	12315	4379	37
H(3)	4549	12899	3455	21
H(5A)	2149	11846	1834	35
H(5B)	2562	12942	2364	35
H(5C)	1036	12175	2681	35
H(113)	7949	9798	6998	23
H(114)	10676	9475	6444	22
H(116)	11195	9628	4917	21

Table C.28. Torsion angles [$^\circ$] for $[\text{Rh}(2,6\text{-Cl}_2\text{-Phony})(\text{CO})_2]$.

Atoms	Angles ($^\circ$)
C(14)-Rh(1)-N(11)-C(2)	-176.67(16)
C(13)-Rh(1)-N(11)-C(2)	-4(2)
O(12)-Rh(1)-N(11)-C(2)	2.54(15)
C(14)-Rh(1)-N(11)-C(111)	7.23(14)
C(13)-Rh(1)-N(11)-C(111)	180(100)
O(12)-Rh(1)-N(11)-C(111)	-173.56(12)
C(14)-Rh(1)-O(12)-C(4)	158.3(15)
C(13)-Rh(1)-O(12)-C(4)	173.20(15)
N(11)-Rh(1)-O(12)-C(4)	-6.54(15)
C(111)-N(11)-C(2)-C(3)	177.34(16)
Rh(1)-N(11)-C(2)-C(3)	1.2(3)
C(111)-N(11)-C(2)-C(1)	-3.0(2)
Rh(1)-N(11)-C(2)-C(1)	-179.12(13)
N(11)-C(2)-C(3)-C(4)	-3.1(3)
C(1)-C(2)-C(3)-C(4)	177.20(18)

Appendix C

Rh(1)-O(12)-C(4)-C(3)	7.0(3)
Rh(1)-O(12)-C(4)-C(5)	-172.89(12)
C(2)-C(3)-C(4)-O(12)	-1.3(3)
C(2)-C(3)-C(4)-C(5)	178.57(18)
C(14)-Rh(1)-C(13)-O(13)	145(10)
O(12)-Rh(1)-C(13)-O(13)	-34(10)
N(11)-Rh(1)-C(13)-O(13)	-27(12)
C(13)-Rh(1)-C(14)-O(14)	-109(30)
O(12)-Rh(1)-C(14)-O(14)	-94(30)
N(11)-Rh(1)-C(14)-O(14)	70(30)
C(2)-N(11)-C(111)-C(115)	-86.4(2)
Rh(1)-N(11)-C(111)-C(115)	90.00(18)
C(2)-N(11)-C(111)-C(112)	95.9(2)
Rh(1)-N(11)-C(111)-C(112)	-87.64(18)
C(115)-C(111)-C(112)-C(113)	1.5(3)
N(11)-C(111)-C(112)-C(113)	179.28(16)
C(115)-C(111)-C(112)-Cl(12)	-178.41(13)
N(11)-C(111)-C(112)-Cl(12)	-0.7(2)
C(111)-C(112)-C(113)-C(114)	0.0(3)
Cl(12)-C(112)-C(113)-C(114)	179.92(15)
C(112)-C(113)-C(114)-C(116)	-1.3(3)
C(112)-C(111)-C(115)-C(116)	-1.8(3)
N(11)-C(111)-C(115)-C(116)	-179.55(16)
C(112)-C(111)-C(115)-Cl(16)	178.15(13)
N(11)-C(111)-C(115)-Cl(16)	0.4(2)
C(111)-C(115)-C(116)-C(114)	0.5(3)
Cl(16)-C(115)-C(116)-C(114)	-179.43(14)
C(113)-C(114)-C(116)-C(115)	1.1(3)

Table C.29. Hydrogen bonds for [Rh(2,6-Cl₂-Phony)(CO)₂] [Å and °].

D-H...A	d(D-H)	d(H...A)	d(D...A)	<(DHA)
C(113)-H(113)...Cl(16) ^{xv}	0.95	2.79	3.663(2)	152.6
C(114)-H(114)...O(12) ^{xv}	0.95	2.50	3.342(2)	147.4
C(115)-H(115)...Rh(1) ^{xvi}	0.95	3.04	3.972(2)	166.1

Symmetry operator: xv) $-x + 1\frac{1}{2}, -y + 2, z + \frac{1}{2}$ xvi) $1 + x, y, z$.

D Appendix: DFT Calculated Data of Dicarbonyl-[4-(Phenylamino)pent-3-en-2-onato]-Rhodium(I) Derivatives

D.1. Dicarbonyl-[4-(phenylamino)pent-3-en-2-onato]-Rhodium(I) [Rh(Phony)(CO)₂]

Table D.1. Calculated atomic coordinates ($\times 10^4$) [Rh(Phony)(CO)₂].

	x	y	z
Rh	-0.926872	-0.813558	-0.000148
O	-2.927454	0.000359	
O	-3.047235	-3.000454	-0.000115
O	-2.513795	0.496210	-0.000151
N	0.406267	0.805515	0.000124
C	3.848943	0.005201	-1.205703
H	4.369402	-0.128900	-2.148552
C	1.110563	3.161414	0.000046
H	1.757983	3.073865	0.876572
H	0.655237	4.151187	0.001319
H	1.756146	3.075373	-0.878012
C	2.494029	0.334248	-1.207697
H	1.954701	0.449928	-2.142050
C	1.810722	0.503689	0.000048
C	0.433186	-2.105965	0.000048
C	2.493901	0.333394	1.207752
H	1.954468	0.448436	2.142122
C	-3.804484	2.458709	0.000353
H	-4.372098	2.141396	-0.880015
H	-3.720607	3.546496	-0.000036
H	-4.371410	2.142022	0.881398

Appendix D

C	0.043062	2.083438	0.000134
C	-2.232986	-2.195218	-0.000282
C	-1.293902	2.543023	0.000158
H	-1.427015	3.616348	0.000299
C	4.531722	-0.159899	-0.000035
H	5.584203	-0.422278	-0.000072
C	-2.456036	1.777215	0.000099
C	3.848817	0.004356	1.205675
H	4.369181	-0.130397	2.148484

D.2. Dicarbonyl-[4-(2-Chlorophenylamino)pent-3-en-2-onato]-Rhodium(I) [Rh(2-Cl-Phony)(CO)₂]

Table D.2. Calculated atomic coordinates (x 10⁴) for [Rh(2-Cl-Phony)(CO)₂].

	x	y	z
Rh	1.134279	-0.832584	-0.067463
Cl	0.685742	2.279291	
N	-0.255730	0.726605	-0.298173
O	2.665932	0.541819	-0.071320
O	3.328849	-2.920708	0.242346
O	-0.948883	-3.020620	0.017891
C	-1.048573	3.042719	-0.511394
H	-1.655484	2.838230	-1.396641
H	-0.632289	4.045445	-0.598751
H	-1.718211	3.021268	0.353005
C	0.057612	2.018076	-0.355040
C	1.369903	2.531623	-0.277870
H	1.462051	3.607571	-0.332260
C	2.558357	1.816457	-0.148378
C	3.874612	2.555476	-0.083775
H	4.349650	2.363391	0.883591
H	3.753653	3.631678	-0.213284
H	4.546411	2.170774	-0.856329
C	2.487782	-2.152330	0.127348
C	-0.173477	-2.175163	-0.023166
C	-1.631121	0.362586	-0.424096

Appendix D

C	-2.487676	0.279051	0.682656
C	-3.811928	-0.133787	0.541122
H	-4.445287	-0.193220	1.418086
C	-4.302823	-0.468456	-0.717990
H	-5.332071	-0.792420	-0.823399
C	-3.466515	-0.391040	-1.832229
H	-3.839354	-0.655328	-2.815649
C	-2.145425	0.017420	-1.680518
H	-1.478880	0.065338	-2.534644

D.3. Dicarboxyl-[4-(4-Chlorophenylamino)pent-3-en-2-onato]-Rhodium(I) [Rh(4-Cl-Phony)(CO)₂]

Table D.3. Calculated atomic coordinates ($\times 10^4$) for [Rh(4-Cl-Phony)(CO)₂].

	x	y	z
Rh	-1.434898	-0.842349	-0.000205
N	-0.188892	0.846100	-0.000148
O	-3.087502	0.383006	0.000287
O	-3.438393	-3.137089	0.000558
O	0.836451	-2.837344	-0.000047
Cl	5.690429	-0.209108	0.000186
C	0.389756	3.236780	0.000016
H	1.039874	3.185357	-0.877425
H	1.039455	3.185581	0.877784
H	-0.116890	4.201080	-0.000211
C	-0.619502	2.104281	-0.000084
C	-1.977912	2.491730	-0.000166
H	-2.168347	3.556347	-0.000236
C	-3.098431	1.664720	0.000052
C	-4.480765	2.273998	0.000245
H	-5.030334	1.927131	0.880835
H	-5.030364	1.927338	-0.880489
H	-4.454401	3.364633	0.000361
C	-2.667524	-2.290720	0.000149
C	-0.009801	-2.062028	-0.000340
C	1.227871	0.620078	-0.000052

Appendix D

C	1.922271	0.485591	-1.205524
H	1.382192	0.569658	-2.142492
C	3.292432	0.233078	-1.211293
H	3.828961	0.126073	-2.146620
C	3.968811	0.111999	0.000094
C	3.292315	0.233165	1.211407
H	3.828758	0.126217	2.146792
C	1.922152	0.485675	1.205496
H	1.381990	0.569772	2.142411

D.4. Dicarbonyl-[4-(2,4-Dichlorophenylamino)pent-3-en-2-onato]-Rhodium(I) [Rh(2,4-Cl₂-Phony)(CO)₂]

Table D.4. Calculated atomic coordinates (x 10⁴ for [Rh(2,4-Cl₂-Phony)(CO)₂].

	x	y	z
Rh	1.540965	-0.896173	-0.077346
Cl	-1.188025	0.899478	2.417772
Cl	-5.569942	-0.399382	-0.461388
O	3.558398	-3.165818	0.153840
O	3.185656	0.336737	-0.180675
O	-0.720462	-2.889762	0.134028
C	0.124567	-2.117679	0.048540
C	2.782126	-2.328945	0.069360
N	0.285215	0.779453	-0.260372
C	3.189007	1.613149	-0.286647
C	2.063156	2.430811	-0.370867
H	2.248459	3.492806	-0.456823
C	4.567110	2.230610	-0.320813
H	5.108242	1.959765	0.591069
H	4.534030	3.317446	-0.408928
H	5.128976	1.817858	-1.164454
C	-1.120873	0.540707	-0.292277
C	0.708925	2.037492	-0.361901
C	-0.308770	3.154880	-0.476630
H	-0.969697	3.003067	-1.333970
H	0.189187	4.117058	-0.589748

Appendix D

H	-0.939966	3.197191	0.415454
C	-3.860554	-0.037448	-0.401048
C	-1.907794	0.541039	0.868402
C	-3.271272	0.254208	0.823978
H	-3.857218	0.256843	1.733874
C	-1.750285	0.235799	-1.505070
H	-1.145024	0.215560	-2.404774
C	-3.109065	-0.049875	-1.573877
H	-3.577871	-0.285351	-2.521509

D.5. Dicarbonyl-[4-(2,6-Dichlorophenylamino)pent-3-en-2-onato]-Rhodium(I) [Rh(2,6-Cl₂-Phony)(CO)₂]

Table D.5. Calculated atomic coordinates ($\times 10^4$) for [Rh(2,6-Cl₂-Phony)(CO)₂].

	x	y	z
Rh	-1.233295	-0.848263	0.000113
N	0.166184	0.726027	-0.001877
O	-2.763884	0.528759	-0.000786
O	-3.439903	-2.945347	0.003249
O	0.846123	-3.039869	0.003049
Cl	1.438008	0.414733	2.725267
Cl	1.444074	0.400577	-2.724946
C	0.964470	3.048157	-0.010690
H	1.605604	2.934524	0.867738
H	0.554389	4.057380	-0.007925
H	1.596130	2.935618	-0.896209
C	-0.147649	2.019899	-0.006259
C	-1.462331	2.526271	-0.007298
H	-1.555192	3.603648	-0.010507
C	-2.655492	1.804379	-0.003316
C	-3.974506	2.540561	0.001520
H	-4.571273	2.221888	-0.858504
H	-3.846942	3.623504	-0.030182
H	-4.535784	2.271690	0.902048
C	-2.593960	-2.174052	0.001897
C	0.069660	-2.194239	0.001567

Appendix D

C	1.540327	0.367589	0.000368
C	2.243200	0.148549	1.198587
C	3.566870	-0.280895	1.211010
H	4.065992	-0.441909	2.158632
C	4.227243	-0.500570	0.005640
H	5.257052	-0.839455	0.007638
C	2.245930	0.142584	-1.195098
C	3.569589	-0.287022	-1.202306
H	4.070802	-0.453105	-2.147952

E Appendix: Crystal Data of **Carbonyl-[4-(Phenylamino)pent-3-en-2-onato]-Triphenylphosphine-Rhodium(I) Derivatives**

E.1. Carbonyl-[4-(4-Chlorophenylamino)pent-3-en-2-onato]-Triphenylphosphine-Rhodium(I) [Rh(4-Cl-Phony)(CO)(PPh₃)]

Table E.1. Atomic coordinates ($\times 10^4$) and equivalent isotropic displacement parameters ($\text{\AA}^2 \times 10^3$) for [Rh(4-Cl-Phony)(CO)(PPh₃)]. $U(\text{eq})$ is defined as one third of the trace of the orthogonalized U^{ij} tensor.

	x	y	z	U(eq)
Rh(1)	8751(1)	5454(1)	2802(1)	13(1)
Cl(14)	14899(1)	2741(1)	4359(1)	23(1)
N(11)	10631(3)	6591(3)	3681(1)	12(1)
O(12)	7890(3)	7301(2)	2919(1)	16(1)
O(14)	9992(4)	2755(3)	2540(1)	28(1)
P(13)	6634(1)	4188(1)	1863(1)	13(1)
C(1)	12355(5)	8655(4)	4681(2)	19(1)
C(2)	10895(4)	7980(3)	4063(2)	14(1)
C(3)	9879(4)	8915(3)	3927(2)	17(1)
C(4)	8512(4)	8569(3)	3389(2)	15(1)
C(5)	7626(5)	9751(4)	3316(2)	21(1)
C(14)	9500(5)	3799(4)	2646(2)	18(1)
C(111)	11740(4)	5745(3)	3885(2)	15(1)
C(112)	13595(4)	6029(4)	3711(2)	17(1)
C(113)	14593(5)	5119(4)	3857(2)	18(1)
C(114)	13691(5)	3930(4)	4188(2)	16(1)
C(115)	11860(5)	3646(4)	4384(2)	18(1)
C(116)	10861(4)	4544(3)	4227(2)	16(1)
C(311)	5663(4)	5471(3)	1540(2)	16(1)

Appendix E

C(312)	4448(5)	5995(4)	1937(2)	20(1)
C(313)	3822(5)	7112(4)	1776(2)	26(1)
C(314)	4385(5)	7708(4)	1217(2)	31(1)
C(315)	5550(5)	7174(4)	814(2)	33(1)
C(316)	6211(5)	6062(4)	976(2)	23(1)
C(321)	4443(4)	2489(3)	1929(2)	15(1)
C(322)	4366(5)	1771(4)	2470(2)	18(1)
C(323)	2710(5)	445(4)	2512(2)	22(1)
C(324)	1147(5)	-160(4)	2024(2)	22(1)
C(325)	1198(5)	557(4)	1490(2)	20(1)
C(326)	2832(5)	1878(4)	1445(2)	18(1)
C(331)	7702(4)	3395(3)	1161(2)	15(1)
C(332)	9502(5)	4416(4)	1023(2)	19(1)
C(333)	10430(5)	3902(4)	508(2)	22(1)
C(334)	9588(5)	2359(4)	136(2)	21(1)
C(335)	7815(5)	1336(4)	274(2)	23(1)
C(336)	6872(5)	1844(4)	783(2)	19(1)

Table E.2. Bond lengths [\AA] and angles [$^\circ$] for $[\text{Rh}(4\text{-Cl-Phony})(\text{CO})(\text{PPh}_3)]$.

Atoms	Bond lengths (\AA)	Atoms	Angles ($^\circ$)
Rh(1)-C(14)	1.810(3)	C(14)-Rh(1)-O(12)	176.63(11)
Rh(1)-O(12)	2.0332(19)	C(14)-Rh(1)-N(11)	93.73(11)
Rh(1)-N(11)	2.078(2)	O(12)-Rh(1)-N(11)	89.05(9)
Rh(1)-P(13)	2.2622(8)	C(14)-Rh(1)-P(13)	86.52(10)
Cl(14)-C(114)	1.748(3)	O(12)-Rh(1)-P(13)	90.76(6)
N(11)-C(2)	1.317(4)	N(11)-Rh(1)-P(13)	178.37(7)
N(11)-C(111)	1.446(4)	C(2)-N(11)-C(111)	117.9(2)
O(12)-C(4)	1.289(4)	C(2)-N(11)-Rh(1)	126.7(2)
O(14)-C(14)	1.151(4)	C(111)-N(11)-Rh(1)	115.45(18)
P(13)-C(321)	1.823(3)	C(4)-O(12)-Rh(1)	127.52(18)
P(13)-C(311)	1.827(3)	C(321)-P(13)-C(311)	103.18(14)
P(13)-C(331)	1.831(3)	C(321)-P(13)-C(331)	103.79(13)
C(1)-C(2)	1.508(4)	C(311)-P(13)-C(331)	104.80(14)
C(1)-H(1A)	0.9800	C(321)-P(13)-Rh(1)	116.77(10)
C(1)-H(1B)	0.9800	C(311)-P(13)-Rh(1)	113.11(10)
C(1)-H(1C)	0.9800	C(331)-P(13)-Rh(1)	113.83(10)

Appendix E

C(2)-C(3)	1.415(4)	C(2)-C(1)-H(1A)	109.5
C(3)-C(4)	1.379(4)	C(2)-C(1)-H(1B)	109.5
C(3)-H(3)	0.9500	H(1A)-C(1)-H(1B)	109.5
C(4)-C(5)	1.513(4)	C(2)-C(1)-H(1C)	109.5
C(5)-H(5A)	0.9800	H(1A)-C(1)-H(1C)	109.5
C(5)-H(5B)	0.9800	H(1B)-C(1)-H(1C)	109.5
C(5)-H(5C)	0.9800	N(11)-C(2)-C(3)	123.5(3)
C(111)-C(112)	1.377(4)	N(11)-C(2)-C(1)	120.0(3)
C(111)-C(116)	1.397(4)	C(3)-C(2)-C(1)	116.5(3)
C(112)-C(113)	1.390(4)	C(4)-C(3)-C(2)	127.3(3)
C(112)-H(112)	0.9500	C(4)-C(3)-H(3)	116.4
C(113)-C(114)	1.377(4)	C(2)-C(3)-H(3)	116.4
C(113)-H(113)	0.9500	O(12)-C(4)-C(3)	126.0(3)
C(114)-C(115)	1.376(4)	O(12)-C(4)-C(5)	114.4(3)
C(115)-C(116)	1.389(4)	C(3)-C(4)-C(5)	119.6(3)
C(115)-H(115)	0.9500	C(4)-C(5)-H(5A)	109.5
C(116)-H(116)	0.9500	C(4)-C(5)-H(5B)	109.5
C(311)-C(316)	1.384(4)	H(5A)-C(5)-H(5B)	109.5
C(311)-C(312)	1.395(4)	C(4)-C(5)-H(5C)	109.5
C(312)-C(313)	1.381(4)	H(5A)-C(5)-H(5C)	109.5
C(312)-H(312)	0.9500	H(5B)-C(5)-H(5C)	109.5
C(313)-C(314)	1.377(5)	O(14)-C(14)-Rh(1)	179.0(3)
C(313)-H(313)	0.9500	C(112)-C(111)-C(116)	119.5(3)
C(314)-C(315)	1.378(5)	C(112)-C(111)-N(11)	121.3(3)
C(314)-H(314)	0.9500	C(116)-C(111)-N(11)	119.1(3)
C(315)-C(316)	1.394(5)	C(111)-C(112)-C(113)	121.2(3)
C(315)-H(315)	0.9500	C(111)-C(112)-H(112)	119.4
C(316)-H(316)	0.9500	C(113)-C(112)-H(112)	119.4
C(321)-C(326)	1.394(4)	C(114)-C(113)-C(112)	118.4(3)
C(321)-C(322)	1.396(4)	C(114)-C(113)-H(113)	120.8
C(322)-C(323)	1.395(4)	C(112)-C(113)-H(113)	120.8
C(322)-H(322)	0.9500	C(115)-C(114)-C(113)	121.6(3)
C(323)-C(324)	1.376(5)	C(115)-C(114)-Cl(14)	119.3(2)
C(323)-H(323)	0.9500	C(113)-C(114)-Cl(14)	119.1(2)
C(324)-C(325)	1.385(5)	C(114)-C(115)-C(116)	119.6(3)
C(324)-H(324)	0.9500	C(114)-C(115)-H(115)	120.2
C(325)-C(326)	1.385(4)	C(116)-C(115)-H(115)	120.2
C(325)-H(325)	0.9500	C(115)-C(116)-C(111)	119.7(3)

Appendix E

C(326)-H(326)	0.9500	C(115)-C(116)-H(116)	120.2
C(331)-C(336)	1.391(4)	C(111)-C(116)-H(116)	120.2
C(331)-C(332)	1.393(4)	C(316)-C(311)-C(312)	119.2(3)
C(332)-C(333)	1.387(4)	C(316)-C(311)-P(13)	124.2(2)
C(332)-H(332)	0.9500	C(312)-C(311)-P(13)	116.2(2)
C(333)-C(334)	1.382(5)	C(313)-C(312)-C(311)	120.6(3)
C(333)-H(333)	0.9500	C(313)-C(312)-H(312)	119.7
C(334)-C(335)	1.380(5)	C(311)-C(312)-H(312)	119.7
C(334)-H(334)	0.9500	C(314)-C(313)-C(312)	119.9(3)
C(335)-C(336)	1.384(4)	C(314)-C(313)-H(313)	120.0
C(335)-H(335)	0.9500	C(312)-C(313)-H(313)	120.0
C(336)-H(336)	0.9500	C(313)-C(314)-C(315)	120.0(3)
		C(313)-C(314)-H(314)	120.0
		C(315)-C(314)-H(314)	120.0
		C(314)-C(315)-C(316)	120.6(3)
		C(314)-C(315)-H(315)	119.7
		C(316)-C(315)-H(315)	119.7
		C(311)-C(316)-C(315)	119.6(3)
		C(311)-C(316)-H(316)	120.2
		C(315)-C(316)-H(316)	120.2
		C(326)-C(321)-C(322)	118.8(3)
		C(326)-C(321)-P(13)	121.3(2)
		C(322)-C(321)-P(13)	119.8(2)
		C(323)-C(322)-C(321)	119.9(3)
		C(323)-C(322)-H(322)	120.0
		C(321)-C(322)-H(322)	120.0
		C(324)-C(323)-C(322)	120.4(3)
		C(324)-C(323)-H(323)	119.8
		C(322)-C(323)-H(323)	119.8
		C(323)-C(324)-C(325)	120.1(3)
		C(323)-C(324)-H(324)	120.0
		C(325)-C(324)-H(324)	120.0
		C(324)-C(325)-C(326)	119.9(3)
		C(324)-C(325)-H(325)	120.1
		C(326)-C(325)-H(325)	120.1
		C(325)-C(326)-C(321)	120.8(3)
		C(325)-C(326)-H(326)	119.6
		C(321)-C(326)-H(326)	119.6

Appendix E

C(336)-C(331)-C(332)	118.9(3)
C(336)-C(331)-P(13)	124.3(2)
C(332)-C(331)-P(13)	116.7(2)
C(333)-C(332)-C(331)	120.5(3)
C(333)-C(332)-H(332)	119.7
C(331)-C(332)-H(332)	119.7
C(334)-C(333)-C(332)	120.0(3)
C(334)-C(333)-H(333)	120.0
C(332)-C(333)-H(333)	120.0
C(335)-C(334)-C(333)	119.9(3)
C(335)-C(334)-H(334)	120.1
C(333)-C(334)-H(334)	120.1
C(334)-C(335)-C(336)	120.5(3)
C(334)-C(335)-H(335)	119.8
C(336)-C(335)-H(335)	119.8
C(335)-C(336)-C(331)	120.2(3)
C(335)-C(336)-H(336)	119.9
C(331)-C(336)-H(336)	119.9

Table E.3. Anisotropic displacement parameters ($\text{\AA}^2 \times 10^3$) for $[\text{Rh}(4\text{-Cl-Phony})(\text{CO})(\text{PPh}_3)]$. The anisotropic displacement factor exponent takes the form: $-2\pi^2 [h^2 a^{*2} U^{11} + \dots + 2 h k a^* b^* U^{12}]$.

	U^{11}	U^{22}	U^{33}	U^{23}	U^{13}	U^{12}
Rh(1)	15(1)	10(1)	15(1)	2(1)	0(1)	7(1)
Cl(14)	26(1)	21(1)	28(1)	6(1)	-1(1)	16(1)
N(11)	13(1)	11(1)	14(1)	4(1)	1(1)	6(1)
O(12)	19(1)	12(1)	18(1)	1(1)	-2(1)	8(1)
O(14)	42(2)	23(1)	27(1)	-1(1)	-2(1)	25(1)
P(13)	15(1)	11(1)	15(1)	2(1)	0(1)	6(1)
C(1)	23(2)	14(2)	18(2)	0(1)	-1(1)	7(1)
C(2)	12(2)	12(2)	18(2)	5(1)	4(1)	3(1)
C(3)	20(2)	7(2)	21(2)	-1(1)	1(1)	6(1)
C(4)	16(2)	13(2)	19(2)	6(1)	5(1)	6(1)
C(5)	24(2)	15(2)	26(2)	4(1)	-1(2)	11(1)
C(14)	19(2)	22(2)	12(2)	2(1)	-3(1)	8(1)
C(111)	19(2)	12(2)	13(2)	-2(1)	-3(1)	7(1)
C(112)	20(2)	13(2)	18(2)	5(1)	2(1)	6(1)

Appendix E

C(113)	17(2)	21(2)	19(2)	3(1)	3(1)	11(1)
C(114)	20(2)	17(2)	16(2)	2(1)	-2(1)	11(1)
C(115)	24(2)	14(2)	18(2)	5(1)	2(1)	7(1)
C(116)	15(2)	14(2)	19(2)	3(1)	3(1)	6(1)
C(311)	13(2)	12(2)	22(2)	2(1)	-5(1)	4(1)
C(312)	23(2)	15(2)	19(2)	-1(1)	-6(1)	7(1)
C(313)	22(2)	16(2)	36(2)	-4(2)	-9(2)	11(1)
C(314)	23(2)	14(2)	55(3)	10(2)	-10(2)	7(1)
C(315)	25(2)	32(2)	49(2)	30(2)	4(2)	8(2)
C(316)	17(2)	23(2)	30(2)	13(2)	5(2)	7(1)
C(321)	20(2)	9(2)	17(2)	0(1)	5(1)	8(1)
C(322)	19(2)	16(2)	20(2)	2(1)	0(1)	9(1)
C(323)	28(2)	17(2)	26(2)	8(2)	10(2)	12(1)
C(324)	22(2)	12(2)	32(2)	3(2)	11(2)	6(1)
C(325)	17(2)	16(2)	25(2)	-2(1)	2(1)	7(1)
C(326)	21(2)	15(2)	18(2)	2(1)	1(1)	9(1)
C(331)	18(2)	14(2)	14(2)	5(1)	-1(1)	9(1)
C(332)	19(2)	17(2)	21(2)	0(1)	1(1)	8(1)
C(333)	19(2)	23(2)	25(2)	6(2)	3(1)	9(1)
C(334)	25(2)	25(2)	18(2)	3(2)	5(1)	15(2)
C(335)	27(2)	17(2)	23(2)	-1(1)	1(2)	10(1)
C(336)	20(2)	15(2)	21(2)	3(1)	1(1)	8(1)

Appendix E

Table E.4. Hydrogen coordinates ($\times 10^4$) and isotropic displacement parameters ($\text{\AA}^2 \times 10^3$) for [Rh(4-Cl-Phony)(CO)(PPh₃)].

	x	y	z	U(eq)
H(1A)	12037	7895	4972	28
H(1B)	12308	9654	4921	28
H(1C)	13668	8857	4550	28
H(3)	10170	9890	4240	20
H(5A)	7572	9842	2849	32
H(5B)	8431	10790	3602	32
H(5C)	6303	9384	3450	32
H(112)	14204	6862	3487	21
H(113)	15867	5313	3731	22
H(115)	11283	2841	4624	22
H(116)	9585	4342	4352	19
H(312)	4047	5580	2321	24
H(313)	3005	7469	2051	31
H(314)	3970	8486	1110	37
H(315)	5907	7566	422	40
H(316)	7033	5713	700	27
H(322)	5439	2185	2810	22
H(323)	2663	-44	2881	26
H(324)	30	-1071	2054	27
H(325)	114	143	1154	24
H(326)	2855	2373	1080	21
H(332)	10098	5471	1285	23
H(333)	11644	4612	411	26
H(334)	10229	2002	-215	25
H(335)	7237	275	17	27
H(336)	5652	1131	875	22

Appendix E

Table E.5. Torsion angles [°] for [Rh(4-Cl-Phony)(CO)(PPh₃)].

Atoms	Angles (°)
C(14)-Rh(1)-N(11)-C(2)	177.3(2)
O(12)-Rh(1)-N(11)-C(2)	-0.8(2)
P(13)-Rh(1)-N(11)-C(2)	-84(2)
C(14)-Rh(1)-N(11)-C(111)	-2.9(2)
O(12)-Rh(1)-N(11)-C(111)	179.0(2)
P(13)-Rh(1)-N(11)-C(111)	96(2)
C(14)-Rh(1)-O(12)-C(4)	-144.4(19)
N(11)-Rh(1)-O(12)-C(4)	1.2(2)
P(13)-Rh(1)-O(12)-C(4)	179.6(2)
C(14)-Rh(1)-P(13)-C(321)	76.15(14)
O(12)-Rh(1)-P(13)-C(321)	-105.83(12)
N(11)-Rh(1)-P(13)-C(321)	-23(2)
C(14)-Rh(1)-P(13)-C(311)	-164.31(15)
O(12)-Rh(1)-P(13)-C(311)	13.70(13)
N(11)-Rh(1)-P(13)-C(311)	97(2)
C(14)-Rh(1)-P(13)-C(331)	-44.83(14)
O(12)-Rh(1)-P(13)-C(331)	133.19(12)
N(11)-Rh(1)-P(13)-C(331)	-144(2)
C(111)-N(11)-C(2)-C(3)	-178.9(3)
Rh(1)-N(11)-C(2)-C(3)	0.8(4)
C(111)-N(11)-C(2)-C(1)	1.5(4)
Rh(1)-N(11)-C(2)-C(1)	-178.7(2)
N(11)-C(2)-C(3)-C(4)	-0.9(5)
C(1)-C(2)-C(3)-C(4)	178.6(3)
Rh(1)-O(12)-C(4)-C(3)	-1.6(4)
Rh(1)-O(12)-C(4)-C(5)	177.7(2)
C(2)-C(3)-C(4)-O(12)	1.4(5)
C(2)-C(3)-C(4)-C(5)	-177.9(3)
O(12)-Rh(1)-C(14)-O(14)	42(20)
N(11)-Rh(1)-C(14)-O(14)	-103(19)
P(13)-Rh(1)-C(14)-O(14)	78(19)
C(2)-N(11)-C(111)-C(112)	-86.0(4)
Rh(1)-N(11)-C(111)-C(112)	94.2(3)
C(2)-N(11)-C(111)-C(116)	98.2(3)
Rh(1)-N(11)-C(111)-C(116)	-81.6(3)

Appendix E

C(116)-C(111)-C(112)-C(113)	1.4(5)
N(11)-C(111)-C(112)-C(113)	-174.4(3)
C(111)-C(112)-C(113)-C(114)	-0.7(5)
C(112)-C(113)-C(114)-C(115)	-1.0(5)
C(112)-C(113)-C(114)-Cl(14)	178.5(2)
C(113)-C(114)-C(115)-C(116)	2.0(5)
Cl(14)-C(114)-C(115)-C(116)	-177.5(2)
C(114)-C(115)-C(116)-C(111)	-1.3(5)
C(112)-C(111)-C(116)-C(115)	-0.4(5)
N(11)-C(111)-C(116)-C(115)	175.5(3)
C(321)-P(13)-C(311)-C(316)	-126.6(3)
C(331)-P(13)-C(311)-C(316)	-18.2(3)
Rh(1)-P(13)-C(311)-C(316)	106.3(3)
C(321)-P(13)-C(311)-C(312)	60.1(3)
C(331)-P(13)-C(311)-C(312)	168.5(2)
Rh(1)-P(13)-C(311)-C(312)	-67.0(2)
C(316)-C(311)-C(312)-C(313)	-1.1(5)
P(13)-C(311)-C(312)-C(313)	172.5(2)
C(311)-C(312)-C(313)-C(314)	0.6(5)
C(312)-C(313)-C(314)-C(315)	0.8(5)
C(313)-C(314)-C(315)-C(316)	-1.7(5)
C(312)-C(311)-C(316)-C(315)	0.3(5)
P(13)-C(311)-C(316)-C(315)	-172.8(3)
C(314)-C(315)-C(316)-C(311)	1.1(5)
C(311)-P(13)-C(321)-C(326)	38.9(3)
C(331)-P(13)-C(321)-C(326)	-70.3(3)
Rh(1)-P(13)-C(321)-C(326)	163.6(2)
C(311)-P(13)-C(321)-C(322)	-141.6(2)
C(331)-P(13)-C(321)-C(322)	109.3(2)
Rh(1)-P(13)-C(321)-C(322)	-16.8(3)
C(326)-C(321)-C(322)-C(323)	1.3(4)
P(13)-C(321)-C(322)-C(323)	-178.3(2)
C(321)-C(322)-C(323)-C(324)	-0.2(5)
C(322)-C(323)-C(324)-C(325)	-0.7(5)
C(323)-C(324)-C(325)-C(326)	0.4(5)
C(324)-C(325)-C(326)-C(321)	0.7(5)
C(322)-C(321)-C(326)-C(325)	-1.6(4)
P(13)-C(321)-C(326)-C(325)	178.0(2)

Appendix E

C(321)-P(13)-C(331)-C(336)	2.0(3)
C(311)-P(13)-C(331)-C(336)	-106.0(3)
Rh(1)-P(13)-C(331)-C(336)	130.0(2)
C(321)-P(13)-C(331)-C(332)	-175.4(2)
C(311)-P(13)-C(331)-C(332)	76.7(2)
Rh(1)-P(13)-C(331)-C(332)	-47.4(2)
C(336)-C(331)-C(332)-C(333)	1.4(4)
P(13)-C(331)-C(332)-C(333)	178.9(2)
C(331)-C(332)-C(333)-C(334)	-1.3(5)
C(332)-C(333)-C(334)-C(335)	0.6(5)
C(333)-C(334)-C(335)-C(336)	0.0(5)
C(334)-C(335)-C(336)-C(331)	0.1(5)
C(332)-C(331)-C(336)-C(335)	-0.8(4)
P(13)-C(331)-C(336)-C(335)	-178.1(2)

E.2. Carbonyl-[4-(2,4-Dichlorophenylamino)pent-3-en-2-onato]-Triphenylphosphine-Rhodium(I) [Rh(2,4-Cl₂-Phony)(CO)(PPh₃)]

Table E.6. Atomic coordinates ($\times 10^4$) and equivalent isotropic displacement parameters ($\text{\AA}^2 \times 10^3$) for [Rh(2,4-Cl₂-Phony)(CO)(PPh₃)]. U(eq) is defined as one third of the trace of the orthogonalized U^{ij} tensor.

	x	y	z	U(eq)
Rh(1)	8621(1)	1807(1)	2894(1)	20(1)
N(11)	7378(8)	2078(4)	3748(3)	21(1)
O(12)	10335(7)	2713(4)	3074(2)	29(1)
O(14)	6362(8)	407(3)	2629(2)	28(1)
P(13)	10094(2)	1591(1)	1971(1)	20(1)
Cl(12)	8431(3)	762(1)	4627(1)	44(1)
Cl(14)	1984(4)	-378(2)	4352(1)	60(1)
C(1)	6753(11)	2787(5)	4746(4)	32(2)
C(2)	7825(11)	2660(5)	4156(4)	26(2)
C(3)	9233(9)	3190(5)	4051(3)	23(1)
C(4)	10375(9)	3202(5)	3550(3)	23(2)
C(5)	11821(12)	3810(5)	3534(4)	33(2)
C(14)	7209(10)	950(5)	2720(3)	23(2)
C(111)	6022(11)	1524(5)	3936(4)	31(1)
C(112)	6405(12)	876(5)	4314(4)	29(2)

Appendix E

C(113)	5155(14)	283(5)	4454(4)	38(2)
C(114)	3463(13)	389(6)	4199(5)	40(2)
C(115)	3043(12)	1030(5)	3834(5)	36(2)
C(116)	4319(10)	1629(5)	3692(4)	31(1)
C(311)	11696(10)	2372(5)	1842(3)	24(2)
C(312)	11151(10)	3143(5)	1686(3)	25(2)
C(313)	12308(11)	3776(5)	1622(4)	27(2)
C(314)	14074(10)	3650(5)	1724(4)	25(2)
C(315)	14662(10)	2887(5)	1885(4)	28(2)
C(316)	13485(10)	2252(4)	1937(4)	26(2)
C(321)	11351(10)	656(4)	1930(3)	20(1)
C(322)	11316(11)	130(5)	2454(4)	28(2)
C(323)	12276(11)	-582(6)	2434(4)	34(2)
C(324)	13265(10)	-758(5)	1915(4)	29(2)
C(325)	13308(11)	-246(5)	1398(4)	31(2)
C(326)	12313(10)	452(4)	1399(4)	24(2)
C(331)	8887(9)	1601(4)	1206(3)	21(2)
C(332)	7241(10)	1268(5)	1166(4)	26(2)
C(333)	6376(12)	1217(5)	588(4)	32(2)
C(334)	7131(11)	1505(5)	38(4)	27(2)
C(335)	8783(12)	1833(5)	61(4)	35(2)
C(336)	9689(11)	1866(6)	649(3)	31(2)

Table E.7. Bond lengths [\AA] and angles [$^\circ$] for $[\text{Rh}(2,4\text{-Cl}_2\text{-Phony})(\text{CO})(\text{PPh}_3)]$.

Atoms	Bond lengths (\AA)	Atoms	Angles ($^\circ$)
Rh(1)-C(14)	1.826(8)	C(14)-Rh(1)-O(12)	176.1(3)
Rh(1)-O(12)	2.033(5)	C(14)-Rh(1)-N(11)	94.0(3)
Rh(1)-N(11)	2.077(6)	O(12)-Rh(1)-N(11)	88.6(2)
Rh(1)-P(13)	2.2678(19)	C(14)-Rh(1)-P(13)	90.1(2)
N(11)-C(2)	1.334(9)	O(12)-Rh(1)-P(13)	87.35(15)
N(11)-C(111)	1.443(9)	N(11)-Rh(1)-P(13)	175.92(18)
O(12)-C(4)	1.286(9)	C(2)-N(11)-C(111)	118.2(6)
O(14)-C(14)	1.127(9)	C(2)-N(11)-Rh(1)	126.2(5)
P(13)-C(311)	1.806(8)	C(111)-N(11)-Rh(1)	115.3(5)
P(13)-C(321)	1.829(7)	C(4)-O(12)-Rh(1)	128.8(5)
P(13)-C(331)	1.849(7)	C(311)-P(13)-C(321)	104.2(3)

Appendix E

Cl(12)-C(112)	1.696(9)	C(311)-P(13)-C(331)	101.8(3)
Cl(14)-C(114)	1.735(9)	C(321)-P(13)-C(331)	103.3(3)
C(1)-C(2)	1.498(11)	C(311)-P(13)-Rh(1)	110.6(2)
C(1)-H(1A)	0.9800	C(321)-P(13)-Rh(1)	115.9(2)
C(1)-H(1B)	0.9800	C(331)-P(13)-Rh(1)	119.2(2)
C(1)-H(1C)	0.9800	C(2)-C(1)-H(1A)	109.5
C(2)-C(3)	1.410(11)	C(2)-C(1)-H(1B)	109.5
C(3)-C(4)	1.367(10)	H(1A)-C(1)-H(1B)	109.5
C(3)-H(3)	0.9500	C(2)-C(1)-H(1C)	109.5
C(4)-C(5)	1.500(11)	H(1A)-C(1)-H(1C)	109.5
C(5)-H(5A)	0.9800	H(1B)-C(1)-H(1C)	109.5
C(5)-H(5B)	0.9800	N(11)-C(2)-C(3)	123.3(7)
C(5)-H(5C)	0.9800	N(11)-C(2)-C(1)	119.3(7)
C(111)-C(112)	1.368(11)	C(3)-C(2)-C(1)	117.4(7)
C(111)-C(116)	1.413(11)	C(4)-C(3)-C(2)	128.2(7)
C(112)-C(113)	1.405(12)	C(4)-C(3)-H(3)	115.9
C(113)-C(114)	1.414(14)	C(2)-C(3)-H(3)	115.9
C(113)-H(113)	0.9500	O(12)-C(4)-C(3)	124.8(7)
C(114)-C(115)	1.350(13)	O(12)-C(4)-C(5)	115.1(6)
C(115)-C(116)	1.426(11)	C(3)-C(4)-C(5)	120.1(7)
C(115)-H(115)	0.9500	C(4)-C(5)-H(5A)	109.5
C(116)-H(116)	0.9500	C(4)-C(5)-H(5B)	109.5
C(311)-C(312)	1.386(11)	H(5A)-C(5)-H(5B)	109.5
C(311)-C(316)	1.400(11)	C(4)-C(5)-H(5C)	109.5
C(312)-C(313)	1.382(11)	H(5A)-C(5)-H(5C)	109.5
C(312)-H(312)	0.9500	H(5B)-C(5)-H(5C)	109.5
C(313)-C(314)	1.387(11)	O(14)-C(14)-Rh(1)	177.7(7)
C(313)-H(313)	0.9500	C(112)-C(111)-C(116)	120.3(8)
C(314)-C(315)	1.386(11)	C(112)-C(111)-N(11)	120.3(8)
C(314)-H(314)	0.9500	C(116)-C(111)-N(11)	119.2(8)
C(315)-C(316)	1.392(10)	C(111)-C(112)-C(113)	121.7(9)
C(315)-H(315)	0.9500	C(111)-C(112)-Cl(12)	120.5(7)
C(316)-H(316)	0.9500	C(113)-C(112)-Cl(12)	117.7(7)
C(321)-C(326)	1.377(10)	C(112)-C(113)-C(114)	117.3(9)
C(321)-C(322)	1.404(10)	C(112)-C(113)-H(113)	121.3
C(322)-C(323)	1.392(11)	C(114)-C(113)-H(113)	121.3
C(322)-H(322)	0.9500	C(115)-C(114)-C(113)	122.1(9)
C(323)-C(324)	1.357(12)	C(115)-C(114)-Cl(14)	121.9(8)

Appendix E

C(323)-H(323)	0.9500	C(113)-C(114)-Cl(14)	116.0(8)
C(324)-C(325)	1.377(11)	C(114)-C(115)-C(116)	120.3(9)
C(324)-H(324)	0.9500	C(114)-C(115)-H(115)	119.8
C(325)-C(326)	1.388(11)	C(116)-C(115)-H(115)	119.8
C(325)-H(325)	0.9500	C(111)-C(116)-C(115)	118.2(8)
C(326)-H(326)	0.9500	C(111)-C(116)-H(116)	120.9
C(331)-C(332)	1.380(10)	C(115)-C(116)-H(116)	120.9
C(331)-C(336)	1.390(10)	C(312)-C(311)-C(316)	117.4(7)
C(332)-C(333)	1.384(11)	C(312)-C(311)-P(13)	119.6(6)
C(332)-H(332)	0.9500	C(316)-C(311)-P(13)	122.9(6)
C(333)-C(334)	1.374(11)	C(313)-C(312)-C(311)	122.2(7)
C(333)-H(333)	0.9500	C(313)-C(312)-H(312)	118.9
C(334)-C(335)	1.379(11)	C(311)-C(312)-H(312)	118.9
C(334)-H(334)	0.9500	C(312)-C(313)-C(314)	119.8(8)
C(335)-C(336)	1.415(10)	C(312)-C(313)-H(313)	120.1
C(335)-H(335)	0.9500	C(314)-C(313)-H(313)	120.1
C(336)-H(336)	0.9500	C(315)-C(314)-C(313)	119.5(7)
		C(315)-C(314)-H(314)	120.2
		C(313)-C(314)-H(314)	120.2
		C(314)-C(315)-C(316)	120.1(7)
		C(314)-C(315)-H(315)	120.0
		C(316)-C(315)-H(315)	120.0
		C(315)-C(316)-C(311)	121.1(7)
		C(315)-C(316)-H(316)	119.5
		C(311)-C(316)-H(316)	119.5
		C(326)-C(321)-C(322)	119.2(7)
		C(326)-C(321)-P(13)	121.9(6)
		C(322)-C(321)-P(13)	118.8(6)
		C(323)-C(322)-C(321)	119.7(8)
		C(323)-C(322)-H(322)	120.2
		C(321)-C(322)-H(322)	120.2
		C(324)-C(323)-C(322)	120.2(8)
		C(324)-C(323)-H(323)	119.9
		C(322)-C(323)-H(323)	119.9
		C(323)-C(324)-C(325)	120.6(8)
		C(323)-C(324)-H(324)	119.7
		C(325)-C(324)-H(324)	119.7
		C(324)-C(325)-C(326)	120.2(8)

Appendix E

C(324)-C(325)-H(325)	119.9
C(326)-C(325)-H(325)	119.9
C(321)-C(326)-C(325)	120.1(7)
C(321)-C(326)-H(326)	120.0
C(325)-C(326)-H(326)	120.0
C(332)-C(331)-C(336)	118.7(7)
C(332)-C(331)-P(13)	120.4(6)
C(336)-C(331)-P(13)	120.5(5)
C(331)-C(332)-C(333)	121.0(8)
C(331)-C(332)-H(332)	119.5
C(333)-C(332)-H(332)	119.5
C(334)-C(333)-C(332)	120.7(8)
C(334)-C(333)-H(333)	119.7
C(332)-C(333)-H(333)	119.7
C(333)-C(334)-C(335)	119.7(7)
C(333)-C(334)-H(334)	120.2
C(335)-C(334)-H(334)	120.2
C(334)-C(335)-C(336)	119.8(7)
C(334)-C(335)-H(335)	120.1
C(336)-C(335)-H(335)	120.1
C(331)-C(336)-C(335)	120.0(7)
C(331)-C(336)-H(336)	120.0
C(335)-C(336)-H(336)	120.0

Table E.8. Anisotropic displacement parameters ($\text{\AA}^2 \times 10^3$) for $[\text{Rh}(2,4\text{-Cl}_2\text{-Phony})(\text{CO})(\text{PPh}_3)]$. The anisotropic displacement factor exponent takes the form: $-2\pi^2 [h^2 a^{*2} U^{11} + \dots + 2 h k a^* b^* U^{12}]$.

	U^{11}	U^{22}	U^{33}	U^{23}	U^{13}	U^{12}
Rh(1)	20(1)	26(1)	14(1)	-3(1)	2(1)	-4(1)
N(11)	24(3)	21(3)	19(3)	-4(2)	7(3)	-2(3)
O(12)	34(3)	36(3)	16(3)	-6(2)	7(2)	-14(3)
O(14)	35(3)	23(3)	27(3)	-2(2)	3(3)	-15(3)
P(13)	18(1)	25(1)	16(1)	-2(1)	1(1)	-3(1)
Cl(12)	36(1)	45(1)	53(1)	16(1)	-9(1)	3(1)
Cl(14)	54(2)	56(2)	70(2)	-12(1)	24(1)	-30(1)
C(1)	37(5)	35(4)	22(4)	-7(3)	2(4)	-2(4)
C(2)	30(4)	31(4)	16(4)	-7(3)	-1(3)	1(3)

Appendix E

C(3)	29(3)	26(3)	14(3)	-1(3)	-4(3)	-2(3)
C(4)	24(3)	30(4)	16(3)	1(3)	-6(3)	-7(4)
C(5)	41(5)	34(4)	25(4)	-6(3)	1(4)	-11(4)
C(14)	23(4)	27(4)	18(4)	2(3)	2(3)	10(3)
C(111)	29(3)	35(3)	27(3)	-16(2)	15(3)	-9(3)
C(112)	25(4)	36(4)	25(4)	-4(3)	3(4)	-8(4)
C(113)	61(6)	24(4)	29(5)	-8(4)	28(5)	-6(4)
C(114)	33(5)	42(5)	45(5)	-21(4)	23(5)	-9(5)
C(115)	27(4)	36(5)	45(5)	-17(4)	14(4)	-2(4)
C(116)	29(3)	35(3)	27(3)	-16(2)	15(3)	-9(3)
C(311)	28(4)	27(4)	16(3)	-3(3)	0(3)	2(3)
C(312)	23(4)	35(4)	16(3)	1(3)	3(3)	-1(4)
C(313)	33(4)	23(4)	26(4)	-1(3)	-1(4)	-8(3)
C(314)	26(4)	30(4)	19(4)	-1(3)	3(3)	-11(3)
C(315)	23(4)	32(4)	30(4)	-5(3)	-2(3)	-3(3)
C(316)	24(3)	21(3)	32(4)	-3(3)	11(4)	-3(3)
C(321)	17(3)	20(3)	23(3)	-1(3)	-2(3)	-2(3)
C(322)	18(3)	36(4)	30(4)	7(3)	1(4)	-2(4)
C(323)	26(4)	46(5)	31(5)	17(4)	-2(4)	11(4)
C(324)	24(4)	25(4)	40(5)	7(3)	-1(4)	2(3)
C(325)	32(5)	31(4)	29(4)	-6(3)	7(4)	0(4)
C(326)	26(4)	19(4)	25(4)	-1(3)	1(3)	-4(3)
C(331)	18(3)	27(4)	19(3)	6(3)	-8(3)	0(3)
C(332)	28(4)	36(4)	15(4)	-3(3)	2(3)	-5(4)
C(333)	21(4)	43(5)	33(4)	1(4)	-7(4)	-4(4)
C(334)	32(4)	27(4)	21(4)	0(3)	-6(3)	2(3)
C(335)	45(5)	40(4)	19(4)	4(4)	1(4)	-10(5)
C(336)	39(4)	41(5)	13(3)	0(4)	2(3)	-8(4)

Appendix E

Table E.9. Hydrogen coordinates ($\times 10^4$) and isotropic displacement parameters ($\text{\AA}^2 \times 10^3$) for $[\text{Rh}(2,4\text{-Cl}_2\text{-Phony})(\text{CO})(\text{PPh}_3)]$.

	x	y	z	U(eq)
H(1A)	5512	2776	4634	47
H(1B)	7043	3310	4935	47
H(1C)	7003	2358	5054	47
H(3)	9410	3590	4369	27
H(5A)	12946	3534	3571	50
H(5B)	11683	4187	3890	50
H(5C)	11779	4106	3129	50
H(113)	5436	-171	4710	46
H(115)	1891	1083	3672	43
H(116)	4032	2085	3439	37
H(312)	9942	3240	1622	30
H(313)	11895	4296	1508	33
H(314)	14876	4083	1684	30
H(315)	15868	2798	1960	34
H(316)	13903	1730	2040	31
H(322)	10642	258	2821	33
H(323)	12239	-944	2785	41
H(324)	13934	-1240	1909	35
H(325)	14021	-371	1041	37
H(326)	12296	789	1032	28
H(332)	6693	1071	1542	31
H(333)	5248	981	570	39
H(334)	6519	1478	-356	32
H(335)	9310	2036	-316	42
H(336)	10846	2070	663	37

Table E.10. Torsion angles [$^\circ$] for $[\text{Rh}(2,4\text{-Cl}_2\text{-Phony})(\text{CO})(\text{PPh}_3)]$.

Atoms	Angles ($^\circ$)
C(14)-Rh(1)-N(11)-C(2)	177.4(7)
O(12)-Rh(1)-N(11)-C(2)	0.3(7)
P(13)-Rh(1)-N(11)-C(2)	-8(3)
C(14)-Rh(1)-N(11)-C(111)	4.1(6)

Appendix E

O(12)-Rh(1)-N(11)-C(111)	-173.0(6)
P(13)-Rh(1)-N(11)-C(111)	179(64)
C(14)-Rh(1)-O(12)-C(4)	-133(4)
N(11)-Rh(1)-O(12)-C(4)	-1.4(7)
P(13)-Rh(1)-O(12)-C(4)	178.0(7)
C(14)-Rh(1)-P(13)-C(311)	175.4(4)
O(12)-Rh(1)-P(13)-C(311)	-7.6(3)
N(11)-Rh(1)-P(13)-C(311)	0(3)
C(14)-Rh(1)-P(13)-C(321)	-66.4(4)
O(12)-Rh(1)-P(13)-C(321)	110.6(3)
N(11)-Rh(1)-P(13)-C(321)	119(3)
C(14)-Rh(1)-P(13)-C(331)	57.9(4)
O(12)-Rh(1)-P(13)-C(331)	-125.0(3)
N(11)-Rh(1)-P(13)-C(331)	-117(3)
C(111)-N(11)-C(2)-C(3)	174.1(7)
Rh(1)-N(11)-C(2)-C(3)	0.9(11)
C(111)-N(11)-C(2)-C(1)	-8.4(11)
Rh(1)-N(11)-C(2)-C(1)	178.5(6)
N(11)-C(2)-C(3)-C(4)	-1.6(13)
C(1)-C(2)-C(3)-C(4)	-179.2(8)
Rh(1)-O(12)-C(4)-C(3)	1.3(12)
Rh(1)-O(12)-C(4)-C(5)	-179.5(5)
C(2)-C(3)-C(4)-O(12)	0.5(13)
C(2)-C(3)-C(4)-C(5)	-178.7(8)
O(12)-Rh(1)-C(14)-O(14)	62(19)
N(11)-Rh(1)-C(14)-O(14)	-69(17)
P(13)-Rh(1)-C(14)-O(14)	111(17)
C(2)-N(11)-C(111)-C(112)	-82.8(9)
Rh(1)-N(11)-C(111)-C(112)	91.1(7)
C(2)-N(11)-C(111)-C(116)	101.2(9)
Rh(1)-N(11)-C(111)-C(116)	-84.9(7)
C(116)-C(111)-C(112)-C(113)	2.3(12)
N(11)-C(111)-C(112)-C(113)	-173.6(7)
C(116)-C(111)-C(112)-Cl(12)	-178.2(6)
N(11)-C(111)-C(112)-Cl(12)	5.9(10)
C(111)-C(112)-C(113)-C(114)	-1.3(12)
Cl(12)-C(112)-C(113)-C(114)	179.2(6)
C(112)-C(113)-C(114)-C(115)	0.0(12)

Appendix E

C(112)-C(113)-C(114)-Cl(14)	177.3(6)
C(113)-C(114)-C(115)-C(116)	0.3(12)
Cl(14)-C(114)-C(115)-C(116)	-176.9(6)
C(112)-C(111)-C(116)-C(115)	-2.0(11)
N(11)-C(111)-C(116)-C(115)	174.0(7)
C(114)-C(115)-C(116)-C(111)	0.7(11)
C(321)-P(13)-C(311)-C(312)	164.2(6)
C(331)-P(13)-C(311)-C(312)	57.0(6)
Rh(1)-P(13)-C(311)-C(312)	-70.6(6)
C(321)-P(13)-C(311)-C(316)	-20.6(7)
C(331)-P(13)-C(311)-C(316)	-127.9(6)
Rh(1)-P(13)-C(311)-C(316)	104.5(6)
C(316)-C(311)-C(312)-C(313)	0.5(11)
P(13)-C(311)-C(312)-C(313)	175.8(6)
C(311)-C(312)-C(313)-C(314)	-1.1(12)
C(312)-C(313)-C(314)-C(315)	0.5(12)
C(313)-C(314)-C(315)-C(316)	0.6(12)
C(314)-C(315)-C(316)-C(311)	-1.3(12)
C(312)-C(311)-C(316)-C(315)	0.7(11)
P(13)-C(311)-C(316)-C(315)	-174.5(6)
C(311)-P(13)-C(321)-C(326)	-57.9(7)
C(331)-P(13)-C(321)-C(326)	48.2(7)
Rh(1)-P(13)-C(321)-C(326)	-179.7(5)
C(311)-P(13)-C(321)-C(322)	122.7(6)
C(331)-P(13)-C(321)-C(322)	-131.2(6)
Rh(1)-P(13)-C(321)-C(322)	0.9(7)
C(326)-C(321)-C(322)-C(323)	1.1(12)
P(13)-C(321)-C(322)-C(323)	-179.5(6)
C(321)-C(322)-C(323)-C(324)	1.2(13)
C(322)-C(323)-C(324)-C(325)	-1.2(13)
C(323)-C(324)-C(325)-C(326)	-1.1(13)
C(322)-C(321)-C(326)-C(325)	-3.4(11)
P(13)-C(321)-C(326)-C(325)	177.2(6)
C(324)-C(325)-C(326)-C(321)	3.4(12)
C(311)-P(13)-C(331)-C(332)	-160.7(6)
C(321)-P(13)-C(331)-C(332)	91.4(7)
Rh(1)-P(13)-C(331)-C(332)	-38.8(7)
C(311)-P(13)-C(331)-C(336)	26.1(7)

Appendix E

C(321)-P(13)-C(331)-C(336)	-81.8(7)
Rh(1)-P(13)-C(331)-C(336)	148.0(6)
C(336)-C(331)-C(332)-C(333)	-1.8(12)
P(13)-C(331)-C(332)-C(333)	-175.1(6)
C(331)-C(332)-C(333)-C(334)	-0.6(13)
C(332)-C(333)-C(334)-C(335)	1.4(13)
C(333)-C(334)-C(335)-C(336)	0.3(13)
C(332)-C(331)-C(336)-C(335)	3.5(13)
P(13)-C(331)-C(336)-C(335)	176.8(7)
C(334)-C(335)-C(336)-C(331)	-2.8(14)

Table E.11. Hydrogen bonds for [Rh(2,4-Cl₂-Phony)(CO)(PPh₃)] [\AA and $^\circ$].

D-H...A	d(D-H)	d(H...A)	d(D...A)	<(DHA)
C(332)-H(332)...O(14)	0.95	2.54	3.447(10)	159.3

E.3. Carbonyl-[4-(2,6-Dichlorophenylamino)pent-3-en-2-onato]-Triphenylphosphine-Rhodium(I) [Rh(2,6-Cl₂-Phony)(CO)(PPh₃)]

Table E.12. Atomic coordinates ($\times 10^4$) and equivalent isotropic displacement parameters ($\text{\AA}^2 \times 10^3$) for [Rh(2,6-Cl₂-Phony)(CO)(PPh₃)]. U(eq) is defined as one third of the trace of the orthogonalized U_{ij} tensor.

	x	y	z	U(eq)
O(01)	4750(5)	1372(8)	289(9)	297(7)
C(02)	4986(10)	451(8)	100(8)	218(7)
C(01)	5836(5)	387(7)	248(10)	173(5)
Rh(1)	2371(1)	5807(1)	1224(1)	10(1)
P(13)	2330(1)	7767(1)	1515(1)	11(1)
Cl(16)	3376(1)	3087(1)	2768(1)	26(1)
Cl(12)	789(1)	3496(1)	-256(1)	25(1)
N(11)	2485(1)	4034(2)	917(2)	12(1)
O(12)	3316(1)	6184(2)	753(1)	15(1)
O(14)	893(1)	5322(2)	1734(1)	20(1)
C(311)	3336(1)	8421(2)	2020(2)	13(1)
C(321)	1755(1)	8259(2)	2254(2)	12(1)
C(335)	1993(2)	9143(3)	-1005(2)	29(1)
C(332)	1306(2)	9491(2)	368(2)	17(1)

Appendix E

C(14)	1479(2)	5532(2)	1565(2)	14(1)
C(323)	1654(2)	9130(2)	3640(2)	16(1)
C(331)	1923(2)	8654(2)	485(2)	14(1)
C(312)	3453(2)	9628(3)	1957(2)	25(1)
C(4)	3610(2)	5511(2)	264(2)	15(1)
C(3)	3433(2)	4329(2)	79(2)	16(1)
C(116)	2382(2)	2732(2)	2150(2)	16(1)
C(325)	461(2)	8347(2)	2540(2)	18(1)
C(1)	2924(2)	2310(2)	233(2)	21(1)
C(115)	1950(2)	1970(2)	2530(2)	21(1)
C(112)	1243(2)	2906(2)	818(2)	17(1)
C(322)	2116(2)	8817(2)	3085(2)	14(1)
C(326)	919(2)	8032(2)	1983(2)	15(1)
C(111)	2048(2)	3210(2)	1283(2)	14(1)
C(315)	4754(2)	8225(3)	2870(2)	23(1)
C(316)	3993(2)	7719(2)	2489(2)	17(1)
C(333)	1037(2)	10138(2)	-431(2)	22(1)
C(113)	795(2)	2158(2)	1192(2)	21(1)
C(336)	2258(2)	8484(3)	-216(2)	22(1)
C(334)	1379(2)	9971(3)	-1116(2)	25(1)
C(314)	4869(2)	9412(3)	2783(2)	24(1)
C(324)	828(2)	8888(2)	3370(2)	18(1)
C(5)	4214(2)	6122(2)	-106(2)	21(1)
C(114)	1157(2)	1686(2)	2047(2)	23(1)
C(2)	2930(2)	3616(2)	431(2)	14(1)
C(313)	4219(2)	10120(3)	2340(2)	31(1)

Table E.13. Bond lengths [\AA] and angles [$^\circ$] for $[\text{Rh}(2,6\text{-Cl}_2\text{-Phony})(\text{CO})(\text{PPh}_3)]$.

Atoms	Bond lengths (\AA)	Atoms	Angles ($^\circ$)
O(01)-C(02)	1.190(9)	C(02) ^{xviii} -C(02)-O(01)	163(3)
C(02)-C(02) ^{xviii}	1.071(15)	C(02) ^{xviii} -C(02)-C(01)	82.0(16)
C(02)-C(01)	1.419(15)	O(01)-C(02)-C(01)	115.1(14)
C(02)-C(01) ^{xviii}	1.655(19)	C(02) ^{xviii} -C(02)-C(01) ^{xviii}	58.1(15)
C(01)-C(02) ^{xviii}	1.655(19)	O(01)-C(02)-C(01) ^{xviii}	104.8(13)
Rh(1)-C(14)	1.809(3)	C(01)-C(02)-C(01) ^{xviii}	140.1(6)
Rh(1)-O(12)	2.0350(17)	C(02)-C(01)-C(02) ^{xviii}	39.9(6)

Appendix E

Rh(1)-N(11)	2.086(2)	C(14)-Rh(1)-O(12)	175.44(10)
Rh(1)-P(13)	2.2690(7)	C(14)-Rh(1)-N(11)	92.94(10)
P(13)-C(321)	1.823(2)	O(12)-Rh(1)-N(11)	88.60(8)
P(13)-C(331)	1.828(3)	C(14)-Rh(1)-P(13)	91.62(8)
P(13)-C(311)	1.828(2)	O(12)-Rh(1)-P(13)	86.81(5)
Cl(16)-C(116)	1.736(3)	N(11)-Rh(1)-P(13)	175.42(6)
Cl(12)-C(112)	1.735(3)	C(321)-P(13)-C(331)	104.01(11)
N(11)-C(2)	1.322(3)	C(321)-P(13)-C(311)	104.03(11)
N(11)-C(111)	1.425(3)	C(331)-P(13)-C(311)	102.00(12)
O(12)-C(4)	1.286(3)	C(321)-P(13)-Rh(1)	118.65(8)
O(14)-C(14)	1.149(3)	C(331)-P(13)-Rh(1)	113.03(9)
C(311)-C(312)	1.388(4)	C(311)-P(13)-Rh(1)	113.32(8)
C(311)-C(316)	1.392(4)	C(2)-N(11)-C(111)	118.0(2)
C(321)-C(322)	1.393(4)	C(2)-N(11)-Rh(1)	126.00(17)
C(321)-C(326)	1.400(3)	C(111)-N(11)-Rh(1)	116.02(16)
C(335)-C(336)	1.382(4)	C(4)-O(12)-Rh(1)	126.72(16)
C(335)-C(334)	1.388(4)	C(312)-C(311)-C(316)	119.0(2)
C(335)-H(335)	0.9500	C(312)-C(311)-P(13)	120.6(2)
C(332)-C(333)	1.387(4)	C(316)-C(311)-P(13)	120.5(2)
C(332)-C(331)	1.396(4)	C(322)-C(321)-C(326)	118.9(2)
C(332)-H(332)	0.9500	C(322)-C(321)-P(13)	122.81(18)
C(323)-C(324)	1.387(4)	C(326)-C(321)-P(13)	118.21(19)
C(323)-C(322)	1.390(4)	C(336)-C(335)-C(334)	120.2(3)
C(323)-H(323)	0.9500	C(336)-C(335)-H(335)	119.9
C(331)-C(336)	1.393(4)	C(334)-C(335)-H(335)	119.9
C(312)-C(313)	1.389(4)	C(333)-C(332)-C(331)	120.3(3)
C(312)-H(312)	0.9500	C(333)-C(332)-H(332)	119.9
C(4)-C(3)	1.382(4)	C(331)-C(332)-H(332)	119.9
C(4)-C(5)	1.508(3)	O(14)-C(14)-Rh(1)	176.0(2)
C(3)-C(2)	1.415(4)	C(324)-C(323)-C(322)	120.2(2)
C(3)-H(3)	0.9500	C(324)-C(323)-H(323)	119.9
C(116)-C(115)	1.388(4)	C(322)-C(323)-H(323)	119.9
C(116)-C(111)	1.394(4)	C(336)-C(331)-C(332)	118.7(2)
C(325)-C(324)	1.386(4)	C(336)-C(331)-P(13)	117.5(2)
C(325)-C(326)	1.387(4)	C(332)-C(331)-P(13)	123.8(2)
C(325)-H(325)	0.9500	C(311)-C(312)-C(313)	120.4(3)
C(1)-C(2)	1.509(4)	C(311)-C(312)-H(312)	119.8
C(1)-H(1A)	0.9800	C(313)-C(312)-H(312)	119.8

Appendix E

C(1)-H(1B)	0.9800	O(12)-C(4)-C(3)	126.3(2)
C(1)-H(1C)	0.9800	O(12)-C(4)-C(5)	113.6(2)
C(115)-C(114)	1.382(4)	C(3)-C(4)-C(5)	120.1(2)
C(115)-H(115)	0.9500	C(4)-C(3)-C(2)	126.6(2)
C(112)-C(113)	1.391(4)	C(4)-C(3)-H(3)	116.7
C(112)-C(111)	1.398(4)	C(2)-C(3)-H(3)	116.7
C(322)-H(322)	0.9500	C(115)-C(116)-C(111)	122.2(3)
C(326)-H(326)	0.9500	C(115)-C(116)-Cl(16)	118.9(2)
C(315)-C(314)	1.372(4)	C(111)-C(116)-Cl(16)	118.9(2)
C(315)-C(316)	1.389(4)	C(324)-C(325)-C(326)	120.3(2)
C(315)-H(315)	0.9500	C(324)-C(325)-H(325)	119.9
C(316)-H(316)	0.9500	C(326)-C(325)-H(325)	119.9
C(333)-C(334)	1.379(4)	C(2)-C(1)-H(1A)	109.5
C(333)-H(333)	0.9500	C(2)-C(1)-H(1B)	109.5
C(113)-C(114)	1.381(4)	H(1A)-C(1)-H(1B)	109.5
C(113)-H(113)	0.9500	C(2)-C(1)-H(1C)	109.5
C(336)-H(336)	0.9500	H(1A)-C(1)-H(1C)	109.5
C(334)-H(334)	0.9500	H(1B)-C(1)-H(1C)	109.5
C(314)-C(313)	1.378(4)	C(114)-C(115)-C(116)	119.4(3)
C(314)-H(314)	0.9500	C(114)-C(115)-H(115)	120.3
C(324)-H(324)	0.9500	C(116)-C(115)-H(115)	120.3
C(5)-H(5A)	0.9800	C(113)-C(112)-C(111)	122.1(3)
C(5)-H(5B)	0.9800	C(113)-C(112)-Cl(12)	119.2(2)
C(5)-H(5C)	0.9800	C(111)-C(112)-Cl(12)	118.7(2)
C(114)-H(114)	0.9500	C(323)-C(322)-C(321)	120.4(2)
C(313)-H(313)	0.9500	C(323)-C(322)-H(322)	119.8
		C(321)-C(322)-H(322)	119.8
		C(325)-C(326)-C(321)	120.3(2)
		C(325)-C(326)-H(326)	119.8
		C(321)-C(326)-H(326)	119.8
		C(116)-C(111)-C(112)	116.6(2)
		C(116)-C(111)-N(11)	121.5(2)
		C(112)-C(111)-N(11)	121.7(2)
		C(314)-C(315)-C(316)	120.6(3)
		C(314)-C(315)-H(315)	119.7
		C(316)-C(315)-H(315)	119.7
		C(315)-C(316)-C(311)	120.0(3)
		C(315)-C(316)-H(316)	120.0

Appendix E

C(311)-C(316)-H(316)	120.0
C(334)-C(333)-C(332)	120.5(3)
C(334)-C(333)-H(333)	119.8
C(332)-C(333)-H(333)	119.8
C(114)-C(113)-C(112)	119.3(3)
C(114)-C(113)-H(113)	120.4
C(112)-C(113)-H(113)	120.4
C(335)-C(336)-C(331)	120.6(3)
C(335)-C(336)-H(336)	119.7
C(331)-C(336)-H(336)	119.7
C(333)-C(334)-C(335)	119.7(3)
C(333)-C(334)-H(334)	120.2
C(335)-C(334)-H(334)	120.2
C(315)-C(314)-C(313)	119.8(3)
C(315)-C(314)-H(314)	120.1
C(313)-C(314)-H(314)	120.1
C(325)-C(324)-C(323)	119.8(2)
C(325)-C(324)-H(324)	120.1
C(323)-C(324)-H(324)	120.1
C(4)-C(5)-H(5A)	109.5
C(4)-C(5)-H(5B)	109.5
H(5A)-C(5)-H(5B)	109.5
C(4)-C(5)-H(5C)	109.5
H(5A)-C(5)-H(5C)	109.5
H(5B)-C(5)-H(5C)	109.5
C(113)-C(114)-C(115)	120.4(3)
C(113)-C(114)-H(114)	119.8
C(115)-C(114)-H(114)	119.8
N(11)-C(2)-C(3)	123.6(2)
N(11)-C(2)-C(1)	119.8(2)
C(3)-C(2)-C(1)	116.6(2)
C(314)-C(313)-C(312)	120.2(3)
C(314)-C(313)-H(313)	119.9
C(312)-C(313)-H(313)	119.9

Symmetry operator: xviii) $-x + 1, -y, -z$.

Appendix E

Table E.14. Anisotropic displacement parameters ($\text{\AA}^2 \times 10^3$) for $[\text{Rh}(2,6\text{-Cl}_2\text{-Phony})(\text{CO})(\text{PPh}_3)]$. The anisotropic displacement factor exponent takes the form: $-2\pi^2 [h^2 a^{*2} U^{11} + \dots + 2 h k a^* b^* U^{12}]$

	U^{11}	U^{22}	U^{33}	U^{23}	U^{13}	U^{12}
O(01)	204(8)	168(7)	580(20)	-134(10)	211(11)	-60(6)
C(02)	420(20)	76(6)	183(10)	-17(6)	130(13)	110(10)
C(01)	114(7)	64(5)	343(17)	-58(7)	74(9)	-3(5)
Rh(1)	11(1)	8(1)	12(1)	0(1)	4(1)	0(1)
P(13)	11(1)	9(1)	12(1)	0(1)	3(1)	0(1)
Cl(16)	21(1)	32(1)	22(1)	8(1)	0(1)	0(1)
Cl(12)	24(1)	21(1)	23(1)	4(1)	-4(1)	-7(1)
N(11)	14(1)	8(1)	14(1)	2(1)	4(1)	-1(1)
O(12)	15(1)	12(1)	19(1)	0(1)	8(1)	0(1)
O(14)	19(1)	19(1)	24(1)	0(1)	11(1)	-3(1)
C(311)	11(1)	14(1)	14(1)	-1(1)	5(1)	-2(1)
C(321)	12(1)	9(1)	14(1)	2(1)	5(1)	0(1)
C(335)	46(2)	26(2)	18(2)	3(1)	15(1)	14(1)
C(332)	18(1)	14(1)	19(1)	1(1)	6(1)	2(1)
C(14)	18(1)	9(1)	14(1)	0(1)	4(1)	0(1)
C(323)	18(1)	16(1)	14(1)	-1(1)	4(1)	1(1)
C(331)	15(1)	12(1)	12(1)	-1(1)	1(1)	-1(1)
C(312)	18(1)	18(1)	33(2)	5(1)	1(1)	-4(1)
C(4)	11(1)	17(1)	16(1)	4(1)	4(1)	3(1)
C(3)	16(1)	15(1)	17(1)	2(1)	8(1)	4(1)
C(116)	18(1)	14(1)	17(1)	-1(1)	6(1)	0(1)
C(325)	14(1)	16(1)	25(2)	4(1)	8(1)	1(1)
C(1)	27(1)	13(1)	27(2)	-2(1)	13(1)	1(1)
C(115)	32(2)	14(1)	22(2)	3(1)	15(1)	1(1)
C(112)	20(1)	12(1)	18(1)	-1(1)	4(1)	1(1)
C(322)	12(1)	14(1)	16(1)	0(1)	2(1)	1(1)
C(326)	13(1)	13(1)	16(1)	1(1)	2(1)	-1(1)
C(111)	17(1)	6(1)	18(1)	-1(1)	7(1)	1(1)
C(315)	13(1)	29(2)	24(2)	-5(1)	2(1)	6(1)
C(316)	17(1)	15(1)	18(1)	-3(1)	3(1)	0(1)
C(333)	23(1)	17(1)	23(2)	1(1)	2(1)	7(1)
C(113)	19(1)	13(1)	32(2)	-5(1)	10(1)	-4(1)
C(336)	29(2)	20(1)	18(1)	2(1)	9(1)	12(1)
C(334)	41(2)	17(1)	15(1)	3(1)	4(1)	7(1)

Appendix E

C(314)	14(1)	32(2)	24(2)	-4(1)	4(1)	-8(1)
C(324)	19(1)	15(1)	21(1)	2(1)	11(1)	5(1)
C(5)	20(1)	16(1)	31(2)	3(1)	16(1)	1(1)
C(114)	32(2)	11(1)	33(2)	-2(1)	20(1)	-3(1)
C(2)	13(1)	13(1)	13(1)	0(1)	1(1)	1(1)
C(313)	25(2)	21(2)	42(2)	4(1)	3(1)	-12(1)

Table E.15. Hydrogen coordinates ($\times 10^4$) and isotropic displacement parameters ($\text{\AA}^2 \times 10^3$) for [Rh(2,6-Cl₂-Phony)(CO)(PPh₃)].

	x	y	z	U(eq)
H(335)	2233	9029	-1474	35
H(332)	1070	9618	838	21
H(323)	1905	9510	4206	19
H(312)	3007	10119	1651	30
H(3)	3674	3958	-324	19
H(325)	-106	8191	2351	21
H(1A)	3183	1879	799	32
H(1B)	3223	2162	-200	32
H(1C)	2361	2039	-29	32
H(115)	2197	1646	3118	25
H(322)	2681	8985	3274	17
H(326)	664	7660	1415	17
H(315)	5200	7743	3195	28
H(316)	3920	6894	2549	20
H(333)	614	10701	-508	27
H(113)	247	1974	864	25
H(336)	2673	7910	-149	26
H(334)	1196	10421	-1660	30
H(314)	5396	9746	3026	29
H(324)	514	9093	3754	21
H(5A)	3968	6839	-432	31
H(5B)	4368	5591	-524	31
H(5C)	4698	6334	398	31
H(114)	858	1163	2303	27
H(313)	4294	10946	2296	37

Appendix E

Table E.16. Torsion angles [°] for [Rh(2,6-Cl₂-Phony)(CO)(PPh₃)].

Atoms	Angles (°)
O(01)-C(02)-C(01)-C(02) ^{xviii}	178(2)
C(01) ^{xviii} -C(02)-C(01)-C(02) ^{xviii}	0.000(2)
C(14)-Rh(1)-P(13)-C(321)	19.28(13)
O(12)-Rh(1)-P(13)-C(321)	-165.00(11)
N(11)-Rh(1)-P(13)-C(321)	-165.7(8)
C(14)-Rh(1)-P(13)-C(331)	-102.86(12)
O(12)-Rh(1)-P(13)-C(331)	72.86(10)
N(11)-Rh(1)-P(13)-C(331)	72.2(8)
C(14)-Rh(1)-P(13)-C(311)	141.72(12)
O(12)-Rh(1)-P(13)-C(311)	-42.56(10)
N(11)-Rh(1)-P(13)-C(311)	-43.2(8)
C(14)-Rh(1)-N(11)-C(2)	164.2(2)
O(12)-Rh(1)-N(11)-C(2)	-11.5(2)
P(13)-Rh(1)-N(11)-C(2)	-10.8(9)
C(14)-Rh(1)-N(11)-C(111)	-16.75(19)
O(12)-Rh(1)-N(11)-C(111)	167.54(18)
P(13)-Rh(1)-N(11)-C(111)	168.2(7)
C(14)-Rh(1)-O(12)-C(4)	-94.5(12)
N(11)-Rh(1)-O(12)-C(4)	15.4(2)
P(13)-Rh(1)-O(12)-C(4)	-164.5(2)
C(321)-P(13)-C(311)-C(312)	-71.9(2)
C(331)-P(13)-C(311)-C(312)	36.0(3)
Rh(1)-P(13)-C(311)-C(312)	157.8(2)
C(321)-P(13)-C(311)-C(316)	106.8(2)
C(331)-P(13)-C(311)-C(316)	-145.2(2)
Rh(1)-P(13)-C(311)-C(316)	-23.4(2)
C(331)-P(13)-C(321)-C(322)	-116.6(2)
C(311)-P(13)-C(321)-C(322)	-10.1(2)
Rh(1)-P(13)-C(321)-C(322)	116.9(2)
C(331)-P(13)-C(321)-C(326)	65.4(2)
C(311)-P(13)-C(321)-C(326)	171.8(2)
Rh(1)-P(13)-C(321)-C(326)	-61.2(2)
O(12)-Rh(1)-C(14)-O(14)	60(4)
N(11)-Rh(1)-C(14)-O(14)	-50(3)
P(13)-Rh(1)-C(14)-O(14)	130(3)

Appendix E

C(333)-C(332)-C(331)-C(336)	-0.1(4)
C(333)-C(332)-C(331)-P(13)	179.2(2)
C(321)-P(13)-C(331)-C(336)	179.1(2)
C(311)-P(13)-C(331)-C(336)	71.2(2)
Rh(1)-P(13)-C(331)-C(336)	-50.9(2)
C(321)-P(13)-C(331)-C(332)	-0.2(3)
C(311)-P(13)-C(331)-C(332)	-108.1(2)
Rh(1)-P(13)-C(331)-C(332)	129.8(2)
C(316)-C(311)-C(312)-C(313)	1.4(4)
P(13)-C(311)-C(312)-C(313)	-179.8(2)
Rh(1)-O(12)-C(4)-C(3)	-11.2(4)
Rh(1)-O(12)-C(4)-C(5)	170.18(17)
O(12)-C(4)-C(3)-C(2)	-3.6(5)
C(5)-C(4)-C(3)-C(2)	174.9(3)
C(111)-C(116)-C(115)-C(114)	-1.2(4)
Cl(16)-C(116)-C(115)-C(114)	179.6(2)
C(324)-C(323)-C(322)-C(321)	0.0(4)
C(326)-C(321)-C(322)-C(323)	0.8(4)
P(13)-C(321)-C(322)-C(323)	-177.3(2)
C(324)-C(325)-C(326)-C(321)	-0.1(4)
C(322)-C(321)-C(326)-C(325)	-0.7(4)
P(13)-C(321)-C(326)-C(325)	177.4(2)
C(115)-C(116)-C(111)-C(112)	1.5(4)
Cl(16)-C(116)-C(111)-C(112)	-179.34(19)
C(115)-C(116)-C(111)-N(11)	177.1(2)
Cl(16)-C(116)-C(111)-N(11)	-3.7(3)
C(113)-C(112)-C(111)-C(116)	-0.5(4)
Cl(12)-C(112)-C(111)-C(116)	178.90(19)
C(113)-C(112)-C(111)-N(11)	-176.1(2)
Cl(12)-C(112)-C(111)-N(11)	3.3(3)
C(2)-N(11)-C(111)-C(116)	91.7(3)
Rh(1)-N(11)-C(111)-C(116)	-87.4(3)
C(2)-N(11)-C(111)-C(112)	-92.9(3)
Rh(1)-N(11)-C(111)-C(112)	88.0(3)
C(314)-C(315)-C(316)-C(311)	-0.6(4)
C(312)-C(311)-C(316)-C(315)	-1.2(4)
P(13)-C(311)-C(316)-C(315)	180.0(2)
C(331)-C(332)-C(333)-C(334)	-0.6(4)

Appendix E

C(111)-C(112)-C(113)-C(114)	-0.8(4)
Cl(12)-C(112)-C(113)-C(114)	179.8(2)
C(334)-C(335)-C(336)-C(331)	-1.0(5)
C(332)-C(331)-C(336)-C(335)	0.9(4)
P(13)-C(331)-C(336)-C(335)	-178.5(2)
C(332)-C(333)-C(334)-C(335)	0.4(5)
C(336)-C(335)-C(334)-C(333)	0.4(5)
C(316)-C(315)-C(314)-C(313)	2.3(5)
C(326)-C(325)-C(324)-C(323)	0.9(4)
C(322)-C(323)-C(324)-C(325)	-0.8(4)
C(112)-C(113)-C(114)-C(115)	1.1(4)
C(116)-C(115)-C(114)-C(113)	-0.2(4)
C(111)-N(11)-C(2)-C(3)	-175.8(2)
Rh(1)-N(11)-C(2)-C(3)	3.2(4)
C(111)-N(11)-C(2)-C(1)	3.6(4)
Rh(1)-N(11)-C(2)-C(1)	-177.41(18)
C(4)-C(3)-C(2)-N(11)	7.7(4)
C(4)-C(3)-C(2)-C(1)	-171.7(3)
C(315)-C(314)-C(313)-C(312)	-2.1(5)
C(311)-C(312)-C(313)-C(314)	0.2(5)

Symmetry operator: xviii) $-x + 1, -y, -z$.

Table E.17. Hydrogen bonds for [Rh(2,6-Cl₂-Phony)(CO)(PPh₃)] [\AA and $^\circ$].

D-H...A	d(D-H)	d(H...A)	d(D...A)	<(DHA)
C(336)-H(336)...O(12)	0.95	2.46	3.266(3)	143.0
C(334)-H(334)...O(14) ^{xix}	0.95	2.52	3.185(4)	127.2

Symmetry operators: xviii) $-x + 1, -y, -z$ xix) $x, -y + 1\frac{1}{2}, z - \frac{1}{2}$

Appendix E

E.4. Carbonyl-[4-(2,3-Dimethylphenylamino)pent-3-en-2-onato]-Triphenylphosphine-Rhodium(I) [Rh(2,3-Me₂-Phony)(CO)(PPh₃)]

Table E.18. Atomic coordinates ($\times 10^4$) and equivalent isotropic displacement parameters ($\text{\AA}^2 \times 10^3$) for [Rh(2,3-Me₂-Phony)(CO)(PPh₃)]. U(eq) is defined as one third of the trace of the orthogonalized U_{ij} tensor.

	x	y	z	U(eq)
Rh(1)	2587(1)	6055(1)	10624(1)	19(1)
N(11)	2658(2)	4330(2)	10317(2)	36(1)
O(12)	3655(1)	6370(1)	9933(1)	22(1)
O(14)	980(1)	5732(2)	11595(1)	29(1)
P(13)	2618(1)	7972(1)	10876(1)	18(1)
C(1)	3204(2)	2591(2)	9641(2)	58(1)
C(2)	3218(2)	3869(2)	9805(2)	33(1)
C(3)	3845(2)	4508(2)	9371(2)	27(1)
C(4)	4032(1)	5655(2)	9447(1)	22(1)
C(5)	4722(2)	6203(2)	8925(2)	32(1)
C(11A)	2241(2)	3512(2)	10870(2)	25(1)
C(12A)	1377(2)	3169(2)	10605(1)	25(1)
C(13A)	912(1)	2400(2)	11083(2)	25(1)
C(14A)	1311(2)	1974(2)	11827(1)	25(1)
C(15A)	2176(2)	2318(2)	12092(1)	25(1)
C(16A)	2641(1)	3086(3)	11613(2)	25(1)
C(18A)	-11(3)	1950(4)	10797(2)	25(1)
C(17A)	953(3)	3664(4)	9799(3)	25(1)
C(11B)	1803(2)	3671(3)	10474(2)	24(1)
C(12B)	1886(2)	3040(3)	11212(2)	24(1)
C(13B)	1158(2)	2418(3)	11474(2)	24(1)
C(14B)	346(2)	2428(3)	10998(2)	24(1)
C(15B)	263(2)	3059(3)	10261(2)	24(1)
C(16B)	991(3)	3680(3)	9999(2)	24(1)
C(17B)	2760(4)	3064(6)	11737(4)	24(1)
C(18B)	1219(4)	1738(5)	12287(3)	24(1)
C(14)	1614(2)	5865(2)	11228(1)	22(1)
C(311)	1982(2)	8522(2)	11725(1)	21(1)
C(312)	2399(2)	8923(2)	12473(2)	26(1)
C(313)	1889(2)	9239(2)	13131(2)	34(1)
C(314)	960(2)	9173(2)	13044(2)	37(1)

Appendix E

C(315)	542(2)	8787(2)	12306(2)	36(1)
C(316)	1042(2)	8460(2)	11649(2)	29(1)
C(321)	2243(2)	8831(2)	9965(1)	24(1)
C(322)	1770(2)	9858(2)	10015(2)	33(1)
C(323)	1525(2)	10472(2)	9292(2)	41(1)
C(324)	1756(2)	10084(2)	8519(2)	38(1)
C(325)	2230(2)	9068(2)	8468(2)	36(1)
C(326)	2470(2)	8442(2)	9186(1)	28(1)
C(331)	3754(2)	8504(2)	11139(1)	22(1)
C(332)	4023(2)	9603(2)	10935(2)	39(1)
C(333)	4886(2)	9988(3)	11196(2)	51(1)
C(334)	5462(2)	9282(3)	11657(2)	43(1)
C(335)	5203(2)	8193(3)	11855(2)	35(1)
C(336)	4353(2)	7797(2)	11594(1)	26(1)

Table E.19. Bond lengths [Å] and angles [°] for [Rh(2,3-Me₂-Phony)(CO)(PPh₃)].

Atoms	Bond lengths (Å)	Atoms	Angles (°)
Rh(1)-C(14)	1.807(2)	C(14)-Rh(1)-O(12)	176.48(9)
Rh(1)-O(12)	2.0280(15)	C(14)-Rh(1)-N(11)	93.62(9)
Rh(1)-N(11)	2.069(2)	O(12)-Rh(1)-N(11)	89.53(7)
Rh(1)-P(13)	2.2635(6)	C(14)-Rh(1)-P(13)	91.86(7)
N(11)-C(2)	1.320(3)	O(12)-Rh(1)-P(13)	84.97(5)
N(11)-C(11A)	1.463(3)	N(11)-Rh(1)-P(13)	174.49(6)
N(11)-C(11B)	1.522(3)	C(2)-N(11)-C(11A)	114.9(2)
O(12)-C(4)	1.290(3)	C(2)-N(11)-C(11B)	117.8(2)
O(14)-C(14)	1.152(3)	C(11A)-N(11)-C(11B)	35.07(17)
P(13)-C(311)	1.821(2)	C(2)-N(11)-Rh(1)	125.77(17)
P(13)-C(331)	1.828(2)	C(11A)-N(11)-Rh(1)	117.14(17)
P(13)-C(321)	1.828(2)	C(11B)-N(11)-Rh(1)	113.14(19)
C(1)-C(2)	1.508(4)	C(4)-O(12)-Rh(1)	126.75(15)
C(1)-H(1A)	0.9800	C(311)-P(13)-C(331)	103.07(10)
C(1)-H(1B)	0.9800	C(311)-P(13)-C(321)	104.96(11)
C(1)-H(1C)	0.9800	C(331)-P(13)-C(321)	103.48(11)
C(2)-C(3)	1.410(3)	C(311)-P(13)-Rh(1)	118.23(8)
C(3)-C(4)	1.366(3)	C(331)-P(13)-Rh(1)	112.44(8)
C(3)-H(3)	0.9500	C(321)-P(13)-Rh(1)	113.14(8)

Appendix E

C(4)-C(5)	1.507(3)	C(2)-C(1)-H(1A)	109.5
C(5)-H(5A)	0.9800	C(2)-C(1)-H(1B)	109.5
C(5)-H(5B)	0.9800	H(1A)-C(1)-H(1B)	109.5
C(5)-H(5C)	0.9800	C(2)-C(1)-H(1C)	109.5
C(11A)-C(12A)	1.3900	H(1A)-C(1)-H(1C)	109.5
C(11A)-C(16A)	1.3900	H(1B)-C(1)-H(1C)	109.5
C(12A)-C(13A)	1.3900	N(11)-C(2)-C(3)	123.8(2)
C(12A)-C(17A)	1.515(5)	N(11)-C(2)-C(1)	120.3(2)
C(13A)-C(14A)	1.3900	C(3)-C(2)-C(1)	115.8(2)
C(13A)-C(18A)	1.516(4)	C(4)-C(3)-C(2)	127.4(2)
C(14A)-C(15A)	1.3900	C(4)-C(3)-H(3)	116.3
C(14A)-H(14A)	0.9500	C(2)-C(3)-H(3)	116.3
C(15A)-C(16A)	1.3900	O(12)-C(4)-C(3)	126.1(2)
C(15A)-H(15A)	0.9500	O(12)-C(4)-C(5)	113.6(2)
C(16A)-H(16A)	0.9500	C(3)-C(4)-C(5)	120.3(2)
C(18A)-H(18A)	0.9800	C(4)-C(5)-H(5A)	109.5
C(18A)-H(18B)	0.9800	C(4)-C(5)-H(5B)	109.5
C(18A)-H(18C)	0.9800	H(5A)-C(5)-H(5B)	109.5
C(17A)-H(17A)	0.9800	C(4)-C(5)-H(5C)	109.5
C(17A)-H(17B)	0.9800	H(5A)-C(5)-H(5C)	109.5
C(17A)-H(17C)	0.9800	H(5B)-C(5)-H(5C)	109.5
C(11B)-C(12B)	1.3900	C(12A)-C(11A)-C(16A)	120.0
C(11B)-C(16B)	1.3900	C(12A)-C(11A)-N(11)	114.94(19)
C(12B)-C(13B)	1.3900	C(16A)-C(11A)-N(11)	125.06(19)
C(12B)-C(17B)	1.506(7)	C(11A)-C(12A)-C(13A)	120.0
C(13B)-C(14B)	1.3900	C(11A)-C(12A)-C(17A)	118.8(2)
C(13B)-C(18B)	1.522(6)	C(13A)-C(12A)-C(17A)	121.2(2)
C(14B)-C(15B)	1.3900	C(12A)-C(13A)-C(14A)	120.0
C(14B)-H(14B)	0.9500	C(12A)-C(13A)-C(18A)	121.9(2)
C(15B)-C(16B)	1.3900	C(14A)-C(13A)-C(18A)	118.0(2)
C(15B)-H(15B)	0.9500	C(15A)-C(14A)-C(13A)	120.0
C(16B)-H(16B)	0.9500	C(15A)-C(14A)-H(14A)	120.0
C(17B)-H(17D)	0.9800	C(13A)-C(14A)-H(14A)	120.0
C(17B)-H(17E)	0.9800	C(14A)-C(15A)-C(16A)	120.0
C(17B)-H(17F)	0.9800	C(14A)-C(15A)-H(15A)	120.0
C(18B)-H(18D)	0.9800	C(16A)-C(15A)-H(15A)	120.0
C(18B)-H(18E)	0.9800	C(15A)-C(16A)-C(11A)	120.0
C(18B)-H(18F)	0.9800	C(15A)-C(16A)-H(16A)	120.0

Appendix E

C(311)-C(312)	1.395(3)	C(11A)-C(16A)-H(16A)	120.0
C(311)-C(316)	1.401(3)	C(12B)-C(11B)-C(16B)	120.0
C(312)-C(313)	1.388(3)	C(12B)-C(11B)-N(11)	112.0(2)
C(312)-H(312)	0.9500	C(16B)-C(11B)-N(11)	128.0(2)
C(313)-C(314)	1.386(4)	C(11B)-C(12B)-C(13B)	120.0
C(313)-H(313)	0.9500	C(11B)-C(12B)-C(17B)	119.6(3)
C(314)-C(315)	1.378(4)	C(13B)-C(12B)-C(17B)	120.4(3)
C(314)-H(314)	0.9500	C(14B)-C(13B)-C(12B)	120.0
C(315)-C(316)	1.379(3)	C(14B)-C(13B)-C(18B)	118.6(3)
C(315)-H(315)	0.9500	C(12B)-C(13B)-C(18B)	121.4(3)
C(316)-H(316)	0.9500	C(13B)-C(14B)-C(15B)	120.0
C(321)-C(326)	1.388(3)	C(13B)-C(14B)-H(14B)	120.0
C(321)-C(322)	1.390(3)	C(15B)-C(14B)-H(14B)	120.0
C(322)-C(323)	1.391(4)	C(16B)-C(15B)-C(14B)	120.0
C(322)-H(322)	0.9500	C(16B)-C(15B)-H(15B)	120.0
C(323)-C(324)	1.381(4)	C(14B)-C(15B)-H(15B)	120.0
C(323)-H(323)	0.9500	C(15B)-C(16B)-C(11B)	120.0
C(324)-C(325)	1.380(4)	C(15B)-C(16B)-H(16B)	120.0
C(324)-H(324)	0.9500	C(11B)-C(16B)-H(16B)	120.0
C(325)-C(326)	1.390(3)	C(12B)-C(17B)-H(17D)	109.5
C(325)-H(325)	0.9500	C(12B)-C(17B)-H(17E)	109.5
C(326)-H(326)	0.9500	H(17D)-C(17B)-H(17E)	109.5
C(331)-C(332)	1.384(4)	C(12B)-C(17B)-H(17F)	109.5
C(331)-C(336)	1.388(3)	H(17D)-C(17B)-H(17F)	109.5
C(332)-C(333)	1.403(4)	H(17E)-C(17B)-H(17F)	109.5
C(332)-H(332)	0.9500	C(13B)-C(18B)-H(18D)	109.5
C(333)-C(334)	1.369(5)	C(13B)-C(18B)-H(18E)	109.5
C(333)-H(333)	0.9500	H(18D)-C(18B)-H(18E)	109.5
C(334)-C(335)	1.366(4)	C(13B)-C(18B)-H(18F)	109.5
C(334)-H(334)	0.9500	H(18D)-C(18B)-H(18F)	109.5
C(335)-C(336)	1.387(3)	H(18E)-C(18B)-H(18F)	109.5
C(335)-H(335)	0.9500	O(14)-C(14)-Rh(1)	178.1(2)
C(336)-H(336)	0.9500	C(312)-C(311)-C(316)	118.8(2)
		C(312)-C(311)-P(13)	122.29(17)
		C(316)-C(311)-P(13)	118.70(17)
		C(313)-C(312)-C(311)	120.4(2)
		C(313)-C(312)-H(312)	119.8
		C(311)-C(312)-H(312)	119.8

Appendix E

C(314)-C(313)-C(312)	120.0(2)
C(314)-C(313)-H(313)	120.0
C(312)-C(313)-H(313)	120.0
C(315)-C(314)-C(313)	120.1(2)
C(315)-C(314)-H(314)	120.0
C(313)-C(314)-H(314)	120.0
C(314)-C(315)-C(316)	120.5(2)
C(314)-C(315)-H(315)	119.7
C(316)-C(315)-H(315)	119.7
C(315)-C(316)-C(311)	120.2(2)
C(315)-C(316)-H(316)	119.9
C(311)-C(316)-H(316)	119.9
C(326)-C(321)-C(322)	119.0(2)
C(326)-C(321)-P(13)	117.40(18)
C(322)-C(321)-P(13)	123.59(18)
C(321)-C(322)-C(323)	120.0(2)
C(321)-C(322)-H(322)	120.0
C(323)-C(322)-H(322)	120.0
C(324)-C(323)-C(322)	120.8(2)
C(324)-C(323)-H(323)	119.6
C(322)-C(323)-H(323)	119.6
C(325)-C(324)-C(323)	119.3(2)
C(325)-C(324)-H(324)	120.3
C(323)-C(324)-H(324)	120.3
C(324)-C(325)-C(326)	120.3(2)
C(324)-C(325)-H(325)	119.9
C(326)-C(325)-H(325)	119.9
C(321)-C(326)-C(325)	120.6(2)
C(321)-C(326)-H(326)	119.7
C(325)-C(326)-H(326)	119.7
C(332)-C(331)-C(336)	119.0(2)
C(332)-C(331)-P(13)	122.3(2)
C(336)-C(331)-P(13)	118.61(18)
C(331)-C(332)-C(333)	119.8(3)
C(331)-C(332)-H(332)	120.1
C(333)-C(332)-H(332)	120.1
C(334)-C(333)-C(332)	120.2(3)
C(334)-C(333)-H(333)	119.9

Appendix E

C(332)-C(333)-H(333)	119.9
C(335)-C(334)-C(333)	120.3(3)
C(335)-C(334)-H(334)	119.9
C(333)-C(334)-H(334)	119.9
C(334)-C(335)-C(336)	120.2(3)
C(334)-C(335)-H(335)	119.9
C(336)-C(335)-H(335)	119.9
C(335)-C(336)-C(331)	120.5(3)
C(335)-C(336)-H(336)	119.7
C(331)-C(336)-H(336)	119.7

Table E.20. Anisotropic displacement parameters ($\text{\AA}^2 \times 10^3$) for $[\text{Rh}(2,3\text{-Me}_2\text{-Phony})(\text{CO})(\text{PPh}_3)]$. The anisotropic displacement factor exponent takes the form: $-2\pi^2 [h^2 a^{*2} U^{11} + \dots + 2 h k a^* b^* U^{12}]$.

	U^{11}	U^{22}	U^{33}	U^{23}	U^{13}	U^{12}
Rh(1)	19(1)	17(1)	22(1)	-1(1)	7(1)	-2(1)
N(11)	47(1)	18(1)	48(1)	-5(1)	33(1)	-7(1)
O(12)	20(1)	22(1)	26(1)	4(1)	7(1)	1(1)
O(14)	24(1)	32(1)	31(1)	-5(1)	11(1)	-8(1)
P(13)	17(1)	18(1)	19(1)	-1(1)	0(1)	-1(1)
C(1)	83(2)	24(2)	73(2)	-11(2)	55(2)	-5(2)
C(2)	38(1)	22(1)	39(1)	-4(1)	20(1)	-1(1)
C(3)	27(1)	25(1)	30(1)	0(1)	13(1)	4(1)
C(4)	17(1)	28(1)	22(1)	5(1)	4(1)	3(1)
C(5)	25(1)	37(2)	35(1)	7(1)	13(1)	0(1)
C(11A)	26(1)	23(1)	26(1)	1(1)	2(1)	-2(1)
C(12A)	26(1)	23(1)	26(1)	1(1)	2(1)	-2(1)
C(13A)	26(1)	23(1)	26(1)	1(1)	2(1)	-2(1)
C(14A)	26(1)	23(1)	26(1)	1(1)	2(1)	-2(1)
C(15A)	26(1)	23(1)	26(1)	1(1)	2(1)	-2(1)
C(16A)	26(1)	23(1)	26(1)	1(1)	2(1)	-2(1)
C(18A)	26(1)	23(1)	26(1)	1(1)	2(1)	-2(1)
C(17A)	26(1)	23(1)	26(1)	1(1)	2(1)	-2(1)
C(11B)	28(1)	20(1)	25(1)	0(1)	4(1)	2(1)
C(12B)	28(1)	20(1)	25(1)	0(1)	4(1)	2(1)
C(13B)	28(1)	20(1)	25(1)	0(1)	4(1)	2(1)
C(14B)	28(1)	20(1)	25(1)	0(1)	4(1)	2(1)

Appendix E

C(15B)	28(1)	20(1)	25(1)	0(1)	4(1)	2(1)
C(16B)	28(1)	20(1)	25(1)	0(1)	4(1)	2(1)
C(17B)	28(1)	20(1)	25(1)	0(1)	4(1)	2(1)
C(18B)	28(1)	20(1)	25(1)	0(1)	4(1)	2(1)
C(14)	24(1)	19(1)	22(1)	-3(1)	3(1)	-5(1)
C(311)	20(1)	19(1)	24(1)	-2(1)	1(1)	0(1)
C(312)	23(1)	28(1)	27(1)	-5(1)	-2(1)	4(1)
C(313)	36(1)	40(2)	24(1)	-12(1)	-1(1)	2(1)
C(314)	32(1)	46(2)	35(1)	-14(1)	11(1)	4(1)
C(315)	20(1)	44(2)	46(2)	-11(1)	7(1)	0(1)
C(316)	24(1)	31(1)	32(1)	-9(1)	1(1)	-1(1)
C(321)	28(1)	20(1)	23(1)	0(1)	-3(1)	0(1)
C(322)	48(2)	23(1)	27(1)	-5(1)	-4(1)	7(1)
C(323)	59(2)	24(1)	39(2)	0(1)	-6(1)	15(1)
C(324)	53(2)	31(2)	30(1)	7(1)	-7(1)	10(1)
C(325)	47(2)	38(2)	23(1)	2(1)	-1(1)	10(1)
C(326)	34(1)	25(1)	25(1)	1(1)	-2(1)	8(1)
C(331)	20(1)	29(1)	19(1)	-3(1)	4(1)	-6(1)
C(332)	41(2)	33(2)	42(2)	5(1)	-2(1)	-14(1)
C(333)	50(2)	49(2)	55(2)	-5(2)	11(2)	-33(2)
C(334)	24(1)	67(2)	39(2)	-20(2)	9(1)	-15(1)
C(335)	19(1)	59(2)	28(1)	-16(1)	3(1)	1(1)
C(336)	21(1)	37(1)	22(1)	-10(1)	5(1)	-1(1)

Appendix E

Table E.21. Hydrogen coordinates ($\times 10^4$) and isotropic displacement parameters ($\text{\AA}^2 \times 10^3$) for $[\text{Rh}(2,3\text{-Me}_2\text{-Phony})(\text{CO})(\text{PPh}_3)]$.

	x	y	z	U(eq)
H(1A)	3099	2180	10161	86
H(1B)	3782	2352	9439	86
H(1C)	2722	2409	9219	86
H(3)	4176	4093	8982	32
H(5A)	4419	6684	8492	48
H(5B)	5068	5601	8662	48
H(5C)	5129	6680	9283	48
H(14A)	994	1449	12154	30
H(15A)	2449	2027	12600	30
H(16A)	3231	3321	11794	30
H(18A)	43	1423	10325	37
H(18B)	-401	2596	10622	37
H(18C)	-271	1539	11258	37
H(17A)	902	4501	9853	37
H(17B)	354	3330	9688	37
H(17C)	1329	3480	9337	37
H(14B)	-152	2003	11178	29
H(15B)	-292	3065	9936	29
H(16B)	934	4111	9495	29
H(17D)	3093	2351	11650	36
H(17E)	2636	3132	12328	36
H(17F)	3119	3724	11574	36
H(18D)	624	1440	12399	36
H(18E)	1436	2241	12747	36
H(18F)	1638	1094	12238	36
H(312)	3036	8980	12531	31
H(313)	2177	9501	13642	40
H(314)	611	9395	13493	45
H(315)	-95	8745	12248	44
H(316)	748	8192	11143	35
H(322)	1615	10140	10544	40
H(323)	1194	11167	9329	49
H(324)	1591	10511	8028	46
H(325)	2393	8796	7939	43

Appendix E

H(326)	2791	7741	9144	34
H(332)	3623	10096	10618	47
H(333)	5073	10740	11053	61
H(334)	6043	9550	11839	52
H(335)	5605	7705	12172	42
H(336)	4181	7035	11729	32

Table E.22. Torsion angles [°] for [Rh(2,3-Me₂-Phony)(CO)(PPh₃)].

Atoms	Angles (°)
C(14)-Rh(1)-N(11)-C(2)	174.7(3)
O(12)-Rh(1)-N(11)-C(2)	-3.8(3)
P(13)-Rh(1)-N(11)-C(2)	0.6(10)
C(14)-Rh(1)-N(11)-C(11A)	-23.0(2)
O(12)-Rh(1)-N(11)-C(11A)	158.5(2)
P(13)-Rh(1)-N(11)-C(11A)	162.9(6)
C(14)-Rh(1)-N(11)-C(11B)	15.6(2)
O(12)-Rh(1)-N(11)-C(11B)	-162.8(2)
P(13)-Rh(1)-N(11)-C(11B)	-158.5(7)
C(14)-Rh(1)-O(12)-C(4)	-145.4(13)
N(11)-Rh(1)-O(12)-C(4)	8.13(19)
P(13)-Rh(1)-O(12)-C(4)	-171.45(18)
C(14)-Rh(1)-P(13)-C(311)	16.41(11)
O(12)-Rh(1)-P(13)-C(311)	-165.13(10)
N(11)-Rh(1)-P(13)-C(311)	-169.5(8)
C(14)-Rh(1)-P(13)-C(331)	136.38(10)
O(12)-Rh(1)-P(13)-C(331)	-45.16(9)
N(11)-Rh(1)-P(13)-C(331)	-49.5(8)
C(14)-Rh(1)-P(13)-C(321)	-106.82(11)
O(12)-Rh(1)-P(13)-C(321)	71.63(10)
N(11)-Rh(1)-P(13)-C(321)	67.2(8)
C(11A)-N(11)-C(2)-C(3)	-164.1(3)
C(11B)-N(11)-C(2)-C(3)	156.7(3)
Rh(1)-N(11)-C(2)-C(3)	-1.5(4)
C(11A)-N(11)-C(2)-C(1)	16.8(4)
C(11B)-N(11)-C(2)-C(1)	-22.4(4)
Rh(1)-N(11)-C(2)-C(1)	179.4(2)

Appendix E

N(11)-C(2)-C(3)-C(4)	5.4(5)
C(1)-C(2)-C(3)-C(4)	-175.5(3)
Rh(1)-O(12)-C(4)-C(3)	-7.5(3)
Rh(1)-O(12)-C(4)-C(5)	171.45(15)
C(2)-C(3)-C(4)-O(12)	-0.5(4)
C(2)-C(3)-C(4)-C(5)	-179.4(3)
C(2)-N(11)-C(11A)-C(12A)	-98.8(3)
C(11B)-N(11)-C(11A)-C(12A)	4.8(3)
Rh(1)-N(11)-C(11A)-C(12A)	97.0(2)
C(2)-N(11)-C(11A)-C(16A)	81.7(3)
C(11B)-N(11)-C(11A)-C(16A)	-174.7(4)
Rh(1)-N(11)-C(11A)-C(16A)	-82.5(2)
C(16A)-C(11A)-C(12A)-C(13A)	0.0
N(11)-C(11A)-C(12A)-C(13A)	-179.5(3)
C(16A)-C(11A)-C(12A)-C(17A)	178.9(3)
N(11)-C(11A)-C(12A)-C(17A)	-0.6(3)
C(11A)-C(12A)-C(13A)-C(14A)	0.0
C(17A)-C(12A)-C(13A)-C(14A)	-178.9(3)
C(11A)-C(12A)-C(13A)-C(18A)	-176.5(3)
C(17A)-C(12A)-C(13A)-C(18A)	4.6(4)
C(12A)-C(13A)-C(14A)-C(15A)	0.0
C(18A)-C(13A)-C(14A)-C(15A)	176.7(3)
C(13A)-C(14A)-C(15A)-C(16A)	0.0
C(14A)-C(15A)-C(16A)-C(11A)	0.0
C(12A)-C(11A)-C(16A)-C(15A)	0.0
N(11)-C(11A)-C(16A)-C(15A)	179.5(3)
C(2)-N(11)-C(11B)-C(12B)	98.0(3)
C(11A)-N(11)-C(11B)-C(12B)	3.6(3)
Rh(1)-N(11)-C(11B)-C(12B)	-101.2(2)
C(2)-N(11)-C(11B)-C(16B)	-84.8(3)
C(11A)-N(11)-C(11B)-C(16B)	-179.2(5)
Rh(1)-N(11)-C(11B)-C(16B)	76.1(3)
C(16B)-C(11B)-C(12B)-C(13B)	0.0
N(11)-C(11B)-C(12B)-C(13B)	177.5(3)
C(16B)-C(11B)-C(12B)-C(17B)	-178.1(4)
N(11)-C(11B)-C(12B)-C(17B)	-0.6(4)
C(11B)-C(12B)-C(13B)-C(14B)	0.0
C(17B)-C(12B)-C(13B)-C(14B)	178.1(4)

Appendix E

C(11B)-C(12B)-C(13B)-C(18B)	-178.8(4)
C(17B)-C(12B)-C(13B)-C(18B)	-0.7(5)
C(12B)-C(13B)-C(14B)-C(15B)	0.0
C(18B)-C(13B)-C(14B)-C(15B)	178.8(4)
C(13B)-C(14B)-C(15B)-C(16B)	0.0
C(14B)-C(15B)-C(16B)-C(11B)	0.0
C(12B)-C(11B)-C(16B)-C(15B)	0.0
N(11)-C(11B)-C(16B)-C(15B)	-177.0(4)
O(12)-Rh(1)-C(14)-O(14)	95(7)
N(11)-Rh(1)-C(14)-O(14)	-58(7)
P(13)-Rh(1)-C(14)-O(14)	121(7)
C(331)-P(13)-C(311)-C(312)	-16.6(2)
C(321)-P(13)-C(311)-C(312)	-124.6(2)
Rh(1)-P(13)-C(311)-C(312)	108.17(19)
C(331)-P(13)-C(311)-C(316)	168.3(2)
C(321)-P(13)-C(311)-C(316)	60.2(2)
Rh(1)-P(13)-C(311)-C(316)	-67.0(2)
C(316)-C(311)-C(312)-C(313)	0.9(4)
P(13)-C(311)-C(312)-C(313)	-174.3(2)
C(311)-C(312)-C(313)-C(314)	-0.9(4)
C(312)-C(313)-C(314)-C(315)	0.4(4)
C(313)-C(314)-C(315)-C(316)	0.1(5)
C(314)-C(315)-C(316)-C(311)	-0.2(4)
C(312)-C(311)-C(316)-C(315)	-0.3(4)
P(13)-C(311)-C(316)-C(315)	175.1(2)
C(311)-P(13)-C(321)-C(326)	-166.46(19)
C(331)-P(13)-C(321)-C(326)	85.8(2)
Rh(1)-P(13)-C(321)-C(326)	-36.2(2)
C(311)-P(13)-C(321)-C(322)	15.4(2)
C(331)-P(13)-C(321)-C(322)	-92.3(2)
Rh(1)-P(13)-C(321)-C(322)	145.7(2)
C(326)-C(321)-C(322)-C(323)	0.6(4)
P(13)-C(321)-C(322)-C(323)	178.7(2)
C(321)-C(322)-C(323)-C(324)	-1.0(4)
C(322)-C(323)-C(324)-C(325)	0.6(5)
C(323)-C(324)-C(325)-C(326)	0.2(5)
C(322)-C(321)-C(326)-C(325)	0.1(4)
P(13)-C(321)-C(326)-C(325)	-178.1(2)

Appendix E

C(324)-C(325)-C(326)-C(321)	-0.5(4)
C(311)-P(13)-C(331)-C(332)	-83.3(2)
C(321)-P(13)-C(331)-C(332)	25.9(2)
Rh(1)-P(13)-C(331)-C(332)	148.32(19)
C(311)-P(13)-C(331)-C(336)	93.63(19)
C(321)-P(13)-C(331)-C(336)	-157.22(18)
Rh(1)-P(13)-C(331)-C(336)	-34.78(19)
C(336)-C(331)-C(332)-C(333)	-0.7(4)
P(13)-C(331)-C(332)-C(333)	176.2(2)
C(331)-C(332)-C(333)-C(334)	-0.4(4)
C(332)-C(333)-C(334)-C(335)	0.9(4)
C(333)-C(334)-C(335)-C(336)	-0.3(4)
C(334)-C(335)-C(336)-C(331)	-0.8(3)
C(332)-C(331)-C(336)-C(335)	1.3(3)
P(13)-C(331)-C(336)-C(335)	-175.74(17)

Table E.23. Hydrogen bonds for [Rh(2,3-Me₂-Phony)(CO)(PPh₃)] [Å and °].

D-H...A	d(D-H)	d(H...A)	d(D...A)	<(DHA)
C(326)-H(326)...O(12)	0.95	2.36	3.177(3)	143.2

E.5. Carbonyl-[4-(2,6-Dimethylphenylamino)pent-3-en-2-onato]-Triphenylphosphine-Rhodium(I) [Rh(2,6-Me₂-Phony)(CO)(PPh₃)

Table E.24. Atomic coordinates ($\times 10^4$) and equivalent isotropic displacement parameters ($\text{\AA}^2 \times 10^3$) for [Rh(2,6-Me₂-Phony)(CO)(PPh₃)]. U(eq) is defined as one third of the trace of the orthogonalized U_{ij} tensor.

	x	y	z	U(eq)
O(01)	4750(5)	1372(8)	289(9)	297(7)
C(02)	4986(10)	451(8)	100(8)	218(7)
C(01)	5836(5)	387(7)	248(10)	173(5)
Rh(1)	2371(1)	5807(1)	1224(1)	10(1)
P(13)	2330(1)	7767(1)	1515(1)	11(1)
Cl(16)	3376(1)	3087(1)	2768(1)	26(1)
Cl(12)	789(1)	3496(1)	-256(1)	25(1)
N(11)	2485(1)	4034(2)	917(2)	12(1)
O(12)	3316(1)	6184(2)	753(1)	15(1)

Appendix E

O(14)	893(1)	5322(2)	1734(1)	20(1)
C(311)	3336(1)	8421(2)	2020(2)	13(1)
C(321)	1755(1)	8259(2)	2254(2)	12(1)
C(335)	1993(2)	9143(3)	-1005(2)	29(1)
C(332)	1306(2)	9491(2)	368(2)	17(1)
C(14)	1479(2)	5532(2)	1565(2)	14(1)
C(323)	1654(2)	9130(2)	3640(2)	16(1)
C(331)	1923(2)	8654(2)	485(2)	14(1)
C(312)	3453(2)	9628(3)	1957(2)	25(1)
C(4)	3610(2)	5511(2)	264(2)	15(1)
C(3)	3433(2)	4329(2)	79(2)	16(1)
C(116)	2382(2)	2732(2)	2150(2)	16(1)
C(325)	461(2)	8347(2)	2540(2)	18(1)
C(1)	2924(2)	2310(2)	233(2)	21(1)
C(115)	1950(2)	1970(2)	2530(2)	21(1)
C(112)	1243(2)	2906(2)	818(2)	17(1)
C(322)	2116(2)	8817(2)	3085(2)	14(1)
C(326)	919(2)	8032(2)	1983(2)	15(1)
C(111)	2048(2)	3210(2)	1283(2)	14(1)
C(315)	4754(2)	8225(3)	2870(2)	23(1)
C(316)	3993(2)	7719(2)	2489(2)	17(1)
C(333)	1037(2)	10138(2)	-431(2)	22(1)
C(113)	795(2)	2158(2)	1192(2)	21(1)
C(336)	2258(2)	8484(3)	-216(2)	22(1)
C(334)	1379(2)	9971(3)	-1116(2)	25(1)
C(314)	4869(2)	9412(3)	2783(2)	24(1)
C(324)	828(2)	8888(2)	3370(2)	18(1)
C(5)	4214(2)	6122(2)	-106(2)	21(1)
C(114)	1157(2)	1686(2)	2047(2)	23(1)
C(2)	2930(2)	3616(2)	431(2)	14(1)
C(313)	4219(2)	10120(3)	2340(2)	31(1)

Appendix E

Table E.25. Bond lengths [\AA] and angles [$^\circ$] for $[\text{Rh}(2,6\text{-Me}_2\text{-Phony})(\text{CO})(\text{PPh}_3)]$.

Atoms	Bond lengths (\AA)	Atoms	Angles ($^\circ$)
O(01)-C(02)	1.190(9)	C(02) ^{xx} -C(02)-O(01)	163(3)
C(02)-C(02) ^{xx}	1.071(15)	C(02) ^{xx} -C(02)-C(01)	82.0(16)
C(02)-C(01)	1.419(15)	O(01)-C(02)-C(01)	115.1(14)
C(02)-C(01) ^{xx}	1.655(19)	C(02) ^{xx} -C(02)-C(01) ^{xx}	58.1(15)
C(01)-C(02) ^{xx}	1.655(19)	O(01)-C(02)-C(01) ^{xx}	104.8(13)
Rh(1)-C(14)	1.809(3)	C(01)-C(02)-C(01) ^{xx}	140.1(6)
Rh(1)-O(12)	2.0350(17)	C(02)-C(01)-C(02) ^{xx}	39.9(6)
Rh(1)-N(11)	2.086(2)	C(14)-Rh(1)-O(12)	175.44(10)
Rh(1)-P(13)	2.2690(7)	C(14)-Rh(1)-N(11)	92.94(10)
P(13)-C(321)	1.823(2)	O(12)-Rh(1)-N(11)	88.60(8)
P(13)-C(331)	1.828(3)	C(14)-Rh(1)-P(13)	91.62(8)
P(13)-C(311)	1.828(2)	O(12)-Rh(1)-P(13)	86.81(5)
Cl(16)-C(116)	1.736(3)	N(11)-Rh(1)-P(13)	175.42(6)
Cl(12)-C(112)	1.735(3)	C(321)-P(13)-C(331)	104.01(11)
N(11)-C(2)	1.322(3)	C(321)-P(13)-C(311)	104.03(11)
N(11)-C(111)	1.425(3)	C(331)-P(13)-C(311)	102.00(12)
O(12)-C(4)	1.286(3)	C(321)-P(13)-Rh(1)	118.65(8)
O(14)-C(14)	1.149(3)	C(331)-P(13)-Rh(1)	113.03(9)
C(311)-C(312)	1.388(4)	C(311)-P(13)-Rh(1)	113.32(8)
C(311)-C(316)	1.392(4)	C(2)-N(11)-C(111)	118.0(2)
C(321)-C(322)	1.393(4)	C(2)-N(11)-Rh(1)	126.00(17)
C(321)-C(326)	1.400(3)	C(111)-N(11)-Rh(1)	116.02(16)
C(335)-C(336)	1.382(4)	C(4)-O(12)-Rh(1)	126.72(16)
C(335)-C(334)	1.388(4)	C(312)-C(311)-C(316)	119.0(2)
C(335)-H(335)	0.9500	C(312)-C(311)-P(13)	120.6(2)
C(332)-C(333)	1.387(4)	C(316)-C(311)-P(13)	120.5(2)
C(332)-C(331)	1.396(4)	C(322)-C(321)-C(326)	118.9(2)
C(332)-H(332)	0.9500	C(322)-C(321)-P(13)	122.81(18)
C(323)-C(324)	1.387(4)	C(326)-C(321)-P(13)	118.21(19)
C(323)-C(322)	1.390(4)	C(336)-C(335)-C(334)	120.2(3)
C(323)-H(323)	0.9500	C(336)-C(335)-H(335)	119.9
C(331)-C(336)	1.393(4)	C(334)-C(335)-H(335)	119.9
C(312)-C(313)	1.389(4)	C(333)-C(332)-C(331)	120.3(3)
C(312)-H(312)	0.9500	C(333)-C(332)-H(332)	119.9
C(4)-C(3)	1.382(4)	C(331)-C(332)-H(332)	119.9

Appendix E

C(4)-C(5)	1.508(3)	O(14)-C(14)-Rh(1)	176.0(2)
C(3)-C(2)	1.415(4)	C(324)-C(323)-C(322)	120.2(2)
C(3)-H(3)	0.9500	C(324)-C(323)-H(323)	119.9
C(116)-C(115)	1.388(4)	C(322)-C(323)-H(323)	119.9
C(116)-C(111)	1.394(4)	C(336)-C(331)-C(332)	118.7(2)
C(325)-C(324)	1.386(4)	C(336)-C(331)-P(13)	117.5(2)
C(325)-C(326)	1.387(4)	C(332)-C(331)-P(13)	123.8(2)
C(325)-H(325)	0.9500	C(311)-C(312)-C(313)	120.4(3)
C(1)-C(2)	1.509(4)	C(311)-C(312)-H(312)	119.8
C(1)-H(1A)	0.9800	C(313)-C(312)-H(312)	119.8
C(1)-H(1B)	0.9800	O(12)-C(4)-C(3)	126.3(2)
C(1)-H(1C)	0.9800	O(12)-C(4)-C(5)	113.6(2)
C(115)-C(114)	1.382(4)	C(3)-C(4)-C(5)	120.1(2)
C(115)-H(115)	0.9500	C(4)-C(3)-C(2)	126.6(2)
C(112)-C(113)	1.391(4)	C(4)-C(3)-H(3)	116.7
C(112)-C(111)	1.398(4)	C(2)-C(3)-H(3)	116.7
C(322)-H(322)	0.9500	C(115)-C(116)-C(111)	122.2(3)
C(326)-H(326)	0.9500	C(115)-C(116)-Cl(16)	118.9(2)
C(315)-C(314)	1.372(4)	C(111)-C(116)-Cl(16)	118.9(2)
C(315)-C(316)	1.389(4)	C(324)-C(325)-C(326)	120.3(2)
C(315)-H(315)	0.9500	C(324)-C(325)-H(325)	119.9
C(316)-H(316)	0.9500	C(326)-C(325)-H(325)	119.9
C(333)-C(334)	1.379(4)	C(2)-C(1)-H(1A)	109.5
C(333)-H(333)	0.9500	C(2)-C(1)-H(1B)	109.5
C(113)-C(114)	1.381(4)	H(1A)-C(1)-H(1B)	109.5
C(113)-H(113)	0.9500	C(2)-C(1)-H(1C)	109.5
C(336)-H(336)	0.9500	H(1A)-C(1)-H(1C)	109.5
C(334)-H(334)	0.9500	H(1B)-C(1)-H(1C)	109.5
C(314)-C(313)	1.378(4)	C(114)-C(115)-C(116)	119.4(3)
C(314)-H(314)	0.9500	C(114)-C(115)-H(115)	120.3
C(324)-H(324)	0.9500	C(116)-C(115)-H(115)	120.3
C(5)-H(5A)	0.9800	C(113)-C(112)-C(111)	122.1(3)
C(5)-H(5B)	0.9800	C(113)-C(112)-Cl(12)	119.2(2)
C(5)-H(5C)	0.9800	C(111)-C(112)-Cl(12)	118.7(2)
C(114)-H(114)	0.9500	C(323)-C(322)-C(321)	120.4(2)
C(313)-H(313)	0.9500	C(323)-C(322)-H(322)	119.8
		C(321)-C(322)-H(322)	119.8
		C(325)-C(326)-C(321)	120.3(2)

Appendix E

C(325)-C(326)-H(326)	119.8
C(321)-C(326)-H(326)	119.8
C(116)-C(111)-C(112)	116.6(2)
C(116)-C(111)-N(11)	121.5(2)
C(112)-C(111)-N(11)	121.7(2)
C(314)-C(315)-C(316)	120.6(3)
C(314)-C(315)-H(315)	119.7
C(316)-C(315)-H(315)	119.7
C(315)-C(316)-C(311)	120.0(3)
C(315)-C(316)-H(316)	120.0
C(311)-C(316)-H(316)	120.0
C(334)-C(333)-C(332)	120.5(3)
C(334)-C(333)-H(333)	119.8
C(332)-C(333)-H(333)	119.8
C(114)-C(113)-C(112)	119.3(3)
C(114)-C(113)-H(113)	120.4
C(112)-C(113)-H(113)	120.4
C(335)-C(336)-C(331)	120.6(3)
C(335)-C(336)-H(336)	119.7
C(331)-C(336)-H(336)	119.7
C(333)-C(334)-C(335)	119.7(3)
C(333)-C(334)-H(334)	120.2
C(335)-C(334)-H(334)	120.2
C(315)-C(314)-C(313)	119.8(3)
C(315)-C(314)-H(314)	120.1
C(313)-C(314)-H(314)	120.1
C(325)-C(324)-C(323)	119.8(2)
C(325)-C(324)-H(324)	120.1
C(323)-C(324)-H(324)	120.1
C(4)-C(5)-H(5A)	109.5
C(4)-C(5)-H(5B)	109.5
H(5A)-C(5)-H(5B)	109.5
C(4)-C(5)-H(5C)	109.5
H(5A)-C(5)-H(5C)	109.5
H(5B)-C(5)-H(5C)	109.5
C(113)-C(114)-C(115)	120.4(3)
C(113)-C(114)-H(114)	119.8
C(115)-C(114)-H(114)	119.8

Appendix E

N(11)-C(2)-C(3)	123.6(2)
N(11)-C(2)-C(1)	119.8(2)
C(3)-C(2)-C(1)	116.6(2)
C(314)-C(313)-C(312)	120.2(3)
C(314)-C(313)-H(313)	119.9
C(312)-C(313)-H(313)	119.9

Symmetry operator: xx) -x + 1, -y, -z.

Table E.26. Anisotropic displacement parameters ($\text{\AA}^2 \times 10^3$) for $[\text{Rh}(2,6\text{-Me}_2\text{-Phony})(\text{CO})(\text{PPh}_3)]$. The anisotropic displacement factor exponent takes the form: $-2\pi^2[h^2a^*2U^{11} + \dots + 2hk a^* b^* U^{12}]$.

	U^{11}	U^{22}	U^{33}	U^{23}	U^{13}	U^{12}
O(01)	204(8)	168(7)	580(20)	-134(10)	211(11)	-60(6)
C(02)	420(20)	76(6)	183(10)	-17(6)	130(13)	110(10)
C(01)	114(7)	64(5)	343(17)	-58(7)	74(9)	-3(5)
Rh(1)	11(1)	8(1)	12(1)	0(1)	4(1)	0(1)
P(13)	11(1)	9(1)	12(1)	0(1)	3(1)	0(1)
Cl(16)	21(1)	32(1)	22(1)	8(1)	0(1)	0(1)
Cl(12)	24(1)	21(1)	23(1)	4(1)	-4(1)	-7(1)
N(11)	14(1)	8(1)	14(1)	2(1)	4(1)	-1(1)
O(12)	15(1)	12(1)	19(1)	0(1)	8(1)	0(1)
O(14)	19(1)	19(1)	24(1)	0(1)	11(1)	-3(1)
C(311)	11(1)	14(1)	14(1)	-1(1)	5(1)	-2(1)
C(321)	12(1)	9(1)	14(1)	2(1)	5(1)	0(1)
C(335)	46(2)	26(2)	18(2)	3(1)	15(1)	14(1)
C(332)	18(1)	14(1)	19(1)	1(1)	6(1)	2(1)
C(14)	18(1)	9(1)	14(1)	0(1)	4(1)	0(1)
C(323)	18(1)	16(1)	14(1)	-1(1)	4(1)	1(1)
C(331)	15(1)	12(1)	12(1)	-1(1)	1(1)	-1(1)
C(312)	18(1)	18(1)	33(2)	5(1)	1(1)	-4(1)
C(4)	11(1)	17(1)	16(1)	4(1)	4(1)	3(1)
C(3)	16(1)	15(1)	17(1)	2(1)	8(1)	4(1)
C(116)	18(1)	14(1)	17(1)	-1(1)	6(1)	0(1)
C(325)	14(1)	16(1)	25(2)	4(1)	8(1)	1(1)
C(1)	27(1)	13(1)	27(2)	-2(1)	13(1)	1(1)
C(115)	32(2)	14(1)	22(2)	3(1)	15(1)	1(1)
C(112)	20(1)	12(1)	18(1)	-1(1)	4(1)	1(1)

Appendix E

C(322)	12(1)	14(1)	16(1)	0(1)	2(1)	1(1)
C(326)	13(1)	13(1)	16(1)	1(1)	2(1)	-1(1)
C(111)	17(1)	6(1)	18(1)	-1(1)	7(1)	1(1)
C(315)	13(1)	29(2)	24(2)	-5(1)	2(1)	6(1)
C(316)	17(1)	15(1)	18(1)	-3(1)	3(1)	0(1)
C(333)	23(1)	17(1)	23(2)	1(1)	2(1)	7(1)
C(113)	19(1)	13(1)	32(2)	-5(1)	10(1)	-4(1)
C(336)	29(2)	20(1)	18(1)	2(1)	9(1)	12(1)
C(334)	41(2)	17(1)	15(1)	3(1)	4(1)	7(1)
C(314)	14(1)	32(2)	24(2)	-4(1)	4(1)	-8(1)
C(324)	19(1)	15(1)	21(1)	2(1)	11(1)	5(1)
C(5)	20(1)	16(1)	31(2)	3(1)	16(1)	1(1)
C(114)	32(2)	11(1)	33(2)	-2(1)	20(1)	-3(1)
C(2)	13(1)	13(1)	13(1)	0(1)	1(1)	1(1)
C(313)	25(2)	21(2)	42(2)	4(1)	3(1)	-12(1)

Appendix E

Table E.27. Hydrogen coordinates ($\times 10^4$) and isotropic displacement parameters ($\text{\AA}^2 \times 10^3$) for $[\text{Rh}(2,6\text{-Me}_2\text{-Phony})(\text{CO})(\text{PPh}_3)]$.

	x	y	z	U(eq)
H(335)	2233	9029	-1474	35
H(332)	1070	9618	838	21
H(323)	1905	9510	4206	19
H(312)	3007	10119	1651	30
H(3)	3674	3958	-324	19
H(325)	-106	8191	2351	21
H(1A)	3183	1879	799	32
H(1B)	3223	2162	-200	32
H(1C)	2361	2039	-29	32
H(115)	2197	1646	3118	25
H(322)	2681	8985	3274	17
H(326)	664	7660	1415	17
H(315)	5200	7743	3195	28
H(316)	3920	6894	2549	20
H(333)	614	10701	-508	27
H(113)	247	1974	864	25
H(336)	2673	7910	-149	26
H(334)	1196	10421	-1660	30
H(314)	5396	9746	3026	29
H(324)	514	9093	3754	21
H(5A)	3968	6839	-432	31
H(5B)	4368	5591	-524	31
H(5C)	4698	6334	398	31
H(114)	858	1163	2303	27
H(313)	4294	10946	2296	37

Appendix E

Table E.28. Torsion angles [°] for [Rh(2,6-Me₂-Phony)(CO)(PPh₃)].

Atoms	Angles (°)
O(01)-C(02)-C(01)-C(02) ^{xx}	178(2)
C(01) ^{xx} -C(02)-C(01)-C(02) ^{xx}	0.000(2)
C(14)-Rh(1)-P(13)-C(321)	19.28(13)
O(12)-Rh(1)-P(13)-C(321)	-165.00(11)
N(11)-Rh(1)-P(13)-C(321)	-165.7(8)
C(14)-Rh(1)-P(13)-C(331)	-102.86(12)
O(12)-Rh(1)-P(13)-C(331)	72.86(10)
N(11)-Rh(1)-P(13)-C(331)	72.2(8)
C(14)-Rh(1)-P(13)-C(311)	141.72(12)
O(12)-Rh(1)-P(13)-C(311)	-42.56(10)
N(11)-Rh(1)-P(13)-C(311)	-43.2(8)
C(14)-Rh(1)-N(11)-C(2)	164.2(2)
O(12)-Rh(1)-N(11)-C(2)	-11.5(2)
P(13)-Rh(1)-N(11)-C(2)	-10.8(9)
C(14)-Rh(1)-N(11)-C(111)	-16.75(19)
O(12)-Rh(1)-N(11)-C(111)	167.54(18)
P(13)-Rh(1)-N(11)-C(111)	168.2(7)
C(14)-Rh(1)-O(12)-C(4)	-94.5(12)
N(11)-Rh(1)-O(12)-C(4)	15.4(2)
P(13)-Rh(1)-O(12)-C(4)	-164.5(2)
C(321)-P(13)-C(311)-C(312)	-71.9(2)
C(331)-P(13)-C(311)-C(312)	36.0(3)
Rh(1)-P(13)-C(311)-C(312)	157.8(2)
C(321)-P(13)-C(311)-C(316)	106.8(2)
C(331)-P(13)-C(311)-C(316)	-145.2(2)
Rh(1)-P(13)-C(311)-C(316)	-23.4(2)
C(331)-P(13)-C(321)-C(322)	-116.6(2)
C(311)-P(13)-C(321)-C(322)	-10.1(2)
Rh(1)-P(13)-C(321)-C(322)	116.9(2)
C(331)-P(13)-C(321)-C(326)	65.4(2)
C(311)-P(13)-C(321)-C(326)	171.8(2)
Rh(1)-P(13)-C(321)-C(326)	-61.2(2)
O(12)-Rh(1)-C(14)-O(14)	60(4)
N(11)-Rh(1)-C(14)-O(14)	-50(3)
P(13)-Rh(1)-C(14)-O(14)	130(3)

Appendix E

C(333)-C(332)-C(331)-C(336)	-0.1(4)
C(333)-C(332)-C(331)-P(13)	179.2(2)
C(321)-P(13)-C(331)-C(336)	179.1(2)
C(311)-P(13)-C(331)-C(336)	71.2(2)
Rh(1)-P(13)-C(331)-C(336)	-50.9(2)
C(321)-P(13)-C(331)-C(332)	-0.2(3)
C(311)-P(13)-C(331)-C(332)	-108.1(2)
Rh(1)-P(13)-C(331)-C(332)	129.8(2)
C(316)-C(311)-C(312)-C(313)	1.4(4)
P(13)-C(311)-C(312)-C(313)	-179.8(2)
Rh(1)-O(12)-C(4)-C(3)	-11.2(4)
Rh(1)-O(12)-C(4)-C(5)	170.18(17)
O(12)-C(4)-C(3)-C(2)	-3.6(5)
C(5)-C(4)-C(3)-C(2)	174.9(3)
C(111)-C(116)-C(115)-C(114)	-1.2(4)
Cl(16)-C(116)-C(115)-C(114)	179.6(2)
C(324)-C(323)-C(322)-C(321)	0.0(4)
C(326)-C(321)-C(322)-C(323)	0.8(4)
P(13)-C(321)-C(322)-C(323)	-177.3(2)
C(324)-C(325)-C(326)-C(321)	-0.1(4)
C(322)-C(321)-C(326)-C(325)	-0.7(4)
P(13)-C(321)-C(326)-C(325)	177.4(2)
C(115)-C(116)-C(111)-C(112)	1.5(4)
Cl(16)-C(116)-C(111)-C(112)	-179.34(19)
C(115)-C(116)-C(111)-N(11)	177.1(2)
Cl(16)-C(116)-C(111)-N(11)	-3.7(3)
C(113)-C(112)-C(111)-C(116)	-0.5(4)
Cl(12)-C(112)-C(111)-C(116)	178.90(19)
C(113)-C(112)-C(111)-N(11)	-176.1(2)
Cl(12)-C(112)-C(111)-N(11)	3.3(3)
C(2)-N(11)-C(111)-C(116)	91.7(3)
Rh(1)-N(11)-C(111)-C(116)	-87.4(3)
C(2)-N(11)-C(111)-C(112)	-92.9(3)
Rh(1)-N(11)-C(111)-C(112)	88.0(3)
C(314)-C(315)-C(316)-C(311)	-0.6(4)
C(312)-C(311)-C(316)-C(315)	-1.2(4)
P(13)-C(311)-C(316)-C(315)	180.0(2)
C(331)-C(332)-C(333)-C(334)	-0.6(4)

Appendix E

C(111)-C(112)-C(113)-C(114)	-0.8(4)
Cl(12)-C(112)-C(113)-C(114)	179.8(2)
C(334)-C(335)-C(336)-C(331)	-1.0(5)
C(332)-C(331)-C(336)-C(335)	0.9(4)
P(13)-C(331)-C(336)-C(335)	-178.5(2)
C(332)-C(333)-C(334)-C(335)	0.4(5)
C(336)-C(335)-C(334)-C(333)	0.4(5)
C(316)-C(315)-C(314)-C(313)	2.3(5)
C(326)-C(325)-C(324)-C(323)	0.9(4)
C(322)-C(323)-C(324)-C(325)	-0.8(4)
C(112)-C(113)-C(114)-C(115)	1.1(4)
C(116)-C(115)-C(114)-C(113)	-0.2(4)
C(111)-N(11)-C(2)-C(3)	-175.8(2)
Rh(1)-N(11)-C(2)-C(3)	3.2(4)
C(111)-N(11)-C(2)-C(1)	3.6(4)
Rh(1)-N(11)-C(2)-C(1)	-177.41(18)
C(4)-C(3)-C(2)-N(11)	7.7(4)
C(4)-C(3)-C(2)-C(1)	-171.7(3)
C(315)-C(314)-C(313)-C(312)	-2.1(5)
C(311)-C(312)-C(313)-C(314)	0.2(5)

Symmetry operator: xx) $-x + 1, -y, -z$.

Table E.29. Hydrogen bonds for [Rh(2,6-Me₂-Phony)(CO)(PPh₃)] [\AA and $^\circ$].

D-H...A	d(D-H)	d(H...A)	d(D...A)	<(DHA)
C(332)-H(332)...O(12)	0.95	2.38	3.201(3)	144.1
C(334)-H(334)...O(14) ^{xxi}	0.95	2.52	3.185(4)	127.2
C(1)-H(1B)...O(01) ^{xxii}	0.98	2.54	3.372(9)	142.4

Symmetry operator: xx) $-x + 1, -y + 1, -z$ xxi) $x, -y + \frac{1}{2}, z + \frac{1}{2}$ xxii) $-x + 1, y + \frac{1}{2}, -z + \frac{1}{2}$